8-2005

Defining the mechanisms of neutrophil exocytosis using proteomic techniques.

George Lominadze 1978-
University of Louisville

DEFINING THE MECHANISMS OF NEUTROPHIL EXOCYTOSIS USING PROTEOMIC TECHNIQUES

By

George Lominadze
B.S. University of Louisville, 2000

A Dissertation
Submitted to the Faculty of the
Graduate School of the University of Louisville
in Partial Fulfillment of the Requirements
for the Degree of

Doctor of Philosophy

Department of Biochemistry
and Molecular Biology
University of Louisville
Louisville, Kentucky

August 2005

DEFINING THE MECHANISMS OF NEUTROPHIL EXOCYTOSIS USING PROTEOMIC TECHNIQUES

By

George Lominadze
B.S., University of Louisville, 20000

A Dissertation Approved on

June 1, 2005

by the following Thesis Committee

Thesis Director

ACKNOWLEDGEMENTS

I would like to thank my mentor, Dr. Kenneth McLeish for his guidance, trust, support, and patience. I would also like to thank Dr. Richard Ward, who has acted as a co-mentor on the granule proteome project. I am very grateful to other members of my dissertation committee, Dr. Jon Klein, Dr. Robert Gray, and Dr. William Dean. I also wish to express my gratitude to Dr. Madhavi Rane for her insightful suggestions, encouragement and advice. I thank Dr. David Powell for carrying out the ESI-MS/MS analysis at Vanderbilt University. Finally, I would like to thank my parents and my brother for being a perfect family.

ABSTRACT

DEFINING THE MECHANISMS OF NEUTROPHIL EXOCYTOSIS USING PROTEOMIC TECHNIQUES

George Lominadze

June 1, 2005

Exocytosis of intracellular granules is critical for conversion of inactive, circulating neutrophils to fully activated cells. The p38 MAPK pathway plays a central role in neutrophil exocytosis, although its mechanism of action is unknown. We used several proteomic approaches to identify granule proteins and find targets of the p38 MAPK and its downstream kinase, MK2, on granules. Our analysis identified 286 proteins on neutrophil granules, four of which were known MK2 substrates. Known p38 substrates were not detected. However, MRP-14 was identified as a novel p38 MAPK substrate. MRP-14 was phosphorylated by p38 MAPK in neutrophils upon cell stimulation and translocated to plasma membranes and gelatinase granules, as well as to Triton X-100-insoluble structures at the base of lamellipodia. Phosphorylation of the MRP-14 by p38 MAPK increased binding to actin *in vitro*. These results suggest that MRP-14 is a potential mediator of p38 MAPK-dependent exocytosis in human neutrophils.

TABLE OF CONTENTS

PAGE

LIST OF TABLES

PAGE

TABLE

LIST OF FIGURES

PAGE

FIGURE

CHAPTER I

GENERAL INTRODUCTION

Role of Neutrophils in Host Defense and Tissue Damage

Neutrophils (also called polymorphonuclear leukocytes or PMNs) are phagocytic granulocytes that are crucial to host defense. These cells provide the initial cellular response at sites of infection and inflammation. Upon exposure to pro-inflammatory chemoattractants, chemokines, and cytokines, neutrophils are transformed from benign circulating cells to cells capable of adhesion to vascular endothelium, migration along chemoattractant gradients to sites of infection or trauma, phagocytosis of opsonized pathogens, and the release of antimicrobial agents [1]. In all of the above-mentioned processes, exocytosis of mobilizable membrane-bound compartments plays a central role.

Although the infiltration of neutrophils into injured tissue protects it from invading pathogens, substantial evidence exists showing that neutrophil-induced host tissue injury contributes to inflammatory diseases, ischemia-reperfusion injury, and impaired wound healing [2-5]. Upon neutrophil activation the secretion of granule proteinases, peroxidases and cationic peptides acts in concert with the release of reactive oxygen intermediates to promote chemotaxis by digestion of extracellular matrix or to directly damage host cells [6,7]. As the intracellular events that lead to neutrophil

exocytosis are poorly characterized, understanding the mechanism of neutrophil degranulation could be of significant clinical importance.

Neutrophil Granules and Their Role in Neutrophil Function

Neutrophils possess four types of mobilizable membrane-bound compartments: secretory vesicles, tertiary (gelatinase) granules, secondary (specific) granules, and primary (azurophil) granules [8,9]. These compartments differ in their protein content, physiological role, and physical characteristics. Differences in density of the granule subsets can be used to separate and enrich these subsets by isopycnic centrifugation on Percoll gradients [10]. Secretory vesicles are derived from the plasma membrane by endocytosis. Their lumen contains plasma proteins, while their membranes are rich in receptors and adhesion molecules, indicating that a major role of exocytosis of this compartment is to enhance plasma membrane expression of these molecules. The azurophil, specific, and gelatinase granules contain a variety of proteins in their luminal spaces and membranes, with distinct proteins being associated with each granule type. Neutrophil granule subsets are differentially mobilized, a process termed graded exocytosis, and the luminal and membrane protein content of each compartment determines the physiological role of exocytosis of secretory vesicles and the three subsets of granules [11,12]. Secretory vesicles are the most easily mobilized, followed in order of the ease of mobilization by gelatinase granules, specific granules, and azurophil granules. Stimulation of cells with optimal concentrations of the chemotactic peptide N-formyl-methionyl-leucyl-phenylalanine (fMLP) results in complete mobilization of secretory vesicles, exocytosis of about 25% of gelatinase granules, and release of 5-7% of specific

granules, while azurophilic granule exocytosis is negligible [12]. Graded exocytosis allows neutrophils to reach a fully activated phenotype in stages that correspond to the events occurring during neutrophil response to inflammatory stimuli, as described next.

Neutrophil stimulation by inflammatory mediators or cross-linking of selectins causes rapid exocytosis of secretory vesicles and gelatinase granules [13-15]. This results in increased plasma membrane expression of integrins, allowing the cell to adhere to vascular endothelium [16,17]. Class IV and class V collagens are substrates of gelatinase (matrix metalloproteinase 9), and local release of gelatinase is believed to play a major role in neutrophil migration through vascular basement membranes [14,18]. Exocytosis of specific and gelatinase granules, whose membranes are the main stores of complement receptor CR3 and flavocytochrome b_{558} [19], enhances bacterial phagocytosis and NADPH oxidase assembly, which generates reactive oxygen species (ROS) [20]. Exocytosis of specific granules releases large amounts of collagenase and lactoferrin. Collagenase is important for cell migration through tissues [21,22], and lactoferrin limits bacterial growth by blocking access to iron [22,23]. Azurophil granules are lysosome-related granules that exhibit limited exocytosis [24]. Azurophil granules fuse with phagosomes, thereby exposing ingested bacteria to hydrolases, proteases, and bactericidal peptides [25,26].

The luminal contents are tightly packaged in neutrophil granules. Most of the luminal proteins, including lactoferrin, myeloperoxidase, and lysozyme are positively charged, which normally would result in strong electrostatic repulsion among proteins within granules. To counter these repulsive forces, neutrophil granules contain negatively charged acidic proteoglycans, such as chondroitin sulfate, that condenses the basic

proteins into a crystalline state, thus both packaging and inactivating them [27,28]. This matrix can act as an ion-exchange gel and release bound proteins upon contact with counter-ions. In neutrophil granules, the vast majority of sulfated proteoglycans (80%) have been localized to azurophil granules, which contain the most basic proteins, while the rest were found distributed in specific and gelatinase granules [29].

The packaging of luminal proteins occurs during granule biogenesis, which takes place throughout myeloid cell maturation. Different granule subsets form at different stages of maturation (Figure 1) [30]. Electron microscopy of neutrophil granules during developmental progression from a myeloblast to a neutrophil revealed that azurophil granules arose by aggregation and fusion of dense core vesicles derived from the *trans*-Golgi complex. These granules were abundant in the cytoplasm of immature cells, but declined in number at later stages of development due to cell division and lack of formation of new azurophil granules. During the middle and late stages of myeloid cell maturation, myeloperoxidase-negative granules (specific and gelatinase granules) formed by a mechanism similar to azurophil granule biogenesis [30].

The differences in the protein content among neutrophil granules are determined by differences in the timing of synthesis of different granule proteins, not by selective targeting of proteins to different granules [31,32]. This conclusion is based on the observation that granule subsets are formed at specific stages of cell development [30]. Granule luminal and membrane proteins that are synthesized at the same time are targeted into the same type of granule [31-34]. The well-known targeting of mannose 6-phosphate-containing glycoproteins to lysosomes via the mannose 6-phosphate receptors [35] does not participate in targeting proteins to neutrophil granules [36,37]. Overlap

Figure 1. A diagram of granule biogenesis during stages of neutrophil maturation. Granules are drawn 1.5 X scale, and only half the average number determined by actual counts are included for a given stage. Myeloperoxidase-positive (azurophil) granules are shown in black and myeloperoxidase-negative (specific and gelatinase) granules in gray. The myeloblast is a small, undifferentiated cell. At progranulocytic and myelocytic stages of maturation cells grow and the amount of endoplasmic reticulum and Golgi apparatus increases in size to allow for protein synthesis and granule biogenesis. Azurophil and specific granule formation occurs at progranulocytic and myelocytic stages, respectively. The metamyelocyte (not shown) and band cell are stages during which there is a progressive decrease in cell size, changes in the shape of the nucleus, a gradual diminution of most cytoplasmic organelles, and a shift to the synthesis of gelatinase granules. The mature neutrophil has a multilobed nucleus and a cytoplasm containing primarily granules. Number of azurophil granules per cell declines after progranulocytic stage due to lack of synthesis of new azurophil granules coupled with cell division. Adapted from Bainton and Farquhar [30].

Figure 1

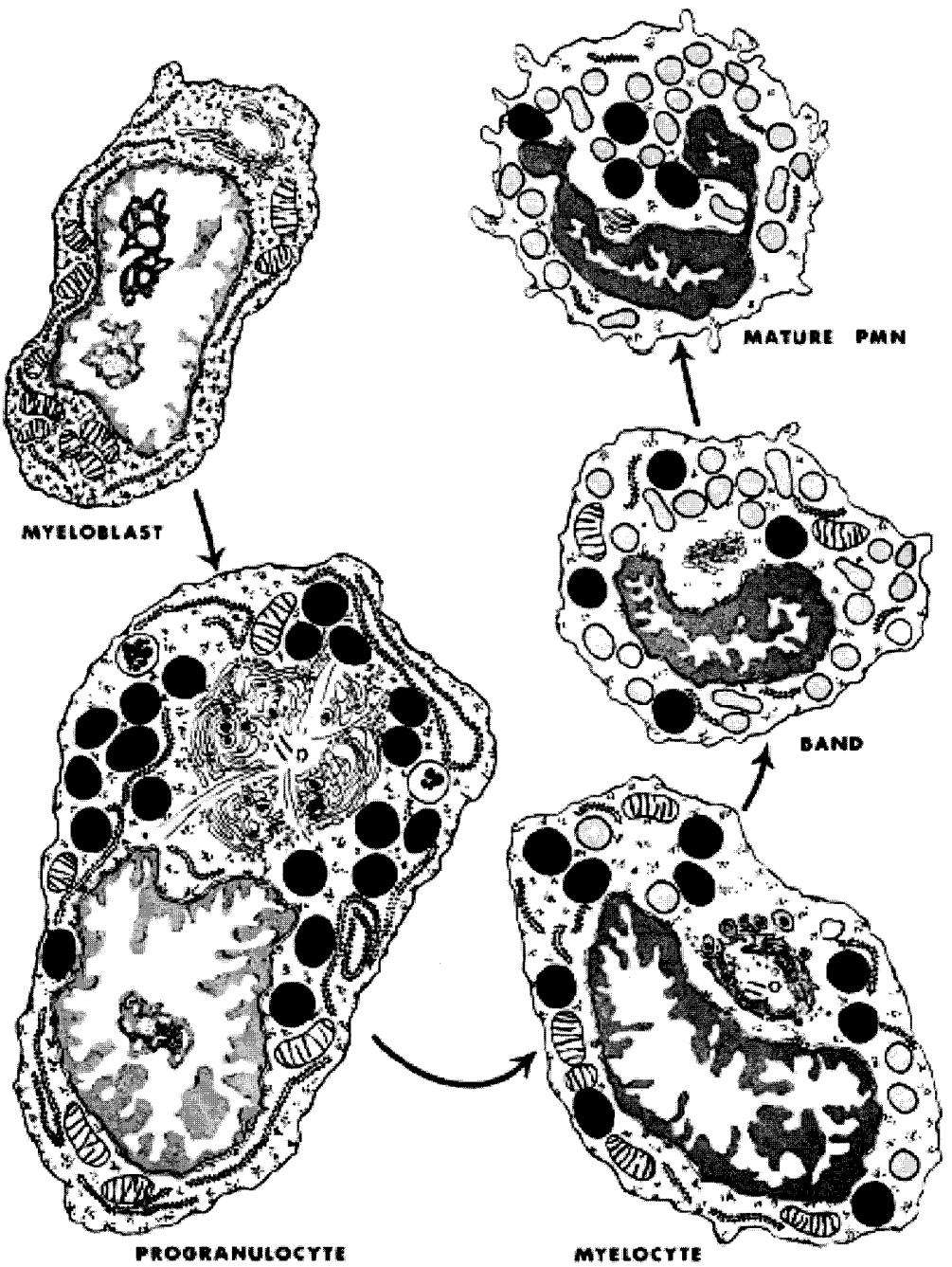

among the windows of synthesis of different granule proteins gives rise to a spectrum of granules that are dominated by the three distinct granule types, some of whose contents overlap [31,32].

Little is known regarding mechanisms that bring luminal and membrane proteins together during granule biogenesis. In many cells targeting of membrane proteins to granules is accomplished by specific sequences in the cytosolic carboxy-terminal tails of these proteins [38,39]. Such signals have been reported only for LAMP-1 and LAMP-2, which are neutrophil specific granule membrane proteins [40], and LAMP-3 (CD63), which is an azurophil granule protein [41]. Thus, the appearance of other membrane proteins in neutrophil granule membranes may be a passive process. Luminal proteins may be directed to granule precursors by matrix proteoglycans by facilitating co-aggregation of granule luminal and membrane proteins in the *trans*-Golgi network [42,43]. Indeed, this role in neutrophil granule formation was recently confirmed for the proteoglycan serglycin [44].

Granule heterogeneity provides the neutrophil with the ability to segregate proteins that cannot be stored in the same compartment, as well as to differentially exocytose proteins that are stored in different granules. For instance, azurophil granules carry terminally processed and active serine proteases, antibiotic peptides, and myeloperoxidase. Specific granules, on the other hand, store metalloproteases and antibiotic peptides as inactive proforms. Mixing of contents from azurophil and specific granules results in the cleavage and activation of the pro- forms of specific granule proteins by azurophil granule proteases [18]. Granule content mixing will also bring the peroxidase-negative granule component flavocytochrome b558 and azurophil granule

myeloperoxidase into close proximity. Myeloperoxidase transforms oxygen radicals made by the NADPH oxidase into even more toxic hypochlorous acid [45]. This mixing was confirmed by studies showing that the interaction of superoxide anion with myeloperoxidase converts luminol to aminophthalate to generate light in intracellular compartments in neutrophils [20]. Since the cytoplasm is loaded with oxygen radical scavengers, diffusion of superoxide anion to the azurophil granule is unlikely to occur, and the fusion of specific granules with azurophil granules is a more plausible explanation. Intracellular granule-to-granule fusion in neutrophils has also been documented by membrane capacitance techniques and electron microscopy [46]. Up to 20 percent of exocytotic events in neutrophils may occur by fusion of granules with each other prior to their fusion with the plasma membrane (compound exocytosis), which includes the fusion of one granule with another that has already fused with the plasma membrane (cumulative fusion) [46].

Neutrophil Granules Exocytosis

General Aspects of Neutrophil Exocytosis

Granule exocytosis can be divided into several steps that lead to the granule membrane fusion with the plasma membrane. [47,48]. The events that occur during exocytosis can vary from cell to cell, and some steps may not occur in a particular cell type. Usually, granule exocytosis involves Ca^{2+}-, ATP-, GTP-, and lipid-mediator-dependent events. These include physical movement of granule to the subplasmalemmal region of the cell, reorganization of the subplasmalemmal and/or granule-associated cytoskeleton to allow granules access to the plasma membrane, tethering and then

docking on the plasma membrane, triggered membrane fusion, and finally, the release of granule contents through a fusion pore (illustrated in Figure 2).

Many cells can regulate the extent of degranulation by maintaining a readily releasable or primed pool of granules that are docked to the plasma membrane, or are immobilized in close proximity to it [49-52]. Granules are not found docked or otherwise segregated in neutrophils [53-55]. Following stimulation, granules are localized to a region near lamellipodia, but they are still randomly distributed [56]. Thus, neutrophils do not utilize physical segregation of different granule subsets as the means of achieving graded exocytosis. Although the mechanism of graded exocytosis is not clear, quantitative or qualitative differences in the expression of membrane proteins that control membrane fusion is one possible explanation.

Membrane Fusion Machinery

Membrane fusion during exocytosis of intracellular vesicles and granules is carried out by similar protein complexes in all eukaryotic cells. This protein complex consists of a hexameric ATPase NSF (N-ethylmaleimide-sensitive fusion protein), α, β, or γ SNAPs (soluble NSF attachment proteins) and SNAREs (SNAP receptors) [57]. Mammalian SNAREs are divided into three families: VAMPs (vesicle associated membrane protein), syntaxins, and SNAP-23/25 (synaptosome-associated protein). Some evidence suggests that SNAREs can reside on vesicles (v-SNAREs) or on target membranes (t-SNAREs), possibly adding specificity to the vesicle-target membrane interaction [58].

Figure 2. Schematic representation of the steps leading to secretory granule exocytosis. This represents the events observed in neuroendocrine cells. In this case, subcortical actin cytoskeleton is disassembled. Concurrently, Ca^{2+}- and ATP-dependent granule-associated cytoskeletal reorganization participates in the granule recruitment to the plasma membrane. Tethering and docking of the granule can then occur. Subsequently, membrane fusion and the release of granule contents takes place. Adapted from Burgoyne and Morgan [47].

Figure 2

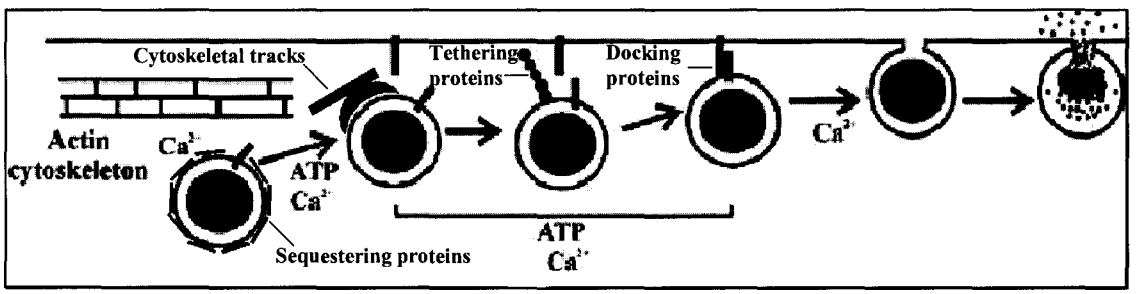
Cytoskeletal tracks
Tethering proteins
Docking proteins
Actin cytoskeleton
Ca^{2+}
ATP
Ca^{2+}
Sequestering proteins
ATP
Ca^{2+}
Ca^{2+}

SNARE proteins are characterized by SNARE helical motifs [59]. An alternative SNARE classification is based on the presence of a conserved glutamine (Q-SNARE) or arginine (R-SNARE) in the SNARE motif [60]. Q-SNAREs are almost always t-SNAREs and R-SNAREs are almost always v-SNAREs. Upon contact between SNAREs, SNARE motifs assemble into parallel four-helix bundles containing 3 Q-helices from two t-SNAREs and one R-helix from a v-SNARE [60,61]. These coiled-coil bundles are stabilized by the burial of hydrophobic helix surfaces in the interior of the structure [62,63]. The coiling of SNARE motifs within complexes brings the membrane of the granule/vesicle and the plasma membrane into close proximity [64]. Assembled SNARE complexes are resistant to SDS and have extremely high thermal stability [65,66]. Thus, the complex formation likely releases sufficient energy to overcome the hydration barrier and initiate bilayer fusion. After the SNARE complex is formed, αSNAP binds to the complex and recruits NSF from the cytoplasm. NSF then uses ATP hydrolysis to dissociate the SNAREs and prepare them for another round of fusion [67].

Access of v-SNAREs to t-SNAREs is regulated by proteins termed SNARE-masters, including Munc-18, Munc-13, and Ca^{2+}-binding synaptotagmin [68-70]. These proteins are regulated by post-translational modifications and/or by binding to second messengers. For example, phosphorylation of Munc-18 releases it from syntaxin-4, allowing syntaxin-4 to interact with VAMP-2 [70]. Munc-13 is recruited to the plasma membrane by binding to diacylglycerol (DAG), where it enhances exocytosis [71].

Only a limited number of membrane proteins have been identified from neutrophil granules [8,9]. They are listed in Table 1. Among the identified proteins are a few SNARE proteins. The v-SNARE, VAMP-2, has been found in the membranes of

Table 1
Known proteins of neutrophil granules

	Gelatinase Granules	Specific Granules	Azurophil Granules
Membrane	CD11b CD18 Cytochrome b_{558} Formyl peptide receptor LAMP-1, LAMP-2 Leukolysin SCAMP SNAP-23 VAMP-2 V-type H^+-ATPase	CD11b CD18 CD66b CD67 Cytochrome b_{558} Fibronectin receptor Formyl peptide receptor G-protein α subunit Laminin receptor Leukolysin Rap1, Rap2 SCAMP Stomatin VAMP-2 Vitronectin receptor	CD63 CD68 Presenilin 1 Stomatin V-type H^+-ATPase
Lumen	Acetyltransferase β2-Microglobulin Gelatinase Lysozyme	β2-Microglobulin Collagenase SGP-28 (CRISP-3) Sialidase Gelatinase hCAP-18 Histaminase Heparanase Lactoferrin Lysozyme NGAL Vitamin B12 binding-protein	Acid β-glycerophosphatase Acid mucopolysaccharide α-Mannosidase Azurocidin BPI β-Glucuronidase Cathepsins Defensins Elastase Lysozyme Myeloperoxidase N–Acetyl–β-glucosaminidase Proteinase-3 Sialidase Ubiquitin-protein

Proteins that have been identified as components of the three neutrophil granule subsets are listed (modified from references 8 and 9).

secretory vesicles and specific and gelatinase granules, but not azurophil granules [72]. The plasma membrane of neutrophils contains t-SNAREs, syntaxin-4 and syntaxin-6 [72,73]. Specific and gelatinase granules contain SNAP-23 [73], which participates in the SNARE complex formation with syntaxin-4 and VAMP-2 in non-neuronal tissues [74,75]. SNAP-23 and VAMP-2 act as v-SNAREs on specific and gelatinase granules, while syntaxin 4 and 6 act as t-SNAREs in the plasma membrane [76]. A v-SNARE for azurophil granules has not been defined. Additionally, syntaxin 7 has been found to be expressed upon neutrophil-like differentiation of HL-60 cells [77]. VAMP-1, VAMP-3, SNAP-25, synaptotagmin, and NSF were not detected in neutrophils, while no data are available regarding the presence of α, β, or γ SNAPs [72,78]. No reports of vesicle tethering proteins or SNARE masters being discovered on neutrophil granules exist.

Role of Cytoskeleton in Neutrophil Degranulation

Most cells, including neutrophils, possess actin filaments organized into a cortical F-actin network beneath the plasma membrane [47]. It has been suggested that this cortical actin network forms a barrier to exocytosis and, thereby, acts as a site of regulation of exocytosis [79,80]. The most compelling indication that cytoskeleton plays an important role in neutrophil exocytosis comes from the fact that pretreatment of neutrophils with an actin-depolymerizing drug, cytochalasin, prior to the cell stimulation, depolymerizes subcortical F-actin and greatly enhances exocytosis of all granule subsets [8]. F-actin depolymerization alone, however, does not lead to granule exocytosis.

Cortical actin disassembly is likely to be carried out by actin-depolymerizing proteins, many of which are activated by elevated calcium [81]. These proteins have been

shown to act in reorganization of subcortical actin during secretion in chromaffin cells, allowing granules to reach the plasma membrane in a calcium-dependent manner [82-84]. Such studies have not yet been carried out in neutrophils, and mechanisms that mediate subcortical actin reorganization during exocytosis in PMNs are unclear.

F-actin is found on granules, and structural changes that occur in this pool of F-actin are required for exocytosis [83,85-87]. Lipid bilayers do not undergo fusion spontaneously, since there is a large electrostatic force between two lipid bilayers that opposes their fusion [88]. Actin was shown to spatially restrict fusogenic proteins to fusion sites and/or apply force to aid membrane fusion during zymogen granule exocytosis in pancreas [80]. Generation of force may be occurring through interaction of F-actin with tropomyosin [81]. F-actin also interacts with myosin motor proteins found on granules, and this interaction is important for granule locomotion through actin network and immobilization of granules near the plasma membrane [89]. Actin cytoskeleton has been shown to interact with SNARE proteins, for example, α-fodrin, a major component of subplasmalemmal cytoskeleton interacts with syntaxins [90], while the actin motor protein myosin V binds VAMPs in a calcium-dependent manner [91].

Apart from actin, cytoskeleton also consists of tubulin (microtubules) and vimentin (intermediate filaments). There is evidence that microtubules and intermediate filaments participate in neutrophil exocytosis. A direct interaction of specific and azurophil granules with microtubules was reported by Rothwell *et al.*, who observed that binding of granules to microtubules increased upon fMLP stimulation [92]. Further studies identified a microtubular motor protein kinesin on both types of granules [93]. Microtubules likely act as tracks for long-range movement of granules. Using colchicine,

a microtubule-depolymerizing drug, it was shown that microtubules directed azurophil granules, and to a lesser extent of specific granules, to phagosomes [94].

Microtubule dynamics in neutrophils are controlled in part by second messengers. It was shown that an increase in intracellular cGMP levels increased the formation of microtubules in neutrophils and enhanced degranulation [95,96], while agents that increase cAMP levels have opposite effects [96,97]. cGMP may also signal to vimentin, which has been implicated in neutrophil degranulation. In fMLP-treated neutrophils vimentin filaments reorganized with a concomitant increase in cGMP levels and degranulation, while inhibition of guanylate cyclase inhibited granule content secretion and vimentin filament reorganization [98].

Like actin, vimentin and tubulin interact with membrane fusion machinery. Vimentin filaments bound SNAP-23 and maintained a reservoir of this SNARE protein in fibroblasts [99]. SNAP-23 dissociated from vimentin filaments upon cell stimulation and translocated to the plasma membrane. Microtubules were shown to interact with Munc-18 in mast cells and participate in its redistribution [100]. In both studies the redistribution of these proteins was important for degranulation. Such studies have not been carried out in neutrophils. It is clear, however, that microfilaments, microtubules, and intermediate filaments are involved in neutrophil granule exocytosis, although their exact functions remain to be elucidated.

Signal Transduction in Neutrophil Exocytosis

Calcium, G proteins, lipid mediators, and protein kinases all mediate signaling events that lead to exocytosis in neutrophils, although the mechanisms of their action are

still largely unclear. The following section provides a brief overview of major pathways and signaling molecules that are involved in neutrophil degranulation.

Role of Calcium in Neutrophil Exocytosis

The best-characterized signal-transduction event leading to a rise in intracellular free Ca^{2+} concentrations ($[Ca^{2+}]_i$) in neutrophils is that induced by agonists that bind to G-protein-coupled receptors. Phospholipase C (PLC) is activated, which cleaves phosphatidylinositol 3,4 bisphosphate (PIP_2) into diacylglycerol (DAG), a PKC agonist, and inositol 1,4,5-trisphosphate (IP_3) [101]. IP_3 induces $[Ca^{2+}]_i$ elevation by releasing Ca^{2+} from intracellular stores into the cytoplasm. This Ca^{2+} release is followed by an influx of extracellular Ca^{2+} via plasma membrane calcium channels (reviewed in ref. [102-104].

It has been documented that neutrophil exposure to various secretagogues, such as fMLP [105], IL-8 [106], and C5a [107] leads to a concomitant increase in $[Ca^{2+}]_i$. TNFα and GM-CSF, both weak secretagogues, did not increase $[Ca^{2+}]_i$ in adherent neutrophils [108]. Chelation of intracellular calcium to levels below the resting level, however, inhibited TNFα- and GM-CSF-induced degranulation in adherent cells. Thus, Ca^{2+}-dependent processes may participate in neutrophil degranulation even when the secretagogue does not induce a measurable increase in $[Ca^{2+}]_i$.

Lew *et al.* showed that buffering of intracellular calcium prevented fMLP-induced degranulation [109]. There were other factors, however, that were important for full exocytotic response upon fMLP-stimulation. Thus, a given rise in $[Ca^{2+}]_i$ elicited by the fMLP was associated with a much greater degree of exocytosis than was the same or

larger rise in $[Ca^{2+}]_i$ produced by calcium ionophore ionomycin. Therefore, fMLP generates an important excitatory signal in addition to a rise in $[Ca^{2+}]_i$.

The sensitivity of granule release to Ca^{2+} follows a hierarchical pattern that reflects the overall hierarchy of granule exocytosis in neutrophils [11,110]. Measurements of dependence of exocytosis of each granule type on $[Ca^{2+}]_i$, showed that the cytosolic Ca^{2+} levels that induce half-maximal exocytosis (EC_{50}) were: for secretory vesicles – 140 nM, for gelatinase granules – 250 nM, for specific granules – 550 nM, and for azurophilic granules – 680 nM [11]. FMLP–induced gelatinase and specific granule exocytosis from MAPTAM-loaded (a calcium chelator) cells placed in a calcium-free buffer were only 42% and 32%, respectively, of the exocytosis in normal neutrophils. Thus, total depletion of intracellular and extracellular Ca^{2+} did not abolish exocytosis in neutrophils.

The differences in granule sensitivity to calcium may be due to the differences in composition of Ca^{2+} binding proteins on granule subsets. The effect of calcium on exocytosis and membrane fusion is likely to be mediated by calcium-binding proteins found in neutrophil cytosol and on granules. The calcium-dependent SNARE modulator, synaptotagmin, is not found in neutrophils. Three calcium binding proteins, annexin I, annexin III, and grancalcin, have been reported to associate with neutrophil granules. Grancalcin is a 28 kDa protein abundant in neutrophils, and its quantity on the granule surface increases upon neutrophil activation [111,112]. Using grancalcin-deficient mice, Roes *et al.* showed that this protein is not essential for leukocyte effector functions required to control microbial infections [113].

Annexins are calcium and phospholipid-binding proteins that are known to aggregate liposomes in a calcium-dependent manner [114,115]. Annexin III was found in the cytosol and also associated with the specific granules in neutrophils [116], and promoted Ca^{2+}-dependent aggregation of isolated specific granules [117]. Additionally, upon introduction of recombinant annexin III into permeabilized cells, degranulation was significantly enhanced upon exposure to calcium, while the addition of annexin I resulted only in a modest increase in secretion [118]. In this study, the authors found that induction of degranulation by calcium was completely inhibited when intracellular ATP was depleted prior to permeabilization. Moreover, exocytosis was rescued upon addition of Mg-ATP to ATP-depleted, permeabilized cells. Thus, in addition to calcium, cells required ATP for exocytosis, and sufficient amounts of ATP remained in cells after permeabilization, but not after ATP-depletion.

Theander *et al.* investigated ATP dependence of calcium-induced neutrophil granule exocytosis in greater detail in cytochalasin B-treated cells [119]. In this study, intracellular ATP concentrations were depleted to different values, and the cells were stimulated by intracellular delivery of Ca^{2+} using cell permeabilization or fMLP stimulation. Depletion of ATP reduced calcium-stimulated exocytosis. Additionally, fMLP-induced granule exocytosis required higher concentrations of ATP than exocytosis induced by ionomycin. This suggests that fMLP-induced exocytosis has ATP-dependent steps even in the presence of cytochalasin B, which are bypassed by ionomycin treatment. Overall, the importance of calcium in neutrophil exocytosis is well documented, however, the requirement of other factors in PMN degranulation is clear.

Role of GTP-binding Proteins in Neutrophil Granule Exocytosis

Chemokines and chemotactic peptides that induce neutrophil degranulation bind to G protein-coupled receptors whose activation induces the dissociation of Gα and $G_{\beta\gamma}$ subunits of heterotrimeric G proteins [120]. As mentioned above, heterotrimeric G proteins are involved in exocytosis through modulation of calcium fluxes. In many cells, including neutrophils, G proteins activate additional pathways that are important for exocytosis. Stimulation of permeabilized neutrophils with the non-hydrolysable analog of GTP, GTP-γ-S, induced calcium flux and exocytosis in permeabilized neutrophils, however, significant exocytosis occurred even when an increase in $[Ca^{2+}]_i$ was prevented by chelation [121-124].

GTPγS activates both heterotrimeric and monomeric G proteins, preventing delineation of which G proteins participate in exocytosis. Both monomeric and heterotrimeric G proteins have been implicated in neutrophil exocytosis. The involvement of heterotrimeric G-proteins was confirmed by using pertussis toxin, which ADP-ribosylates $G\alpha_i$ and $G\alpha_o$ subunits and inhibits their activation. This toxin inhibited neutrophil granule exocytosis induced by fMLP, C5a, or leukotriene B_4 [125]. It did not affect granule enzyme release initiated by Ca^{2+} ionophore or PMA. This is reflective of the locus of action of heterotrimeric G proteins, which transmit activation signal from surface receptors to downstream signals leading to a rise in intracellular Ca^{2+}. This conclusion is demonstrated by the finding that the rise in intracellular Ca^{2+} induced by fMLP or LTB4, is greatly reduced in pertussis toxin-treated neutrophils [126].

$G\alpha_i$ inhibits adenylyl cyclase and $G\alpha_o$ activates PLCβ [127]. Inhibition of $G\alpha_i$ by pertussis toxin could lead to a rise in the levels of cAMP, which would inhibit exocytosis

by negatively affecting microtubule assembly [96,97]. Likewise, inhibition of $G\alpha_o$ would prevent activation of PLCβ and generation of IP_3, which releases Ca^{2+} from intracellular stores, and DAG, which activates PKC. Inhibition of these processes may negatively influence exocytosis. $G_{\beta\gamma}$ subunits of heterotrimeric G-proteins are involved in neutrophil exocytosis by their ability to activate PLCβ as well as phosphatidylinositol-3-kinase (PI3K), which has also been implicated in degranulation [127,128]. Thus, G proteins regulate multiple pathways involved in exocytosis.

Monomeric or small G-proteins are also involved in exocytosis. Ras-like GTPases Rap1 and Rap2 are present on specific and gelatinase granules [129,130], while a G protein of the Rho family, Rac2, associates with the azurophil granules [130]. Rac2 regulates cytoskeletal actin dynamics in neutrophils and together with another small G protein, Cdc42, stimulates actin filament assembly [131]. Viral transfection of neutrophils with dominant-negative Rac2 or Cdc42 revealed that Rac2 plays a major role in the control of directed granule mobilization toward *Candida albicans* phagosomes [132]. In addition, using neutrophils from $rac2^{-/-}$ mice, Rac2 was found to be indispensable for azurophil granule exocytosis in cytochalasin-treated cells, while specific and gelatinase granule release was normal [133].

Role of Lipid Mediators in Neutrophil Degranulation

Lipid mediators released by phospholipases participate in neutrophil degranulation. Phospholipase A_2 (PLA_2) inhibition significantly reduces exocytosis, and arachidonic acid, a PLA_2 product, augments fusion between liposomes and aggregated

specific granules [134,135]. Similar data exist regarding phospholipase D, which is activated by various secretagogues, and its product, phosphatidic acid [136-140]. Additionally, phosphatidic acid is a precursor of another lipid mediator, DAG. DAG is also generated by PLC [141], however, DAG has only a marginal effect on neutrophil exocytosis [139]. The artificial analogue of DAG, PMA, is a strong stimulant of neutrophil degranulation [73]. PMA and DAG may influence exocytosis by activating certain isoforms of PKC, which has been implicated in degranulation of mast cells [142]. PKC does not play a major role in neutrophil degranulation [143,144]. Both DAG and PMA, however, also directly bind and activate Munc13, which is important in membrane fusion [71,145].

Phosphatidic acid itself may augment neutrophil degranulation by inducing non-receptor tyrosine kinase activity in neutrophils, especially that of Fgr tyrosine kinase [146]. Activation of Fgr by direct binding of phosphatidic acid leads to neutrophil calcium mobilization and F-actin polymerization [146,147]. Tyrosine kinases may also act through phosphorylation of neutrophil PLD [148], as genistein-sensitive PLD tyrosine phosphorylation controls its activity and augments PMN degranulation [149].

Role of Kinases in Neutrophil Degranulation

As alluded to above, tyrosine kinases have been implicated in neutrophil exocytosis. Tyrosine kinases are activated by various secretagogues [150,151], and tyrosine kinase inhibitors reduce degranulation [151,152]. In addition, tyrosine kinases

have been localized to neutrophil granules. For example, Fgr associates with specific granules [153], while Hck is on azurophil granules [154]. Using gene knockout mice, Mocsai *et al.* showed that $hck^{-/-}fgr^{-/-}$ mouse neutrophils were deficient in adhesion-dependent and fMLP-induced degranulation [155]. Syk, Yes, and Lyn formed a complex with, and activated another kinase that plays an important role in neutrophil degranulation, phosphatidylinositol-3-kinase (PI3K) [156, 157].

PI3K is also activated by βγ subunit of heterotrimeric G proteins [128,158]. Inhibition of PI3K reduced neutrophil degranulation [159-162]. PI3K activates various signaling proteins that are relevant to exocytosis, for example PLC and PLD [163], as well as guanylate cyclase [164]. In addition, PI3K activates a protein kinase that seems to play a central role in neutrophil exocytosis, the p38 mitogen-activated protein kinase (MAPK), which is described next.

The p38 MAPK Pathway and Its Role in Neutrophil Exocytosis

P38 MAPK, of which there are four isoforms (α,β,γ,δ), is one of four members of a family of proline-directed serine/threonine kinases that also includes extracellular signal-regulated kinases (ERK1/2), c-jun N-terminal kinases (JNKs), and atypical MAPKs such as ERK5 [165-167]. MAPKs exist as three-kinase modules composed of a MAPK kinase kinase (MAP3K), a MAPK kinase (MAP2K), and a MAPK. MAPKs are activated by dual phosphorylation on the Thr-X-Tyr motif by a MAP2K. MAP2Ks are controlled by phosphorylation on a serine or threonine by a MAP3K. MAP3Ks are activated by other kinases and/or by small GTP-binding proteins of the Ras and Rho family. The components of three-kinase modules are specific to each MAPK. MKK3 and

MKK6 phosphorylate and activate p38 MAPK, while the upstream MAP3Ks for the p38 MAPK module include transforming growth factor beta-activated kinase 1 (TAK1), apoptosis signal-regulating kinase 1(ASK1), mixed lineage kinase (MLK), tumor progression locus 2 (Tpl-2), p21-associated kinase (PAK), and thousand and one amino acid protein kinase (TAO) kinases. The actual composition of this module is cell type-specific.

Similarly to other MAPKs, p38 MAPK is activated by a wide array of mitogenic and stress-related stimuli. Upon activation it phosphorylates numerous substrates, including various transcription factors and protein kinases, one of which is MAPK-activated protein kinase 2 (MK2) [165,166,168]. The expression of p38 isoforms is also cell type-dependent. Neutrophils express only p38α and p38δ isoforms [169], of which only p38α is inhibited by pyridinyl-imidazoles (e.g. SB203580) [170]. These compounds inhibit p38 kinase activity by competing for the ATP-binding site. Their selectivity is determined by differences in nonconserved regions within or near the ATP binding pocket [171]. As neutrophils are short lived, terminally differentiated cells, genetic manipulation of the p38 MAPK pathway cannot be accomplished. Therefore, SB203580 and related inhibitors have been invaluable in elucidating p38 functions in these cells.

A large number of secretagogues activate p38 MAPK in neutrophils. Chemoattractants stimulate p38 activity in a G-protein, PI-3K-and calcium-dependent manner [172-176], while stimulation by TNFα is PI-3K independent [173] and Src family tyrosine kinase-dependent [177]. Cross-linking of Fc receptors also leads to degranulation [178], and homotypic or heterotypic crosslinking of FcγRIIa or FcγRIIIb activates p38 in a Src family kinase- and PI3K-dependent manner [179]. P38α is also

activated by LPS [169,180] and this activation is cGMP-dependent kinase- (PKG-) dependent [181,182]. PLCγ is involved in the activation of p38 MAPK in PMNs challenged with *Mycobacterium tuberculosis* [183].

The requirement of p38 MAPK activity in neutrophil degranulation has been well documented. Inhibition of p38 MAPK by pyridinyl-imidazole compounds in neutrophils substantially reduced surface upregulation of granule membrane markers induced by *Staphylococcus aureus* [184], TNFα [185,186], IL-8 or L-selectin cross-linking [15], IL-18 [187], fMLP [188], and LTB_4 [189]. Although activation of p38 is essential for neutrophil granule exocytosis, selective activation of p38 alone by anisomysin does not result in PMN degranulation [190]. Thus, other signals are required. Mocsai, *et al.* showed that fMLP-induced p38 activation and degranulation required Hck, Fgr, and Lyn activities [188], while Yes tyrosine kinase was required for LTB_4-induced exocytosis [189]. Unlike p38 MAPK, ERK inhibition does not affects degranulation [152,186,191], while JNK is not activated by proinflammatory stimuli in neutrophils in suspension [172,183,192].

The mechanism by which p38 MAPK controls neutrophil degranulation is not known, as the substrates of p38 MAPK that mediate this process are unknown. P38 MAPK substrates include kinases – MAPK-activating protein kinase-2 and 3 (MK2 and MK3), p38-regulated kinase (PRAK), MAPK-interacting protein kinase 1 (MNK1), mitogen- and stress-activated protein kinases-1 and -2 (MSK1 and MSK2), and casein kinase 2 (CK2); transcription factors – MEF 2C and 2A, Elk-1, CHOP/GADD153, CEBPβ, p53, STAT 1, ATF-1 and -2, CREB, Usf-1, NFATp, CDX3, PGC-1, and SAP-1; and other substrates – cytosolic PLA_2, stathmin, Na/H exchanger, Cdc25b, and $p47^{phox}$

[175,193] Of the known p38 substrates, only MK2 and $p47^{phox}$ phosphorylation by p38 have been demonstrated in neutrophils [175,194,195]. $P47^{phox}$ participates in NADPH oxidase activation and MK2 phosphorylates the small heat shock protein Hsp27 that functions in actin remodeling [175,196]. Recently, inhibition of MK2 was shown to reduce TNFα-induced neutrophil degranulation, but had no effect on fMLP-stimulated exocytosis [195]. MK2 phosphorylates LSP1, 14-3-3ζ and p16-Arc in neutrophils, which are involved in cytoskeletal reorganization [197-199], and 5-lipoxygenase, which functions in the pathway of conversion of arachidonic acid to leukotrienes [200]. The role of phosphorylation of these proteins in neutrophil exocytosis has not been examined. MK2 phosphorylates vimentin [201] and myosin regulatory light chain [202], but these phosphorylation events have not been examined in neutrophils and their role in exocytosis is unclear. A recent proteomic study identified 25 proteins as downstream targets of the ERK pathway, of which only 5 were previously characterized ERK effectors [203]. This suggests that a number of substrates of the p38 MAPK pathway remain to be identified in order to better understand the role of p38 MAPK in neutrophil exocytosis.

Application of Proteomics to Protein and Phosphoprotein Identification

Proteomic Technology for Protein Identification

The term "proteomics" refers to the large-scale analysis of complex protein mixtures. The technology used in proteomic analysis consists of sample deconvolution and identification of its protein content. Gel electrophoresis and liquid chromatography

are the most common methods for the protein deconvolution, while mass spectrometry (MS) is used for the identification of proteins.

Two-dimensional gel electrophoresis (2DE) is a powerful method for protein separation [204]. It separates proteins first by isoelectric focusing (IEF) in a pH gradient and then by mass using sodium dodecyl sulfate-polyacrylamide gel electrophoresis (SDS-PAGE). Introduction of immobilized pH gradient (IPG) acrylamide strips of various pH range and the precast gradient acrylamide gels for SDS-PAGE have made 2DE a relatively simple and widely available method [205]. 2DE has inherent limitations, such as inability to effectively resolve proteins with isoelectric points below 3 and above 9, and with masses above 100 kDa and below 10 kDa [205,206]. Hydrophobic and membrane proteins are also significantly underrepresented among proteins identified by - 2DE [207-209]. Introduction of high sensitivity fluorescent protein dyes such as SYPRO Ruby [210], novel zwitterionic detergents such as ASB-14 [211,212], and non-ionizable thiol-reducing agents as tributyl phosphine [213] have generally resulted in improved visualization and identification only of the type of proteins that were amenable to 2DE analysis, but has not enlarged the spectrum of proteins detected. Identification of proteins following their separation by 2DE requires excision of the protein spot from a gel, in-gel digestion using a protease or a chemical agent, and preparation of the resultant peptides for MS analysis.

Liquid chromatographic separation of proteolytic peptides and their subsequent analysis by MS avoids problems associated with 2DE. Although proteins in simple mixtures can be successfully identified by combining single-dimensional liquid chromatography and mass spectrometry, the presence of a large number of peptides from

complex protein mixtures overwhelms the resolution capability of one-dimensional chromatography [214]. To address this problem, a recently developed method called the direct analysis of large protein complexes (DALPC) couples multidimensional liquid chromatography with tandem mass spectrometry (MS/MS) [215,216]. This method employs direct proteolytic digestion of complex protein mixtures and fractionation of resultant peptides by two-dimensional chromatography prior to their analysis by MS/MS. The first chromatographic step separates peptides by charge using an acidified sample and a strong cation-exchange (SCX) microcapillary column. Peptides in individual SCX fractions are then further fractionated by hydrophobicity over a reversed-phase high-pressure liquid chromatography (RP-HPLC) column and eluted with an acetonitrile gradient. Peptides in the eluate are directly analyzed by electrospray ionization (ESI)-MS/MS and the protein content of the original sample is then deduced from the thousands of collected MS/MS spectra by genome-assisted computer analysis [214]. Using this approach, large protein complexes such as ribosomes and transcriptional machinery have been successfully analyzed [215,216].

Mass spectrometry allows identification of proteins at femtomol quantities [217]. Mass spectrometers deliver peptides to a mass detector by ionizing them and accelerating the ionized peptides using magnetic fields [218]. Two common methods of ionization are matrix-assisted laser desorption/ionization (MALDI), and electrospray ionization (ESI). MALDI ionizes peptides by laser light-induced energy transfer from the light-absorbing matrix to the matrix-embedded peptides. ESI causes ionization by electrically generating a fine mist of peptide-containing liquid droplets that reach a size limit at which charge repulsion exceeds the surface tension of the droplet, resulting in desorption of peptides

from droplets as bare ions. The mass to charge ratios (m/z) of the resultant ions are then analyzed by time of flight (TOF) analysis, quadrupole (Q) MS, or Fourier transform ion cyclotron resonance (FT-ICR) MS. When used in tandem (MS/MS), TOF and Q MS instruments can generate peptide sequence data (FT-ICR is a tandem spectrometer in itself). The first MS analysis obtains m/z values for peptides generated by protein digestion, which is followed by gas-generated collision-induced dissociation (CID) or fragmenting of selected peptides into smaller ions, which can also be analyzed for m/z values. Comparison of the acquired spectra with the predicted spectra from genome databases using mathematical algorithms, allows for matching of the obtained spectrum with the spectra of proteins in the database, thus identifying the proteins present in the sample.

Proteomic Methods for Identification of Phosphoproteins

Detection and identification of phosphoproteins is a challenging task due to the low abundance of these proteins, low stoichiometry of phosphorylation, and the complexity of protein mixtures. Advances in proteomics technology resulted in availability of several approaches for phosphoprotein identification. These include gel electrophoresis-based, chromatography-based, and mass spectrometry-based approaches [219].

The oldest method of phosphoprotein detection is the radioactive labeling of proteins using [^{32}P]ATP *in vitro* or [^{32}P]orthophosphate *in vivo* prior to separation of proteins by 2DE. This is followed by total protein staining, comparison of autoradiographs with stained gels and identification of phosphoproteins using MS. *In vivo*

labeling of proteins with [^{32}P]orthophosphate does not allow detection of phosphoproteins with low phosphate turnover, and identification of substrates of a specific kinase for the large number of phosphoproteins is difficult. *In vitro* labeling of proteins with [^{32}P]ATP has been used to successfully identify substrates of a specific kinase [198,199]. This approach uses solubilization of cellular proteins in 9M urea buffer to effectively extract proteins and inactivate endogenous kinases by denaturation. This is followed by reduction of the urea concentration to 1M to allow activity of the endogenously added recombinant kinase, which phosphorylates proteins in the presence of [^{32}P]ATP. Proteins are then subjected to 2DE, phosphoproteins visualized by autoradiography, and identified by MS.

Western blotting can also be used for phosphoprotein identification. Western blotting of gels using antibodies against phosphoserine, phosphothreonine, or phosphotyrosine can be carried out and the obtained pattern of spots can be compared to a pattern of protein spots on a gel that was run in parallel to the transferred gel and stained for total protein [220]. The spots visualized by western blotting are matched against the corresponding spots on the gel, and the protein in this spot is then identified using MS. This method is limited by the quality and specificity of anti-phosphoamino acid antibodies.

Another method that utilizes 2DE for phosphoprotein identification takes advantage of detection of a pI shift upon protein phosphorylation [203]. In this approach, the protein pI shifts are compared between gels loaded with protein extracts from untreated cells, cells treated with kinase activators in the presence or absence of specific kinase inhibitors, and cells with constitutively active kinase. Proteins in question are then

identified using MS. Although quite successful at identifying novel kinase substrates, the limitation of this approach is that some shifts in the pI are too small to observe, or may be produced by post-translational modifications other than phosphorylation.

A novel and promising approach to phosphoprotein detection and identification is the use a recently described phosphoprotein-specific fluorescent dye ProQ Diamond (Molecular Probes) [221,222]. It discriminates between phosphorylated and unphosphorylated proteins with a high specificity, and it is compatible with protein dyes such as SYPRO Ruby. It can be used to stain phosphoproteins in acrylamide gels and its compatibility with SYPRO Ruby allows the simultaneous identification of proteins and phosphoproteins for more effective localization of phosphoprotein spots for excision and identification by MALDI-MS. Although the ProQ Diamond dye is novel and its usefulness is not yet completely characterized, it appeared to permit identification of phosphoproteins in nanogram quantities per spot [222].

Phosphoproteome analysis in a complex sample is difficult. Immunoprecipitation of phosphorylated proteins is possible only with anti-phosphotyrosine antibodies, as they possess sufficient affinity to immunoprecipitate proteins that contain phosphorylated tyrosine residues [223]. The antibodies that recognize phosphoserine and phosphothreonine are typically sensitive to surrounding amino acids and have lower affinity, thus not permitting enrichment of phosphorylated proteins by immunoprecipitation [220]. To address this problem of sample deconvolution, immobilized metal-affinity chromatography (IMAC) has been adopted for the enrichment of phosphopeptides and phosphoproteins. In this technique, trivalent metals (most commonly Ga^{3+} or Fe^{3+}) are immobilized on a solid-phase support conjugated to metal-

chelating moieties (iminodiacetc acid - IDA, or nitrilotriacetic acid - NTA), and the peptide or protein mixture is applied [224,225]. Acidic phosphate residues bind noncovalently to trivalent metals and can be eluted by phosphoric acid. Modification of acidic amino acids by methylesterification is advantageous in elimination of non-specific binding of peptides [226], but results in loss of some phosphorylated peptides [227]. When IMAC was coupled with HPLC-ESI-MS/MS, hundreds of phosphopeptides were detected (sensitivity was 5 fmol per phosphorylated peptide) [225,226]. Peptide IMAC is characterized by bias toward enrichment of multipely phosphorylated peptides, which bind trivalent cations better than singly phosphorylated ones. This bias is reduced and more phosphopeptides are detected when protein IMAC is combined with the peptide IMAC [228].

Advances in mass spectrometry have also improved phosphoproteome identification and allowed identification of phosphorylation sites in proteins [219,229]. Two methods that have contributed significantly to the MS analysis of phosphoproteins are precursor-ion scanning and neutral-loss scanning of peptides, which rely on tandem mass spectrometry. In precursor ion scanning for peptides with phosphoserines and/or phosphothreonines, the mass spectrometer is usually operated in a negative mode (analyzes negatively charged peptides, which will include the phosphopeptides). When sufficiently stringent CID conditions are chosen, the loss of a molecule of phosphoric acid will generate a negative PO_3 ion (79 Da). Following a survey analysis of the spectrum, the instrument can be operated in the positive-ion mode to select those peptides and obtain MS/MS spectra from them. That approach, however, does not allow identification and sequencing in the same run. Operation of the instrument in the positive

ion mode can be used for the analysis of peptides with phosphotyrosine, which is much more stable than phosphoserine and phosphothreonine, but will usually generate a positive immonium ion at m/z 216. Precursor ion detection and MS/MS are performed in the positive-ion mode that allows the identification and sequencing in the same analysis. The disadvantage is that the identification of phosphotyrosine in that approach might not be specific, because some amino acid doublets or triplets generate ions with m/z values very close to 216 [230].

Another approach to the identification and analysis of phosphopeptides is the use of neutral-loss scanning. In the CID of phosphoserine- and phosphothreonine-containing peptides, phosphoric acid can be lost through β-elimination. That neutral loss of phosphoric acid (98 Da) is used to identify phosphorylated peptides from a complex peptide mixture. After peptides with a loss of 98 Da in mass are identified, the MS/MS spectra can be acquired from to obtain amino acid sequence information. This approach can also be used to identify phosphotyrosine by a search for the immonium ion at m/z 216 after fragmentation. Thus, acquisition of peptide spectra with and without fragmentation can be accomplished simultaneously.

Project Goals and Specific Aims

The signaling pathways that govern the mobilization of neutrophil granules are largely unknown. It has been shown in our laboratory that p38 mitogen-activated protein kinase (MAPK) and its downstream target, MAPK-activated protein kinase-2 (MK2), play a role in neutrophil exocytosis. The mechanism by which the p38 MAPK cascade mediates this process is not clear. Understanding the role of p38 MAPK and MK2 in neutrophil exocytosis will require identification of downstream targets that mediate

exocytosis. **We examined the hypothesis that p38 MAPK and/or MK2 regulate neutrophil degranulation by phosphorylating granule membrane proteins that modulate exocytosis.** Proteomics were used to identify the substrates of the p38 MAPK pathway that are associated with neutrophil granules. These data may identify targets for pharmacological regulation of neutrophil function during autoimmune and inflammatory diseases. The specific aims of the project were:

1 – Identify potential p38 MAPK and MK2 substrates on granules using proteomics.

Experimental Approaches. We used 2DE and liquid chromatography and mass spectrometry-based approaches to investigate the proteome of each granule subset and identify known MK2 and/or p38 MAPK substrates on granules. To discover novel substrates on granules we utilized the *in vitro* labeling of urea-solubilized granule proteins with [^{32}P]ATP using recombinant MK2 and p38 MAPK followed by separation and identification of labeled proteins using 2DE and mass spectrometry.

2 – Confirm the ability of p38 MAPK and/or MK2 to interact with and phosphorylate these substrates in vitro and in situ.

Experimental Approaches. *In vitro* kinase reactions were carried out under non-denaturing conditions using [^{32}P]ATP, the recombinant kinase, and the purified substrate, to confirm that the identified protein was indeed a substrate for the kinase *in vitro*. Immobilized metal affinity chromatography (IMAC) and mass spectrometry were used to identify the putative phosphorylation site on the protein. Identity of the phosphorylated residue was confirmed by expressing a

mutant recombinant protein with the putative phosphorylated residue changed to an alanine, and subjecting wild-type and mutant recombinant proteins to an *in vitro* kinase reaction using recombinant kinase and [^{32}P]ATP. *In situ* phosphorylation of the candidate substrate was screened by labeling neutrophils with [^{32}P]orthophosphate and observing the phosphorylation of the candidate substrate in stimulated cells using 2DE and autoradiography in the presence or absence of the specific inhibitor of the kinase.

3 – Determine the role of phosphorylation of selected p38 and MK2 substrates in granule exocytosis.

Experimental Approaches. The biological significance of substrate phosphorylation was assessed by investigating the phosphorylation-dependence of substrate translocation to granules and cytoskeleton in stimulated neutrophils in the presence or absence of the kinase inhibitor. Confocal microscopy of neutrophils and western blot analysis of isolated granule subsets was utilized for this purpose. Furthermore, the dependence of substrate binding to actin cytoskeleton on the phosphorylation of the substrate by the kinase was investigated by an *in vitro* binding assay using F-actin and purified phosphorylated or unphosphorylated substrate.

CHAPTER II

PROTEOMIC ANALYSIS OF HUMAN NEUTROPHIL GRANULES

Foreword

The goal of the project was to define targets of the p38 MAPK pathways that regulate neutrophil exocytosis. Previous studies showed that inhibition of p38 MAPK significantly attenuates exocytosis stimulated by IL-8, TNFα, fMLP, and LTB4 [15,185,188,189]. The downstream kinase of p38 MAPK, MAPKAPK2, was shown to mediate p38 MAPK-dependent exocytosis of specific granules [195]. The molecular mechanism by which p38 MAPK and/or MAPKAPK2 regulate exocytosis is unknown. To accomplish the goal of the project, two separate proteomic approaches were applied. First, to identify potential mediators of p38 MAPK-dependent exocytosis, the proteome of neutrophil granule subsets was defined. This proteome was used to identify known targets of p38 MAPK and MAPKAPK2 on granules. Second, the p38 MAPK and MK2 phosphoproteome on neutrophil granules was determined by proteomic technology (described in Chapter III). The following chapter presents the proteome, defined by two-dimensional gel electrophoresis (2DE) followed by matrix-assisted laser desorption and ionization mass spectrometry (MALDI-MS) and by two-dimensional HPLC and electrospray ionization tandem mass spectrometry (2D-HPLC ESI-MS/MS), of

neutrophil granule subsets enriched by subcellular fractionation using Percoll density-gradient centrifugation.

Introduction

Stimulated exocytosis of membrane-bound compartments plays a critical role in converting inactive, circulating neutrophils to fully activated cells capable of directed migration, phagocytosis, and killing of microbes [9]. Four subsets of membrane-bound compartments exist in neutrophils: secretory vesicles, gelatinase (tertiary) granules, specific (secondary) granules, and azurophil (primary) granules [8,9]. Secretory vesicles are generated by endocytosis, resulting in membranes rich in receptors, signaling proteins, and adhesion molecules, while their lumen contains plasma [8]. Azurophil, specific, and gelatinase granules contain various enzymes and host defense proteins in their luminal spaces, while their membranes contain receptors, signaling proteins, adhesion molecules, and enzymes [8,24]. The targeting of proteins to individual granule compartments is determined by the timing of protein synthesis during myeloid progenitor cell differentiation, not by granule-specific sorting [31]. Thus, granule proteins that are synthesized at a given stage of cellular differentiation will be localized to the same type of granule [231,232]. The overlap between the timing of synthesis of different granular proteins gives rise to some overlap of contents among different granule subsets [32,232].

The extent of mobilization of the three types of granule depends on the stimulus intensity, while the order of mobilization is fixed, a process termed graded exocytosis [11,12]. Gelatinase granules are most easily mobilized, followed by specific granules, and then azurophil granules. Graded exocytosis results in stepwise addition of granule

membrane proteins to the plasma membrane and stepwise release of granule luminal contents into the extracellular space. The controlled exocytosis of neutrophil granules allows sequential acquisition of functional responses and targeted delivery of toxic granule proteins, thereby reducing damage to normal host tissue.

In addition to graded granule release, neutrophil exocytosis is distinguished by two other attributes. The first is a lack of spatial organization of granules [30,233,234]. The random distribution of granules in the cytosol of circulating neutrophils suggests that graded exocytosis requires a mechanism to discriminate among granule subsets. The second attribute is compound exocytosis, the fusion of two or more granules prior to their fusion with the plasma membrane [46]. Compound exocytosis requires recognition of granule subsets as target membranes to allow for homotypic or heterotypic fusion. Homotypic fusion enhances the localized delivery of granule contents. Heterotypic fusion allows processing of certain granule constituents into active forms by proteolytic cleavage [235].

The molecular mechanisms that control exocytosis of neutrophil granules are poorly defined. Additionally, the full complement of functional changes resulting from exocytosis of different granule subsets remains to be identified. A major reason for this limited understanding of neutrophil exocytosis is an incomplete identification of membrane and luminal proteins of each granule subset. To address this problem, we performed proteomic profiling of the components of azurophil, specific, and gelatinase granules from human neutrophils. Two different methods for granule protein identification were applied. One used two-dimensional gel electrophoresis (2DE) followed by matrix-assisted laser desorption ionization time of flight mass spectrometry

(MALDI-TOF MS) analysis of peptides obtained by in-gel trypsin digestion of proteins. In the other, peptides from tryptic digests of granule membrane proteins were separated by two-dimensional microcapillary chromatography using strong cation exchange and reverse phase microcapillary high pressure liquid chromatography and analyzed with electrospray ionization tandem mass spectrometry (2D-HLPC ESI-MS/MS). Our analysis identified 286 proteins on the three granule subsets. Additionally, optimal methods for protein identification differed among granule subsets based on their physical .properties and luminal components.

Methods

Neutrophil Isolation

Neutrophils (8×10^8 cells) were isolated from healthy donors using plasma-Percoll gradients as described by Haslett *et al.* [236]. Trypan blue staining revealed that at least 97% of cells were neutrophils with >95% viability. After isolation neutrophils were suspended in Krebs-Ringer phosphate buffer (pH 7.2) at 4×10^7 cells/ml and treated with 10 μM diisopropyl fluorophosphate for 10 minutes on ice to inhibit proteases [237]. The Human Studies Committee of the University of Louisville approved the use of human donors.

Subcellular Fractionation for Granule Enrichment

Neutrophil granules were enriched by centrifugation on a three-layer Percoll density gradient as described by Kjeldsen *et al.* [19]. Briefly, isolated neutrophils (4×10^7/ml) were resuspended in disruption buffer containing 100 mM KCl, 1 mM NaCl, 1

mM $ATPNa_2$, 3.5 mM $MgCl_2$, 10 mM PIPES, and 0.5 mM PMSF, and disrupted by nitrogen cavitation at 380 psi and 4°C. The cavitate was collected, supplemented with 1.5 mM EGTA, and nuclei and intact cells were removed by centrifugation at 500 × g for 5 minutes. The postnuclear supernatant was layered onto a discontinuous Percoll gradient formed from three 9 ml layers of Percoll prepared in a buffer containing 100 mM KCl, 3 mM NaCl, 1 mM $ATPNa_2$, 3.5 mM $MgCl_2$, 1.25 mM EGTA, 10 mM PIPES, and 0.5 mM PMSF, to achieve final densities of 1.050 g/ml, 1.090 g/ml and 1.120 g/ml. The gradient was centrifuged at 37,000 × g for 30 minutes in an SS-34 fixed angle rotor in a Sorvall RC-5B centrifuge. The separated granule fractions were recovered from the gradient interfaces by aspiration, and Percoll was removed by ultracentrifugation of each granule subset at 100,000 × g for 90 minutes.

Sample Preparation for 2DE

Preparation of Whole Granules. Whole granule fractions were resuspended in 4 ml of disruption buffer, and centrifuged at 100,000 × g for 20 minutes to obtain a solid pellet. Buffer was removed by aspiration and the pellets were washed briefly with deionized water to remove residual salt.

Fractionation of Granule Proteins. To separate granule proteins into membrane and luminal fractions, granules were resuspended in 10 volumes of 0.1 M sodium carbonate, sonicated at high setting for 5 seconds, and subjected to three freeze-thaw cycles each followed by sonication [238]. Disrupted granules were incubated on ice for 30 minutes and carbonate-washed membranes were pelleted at 100,000 × g. The supernatant from the carbonate wash was concentrated by ultrafiltration through 1 kDa

cutoff centrifugal devices (Microsep Omega, Pall, East Hills, NY), and the retentate proteins were precipitated using chloroform-methanol desalting-precipitation [239]. The precipitate was dried on room air and subjected to 2DE.

To separate granule proteins based on differential solubility in ammonium sulfate solution, whole granules were solubilized in 3 volumes of lysis buffer containing 50 mM Tris pH 7.2 and 2% Triton X-100, and centrifuged at 20,000 × g to remove insoluble proteins. The Triton X-100-insoluble pellet was subjected to 4-12% acrylamide gradient SDS-PAGE and MALDI-MS analysis, while the cleared lysate was used for fractionation by ammonium sulfate precipitation of proteins. One volume of 100% saturated ammonium sulfate solution was added to the cleared lysate. The resulting precipitate was pelleted (subfraction one) and supernatant was removed. Solid ammonium sulfate was added to the supernatant until saturation, and the protein precipitate was pelleted (subfraction two). Precipitated protein pellets were re-dissolved in the lysis buffer and subjected to chloroform-methanol desalting-precipitation [239].

Protein Separation by 2DE and Identification by MALDI-TOF MS

Whole granules and granule subfractions were dissolved in 160 μL of 7 M urea, 2 M thiourea rehydration buffer (Genomic Solutions, Ann Arbor, MI). Proteins in all samples were separated by 2DE using non-linear pH 3-10 IPG strips for the first dimension and 4-12% gradient acrylamide gels for the second dimension (Invitrogen, Carlsbad, CA). The gels were visualized by colloidal Coomassie staining. Proteins were excised, in-gel trypsin digested, and the resulting peptides analyzed by MALDI-TOF MS using the thin film sample preparation method, as previously described [198,199]. Protein

identification was carried out by searching peptide spectra against the NCBI database using the Mascot web-based search engine. The search parameters used were: taxonomy - *H. Sapiens*, allowed error – 150 ppm, fixed modification – carbamidomethylation, variable modification – methionine oxidation, mass values – MH^+, maximum allowed missed cleavage – 1.

Protein Identification by 2D-HPLC ESI-MS/MS

Granule membranes obtained following treatment with 0.1 M sodium carbonate, as described above, were washed in 50 mM ammonium bicarbonate and then resuspended by sonication in 300 µl of 50 mM ammonium bicarbonate. Trypsin digestion was performed by addition of 20 ng/ml trypsin to the suspension, and samples were incubated on a rotator overnight at 37°C. Residual particulate material was removed by centrifugation at 100,000 × g, and the trypsin generated mixture was analyzed using an approach that combined two-dimensional microcapillary high-pressure liquid chromatography (HPLC) with electrospray ionization tandem mass spectrometry (ESI-MS/MS) [216]. All tandem spectra were searched against *H. Sapiens* Open Reading Frame database (human.nci) using the SEQUEST algorithm [214]. For singly charged peptides, spectra with a cross-correlation score of greater than 1.5 were retained, while for multiply charged peptides, spectra with a cross-correlation score of greater than 2 were retained [215]. The analysis was repeated three times for each granule subset and only proteins identified in at least two out of three experiments were assumed to be present on granules.

Quantitation of Granule Membranes and Western Blot analysis of Granules

Whole granule fractions were resuspended in 2 ml of disruption buffer, and centrifuged at 100,000 × g for 20 minutes to obtain a solid pellet. Buffer was removed by aspiration and the pellets were resuspended in 100 µl of disruption buffer. Sample volume was brought up to 1 ml by water and preincubated at 37°C. To quantitate phospholipid bilayers, TMA-DPH (Molecular Probes, Eugene, OR) was added at a final concentration of 1×10^{-7} M and fluorescence intensity was monitored continuously at excitation of 350 nm and emission of 430 nm for 20 seconds on Hitachi 4500 fluorescence spectrometer. Proteins associated with equal amounts of membrane from each granule subset were loaded onto a gel for SDS-PAGE. Proteins were separated, transferred to nitrocellulose membrane, and probed with an anti-actin antibody.

Results

Prior to subjecting granules to proteomic analysis, the purity of each of the three granule subsets was determined. Granule subsets were analyzed by western blotting for CD66b (specific granule marker), and by ELISA for gelatinase and myeloperoxidase (MPO), markers for gelatinase and azurophil granules, respectively (Figure 3). The western blot showed that CD66b was present in the specific granule fraction, but essentially absent in gelatinase granule and azurophil granule fractions. ELISA for gelatinase showed that 75% of total gelatinase was present in gelatinase granules, 20% in specific granules and 5% in azurophil granules, while 73% of MPO was in azurophil granules, 20% in specific granules, and 7% in gelatinase granules. This distribution of

Figure 3. Assessment of purity of granule fractions. Granule fractions separated by centrifugation on Percoll gradients were analyzed for the content of CD66b (specific granule marker), gelatinase (gelatinase granule marker), and myeloperoxidase (azurophil granule marker). A) Western blotting analysis of CD66b content in granule fractions. 50 μg of protein was loaded into each lane. B) ELISA for gelatinase. C) ELISA for myeloperoxidase.

Figure 3

A)

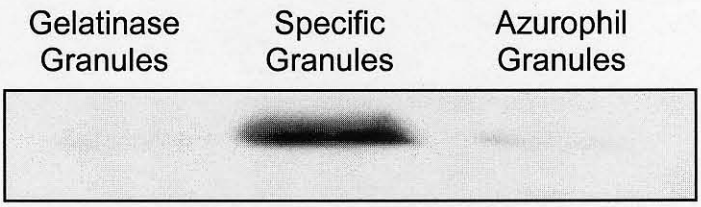
Gelatinase Granules
Specific Granules
Azurophil Granules

B)

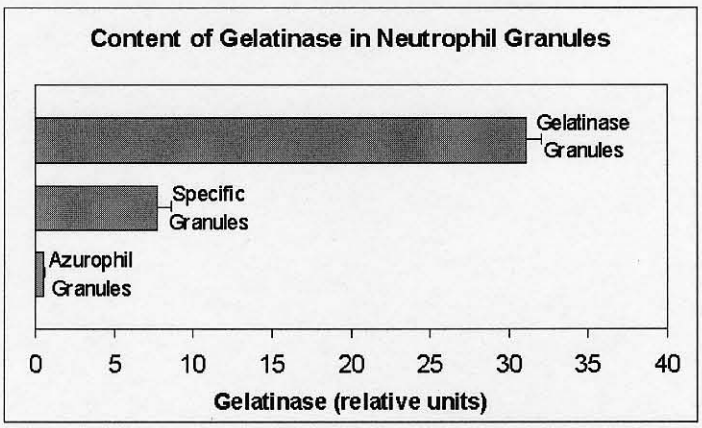
Content of Gelatinase in Neutrophil Granules
Gelatinase Granules
Specific Granules
Azurophil Granules
0
5
10
15
20
25
30
35
40
Gelatinase (relative units)

C)

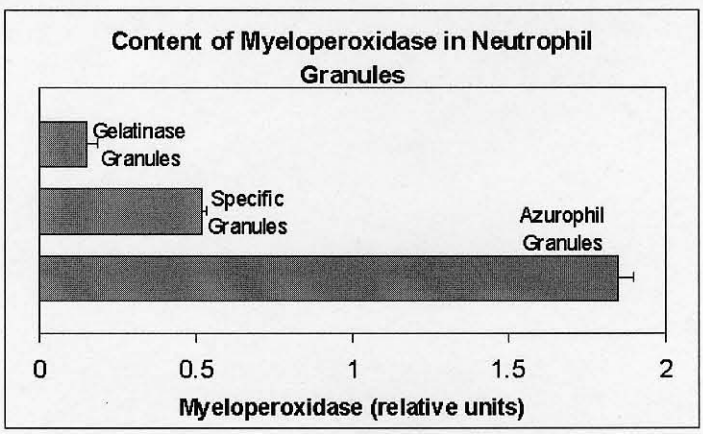
Content of Myeloperoxidase in Neutrophil Granules
Gelatinase Granules
Specific Granules
Azurophil Granules
0
0.5
1
1.5
2
Myeloperoxidase (relative units)

granule markers was similar to that reported by Kjeldsen *et al.* [10, 19]. Thus, optimal levels of granule subset enrichment were obtained.

The initial analysis of granule subset proteomes was carried out by subjecting whole granules to 2DE. Figure 4A shows the separation of gelatinase granule proteins. A total of 38 proteins were identified by peptide mass fingerprint analysis of MALDI-MS spectral data. Thirty of these proteins were cytoskeletal and luminal proteins. The 2D gels of specific granule proteins were dominated by large amounts of luminal proteins, such as lactoferrin and lipocalin (NGAL), which were present in such high abundance that proteins focused poorly (Figure 4B). A total of 26 proteins were identified by peptide mass fingerprinting. The only cytoskeletal protein identified was actin (Figure 4B). Separation of azurophil granule proteins by 2DE revealed large amounts of highly basic proteins, such as myeloperoxidase, which focused poorly, leading to extensive smearing on the basic end of the gel (Figure 4C). Only 8 proteins were identified from the azurophil granule gel.

To address the problem of overabundance of luminal proteins, granule proteins were fractionated by one of two methods prior to their separation by 2DE. First, the luminal contents of granules were separated from membranes by lysing the granules in 0.1 M sodium carbonate, pH 11. At high pH luminal cationic proteins lose their positive charge and dissociate from negatively charged matrix [238,240,241]. Additionally, alkaline sodium carbonate treatment has been reported to remove the actin cytoskeleton from neutrophil membranes [242]. To determine what proteins were removed from granule membranes, carbonate-soluble proteins were also subjected to 2DE. Second, differential solubility of proteins in ammonium sulfate solutions was applied to granule

Figure 4. 2D gels of whole granules. Neutrophil granules were subjected to 2DE, gels were stained with colloidal Coomassie Blue dye, the spots were excised, in-gel digested with trypsin and the resultant peptides were analyzed by MALDI-TOF MS. A) Gelatinase granules, B) Specific granules, C) Azurophil granules.

Figure 4

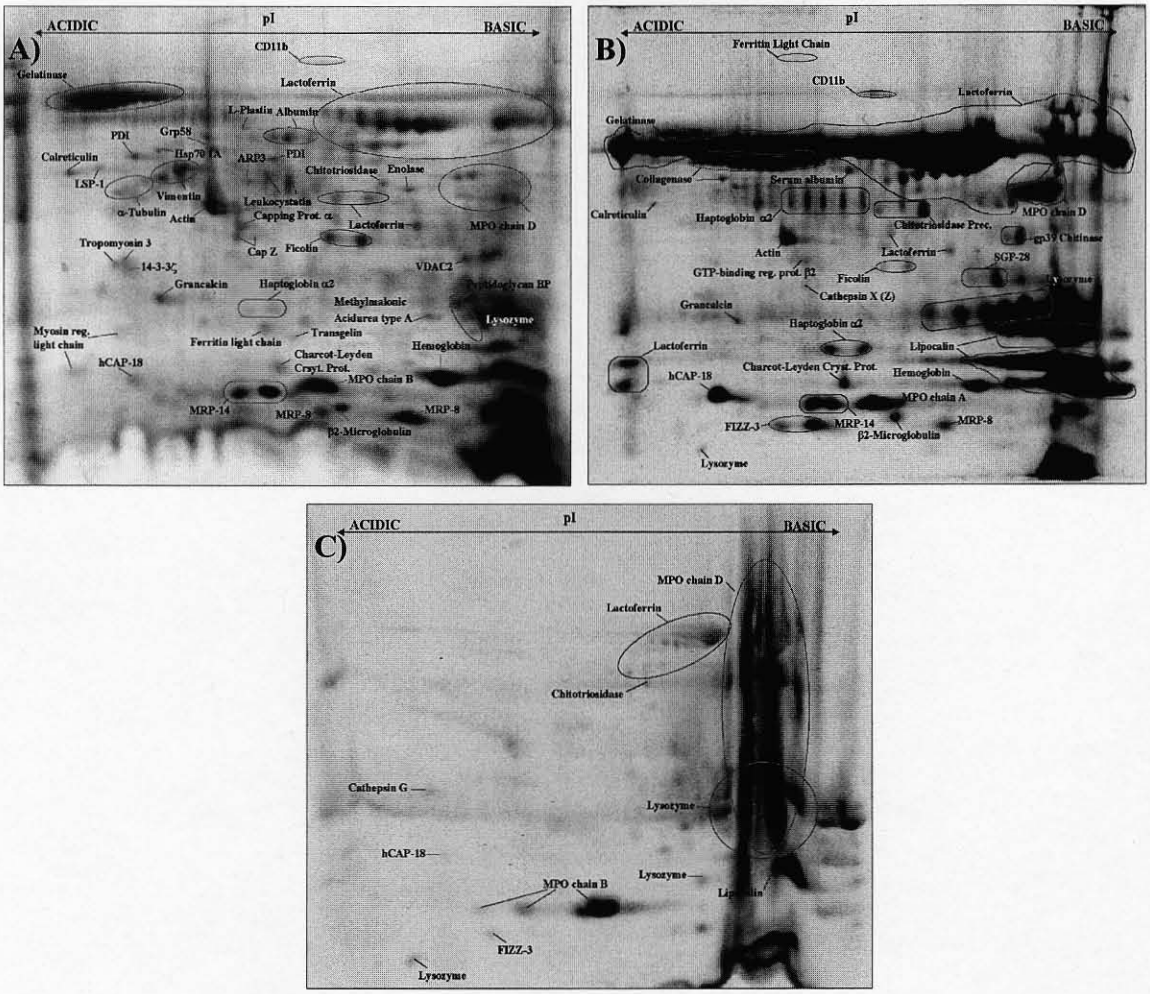
A)
ACIDIC
pI
BASIC
CD11b
Gelatinase
Lactoferrin
L-Plastin
Albumin
PDI
Grp58
Calreticulin
Hsp70 1A
ARP3
PDI
LSP-1
Chitotriosidase
Enolase
Vimentin
α-Tubulin
Actin
Leukocystatin
Capping Prot. α
Lactoferrin
MPO chain D
Tropomyosin 3
Cap Z
Ficolin
14-3-3ζ
VDAC2
Grancalcin
Haptoglobin α2
Peptidoglycan BP
Methylmalonic
Aciduresa type A
Lysozyme
Myosin reg. light chain
Ferritin light chain
Transgelin
Hemoglobin
hCAP-18
Charcot-Leyden Cryst. Prot.
MPO chain B
MRP-14
MRP-8
MRP-8
β2-Microglobulin
B)
ACIDIC
pI
BASIC
Ferritin Light Chain
CD11b
Lactoferrin
Gelatinase
Collagenase
Serum albumin
Calreticulin
Haptoglobin α2
MPO chain D
Chitotriosidase Prec.
gp39 Chitinase
Actin
Lactoferrin
SGP-28
GTP-binding reg. prot. β2
Ficolin
Cathepsin X (Z)
Grancalcin
Haptoglobin α2
Lactoferrin
Lipocalin
hCAP-18
Charcot-Leyden Cryst. Prot.
Hemoglobin
MPO chain A
FIZZ-3
MRP-14
MRP-8
β2-Microglobulin
Lysozyme
C)
ACIDIC
pI
BASIC
MPO chain D
Lactoferrin
Chitotriosidase
Cathepsin G
Lysozyme
hCAP-18
Lysozyme
MPO chain B
FIZZ-3
Lysozyme

proteins prior to 2DE. Whole granules were solubilized in a buffer containing Triton X-100, and proteins were separated based on precipitation at different concentrations of ammonium sulfate. The first subfraction contained proteins precipitated in a 20% ammonium sulfate solution, while the second subfraction contained the proteins soluble in 20% ammonium sulfate, but insoluble in 100% ammonium sulfate.

Fractionation of gelatinase granules with sodium carbonate prior to 2DE resulted in identification of 26 proteins, of which eight proteins were not detected on whole granule gels (Figures 5A and 5B). On the other hand, 20 proteins identified by 2DE of whole granules were not observed on either carbonate-washed membrane or carbonate-soluble protein gels. Most of these proteins were below 30 kDa, suggesting that low molecular weight proteins were lost during fractionation. Figures 5C and 5D show 2DE separation of ammonium sulfate precipitated proteins from gelatinase granules. This fractionation allowed identification of 38 proteins, 22 of which were not previously identified. Use of ammonium sulfate precipitation also identified all but three proteins detected following fractionation with sodium carbonate. Ten proteins seen in whole gelatinase granule gels were not detected after either fractionation method, indicating that protein fractionation is complementary to analysis of intact gelatinase granules. A total of 62 proteins were identified from gelatinase granules by 2DE protein separation and MALDI-MS (Table 2).

Fractionation of specific granule proteins with sodium carbonate resulted in identification of more proteins than extraction by ammonium sulfate precipitation. Sodium carbonate treatment prior to 2DE resulted in identification of 51 proteins from membranes and 27 proteins in the supernatant, of which 42 proteins were not detected on

Figure 5. 2D gels of gelatinase granule proteins fractionated by carbonate lysis and by ammonium sulfate precipitation of Triton X-100 solubilized proteins. Fractionation of gelatinase granule proteins by carbonate lysis (A and B) and by ammonium sulfate precipitation (C and D). A) A 2D gel of proteins that remained on the membrane after granule lysis in 0.1 M sodium carbonate buffer. B) Proteins that were solubilized in 0.1 M sodium carbonate. C) Proteins precipitated in 20% ammonium sulfate solution. D) Proteins that remained in solution in 20% ammonium sulfate but were precipitated in 100 percent ammonium sulfate solution.

Figure 5

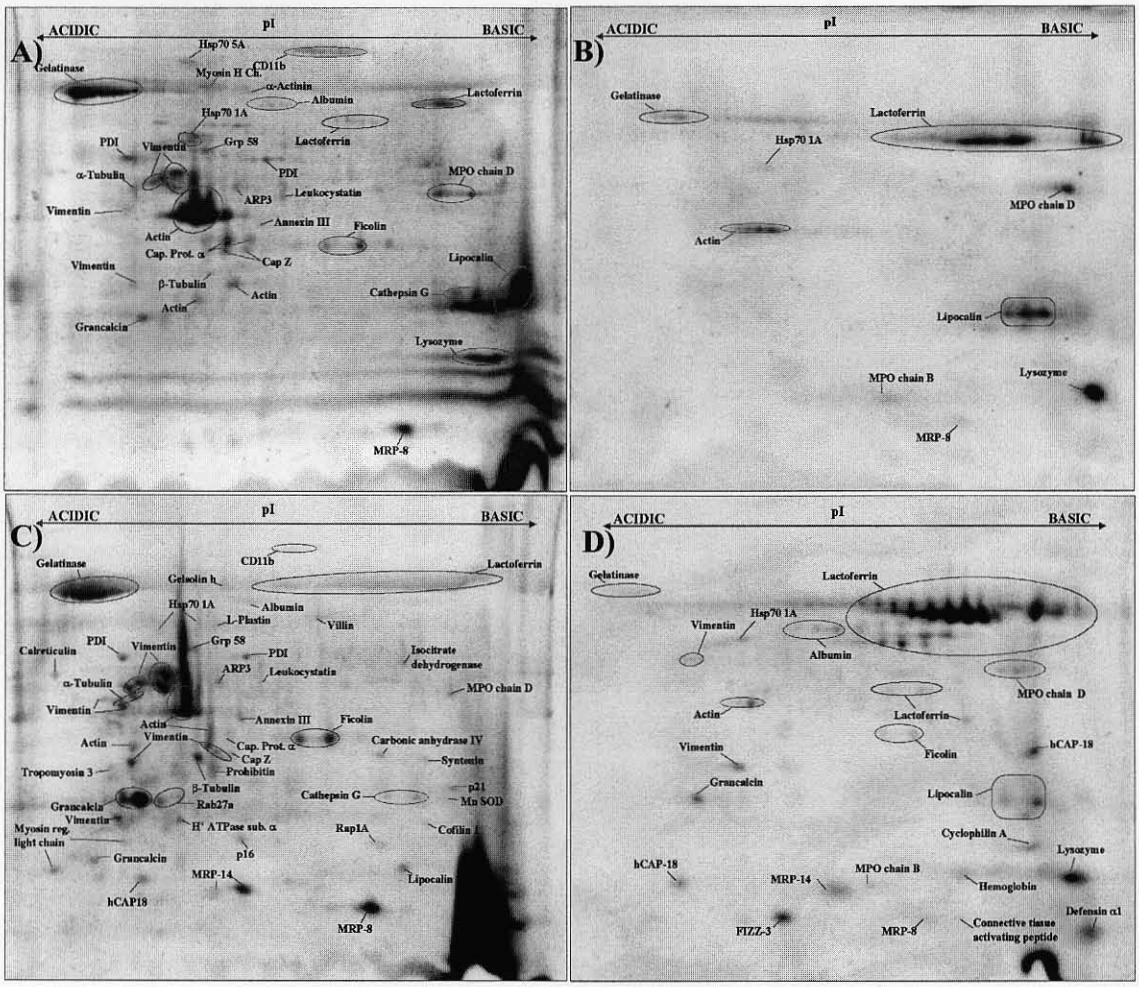
A)
ACIDIC
pI
BASIC
Hsp70 5A
Gelatinase
Myosin H Ch.
CD11b
α-Actinin
Albumin
Lactoferrin
Hsp70 1A
PDI
Vimentin
Grp 58
Lactoferrin
α-Tubulin
PDI
MPO chain D
ARP3
Leukocystatin
Vimentin
Annexin III
Ficolin
Actin
Cap. Prot. α
Cap Z
Lipocalin
Vimentin
β-Tubulin
Actin
Cathepsin G
Actin
Grancalcin
Lysozyme
MRP-8
B)
ACIDIC
pI
BASIC
Gelatinase
Lactoferrin
Hsp70 1A
MPO chain D
Actin
Lipocalin
MPO chain B
Lysozyme
MRP-8
C)
ACIDIC
pI
BASIC
Gelatinase
CD11b
Lactoferrin
Gelsolin h
Hsp70 1A
Albumin
L-Plastin
Villin
Calreticulin
PDI
Vimentin
Grp 58
PDI
Isocitrate dehydrogenase
ARP3
Leukocystatin
α-Tubulin
MPO chain D
Vimentin
Actin
Annexin III
Ficolin
Actin
Vimentin
Cap. Prot. α
Carbonic anhydrase IV
Cap Z
Syntenin
Tropomyosin 3
Prohibitin
β-Tubulin
Cathepsin G
p21
Mn SOD
Grancalcin
Rab27a
Vimentin
H+ ATPase sub. α
Rap1A
Cofilin
Myosin reg. light chain
Grancalcin
p16
MRP-14
Lipocalin
hCAP18
MRP-8
D)
ACIDIC
pI
BASIC
Gelatinase
Lactoferrin
Vimentin
Hsp70 1A
Albumin
MPO chain D
Actin
Lactoferrin
hCAP-18
Vimentin
Ficolin
Grancalcin
Lipocalin
Cyclophilin A
Lysozyme
hCAP-18
MRP-14
MPO chain B
Hemoglobin
FIZZ-3
MRP-8
Connective tissue activating peptide
Defensin α1

gels from whole specific granules (Figures 6A and 6B). Ammonium sulfate precipitation allowed identification of 45 proteins, only ten of which were not seen on gels from whole granules. Ammonium sulfate precipitation did not lead to identification of any protein not identified after fractionation with sodium carbonate (Figures 6C and 6D). Collagenase and cathepsin X were identified on the whole specific granule gels, but not after extraction by sodium carbonate. A total of 70 proteins were identified from specific granules (Table 2).

Fractionation of azurophil granule proteins by sodium carbonate or by ammonium sulfate precipitation failed to improve visualization and identification of proteins. The 2D gels of carbonate-washed membranes were largely devoid of proteins (only 4 proteins were identified), while 2DE of carbonate-soluble proteins failed to reveal proteins not found on gels of whole granule proteins (data not shown). Likewise, fractionation of azurophil granule proteins by ammonium sulfate precipitation failed to improve the number of proteins visualized by 2DE (data not shown). Thus, only 8 proteins from azurophil granules were identified by 2DE (Table 2).

For all granule subsets, the protein fraction precipitated by 100% ammonium sulfate contained primarily luminal proteins. Only two proteins remained in solution after precipitation of specific and gelatinase granule proteins with 100% ammonium sulfate, MRP-14 and MRP-8, while the corresponding sample from azurophil granules was devoid of protein (data not shown). To identify any proteins that failed to dissolve in the TX-100-containing buffer and thus could not be detected in ammonium sulfate precipitated fractions, TX-100-insoluble pellets were also subjected to SDS-PAGE. Only actin, vimentin, CD11b, lactoferrin and gelatinase were detected in pellets from specific

Figure 6. 2D gels of specific granule proteins fractionated by carbonate lysis and by ammonium sulfate precipitation of TX-100 solubilized proteins. Fractionation of specific granule proteins by carbonate lysis (A and B) and by ammonium sulfate precipitation (C and D). A) A 2D gel of proteins that remained on the membrane after granule lysis in 0.1 M sodium carbonate buffer. B) Proteins that were solubilized in 0.1 M sodium carbonate. C) Proteins precipitated in 20% ammonium sulfate solution, D) Proteins that remained in solution in 20% ammonium sulfate but were precipitated in 100 percent ammonium sulfate solution.

Figure 6

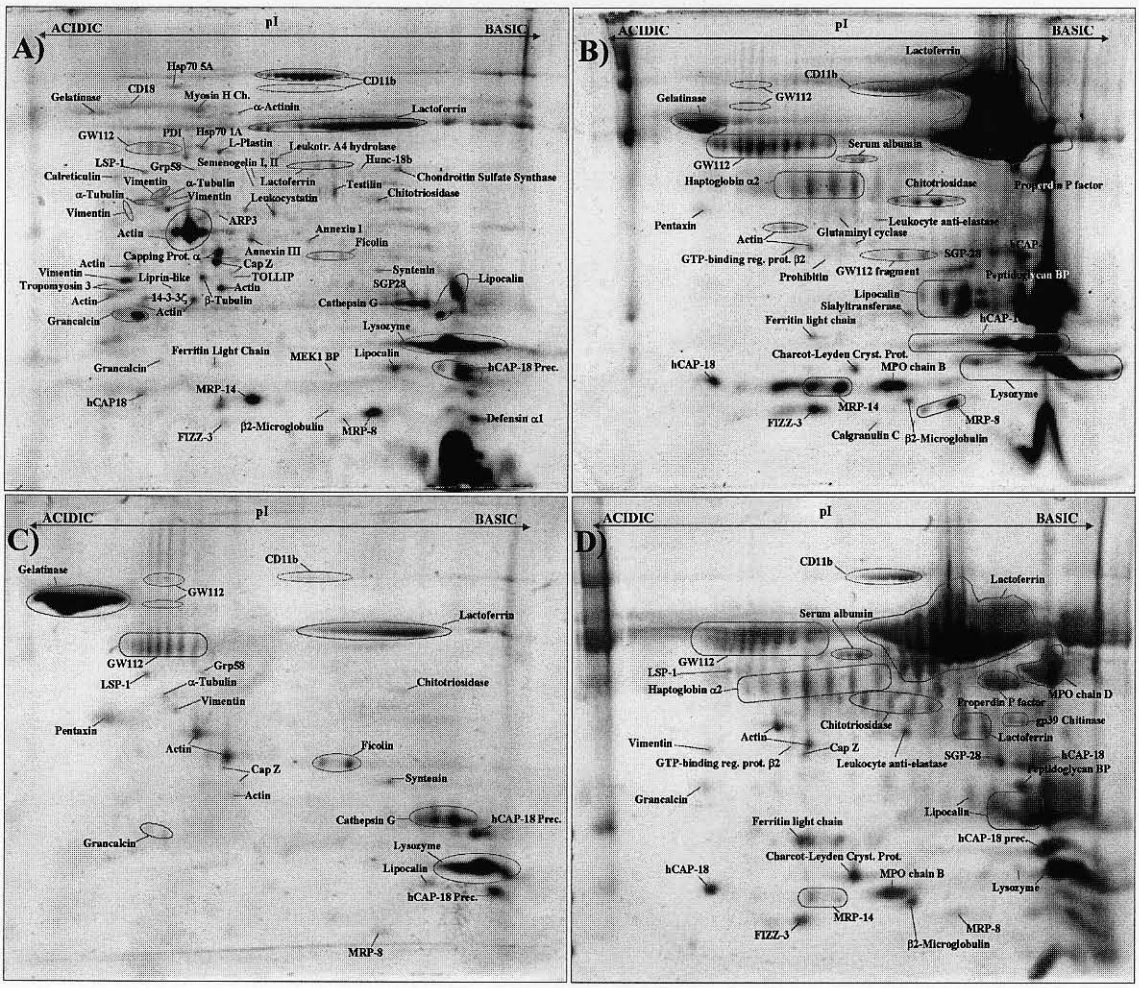
A)
ACIDIC
pI
BASIC
Hsp70 5A
CD11b
CD18
Myosin H Ch.
Gelatinase
α-Actinin
Lactoferrin
GW112
PDI
Hsp70 1A
L-Plastin
Leuktr. A4 hydrolase
LSP-1
GrpS8
Semenogelin I, II
Hunc-18b
Calreticulin
Vimentin
α-Tubulin
Lactoferrin
Testilin
Chondroitin Sulfate Synthase
Leukocystatin
Chitotriosidase
ARP3
Annexin I
Ficolin
Annexin III
Capping Prot. α
Cap Z
TOLLIP
Syntenin
SGP28
Lipocalin
Liprin-like
Actin
β-Tubulin
Cathepsin G
14-3-3ζ
Lysozyme
Ferritin Light Chain
MEK1 BP
hCAP-18 Prec.
MRP-14
bCAP18
β2-Microglobulin
MRP-8
FIZZ-3
Defensin α1
B)
ACIDIC
pI
BASIC
Lactoferrin
CD11b
Gelatinase
GW112
Serum albumin
Haptoglobin α2
Chitotriosidase
Pentaxin
Leukocyte anti-elastase
Actin
Glutaminyl cyclase
GTP-binding reg. prot. β2
SGP-28
Prohibitin
GW112 fragment
Lipocalin
Sialyltransferase
Ferritin light chain
Charcot-Leyden Cryst. Prot.
MPO chain B
hCAP-18
Lysozyme
MRP-14
MRP-8
FIZZ-3
Calgranulin C
β2-Microglobulin
C)
ACIDIC
pI
BASIC
CD11b
Gelatinase
GW112
Lactoferrin
GW112
GrpS8
LSP-1
α-Tubulin
Chitotriosidase
Vimentin
Pentaxin
Actin
Ficolin
Cap Z
Syntenin
Actin
Cathepsin G
hCAP-18 Prec.
Grancalcin
Lysozyme
Lipocalin
hCAP-18 Prec.
MRP-8
D)
ACIDIC
pI
BASIC
CD11b
Lactoferrin
Serum albumin
GW112
LSP-1
Haptoglobin α2
MPO chain D
Properdin P factor
Chitotriosidase
gp-39 Chitinase
Actin
Lactoferrin
Vimentin
Cap Z
GTP-binding reg. prot. β2
Leukocyte anti-elastase
SGP-28
hCAP-18
Peptidoglycan BP
Grancalcin
Lipocalin
Ferritin light chain
hCAP-18 prec.
Charcot-Leyden Cryst. Prot.
hCAP-18
MPO chain B
Lysozyme
MRP-14
MRP-8
FIZZ-3
β2-Microglobulin

Table 2
Proteins identified from 2D gels of neutrophil granules

Proteins Identified from 2D Gels						
Entrez Gene	Entrez ID	Protein Name	Granule	Peptides Matched/Total	% Coverage	MOWSE score
CA4	gi|409725	Carbonic anhydrase IV	GE	10/30	36	101
CFL1	gi|57099669	Cofilin 1	GE	16/53	70	153
1F9PA	gi|34810160	Connective Tissue Activating Pept.	GE	7/33	67	85
ENO1	gi|4503571	Enolase	GE	16/38	42	144
GSN	gi|38044288	Gelsolin	GE	15/58	26	83
ATP5A1	gi|50345982	H+-ATP-ase F0 sub. α	GE	16/55	39	110
IDH2	gi|28178832	Isocitrate dehydrogenase	GE	12/47	27	74
MMAA	gi|26892295	Methylmalonic Acidurea	GE	7/14	16	69
SOD2	gi|7546412	Mn SOD chain b	GE	8/52	57	72
ARPC5	gi|56204524	p16 Arc	GE	11/22	58	142
ARPC3	gi|5031597	p21 Arc	GE	6/20	40	68
PPIA	gi|31615559	Cyclophilin A	GE	7/29	37	65
RAB27A	gi|34485711	Rab27A	GE	9/33	37	93
RAP1A	gi|54696200	Rap1A	GE	9/30	43	105
TAGLN	gi|55960374	Transgelin 2	GE	10/33	44	88
VDAC2	gi|48146045	VDAC2	GE	7/31	32	65
VIL2	gi|46249758	Villin 2	GE	28/58	41	170
VIM	gi|340234	Vimentin 35 kDa	GE	9/34	30	73
YWHAZ	gi|49119653	14-3-3ζ	GE,SG	9/21	36	106
ACTB	gi|14250401	Actin β	GE,SG	9/26	30	88
ACTG1	gi|178045	Actin γ	GE,SG	7/21	37	82
ACTN1	gi|4501891	α-actinin	GE,SG	11/19	13	93
ALB	gi|28592	Albumin	GE,SG	19/35	30	161
ANXA3	gi|4826643	Annexin III	GE,SG	8/12	28	104
ACTR3	gi|27806335	ARP3	GE,SG	9/20	23	83
B2M	gi|1195503	β2-Microglobulin	GE,SG	8/22	77	107
CALR	gi|30583735	Calreticulin	GE,SG	8/21	19	79
CAPZA1	gi|12652785	Cap Z	GE,SG	11/26	56	134
CAPZA2	gi|433308	Capping protein α	GE,SG	8/27	36	83
ITGAM	gi|386975	CD11b	GE,SG	10/16	10	85
CLC	gi|17942629	Charcot-Leyden protein	GE,SG	9/35	43	81
FTL	gi|48145547	Ferritin Light Chain	GE,SG	11/20	53	143
FCN1	gi|8051584	Ficolin 1 precursor	GE,SG	14/24	46	156
MMP9	gi|22532481	Gelatinase	GE,SG	11/21	18	103
GCA	gi|6912388	Grancalcin	GE,SG	12/29	48	109
PDIA3	gi|7437388	Grp58	GE,SG	22/43	44	181
HP	gi|47124562	Haptoglobin α2	GE,SG	14/26	39	151
HBB	gi|4504349	Hemoglobin	GE,SG	12/26	93	184
HSPA1A	gi|5123454	Hsp70 1A	GE,SG	15/23	32	168
HSPA5	gi|1143492	Hsp70 5A	GE,SG	20/50	37	149
CST7	gi|9836652	Leukocystatin	GE,SG	7/16	28	74
LCP1	gi|4504965	L-Plastin	GE,SG	9/19	17	84
LSP1	gi|12804709	LSP-1	GE,SG	6/10	36	86
S100A9	gi|4506773	MRP-14	GE,SG	15/34	92	150
S100A8	gi|30583595	MRP-8	GE,SG	10/23	83	132
MRCL3	gi|5453740	Myosin Regulatory Light Chain	GE,SG	10/36	65	90
P4HB	gi|20070125	PDI	GE,SG	7/18	17	65
PGLYRP1	gi|37182990	Peptidoglycan recog. prot.	GE,SG	8/38	48	70
PHB	gi|49456373	Prohibitin	GE,SG	10/37	47	100
SDCBP	gi|55749523	Syntenin	GE,SG	8/20	43	94
TPM3	gi|55665783	Tropomyosin 3	GE,SG	9/19	29	100
TUBA3	gi|18088719	Tubulins α	GE,SG	9/17	27	104
TUBB1	gi|57013276	Tubulins β	GE,SG	10/15	31	129
VIM	gi|4507895	Vimentin 50 kDa	GE,SG	14/19	36	168
ANXA1	gi|54696696	Annexin I	SG	9/18	34	101

S100A12	gi|5032059	Calgranulin C	SG	4/11	40	65
CTSZ	gi|7546546	Cathepsin X	SG	6/16	24	73
ITGB2	gi|46255730	CD18	SG	7/14	12	64
CHI3L1	gi|4557018	gp39 chitinase	SG	20/37	55	195
CHSY1	gi|37182181	Chondroitin sulfate synthase	SG	13/33	20	87
MMP8	gi|4505221	Collagenase	SG	10/23	25	83
DEFA1	gi|4758146	Defensin α1	SG	5/22	28	68
QPCT	gi|525241	Glutaminyl cyclase	SG	9/17	41	123
GNB2	gi|29789261	GTP-binding prot. β2	SG	7/23	20	67
OLFM4	gi|29126831	GW112	SG	7/15	20	78
STXBP2	gi|1944130	Hunc-18b	SG	8/19	22	74
SLPI	gi|13489087	Leukocyte Anti-elastase	SG	7/15	25	72
LTA4H	gi|4505029	Leukotriene A4 Hydrolase	SG	7/12	14	76
PPFIBP1	gi|28278230	Liprin-like	SG	7/19	40	71
MAP2K1IP1	gi|11496277	MEK1 BP	SG	5/16	62	75
MYH9	gi|189036	Myosin Heavy Ch.	SG	12/21	14	78
PTX3	gi|4506333	Pentaxin 3	SG	11/25	34	107
PFC	gi|3183860	Properdin P factor	SG	14/30	33	134
SEMG1	gi|1147569	Semenogelin I	SG	16/38	38	146
SEMG2	gi|4506885	Semenogelin II	SG	12/38	25	84
ST6GALNAC3	gi|37182203	Sialyltransferase 3	SG	7/25	45	75
EHD1	gi|30240932	Testilin	SG	15/26	25	138
TOLLIP	gi|21361619	TOLLIP	SG	8/33	36	65
CRISP3	gi|2136189	SGP-28	SG,AG	7/25	23	74
CTSG	gi|2392230	Cathepsin G	GE,SG,AG	7/24	24	70
CHIT1	gi|47480958	Chitotriosidase	GE,SG,AG	12/26	30	113
RETN	gi|37183250	FIZZ-3 (Resistin)	GE,SG,AG	8/24	76	85
CAMP	gi|39753970	hCAP-18	GE,SG,AG	9/22	45	109
LTF	gi|640200	Lactoferrin	GE,SG,AG	10/22	16	83
LCN2	gi|38455402	Lipocalin (NGAL)	GE,SG,AG	12/27	64	163
LYZ	gi|442591	Lysozyme	GE,SG,AG	8/24	53	102
MPO	gi|494396 gi|494397	Myeloperoxidase (MPO) Chain B,D	GE,SG,AG	6/29 26/52	69 53	78 191

Eighty-seven proteins were identified from all 2D gels of neutrophil granules using MALDI-TOF MS. The table lists the gene and protein designation, granule type, number of peptides matched, the percent protein coverage by these peptides, and the calculated molecular weight search (MOWSE) score for each protein.

and gelatinase granules (data not shown), while myeloperoxidase, cathepsin G, and lysozyme were found in the TX-100-insoluble fraction of azurophil granules. A total of 87 proteins were identified from granule subsets by the three 2DE approaches, of which 56 were cytoskeletal or luminal proteins. Membrane proteins, except for CD11b and CD18, were not visualized by 2DE.

2DE-based approaches are biased against membrane proteins, low abundance proteins, and proteins at the extremes of isoelectric point and molecular mass. To address these issues, we used an approach that couples two-dimensional microcapillary HPLC (2D-HPLC) with ESI-MS/MS analysis [215,216]. This high-sensitivity mass spectrometry-based approach that allows direct analysis of complex protein mixtures was applied to granule membranes following removal of luminal and cytoskeletal proteins with sodium carbonate. Only proteins present in at least two out of three experiments or proteins also identified by 2DE-MALDI-MS were considered as valid granule proteins. By this criteria a total of 247 proteins were identified from all granule subsets, of which 48 were also identified by 2DE. Table 3 lists identified proteins by granule subset, method of identification and functional classification of the protein. A total of 86 proteins were identified only from gelatinase granules, 28 proteins from only specific granules, and 26 proteins from only azurophil granules. A number of proteins were identified on multiple granule subsets, including 79 proteins from gelatinase and specific granules, 5 proteins from specific and azurophil granules and 61 proteins from all three granule subsets. The peptide sequences detected by 2D-HPLC-ESI-MS/MS can be found in Supplementary Tables 1 and 2. Supplementary Table 1 lists the proteins identified at least twice out of three experiments and the sequences of corresponding peptides. Proteins

Table 3
A complete list of proteins identified on neutrophil granules

Receptors and Transmembrane Cytoskeletal Anchors			
Entrez Gene	**Entrez Protein**	**Protein Name**	**Granule Type$_{METHOD}$**
BZRP	NP_000705	Benzodiazepine receptor	GE_{LCMS}
FCGR3B	NP_000561	CD16, FcγRIIIb	GE_{LCMS}
CR1	NP_000564 NP_000642	CD35, complement receptor-1 (CR1)	GE_{LCMS}
SPN	NP_003114	CD43, sialophorin	GE_{LCMS}
CD9	NP_001760	CD9, motility related protein	GE_{LCMS}
FLOT2	NP_004466	Flotillin 2	GE_{LCMS}
LBR	NP_919424 NP_002287	Lamin B receptor	GE_{LCMS}
GP9	NP_000165	Platelet glycoprotein IX	GE_{LCMS}
SELPLG	NP_002997	P-selectin glycoprotein ligand-1	GE_{LCMS}
UNC84B	NP_056189	Sad1	GE_{LCMS}
SCAMP1	NP_004857	SCAMP1	GE_{LCMS}
SCAMP2	NP_005688	SCAMP2	GE_{LCMS}
CEACAM1	NP_001703	CAECAM-1	GE_{LCMS},SP_{LCMS}
ITGAM	NP_000623	CD11b, complement component receptor 3 (CR3)	$GE_{2D\ LCMS}$,$SP_{2D\ LCMS}$
ADAM8	NP_001100	CD156, ADAM-8	GE_{LCMS}, SP_{LCMS}
ITGB2	NP_000202	CD18, macrophage antigen 1 (mac-1) beta subunit	GE_{LCMS},$SP_{2D\ LCMS}$
ITGA2B	NP_000410	CD41, platelet fibrinogen receptor, alpha subunit	GE_{LCMS},SP_{LCMS}
ITGB3	NP_000203	CD61, platelet glycoprotein IIIa	GE_{LCMS},SP_{LCMS}
C5R1	NP_001727	CD88, C5aR1	GE_{LCMS},SP_{LCMS}
DSG1	NP_001933	Desmoglein preproprotein	GE_{LCMS},SP_{LCMS*}
FPR1	NP_002020	Formyl peptide receptor	GE_{LCMS}, SP_{LCMS}
GP1BB	NP_000398	Glycoprotein Ib beta precursor	GE_{LCMS},SP_{LCMS}
HLA-A	NP_002107	HLA-A1	GE_{LCMS}, SP_{LCMS*}
ICAM3	NP_002153	ICAM-3 precursor	GE_{LCMS}, SP_{LCMS*}
LAIR1	NP_002278 NP_068352 NP_068354	Leukocyte-associated Ig-like receptor 1	GE_{LCMS}, SP_{LCMS*}
LILRB2	NP_005865	Leukocyte Ig-like receptor 2	GE_{LCMS},SP_{LCMS}
CLEC12A	NP_612210 NP_963917	Myeloid inhibitory C-type lectin-like receptor	GE_{LCMS},SP_{LCMS}
SIGLEC5	NP_003821	Sialic acid binding Ig-like lectin 5	GE_{LCMS},SP_{LCMS}
SDCBP	NP_005616	Syntenin	GE_{2D},SP_{2D}
VNN1	NP_004657	Vanin 1 precursor	GE_{LCMS},SP_{LCMS*}
VNN2	NP_004656 NP_511043	Vanin 2	GE_{LCMS}, SP_{LCMS*}
CANX	NP_001737	Calnexin	GE_{LCMS},SP_{LCMS},AZ_{LCMS*}
FLOT1	NP_005794	Flotillin 1	GE_{LCMS},SP_{LCMS*},AZ_{LCMS*}
FCER1G	NP_004097	Fc receptor for IgE, high affinity I, gamma polypeptide	GE_{LCMS},SP_{LCMS},AZ_{LCMS*}
ITGB5	NP_002204	Integrin, β 5	GE_{LCMS*},SP_{LCMS*},AZ_{LCMS}
LAMP2	NP_002285 NP_054701	LAMP2	GE_{LCMS},SP_{LCMS*},AZ_{LCMS*}
STOM	NP_004090	Stomatin	GE_{LCMS},SP_{LCMS},AZ_{LCMS}
CD63	NP_001771	CD63, LAMP-3	AZ_{LCMS}
TM7SF3	NP_057635	Seven transmembrane receptor	AZ_{LCMS}
STOML3	NP_660329	Stomatin-like 3	AZ_{LCMS}

Channels and Transporters			
Entrez Gene	**Entrez Protein**	**Protein Name**	**Granule Type$_{METHOD}$**
SLC25A5	NP_001143	Adenine nucleotide translocator 2	GE_{LCMS}
SLC25A6	NP_001627	Adenine nucleotide translocator 3	GE_{LCMS}
SLC4A1	NP_000333	Anion exchanger, member 1	GE_{LCMS}
ATP5A1	NP_004037	ATP synthase, H+ transporting, mitochondrial F1 complex, alpha subunit	$GE_{2D\ LCMS}$
ATP6V1C2	NP_653184	ATPase, H+ transporting, lysosomal 42kDa, V1 subunit C isoform 2	GE_{LCMS}

ATP6V0A1	NP_005168	ATPase, H+ transporting, lysosomal V0 subunit a isoform 1	GE_{LCMS}
ATP6V0A2	NP_036595	ATPase, H+ transporting, lysosomal V0 subunit a isoform 2	GE_{LCMS}
SLC2A3	NP_008862	Glucose transporter type 3	GE_{LCMS}
TMED9	NP_059980	gp25L2 protein, protein transporter	GE_{LCMS}
MTCH2	NP_055157	Mitochondrial carrier homolog 2	GE_{LCMS}
SFXN1	NP_073591	Sideroflexin 1	GE_{LCMS}
SLCO4C1	NP_851322	Solute carrier organic anion transporter family, member 4C1	GE_{LCMS}
VDAC2	NP_003366	Voltage-dependent anion channel 2	$GE_{2D\ LCMS}$
SLC25A4	NP_001142	Adenine nucleotide translocator 1	GE_{LCMS},SP_{LCMS}
ATP5F1	NP_001679	ATP synthase, H+ transporting, mitochondrial F0 complex, subunit b	GE_{LCMS},SP_{LCMC^*}
ATP5H	NP_006347	ATP synthase, H+ transporting, mitochondrial F0 complex, subunit d	GE_{LCMS},SP_{LCMS^*}
SLC25A24	NP_037518	Calcium-binding transporter	GE_{LCMS},SP_{LCMS^*}
MVP	NP_059447 NP_005106	Major vault protein	GE_{LCMS^*},SP_{LCMC}
SLC25A3	NP_005879 NP_002626	Mitochondrial phosphate carrier precursor isoform 1	GE_{LCMS},SP_{LCMS^*}
PLSCR1	NP_066928	Phospholipid scramblase 1	GE_{LCMS},SP_{LCMS^*}
ATP2A3	NP_005164 NP_777613 NP_777614 NP_777615 NP_777617 NP_777618	Sarco/endoplasmic reticulum Ca^{2+} -ATPase	GE_{LCMS},SP_{LCMS}
VDAC1	NP_003365	Voltage-dependent anion channel 1	GE_{LCMS},SP_{LCMC^*}
VDAC3	NP_005653	Voltage-dependent anion channel 3	GE_{LCMS},SP_{LCMC^*}
ATP6V0D1	NP_004682	ATPase, H+ transporting, lysosomal, V0 subunit D isoform 1	GE_{LCMS},SP_{LCMS^*},AZ_{LCMS}
TCIRG1	NP_006010	ATPase, H+ transporting, 116kD, vacuolar, T cell imune regulator	GE_{LCMS},SP_{LCMS^*},AZ_{LCMS}
ATP8A1	NP_006086	Aminophospholipid transporter ATPase	AZ_{LCMS}
VAT1	NP_006364	Vesicle amine transport protein 1	AZ_{LCMS}

GTP-ases			
Entrez Gene	**Entrez Protein**	**Protein Name**	**Granule Type$_{METHOD}$**
HSPC121	NP_057479	Butyrate-induced transcript 1, GTPase activating protein	GE_{LCMS}
IQGAP1	NP_003861	IQ motif containing GTPase activating protein 1	GE_{LCMS}
RAB7	NP_004628	RAB7	GE_{LCMS}
RAB10	NP_057215	RAB10	GE_{LCMS}
RAB11A	NP_004654	RAB11A	GE_{LCMS}
RAB11B	NP_004209	RAB11B	GE_{LCMS}
RAB14	NP_057406	Rab14	GE_{LCMS}
RAB21	NP_055814	RAB21	GE_{LCMS}
RAB32	NP_006825	RAB32	GE_{LCMS}
RAP2A RAP2B RAP2C	NP_066361 NP_002877 NP_067006	RAP2	GE_{LCMS}
RAB31	NP_006859	RAB31	SP_{LCMS}
RAB2	NP_002856	RAB2	GE_{LCMS},SP_{LCMS^*}
RAB5C	NP_958842 NP_004574	RAB5C	GE_{LCMS},SP_{LCMS}
CDC42	NP_001782	Cdc42	GE_{LCMS},SP_{LCMS^*},AZ_{LCMS}
GNAI2	NP_002061	G_i α2	GE_{LCMS},SP_{LCMS},AZ_{LCMS}
GNB1 GNB2	NP_002065 NP_005264	G β1,2	GE_{LCMS^*},$SP_{2D\ LCMS^*}$,AZ_{LCMS}
RAB1A RAB1B	NP_004152 NP_112243	RAB1	GE_{LCMS},SP_{LCMS^*},AZ_{LCMS}
RAB3A RAB3B RAB3C	NP_002857 NP_002858 NP_612462	RAB3	GE_{LCMS},SP_{LCMS},AZ_{LCMS}
RAB3D	NP_004274	RAB3D	GE_{LCMS},SP_{LCMS},AZ_{LCMS^*}

RAB27A	NP_004571 NP_899057 NP_899058 NP_899059	Rab27A	$GE_{2D\ LCMS}$,SP_{LCMS},AZ_{LCMS}
RAP1A RAP1B	NP_002875 NP_056461	RAP1	GE_{2D},SP_{LCMS},AZ_{LCMS}

Structural Proteins and Adaptors			
Entrez Gene	Entrez Protein	Protein Name	Granule $Type_{METHOD}$
AP2A1	NP_055018 NP_570603	Adaptin	GE_{LCMS}
CFL1	NP_005498 NP_068733 NP_619579	Cofilin 1	$GE_{2D\ LCMS*}$
CORO7	NP_078811	Coronin 7	GE_{LCMS}
ARPC5	NP_005708	p16 Arc	GE_{2D}
ARPC3	NP_005710	p21 Arc	GE_{2D}
MYL6	NP_066299 NP_524147 NP_524149 NP_524148	Myosin alkali light chain	GE_{LCMS}
TAGLN	NP_003177	Transgelin	GE_{2D}
TUBB1	NP_110400	Tubulin beta 1	GE_{LCMS}
URP2	NP_848537 NP_113659	UNC-112 related protein 2	GE_{LCMS}
VIL2	NP_003370	Villin 2	GE_{2D}
RP2	NP_008846	XRP2	GE_{LCMS}
YWHAZ	NP_003397 NP_663723	14-3-3ζ	GE_{2D},SP_{2D}
ACTN1	NP_001093	Actinin, alpha 1	$GE_{2D\ LCMS}$,$SP_{2D\ LCMS}$
ANXA3	NP_005130	Annexin III	GE_{2D},SP_{2D}
ACTR3	NP_005712	ARP3	GE_{2D},SP_{2D}
CAPZA1	NP_006126	Cap Z	GE_{2D},SP_{2D}
CAPZA2	NP_006127	Capping protein a	GE_{2D},SP_{2D}
CORO1A	NP_009005	Coronin 1A	GE_{LCMS},SP_{LCMS}
GSN	NP_000168 NP_937895	Gelsolin	$GE_{2D\ LCMS}$,SP_{LCMS}
TLN1	NP_006280	Talin 1	GE_{LCMS},SP_{LCMS}
TPM3	NP_689476	Tropomyosin 3	GE_{2D},SP_{2D}
TUBA2 TUBA3	NP_005992 NP_524575 NP_006000	Tubulin alpha 2,3	GE_{LCMS},SP_{LCMS}
MRCL3	NP_006462	Myosin regulatory light chain	GE_{2D},SP_{2D}
LSP1	NP_002330	LSP1	GE_{2D},SP_{2D}
CALD1	NP_149129 NP_004333 NP_149347 NP_149130 NP_149131	Caldesmon 1	SP_{LCMS}
CYLC2	NP_001331	Cylicin 2	SP_{LCMS}
MSN	NP_002435	Moesin	SP_{LCMS}
TUBA4	NP_079295	Tubulin alpha 4	SP_{LCMS}
ACTA1 ACTA2	NP_001091 NP_001604	Actin, alpha	GE_{LCMS},SP_{LCMS},AZ_{LCMS}
ACTB ACTG1	NP_001092 NP_001605	Actin, beta or gamma	$GE_{2D\ LCMS}$,$SP_{2D\ LCMS}$,AZ_{LCMS}
ANXA1	NP_000691	Annexin I, (lipocortin I)	GE_{LCMS},SP_{2D},AZ_{LCMS*}
FLNA	NP_001447	Filamin 1	GE_{LCMS},SP_{LCMS},AZ_{LCMS*}
LCP1	NP_002289	L-plastin	$GE_{2D\ LCMS}$,$SP_{2D\ LCMS}$,AZ_{LCMS*}
MYH9	NP_002464	Myosin heavy chain	GE_{LCMS},$SP_{2D\ LCMS}$,AZ_{LCMS}
PFN1	NP_005013	Profilin 1	GE_{LCMS},SP_{LCMS*},AZ_{LCMS*}
TUBA1	NP_005991	Tubulin alpha 1	$GE_{2D\ LCMS}$,$SP_{2D\ LCMS}$,AZ_{LCMS*}
TUBB2	NP_001060	Tubulin beta 3	$GE_{2D\ LCMS}$,$SP_{2D\ LCMS}$,AZ_{LCMS}
VIM	NP_003371	Vimentin	$GE_{2D\ LCMS}$,$SP_{2D\ LCMS*}$,AZ_{LCMS}
HCLS1	NP_005326	Hematopoietic lineage cell-specific protein 1	AZ_{LCMS}
ZYX	NP_003452	Zyxin	AZ_{LCMS}

Kinases and Phosphatases			
Entrez Gene	Entrez Protein	Protein Name	Granule Type$_{METHOD}$
HCK	NP_002101	Hck tyrosine kinase	GE_{LCMS}
FGR	NP_005239	Fgr tyrosine kinase	GE_{LCMS},SP_{LCMS}
PTPRJ	NP_002834	Protein tyrosine phosphatase, receptor type J	GE_{LCMS},SP_{LCMS}
PTPN7	NP_002823 NP_542155	Protein tyrosine phosphatase, non-receptor type 7	GE_{LCMS},SP_{LCMS*}
PTPNS1	NP_542970	Protein tyrosine phosphatase, non-receptor type substrate 1	GE_{LCMS},SP_{LCMS}
TTBK2	NP_775771	Tau tubulin kinase	SP_{LCMS}
MAP2K1IP1	NP_068805	MEK1 Binding Protein, MP1	SP_{2D}
PTPRC	NP_002829 NP_563578 NP_563579	Protein tyrosine phosphatase, receptor type C	GE_{LCMS},SP_{LCMS},AZ_{LCMS}

Luminal and Host Defense Proteins			
Entrez Gene	Entrez Protein	Protein Name	Granule Type$_{METHOD}$
C10orf42	NP_612366	Chromosome 10 ORF 42	GE_{LCMS}
SPCS2	NP_055567	KIAA0102 gene product (signal peptidase)	GE_{LCMS}
MME	NP_000893 NP_009218 NP_009219 NP_009220	Neprilysin	GE_{LCMS}
1F9PA	NP_002695	Connective Tissue Activitating Peptide	GE_{2D}
CLC	NP_001819	Charcot-Leyden crystal protein	GE_{2D},SP_{2D}
DEFA1	NP_004075	Defensin α1	GE_{2D},SP_{2D}
DCD	NP_444513	Dermcidin precursor	GE_{LCMS},SP_{LCMS}
FCN1	NP_001994	Ficolin 1 precursor	$GE_{2D\ LCMS*}$,$SP_{2D\ LCMS}$
HP	NP_005134	Haptoglobin α2	GE_{2D},SP_{2D}
PGLYRP1	NP_005082	Peptidoglycan recognition protein 1	GE_{2D},SP_{2D}
PADI4	NP_036519	Peptidyl arginine deiminase, type IV	GE_{LCMS},SP_{LCMS*}
B2M	NP_004039	β2-Microglobulin	GE_{2D},SP_{2D}
MGAM	NP_004659	Maltase-glucoamylase	GE_{LCMS},SP_{LCMS}
MMP25	NP_071913 NP_073209	Matrix metalloprotease 25 (leukolysin)	GE_{LCMS},SP_{LCMS*}
ANPEP	NP_001141	Membrane alanine aminopeptidase	GE_{LCMS},SP_{LCMS*}
SIGLEC5	NP_003821	Sialic acid binding Ig-like lectin	GE_{LCMS},SP_{LCMS}
THBS1	NP_003237	Thrombospondin 1 precursor	GE_{LCMS},SP_{LCMS*}
CAT	NP_001743	Catalase	SP_{LCMS}
CHI3L1	NP_001267	gp-39 chitinase	SP_{2D}
CHSY1	NP_055733	Chondroitin sulfate synthase	SP_{2D}
CHGA	NP_001266	Chromogranin A	SP_{LCMS}
QPCT	NP_036545	Glutaminyl cyclase	SP_{2D}
SLPI	NP_003055	Leukocyte anti-elastase	SP_{2D}
LTA4H	NP_000886	Leukotriene A4 Hydrolase	SP_{2D}
MMP8	NP_002415	Neutrophil collagenase	$SP_{2D\ LCMS}$
PTX3	NP_002843	Pentraxin-3	$SP_{2D\ LCMS}$
PFC	NP_002612	Properdin P factor	SP_{2D}
T6GALNAC3	NP_694541	Sialyltransferase 3	SP_{2D}
AZU1	NP_001691	Azurocidin 1 preproprotein	GE_{LCMS*},SP_{LCMS},AZ_{LCMS}
BPI	NP_001716	Bactericidal/permeability-increasing protein	GE_{LCMS},SP_{LCMS},AZ_{LCMS}
CALR	NP_004334	Calreticulin precursor	GE_{2D},$SP_{2D\ LCMS*}$,AZ_{LCMS*}
CAMP	NP_004336	hCAP-18	GE_{2D},$SP_{2D\ LCMS}$,$AZ_{2D\ LCMS}$
CTSG	NP_001902	Cathepsin G preproprotein	$GE_{2D\ LCMS}$,$SP_{2D\ LCMS}$,$AZ_{2D\ LCMS}$
CHIT1	NP_003456	Chitotriosidase	GE_{2D},$SP_{2D\ LCMS*}$,AZ_{LCMS*}
EPX	NP_000493	Eosinophil peroxidase	GE_{LCMS},SP_{LCMS},AZ_{LCMS}
FTL	NP_000137	Ferritin, light polypeptide	GE_{2D},SP_{2D},AZ_{LCMS}
RETN	NP_065148	FIZZ-3, resistin	GE_{2D},SP_{2D},AZ_{2D}
OLFM4	NP_006409	GW112	GE_{LCMS*},$SP_{2D\ LCMS}$,AZ_{LCMS*}
LTF	NP_002334	Lactoferrin	$GE_{2D\ LCMS}$,$SP_{2D\ LCMS}$,$AZ_{2D\ LCMS}$
CST7	NP_003641	Leukocystatin; Cystatin	GE_{2D},SP_{2D},AZ_{LCMS}
LCN2	NP_005555	Lipocalin 2; NGAL	$GE_{2D\ LCMS}$,$SP_{2D\ LCMS}$,AZ_{LCMS}

LYZ	NP_000230	Lysozyme precursor	GE_{2D},$SP_{2D\ LCMS}$,$AZ_{2D\ LCMS}$
MMP9	NP_004985	Gelatinase	$GE_{2D\ LCMS}$,$SP_{2D\ LCMS}$,AZ_{LCMS}
MPO	NP_000241	Myeloperoxidase	$GE_{2D\ LCMS}$,$SP_{2D\ LCMS}$,$AZ_{2D\ LCMS}$
PRTN3	NP_002768	Proteinase 3	GE_{LCMS},SP_{LCMS},AZ_{LCMS}
PRG2	NP_002719	Proteoglycan 2	GE_{LCMS},SP_{LCMS},AZ_{LCMS}
CTSZ	NP_001327	Cathepsin Z (X)	SP_{2D},AZ_{LCMS*}
ELA2	NP_001963	Elastase 2	SP_{LCMS*},AZ_{LCMS}
CRISP3	NP_006052	sgp-28	SP_{2D},$AZ_{2D\ LCMS*}$
PPGB	NP_000299	Cathepsin A	AZ_{LCMS}
CTSC	NP_001805	Cathepsin C	AZ_{LCMS}
TPP1	NP_000382	Tripeptidyl-peptidase I	AZ_{LCMS}
DPP7	NP_037511	Dipeptidyl peptidase 7 preproprotein	AZ_{LCMS}
GGH	NP_003869	Gamma-glutamyl hydrolase precursor	AZ_{LCMS}
GUSB	NP_000172	Glucuronidase, beta	AZ_{LCMS}
HEXA	NP_000511	Hexosaminidase A preproprotein	AZ_{LCMS}
HEXB	NP_000512	Hexosaminidase B preproprotein	AZ_{LCMS}
HYAL3	NP_003540	Hyaluronidase 3	AZ_{LCMS}
ACP6	NP_057445	Lysophosphatidic acid phosphatase	AZ_{LCMS}
ACP2	NP_001601	Lysosomal acid phosphatase 2	AZ_{LCMS}
GAA	NP_000143	Lysosomal alpha-glucosidase	AZ_{LCMS}
MAN2B1	NP_000519	Mannosidase, alpha B, lysosomal	AZ_{LCMS}

Membrane Traffic and Fusion Proteins			
Entrez Gene	**Entrez Protein**	**Protein Name**	**Granule Type$_{METHOD}$**
MBC2	NP_056107	KIAA0747 protein (membrane bound C2 domain-containing)	GE_{LCMS}
SNAP23	NP_003816	SNAP-23A	GE_{LCMS}
SACM1L	NP_054735	Synaptojanin	GE_{LCMS}
UNC13D	XP_113950 NP_954712	Unc-13 homolog D	GE_{LCMS}
DYSF	NP_003485	Dysferlin	GE_{LCMS},SP_{LCMS}
CLTC	NP_004850	Clathrin heavy chain 1	SP_{LCMS}
STXBP2	NP_008880	Hunc18b	SP_{2D}
DNAJC5	NP_079495	DnaJ (Hsp40) homolog, subfamily C, member 5	GE_{LCMS},SP_{LCMS*},AZ_{LCMS*}
STX7	NP_003560	Syntaxin 7	GE_{LCMS},SP_{LCMS*},AZ_{LCMS}
VAMP2	NP_004772 NP_055047	VAMP 2	GE_{LCMS},SP_{LCMS*},AZ_{LCMS*}
VAMP8	NP_003752	VAMP 8	GE_{LCMS},SP_{LCMS},AZ_{LCMS}
SYTL1	NP_116261	Synaptotagmin-like 1	AZ_{LCMS}
C20orf178	NP_789782	Snf7 homologue associated with Alix 1	AZ_{LCMS}

Redox Proteins			
Entrez Gene	**Entrez Protein**	**Protein Name**	**Granule Type$_{METHOD}$**
DIA1	NP_000389 NP_015565	Cytochrome b5 reductase	GE_{LCMS}
NQO3A2	NP_057327	Cytochrome b5 reductase 1 (B5R.1)	GE_{LCMS}
GSTK1	NP_057001	Glutathione transferase kappa 1	GE_{LCMS}
SOD2	NP_000627	Mn SOD chain b	GE_{2D}
NDUFB8	NP_004995	NADH dehydrogenase 1 beta subcomplex, 8	GE_{LCMS}
ND5	NP_536853 NP_776061	NADH dehydrogenase subunit 5	GE_{LCMS}
NDUFB11	NP_061929	Neuronal protein 17.3	GE_{LCMS}
HSD17B12	NP_057226	Steroid dehydrogenase homolog	GE_{LCMS}
SQRDL	NP_067022	Sulfide dehydrogenase	GE_{LCMS}
TXNDC	NP_110382	Thioredoxin-related transmembrane protein	GE_{LCMS}
DHRS8	NP_057329	Dehydrogenase/reductase member 8	GE_{LCMS},SP_{LCMS}
GAPD	NP_002037	Glyceraldehyde-3-phosphate dehydrogenase	SP_{LCMS}
PRDX5	NP_036226 NP_857634	Peroxiredoxin 5 precursor	SP_{LCMS}
CYBA	NP_000092	p22-phox	GE_{LCMS},SP_{LCMS},AZ_{LCMS*}
PDIA3	NP_005304	Grp58	$GE_{2D\ LCMS}$,$SP_{2D\ LCMS*}$,AZ_{LCMS}
CYBB	NP_000388	gp91-phox	GE_{LCMS},SP_{LCMS},AZ_{LCMS}

Miscellaneous Proteins			
Entrez Gene	Entrez Protein	Protein Name	Granule Type$_{METHOD}$
CA4	NP_000708	Carbonic anhydrase IV	GE_{2D}
CGI-51	NP_056195	CGI-51 protein	GE_{LCMS}
ENO1	NP_001419	Enolase	GE_{2D}
FGG	NP_000500 NP_068656	Fibrinogen γ chain precursor	GE_{LCMS}
GPI	NP_000166	Glucose phosphate isomerase	GE_{LCMS}
E2IG5	NP_055182	Growth and transformation-dependent protein	GE_{LCMS}
HNRPU	NP_004492 NP_114032	hnRNP U protein	GE_{LCMS}
ATAD3A	NP_060658	Hypothetical protein FLJ10709	GE_{LCMS}
TNFAIP9	NP_078912	Hypothetical protein FLJ23153	GE_{LCMS}
EFHA1	NP_689939	Hypothetical protein FLJ34588	GE_{LCMS}
TMEM43	NP_077310	Hypothetical protein MGC3222	GE_{LCMS}
LOC255809	XP_172995	Hypothetical protein XP_172995	GE_{LCMS}
IDH2	NP_002159	Isocitrate dehydrogenase	GE_{2D}
KIAA0792	XP_375848	KIAA0792 gene product	GE_{LCMS}
LAP1B	NP_056417	Lamina-associated polypeptide 1B	GE_{LCMS}
LST1	NP_995309 NP_995310 NP_995311 NP_995312	Leukocyte specific transcript 1	GE_{LCMS}
MMAA	NP_758454	Methylmalonic acidurea	GE_{2D}
PHB2	NP_009204	Prohibitin-like	GE_{LCMS}
RPN1	NP_002941	Ribophorin I	GE_{LCMS}
RPN2	NP_002942	Ribophorin II precursor	GE_{LCMS}
TMEM16F	XP_113743	Similar to RIKEN cDNA F730003B03	GE_{LCMS}
ALB	NP_000468	Albumin	$GE_{2D\ LCMS^*}$,$SP_{2D\ LCMS^*}$
C20orf3	NP_065392	C20 ORF 3; adipocyte plasma membrane-associated	GE_{LCMS},SP_{LCMS}
DSP	NP_004406	Desmoplakin	GE_{LCMS},SP_{LCMS^*}
FGB	NP_005132	Fibrinogen β chain preproprotein	GE_{LCMS},SP_{LCMS^*}
GCA	NP_036330	Grancalcin	$GE_{2D\ LCMS}$,$SP_{2D\ LCMS}$
HBB	NP_000509	Hemoglobin	GE_{2D},SP_{2D}
HSPA1A	NP_005336	Hsp70 1A	$GE_{2D\ LCMS^*}$,SP_{2D}
LOC199675	NP_777578	Hypothetical protein LOC199675	GE_{LCMS},SP_{LCMS}
PHB	NP_002625	Prohibitin	$GE_{2D\ LCMS}$,$SP_{2D\ LCMS}$
P4HB	NP_000909	PDI	$GE_{2D\ LCMS}$,SP_{2D}
PKM2	NP_002645 NP_872270 NP_872271	Pyruvate kinase 3 isoform	GE_{LCMS},SP_{LCMS}
RTN4	NP_065393 NP_722550 NP_008939 NP_997403 NP_997404	Reticulon 4	GE_{LCMS},SP_{LCMS^*}
LOC388015	XP_370776	Similar to RTI1	GE_{LCMS},SP_{LCMS}
HRNR	XP_373868 NP_001009931	Similar to hornerin	GE_{LCMS},SP_{LCMS^*}
SEMG1	NP_002998 NP_937782	Semenogelin I	GE_{LCMS^*},SP_{2D}
SEMG2	NP_002999	Semenogelin II	GE_{LCMS^*},SP_{2D}
B3GTL	NP_919299	β 3-glycosyltransferase-like	SP_{LCMS}
S100A12	NP_005612	Calgranulin C	SP_{2D}
EP300	NP_001420	E1A binding protein p300	SP_{LCMS}
GALIG	NP_919308	Galectin-3 internal gene	SP_{LCMS}
PPFIBP1	NP_003613 NP_803193	Liprin-like	SP_{2D}
EHD1	NP_006786	Testilin	$SP_{2D\ LCMS^*}$
PPIA	NP_066953 NP_982254 NP_982255	Cyclophilin A	GE_{2D},SP_{LCMS^*},AZ_{LCMS^*}
HCLS1	NP_005326	Hematopoietic cell-specific Lyn substrate 1	GE_{LCMS^*},SP_{LCMS^*},AZ_{LCMS}
HIST1H1C	NP_005310	Histone H1 family	GE_{LCMS},SP_{LCMS^*},AZ_{LCMS}
HIST1H2BG	NP_003509	Histone H2B	GE_{LCMS},SP_{LCMS^*},AZ_{LCMS}

HIST1H4I	NP_003486	Histone H4	GE_{LCMS},SP_{LCMS},AZ_{LCMS}
HSPA5	NP_005338	Hsp70 5A	GE_{2D},$SP_{2D\ LCMS}$,AZ_{LCMS}*
S100A8	NP_002955	MRP-8	$GE_{2D\ LCMS}$,$SP_{2D\ LCMS}$,AZ_{LCMS}*
S100A9	NP_002956	MRP-14	$GE_{2D\ LCMS}$,$SP_{2D\ LCMS}$,AZ_{LCMS}*
TOLLIP	NP_061882	Toll-interacting protein	GE_{LCMS}*,SP_{2D},AZ_{LCMS}
RPS27A UBB UBA52 UBC	NP_002945 NP_061828 NP_003324 NP_066289	Ubiquitin precursor	GE_{LCMS},SP_{LCMS},AZ_{LCMS}
C9orf19	NP_071738	C9orf19, GAPR-1	SP_{LCMS},AZ_{LCMS}
TMEM30A	NP_060717	Hypothetical protein FLJ10856	SP_{LCMS},AZ_{LCMS}
DDX4	NP_061912	DEAD (Asp-Glu-Ala-Asp) box polypeptide 4	AZ_{LCMS}
ARL10B	NP_620150	Hypothetical protein BC015408	AZ_{LCMS}
FLJ22662	NP_079105	Hypothetical protein FLJ22662	AZ_{LCMS}
SQSTM1	NP_003891	Sequestosome 1	AZ_{LCMS}

All proteins identified on neutrophil granules by 2DE MALDI-TOF MS and 2D-HPLC ESI-MS/MS are listed. A total of 286 proteins were identified and proteins were catalogued by function based on a literature search for each protein in the PubMed database. The gene and protein designation, method of identification, and granule subset on which the protein was found are listed. To be listed as a component of the granule subset, a protein was either identified from a granule subset by MALDI-MS analysis of 2D gels, detected by at least 2 of 3 2D-HPLC ESI-MS/MS experiments, or detected by 2D-HPLC ESI MS/MS experiment once in one granule subset, and additionally detected by 2DE MALDI-MS or at least twice by 2D-HPLC ESI-MS/MS in a different granule subset (indicated by an asterisk near the method designation in "Granule $Type_{METHOD}$" column of Table 2). In the method designation, LCMS is an abbreviation for 2D-HPLC ESI-MS/MS and 2D is an abbreviation for 2DE MALDI-TOF MS.

identified once in a given granule subset by 2D-HPLC ESI-MS/MS, and identified by either 2DE or at least twice by 2D-HPLC ESI-MS/MS in another granule subset, are listed in the Supplementary Table 2. Sequences of corresponding peptides and the percent coverage of identified proteins are also shown.

To eliminate proteins present as contaminants of granule subsets, proteins that were detected by only one of the three 2D-HPLC-ESI-MS/MS experiments were classified as rejected proteins. Supplementary Table 3 lists the rejected proteins for each granule subset. A total of 344 proteins were rejected from gelatinase granules, 211 from specific granules, and 230 from azurophil granules. Most rejected proteins were of ribosomal, nuclear and mitochondrial origin, or were hypothetical proteins, suggesting that the granule isolation method resulted in contamination with small amounts of other subcellular organelles. That some contamination did occur is supported by identification of several proteins listed in Table 3. The benzodiazepine receptor was described previously to be present on mitochondria [243]. Lamin B receptor and Sad1 are of nuclear origin [244,245], suggesting that membranes from these structures contaminated granule preparations. The presence of signaling proteins (GRK6, PAK5, small GTPases of the Ras, Rab, and Rho family, and heterotrimeric G protein subunits) and membrane trafficking proteins (syntaxin 2, syntaxin 3A, syntaxin 8, syntaxin 10, and syntaxin 11) in the list of rejected proteins suggests the exclusion criteria eliminated some proteins that are likely components of the granule proteome. Functional classification of proteins was performed by a literature search for each protein in the PubMed database.

Receptors and Cytoskeletal Membrane Anchors. This group included transmembrane proteins involved in adhesion, transmigration, cellular activation, and

cytoskeletal anchoring to the membrane, including components of lipid rafts. Of the 40 proteins, 12 were identified only from gelatinase granules, 19 were found on both specific and gelatinase granules, 6 were found on all three granule types, and three were found only on azurophil granules. Proteins unique to specific granules were not found in this group. Formyl peptide receptors, CR1, CD11b, CD18, SCAMPs Stomatin, CD63, and LAMPs have been identified previously as components of neutrophil granules [8,9,40].

Channels and Transporters. Proteins that function in facilitating the movement of solutes across lipid bilayers were included in this category. Thirteen proteins were identified only on gelatinase granules, 10 from gelatinase and specific granules, two from all three granule subtypes, and two only from azurophil granules. These proteins included proton pumps and transporters for metal ions, glucose, adenine nucleotides, amines, and steroids. Eleven of these proteins were described previously to be of mitochondrial origin.

GTPases. This group included both monomeric and heterotrimeric GTPases, and two GTPase-activating protein. Of the total of 21 identified proteins, 10 were found on gelatinase granules only, one was only from specific granules, two from specific and gelatinase granules, and 8 from all three granule subsets. Monomeric GTPases of the Rab family and Cdc42 have been shown to be involved in granule exocytosis in other cell types [246-248]. Of note, Rab27A was shown previously to associate with many types of granules and play a crucial role in exocytosis by modulating granule binding with cytoskeleton and with proteins that control membrane fusion [249]. Rab27A was a component of all three granule types. To our knowledge this is the first report of the

presence of Rab27A in neutrophils. Cdc42 was also found on all three granule subsets. This Rho family GTPase stimulates exocytosis by activating the IP_3 and calcium second messenger signaling pathway [248].

Structural Proteins and Adaptors. We included cytoskeletal proteins and actin-binding proteins in this group. Eleven proteins were identified only on gelatinase granules, 13 from gelatinase and specific granules, four from specific granules only, ten from all three granule types, and two from only azurophil granules. The presence of actin, tubulin, and vimentin on all three granule subtypes is consistent with a role for these cytoskeletal structures in neutrophil exocytosis [8,9,92,98]. Visual inspection of 2D gels suggested that greater amounts of cytoskeletal proteins were associated with gelatinase granules than specific granules, which in turn had more than azurophil granules. To confirm this observation, western blotting of whole granules for actin was performed following normalization for membrane content using a membrane-binding fluorescent dye (Figure 7). The amount of actin associated with gelatinase granules was dramatically greater than that associated with specific granules. A minimal amount of actin was associated with azurophil granules.

Kinases and Phosphatases. This group included tyrosine kinases, tyrosine phosphatases, and one kinase scaffolding protein, MEK1-binding protein. Tyrosine kinases were previously identified on neutrophil granules, and inhibition of tyrosine kinase activity prevents neutrophil degranulation [152-155]. To our knowledge, this is the first report of a tyrosine phosphatase association with neutrophil granules. Tyrosine phosphatases are localized to granules in other cells, and they have been shown to participate in signaling leading to exocytosis [250-253].

Figure 7. Assessment of actin content on neutrophil granules by western blotting. Membrane lipid content was quantitated in neutrophil granules by TMA-DPH lipophilic dye and granule proteins were loaded such that amounts of granule membranes loaded were equal among different granule subsets. Proteins were transferred to nitrocellulose and probed for actin with an anti-actin antibody.

Figure 7

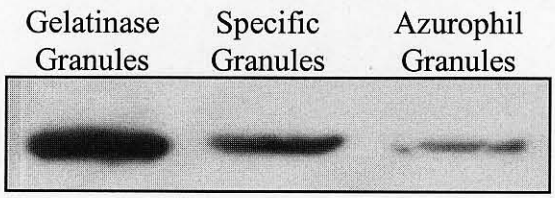
Gelatinase Granules
Specific Granules
Azurophil Granules

Luminal and Host Defense. This group included proteins localized to granule lumens and luminal and membrane proteins that participate in host defense, such as the membrane proteases neprilysin and leukolysin. Four proteins were identified on gelatinase granules only, 13 proteins from gelatinase and specific granules, eleven proteins only from specific granules, 18 from all three granule subsets, three from specific and azurophil granules, and 13 from azurophil granules only. All of the luminal proteins in this list are annotated on the NCBI database as proteins destined either to lysosomal or to secretory compartments. Proteins of lysosomal origin were found previously in azurophil granules, in agreement with the hypothesis that azurophil granules are lysosome-related organelles [8,9]. Among the identified proteins in this group was calreticulin, a component of the endoplasmic reticulum [254]. Calreticulin may also be a *bona fida* granule protein, however, as it acts as a chaperone for neutrophil granule luminal proteins [255] and is present on the extracellular surface of the neutrophil plasma membrane [256]. Calreticulin was identified as a cytolytic component of T lymphocyte granules [257].

Membrane Traffic and Fusion. In this group 4 proteins were found on gelatinase granules only, one from gelatinase and specific granules, two from specific granules alone, four from all three granule types, and two from azurophil granules only. Hunc18b (Munc18-2) and Unc-13 homolog 3 (Munc-13), have not been previously identified in neutrophils. These proteins are members of a family of proteins that bind to and modulate the activity of membrane fusion proteins [47,57]. A hypothetical protein with a C2 domain, which is known to be involved in membrane fusion events [258], was identified on gelatinase granules. Syntaxin 7 and VAMP 8 were expressed on all three granule

subsets. These two membrane fusion proteins have not been previously identified from neutrophil granules.

Redox Proteins. Proteins involved in redox reactions, including a transmembrane protein related to thioredoxin and the components of the neutrophil NADPH oxidase, p22-phox and gp91-phox, were included in this group. Ten proteins were found only on gelatinase granules, one from gelatinase and specific granules, two from specific granules alone, and three from all three granules. Components of the NADPH oxidase were found on all three granule subsets.

Miscellaneous Proteins. This group included proteins not classified into the other groups or for which no function has been described. Twenty-one proteins were identified on gelatinase granules, 16 from gelatinase and specific granules, 6 from specific granules only, 10 from all three granule types, two from specific and azurophil granules, and four from azurophil granules only. Among the proteins found were chaperones such as PDI and Hsp70 and 11 hypothetical proteins. Hemoglobin was also found on gelatinase and specific granules, suggesting that hemoglobin from lysed red blood cells binds to phospholipid membranes. Hemoglobin was completely removed from granule membranes by sodium carbonate treatment.

Discussion

Using two approaches, 2DE followed by MALDI-MS and 2D-HPLC ESI-MS/MS, 286 granule and granule-associated proteins from human neutrophils were identified. Only 87 proteins were identified by 2DE and MALDI-MS, of which 56 were abundant structural or luminal proteins. The only transmembrane spanning proteins

identified after 2DE were the integrins, CD11b and CD18, both of which have a single transmembrane domain. The limited protein identification using intact granules was marginally enhanced by fractionation of granule proteins using sodium carbonate treatment or ammonium sulfate precipitation. These results emphasize the recognized limitations to 2DE-based proteomics, namely, the bias against low abundance proteins, transmembrane proteins, and proteins at the extremes of isoelectric point and molecular mass [206,259]. Despite these limitations, 39 proteins were identified only by the 2DE-based approach.

The 2DE analysis of whole granules revealed that the quality of protein separation paralleled the density of the lumen matrix for each granule subset [8-10,19]. This is likely due to the presence of large amounts of basic proteins in the granule lumens that interfere with IEF and render the less abundant membrane-associated proteins unable to focus. This observation led to attempts to fractionate granule proteins with alkaline sodium carbonate or precipitation with various concentrations of ammonium sulfate. The sodium carbonate method fractionated granule proteins largely into luminal and membrane fractions. This method resulted in effective 2DE separation of specific granule proteins, possibly because these granules contain large amounts of moderately cationic luminal proteins that can be dissociated from the luminal matrix and granule membranes. The less dense granule matrix of gelatinase granules was associated with adequate protein resolution by 2D gels, resulting in minimal improvement after sodium carbonate extraction of luminal proteins. Sodium carbonate extraction did not improve separation and identification of proteins from azurophil granules, which contain a highly packed matrix of acid mucopolysaccharide and highly cationic myeloperoxidase [260]. Sodium

carbonate treatment of gelatinase, but not specific granules, also resulted in the significant loss of low molecular weight proteins, compared to 2DE of whole granules (compare Figure 4A with Figures 5A and 5B).

The failure of sodium carbonate extraction to improve protein identification of gelatinase or azurophil granules prompted us to seek an alternative method of protein fractionation based on a different physical characteristic. Ammonium sulfate precipitation fractionates proteins according to their solubility in concentrated ammonium sulfate solutions. For neutrophil granules, this method separated cytoskeletal and cytoskeleton-binding proteins from more hydrophilic luminal proteins. This fractionation method enhanced protein separation and identification of gelatinase granule proteins (Figure 5C and 5D). Fractionation of specific and azurophil granule proteins by ammonium sulfate precipitation did not improve protein separation or identification. This was likely due to the fact that most of the protein content in these granules was of luminal origin and, therefore, hydrophilic. Such proteins precipitate at high concentrations of ammonium sulfate and therefore they precipitated in the 100% ammonium sulfate solution. More hydrophobic proteins, which were mostly cytoskeletal and were less abundant, precipitated in the 20% ammonium sulfate solution. The use of other concentrations of ammonium sulfate did not result in improved fractionation of granule proteins (data not shown). Thus, sodium carbonate treatment was more effective for identification of specific granule proteins, while ammonium sulfate precipitation was more effective for identification of gelatinase granule proteins. Neither approach improved protein identification from azurophil granules. These results indicate that optimal protein

extraction and separation of granule proteins by 2DE is highly dependent on the properties of the granule matrix and luminal proteins.

To overcome the limitations of 2DE-based protein identification, granule proteins were also identified by strong cation exchange reversed-phase two-dimensional chromatography combined with ESI-MS/MS, commonly referred to as DALPC or MudPIT [214-216,261]. To enhance the sensitivity of this approach for membrane spanning and membrane-associated proteins, sodium carbonate extraction was used to remove luminal and cytoskeletal proteins [238,240-242,262]. As shown by the comparison of Figure 4 with Figures 5 and 6, the use of sodium carbonate significantly reduced high abundance luminal proteins, while the reduction in cytoskeleton was modest. 2D-HPLC ESI-MS/MS identified 247 proteins from the three granule subsets.

The distribution of proteins among the granule subsets indicates that approximately half were present on more than one granule subset. The presence of proteins in more than one granule subset could be due to neutrophil granule biogenesis or to cross-contamination among the granule subsets following separation by Percoll gradient centrifugation. Granule biogenesis occurs during myeloid cell maturation, with different granules forming at different stages of differentiation. The protein content of these granules is determined by the timing of protein synthesis relative to formation of different granule subsets, not by selective targeting of proteins to different granules [8,9,24,31,32,231,232]. The relative purity of granule subset preparations was addressed to determine the quality of the proteome for each granule. The distribution of markers for each granule subset showed granule separation similar to that reported by other groups [10,19]. Western blot analysis for CD66b, a marker for specific granules, showed that

gelatinase and azurophil granules were not contaminated by specific granules. The presence of gelatinase in the specific granule preparation is consistent with a previous study showing that 60% of myeloperoxidase-negative granules contain gelatinase, in addition to a marker of specific granules, lactoferrin [8,9]. The presence of myeloperoxidase in specific and gelatinase granules may be due to the extremely basic nature of this protein, which allows myeloperoxidase released from azurophil granules to bind to phospholipid membranes of other granules. Based on current separation techniques and known granule markers, however, minimal cross-contamination among the granule subsets cannot be excluded.

We attempted to establish a valid list of proteins for each granule type by rejecting proteins that were identified in only one of three 2D-HPLC ESI-MS/MS experiments. A total of over 500 proteins, including nuclear, mitochondrial, ribosomal, and cytosolic proteins were rejected using this exclusion criterion. A few contaminating proteins may have still been present in granule proteomes, as several mitochondrial membrane transporters were identified in more than one granule preparation, especially in the lighter gelatinase granule fraction. This is likely due to the fact that gelatinase granules sediment at a density of 1.08 g/ml in Percoll [10,19], while mitochondria sediment at a density of 1.05 g/ml [263]. Histones were also identified in all three granule subsets. Their presence may reflect nuclear contamination from the reported breakage of 16% of nuclei during nitrogen cavitation of neutrophils [10,19] and subsequent non-specific binding to granule membranes. Histones recently were described to co-localize with granule enzymes in neutrophil extracellular traps [264]. Subcellular fractionation showed that murine macrophage granules contained histones [265]. Histones were also

secreted by amnion cells [266]. Thus, histones may be components of neutrophil granules. The list of rejected proteins contained several proteins, including syntaxins and synaptobrevin-like proteins, that regulate granule membrane fusion. Although none of these proteins have been identified previously on neutrophil granules, these results suggest the possibility that some granule proteins may have been excluded by the criteria used in this study. The presence of false positive and false negative results indicates that defining subcellular organelle proteomes using highly sensitive mass spectrometry-based techniques is limited by the ability to purify these organelles. Ultimately, confirmation that a specific protein is present in an organelle will require histologic studies.

Analysis of the distribution of proteins among the granule subsets revealed differences among the subsets that suggest functional heterogeneity. The total number of proteins and the number of proteins in each functional classification, except for luminal proteins, increased from azurophil to specific to gelatinase granules. The number of luminal proteins identified was greatest in specific granules (45 proteins) while azurophil (34) and gelatinase (35) granules contained similar number of proteins. Gelatinase granules are the most easily mobilized granules in neutrophils, and, therefore, these granules will undergo exocytosis at an earlier stage of neutrophil activation than specific or azurophil granules. Gelatinase granule membranes contain a large number of membrane receptors and adhesion molecules, as well as being associated with the largest amount of actin cytoskeleton and cytoskeletal regulatory proteins. These results support a role for gelatinase granules in enhancing the plasma membrane expression of molecules necessary for neutrophil adherence to and migration through inflamed vascular endothelium and for subsequent chemotaxis. On the other hand, azurophil granules

primarily fuse with phagosomes, while exocytosis is negligible. These granules contain the largest number of luminal bactericidal proteins, while there is a paucity of membrane, cytoskeletal, and GTP-binding proteins. The greater complexity of the specific granule lumen and the presence of a significant number of transmembrane and membrane-associated proteins suggests that these granules represent a transitional phase that can contribute to neutrophil activation through exocytosis or provide bactericidal proteins to phagosomes. Our results also suggest a differential role of the actin cytoskeleton in regulation of granule exocytosis. Gelatinase granules, the most easily mobilizable granule subset, are associated with the largest amount of actin cytoskeleton. On the other hand, azurophil granules are associated with very little actin, and they fail to exhibit exocytosis unless the subplasma membrane actin cytoskeleton is disrupted [8,9]. Once again, specific granules represent a transition between these two extremes. Previous reports have emphasized the role of the subplasma membrane actin cytoskeleton as a barrier to granule exocytosis [79]. The present study suggests that the actin cytoskeleton associated with granules also plays an active role in mediating exocytosis.

To our knowledge, this is the first proteomic study of neutrophil granules. The importance of regulated exocytosis in determining the activation state of neutrophils, and the use of regulated exocytosis by a large number of other cells, indicates the value of defining granule proteomes. The methodology described herein provides an approach to defining granule proteomes. In our experience, 2DE identified and revealed relative distribution of more abundant proteins in granules, while 2D-HPLC ESI-MS/MS identified less abundant proteins and hydrophobic proteins not amenable to detection by 2DE. The sensitivity of this latter approach demands that granules be isolated to a high

degree of purity and/or experimental approaches be employed to eliminate false positive protein identification. Our data show that neutrophil granules are complex organelles. Analysis of the more than 200 proteins associated with neutrophil granules will allow a better understanding of the contribution of each of the granule subsets to neutrophil biology.

CHAPTER III

MYELOID-RELATED PROTEIN-14 IS A P38 MAPK SUBSTRATE IN HUMAN NEUTROPHILS

Foreword

Proteomic analysis of neutrophil granules revealed the presence of four confirmed MK2 substrates, 14-3-3ζ, LSP-1, p16-Arc, and vimentin, on neutrophil granules. These proteins may play an indirect role in exocytosis by affecting actin polymerization, and thus are likely to influence a number of other cellular functions. No known p38 substrate was identified. To identify novel substrates, we screened granule proteome for MK2 and p38 MAPK-mediated phosphorylation by using recombinant active kinases and urea lysates of gelatinase granules [198,199]. We chose gelatinase granules due to the relative ease of separation of proteins from these granules on 2D gels, compared to specific or azurophil granules. Screening of gelatinase granule proteins for phosphorylation by MK2 revealed two spots on autoradiographs that were specific to the presence of the kinase in the reaction mixture (Figure 8A). One of these spots matched to a spot on the Coomassie stained gel, and was identified as vimentin. A similar assay identified MRP-14 as a novel substrate of p38 MAPK (Figure 8B). Because of its novelty as a substrate, its ability to bind calcium and arachidonate (mediators involved in exocytosis), and its abundance in neutrophils, we decided to further study the phosphorylation of this protein.

Figure 8. Phosphorylation of urea-solubilized gelatinase granule proteins by MAPKAPK-2 and p38 MAPK in the presence of [γ^{32}P]ATP. Granule proteins were solubilized in a kinase buffer containing 9 M urea, urea concentration was subsequently reduced by buffer exchange to 1 M and [γ^{32}P]ATP and a recombinant kinase were added to the reaction mixture [198,199]. Proteins were separated by 2DE, gels were stained with Coomassie blue dye and autoradiograms were obtained. Proteins were identified by MALDI-TOF MS. Panel A shows that only vimentin phosphorylation was observed when active recombinant MAPKAPK-2 (MK2) was included in the reaction mixture. When active recombinant p38 MAPK (p38) was included in the reaction mixture, MRP-14 was phosphorylated (Panel B).

Figure 8

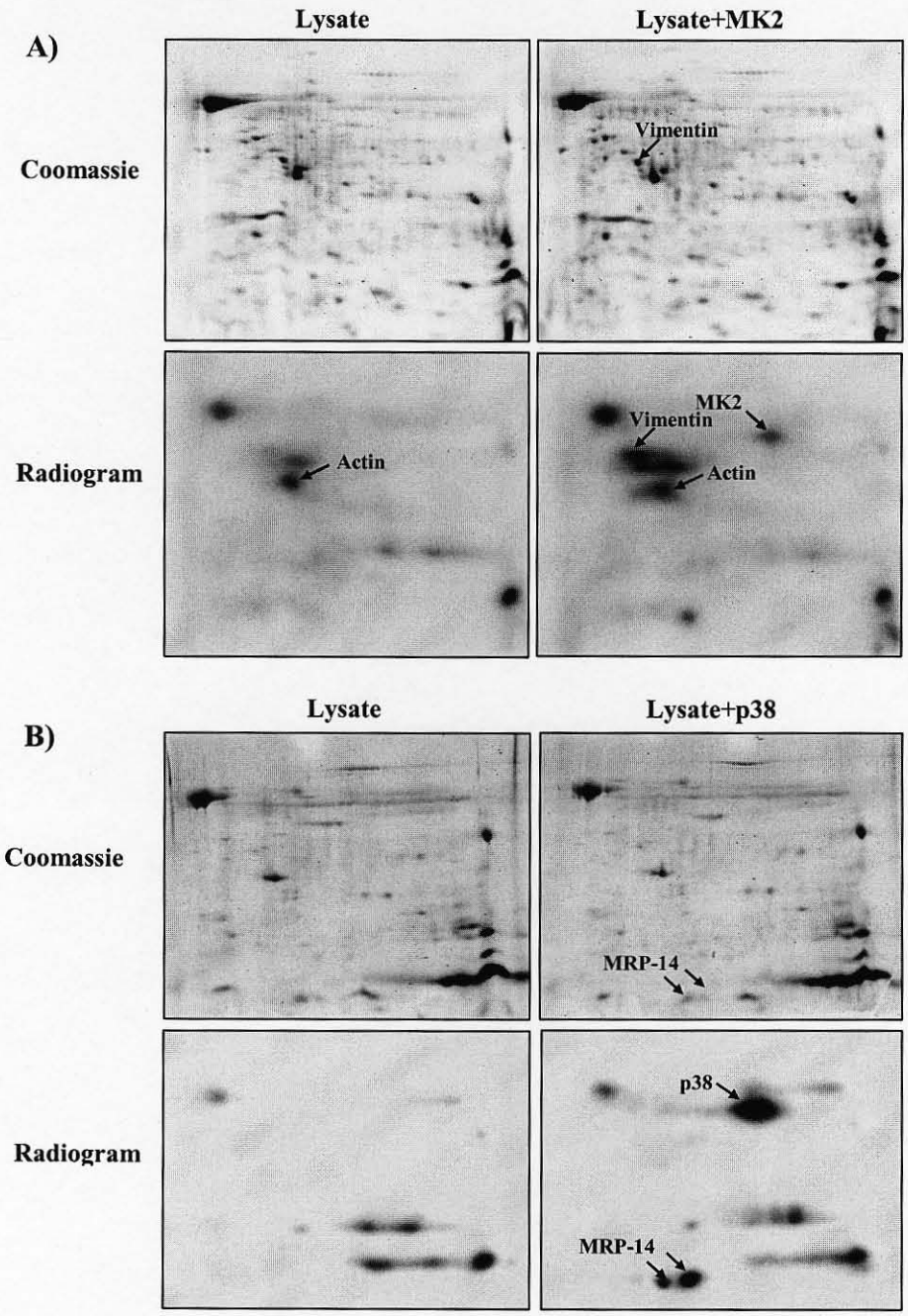
A)
Lysate
Lysate+MK2
Coomassie
Vimentin
Radiogram
Actin
MK2
Vimentin
Actin
B)
Lysate
Lysate+p38
Coomassie
MRP-14
Radiogram
p38
MRP-14

Introduction

Circulating neutrophils are relatively benign cells that undergo a series of phenotypic changes in response to inflammatory stimuli, converting them into cells capable of adherence to vascular endothelium; migration to sites of infection; phagocytosis of bacteria; and rapid bacterial killing through exposure to proteolytic enzymes, antimicrobial peptides, and reactive oxygen species. A number of neutrophil responses, including chemotaxis, granule exocytosis, respiratory burst activity, and production of chemokines, are dependent on the activation of the p38 MAPK pathway [15,172-175,180,186,188,194,195,267,268]. MAPK pathways consist of three-kinase modules formed by the terminal MAPKs, which in turn are activated by dual-specificity serine-threonine/tyrosine kinases termed MAP2Ks, which in turn are activated by serine-threonine kinases termed MAP3Ks [166,168,269]. For the p38 MAPK pathway MKK3 and MKK6 serve as MAP2Ks, and MEKK2, MEKK3, ASK1, Tpl-2, and TAK1 have been identified as MAP3Ks. [165,166]. The p38 MAPK pathway is activated in neutrophils by mediators of inflammation, including chemoattractants, cytokines, chemokines, bacterial lipopolysaccharide, tumor necrosis factor-α, and granulocyte-macrophage colony-stimulating factor [172-175,180,267,268].

The signal transduction pathways that lead from p38 MAPK to specific neutrophil functional responses are not well defined. Delineating these signal transduction pathways requires identification of p38 MAPK substrates in neutrophils. A number of p38 MAPK substrates have been identified previously in other cell types, including transcription factors such as ATF2, kinases such as p38-regulated and -activated kinase (PRAK) and MAPK-activated protein kinase 2 (MAPKAPK-2), and cell cycle regulators such as

cyclin D [270-273]. The only p38 MAPK substrates that have been identified in human neutrophils, however, are MAPKAPK-2 and $p47^{phox}$ [175,194,195,274]. The goal of the present study was to identify p38 MAPK substrates in human neutrophils using a functional proteomic approach developed in our laboratory that combines *in vitro* phosphorylation of neutrophil lysate by recombinant kinase, separation of proteins by two-dimensional gel electrophoresis, and phosphoprotein identification by MALDI-TOF mass spectrometry (MALDI-TOF MS) [198,199]. One of the proteins identified was myeloid related protein-14 (MRP-14), a member of the S100 protein family of calcium binding proteins [275,276]. MRP-14 and its binding partner, MRP-8, are highly expressed in neutrophils and monocytes, comprising up to 30% of the total cytosolic protein mass in neutrophils [277,278]. In addition to the unmodified protein of 114 amino acids, an isoform with deletion of the N-terminal four amino acids (MRP-14*) also exists [275-278]. Edgeworth *et al.* [279] reported that MRP-14 and MRP-14* were phosphorylated on Thr-113 in a PKC-independent manner in neutrophils and monocytes after treatment with ionomycin. Bengis-Garber and Gruener [280] also reported that MRP-14 was phosphorylated in neutrophils upon cell exposure to fMLP. Phosphorylation has been implicated in translocation of the MRP-14/MRP-8 heterodimer to membranes and cytoskeleton in monocytes [281]. MRP-14 was also reported to participate in the initiation of NADPH oxidase activity in human neutrophils [282,283]. The present study showed that p38 MAPK phosphorylates MRP-14 on Thr-113. FMLP stimulation of intact neutrophils induced p38 MAPK-dependent phosphorylation and translocation of MRP-14 to Triton X-100 insoluble cytoskeleton. Thus, MRP-14 is a potential mediator of p38 MAPK-dependent functional responses in human neutrophils.

Materials and Methods

Neutrophil Isolation.

Neutrophils were isolated from healthy volunteers using plasma-Percoll gradients as described by Haslett et al. [236]. Trypan blue staining showed that >97% of cells were neutrophils with >95% viability. After isolation, neutrophils were suspended in Krebs-Ringer phosphate buffer (pH 7.2) (KRPB) at the desired concentration. The Human Studies Committee of the University of Louisville approved the use of human donors.

Neutrophil Lysate Preparation

Neutrophil lysate was prepared as previously described [198,199]. In brief, 10^8 cells were lysed in 500 μl of lysis buffer containing 2 M thiourea, 7 M urea, 65 mM CHAPS (3-[(3-cholamidopropyl)-dimethylammmonio]-1-propane-sulfinate), 58 mM dithiothreitol (DTT), and 4.5% ampholytes (pH 3 to 10). Lysates were cleared by centrifugation at 12,000 × g for 20 min at 15°C. Prior to addition of exogenous p38 MAPK, lysate urea concentration was reduced to 1 M by size exclusion chromatography as previously described [198,199].

p38 MAPK Substrate Identification

Neutrophil lysates (400 μg of total protein) were incubated with 10 μCi of [γ-^{32}P]ATP (ICN Biomedicals, Inc.) in the presence and absence of 400 ng of active recombinant p38 MAPKα (Upstate Biotechnology, Lake Placid, NY) at 30°C for 1 h. Kinase reactions were stopped by adding rehydration buffer (8 M urea, 2% CHAPS, 0.01 M dithiothreitol, 2% ampholytes 3–10, and 0.01% bromophenol blue) to give a total

volume of 450 µl. Proteins were separated by isoelectric focusing with 18 cm, pH 3–10 immobilized pH gradient (IPG) strips, followed by size separation with 10% Duracryl™ (Genomic Solutions, Ann Arbor, MI), as previously described [199]. Proteins were stained with SYPRO Ruby fluorescent stain (Molecular Probes, Eugene, OR), and phosphorylation was visualized by autoradiography.

Identification of Proteins by Mass Spectrometry

Protein spots were excised and digested with trypsin by modification of the method of Jensen et al. [284]. The excised gel pieces were incubated for 15 min in 100 mM NH_4HCO_3 and 50% acetonitrile and dried by vacuum centrifugation. Proteins were then reduced by incubation with 20 mM DTT at 56 °C for 45 min, followed by alkylation with 65 mM iodoacetamide in the dark at room temperature for 30 min. Post-alkylation gel pieces were incubated for 15 min in 100 mM NH_4HCO_3 and 50% acetonitrile and dried by vacuum centrifugation. Proteins were hydrolyzed by incubation in 20 ng/ml modified trypsin (Promega) at 37°C overnight. Trypsin-generated peptides were applied by a thin film-spotting procedure for MALDI-TOF MS analysis using α-cyanohydroxycinnamic acid as the matrix on stainless steel targets. Mass spectral data were obtained using a Tof-Spec 2E mass spectrometer (Micromass, Manchester, UK) and a 337-nm N_2 laser at 20–35% power in the reflector mode. Spectral data were obtained by averaging 10 spectra, each of which was the composite of 40 laser firings. Mass axis calibrations were accomplished using peaks from tryptic auto-hydrolysis. Peptide masses obtained by MALDI-TOF MS analysis were used to search the National Center for Biotechnology Information database (NCBI, www.matrixscience.com) to identify the

intact proteins. A MOWSE score >71 was a priori assumed to indicate a significant match, indicating the probability that the match was not a random event.

Isolation of MRP-14/MRP-8 Complex for *In Vitro* Phosphorylation

High solubility of MRP-14/MRP-8 complex in concentrated ammonium sulfate solution was used to isolate these proteins [285]. Neutrophils (3×10^8 cells) were resuspended in 3 ml of lysis buffer containing 20 mM Tris, pH 7.2, 0.5% Triton X-100, 0.5% NP-40, 150 mM NaCl, 20 mM NaF, 0.2 mM orthovanadate, 1 mM EDTA, 1 mM EGTA, 1 mg/mL AEBSF, 0.005 mg/ml leupeptin, and 0.02 mg/mL aprotinin, and disrupted by rotating the tube at room temperature for 15 minutes. Lysates were centrifuged at 14,000 × g for 15 min to pellet the insoluble material and supernatants were removed. Proteins in the supernatant were subjected to precipitation at room temperature by adding 100% saturated ammonium sulfate solution to reach the final concentration of 80% ammonium sulfate. Precipitated proteins were pelleted by centrifugation at 5,000 × g for 15 min and the supernatant was dialyzed overnight at 4°C against a buffer containing 0.1 M Tris-HCl, pH 7.4, 50 mM KCl and 20% glycerol. Protein concentration was adjusted to 1 mg/ml and aliquots were stored at –20 °C.

***In Vitro* Kinase Reactions**

Phosphorylation of purified MRP-14 by p38 MAPKα was performed by incubation of active recombinant p38 MAPK (1 μg) with 10 μCi of [γ-^{32}P]ATP and 12 μg of purified MRP-14/MRP-8 complex in 30 μl of kinase buffer containing 25 mM HEPES, 25 mM β-glycerophosphate, 25 mM $MgCl_2$, 2 mM dithiothreitol, and 0.1 mM $NaVO_3$,

pH 7.2. Reactions were incubated at 30°C for 30 min. Reactions were terminated with SDS sample dilution buffer, proteins were separated by SDS-PAGE on 4-12% Novex™ bis-tris gels (Invitrogen, Carlsbad, CA), gels were stained with Coomassie blue dye, and phosphorylation was visualized by autoradiography.

Identification of the Phosphorylation Site in MRP-14 by Mass Spectrometry

MRP-14/MRP-8 complex (40 μg protein) was incubated for two hours in 60 μl of kinase buffer (50 mM Tris-HCl, pH 7.5, 30 mM $MgCl_2$) containing 5 mM Na_2ATP in the presence or absence of active recombinant p38 MAPKα (1 μg). Proteins were transferred to 100 mM ammonium bicarbonate buffer by ultrafiltration using Nanosep™ 3K Omega ultrafiltration devices (Pall, East Hills, NY) to the final volume of 100 μl. Five nanograms of sequencing grade modified porcine trypsin (Promega, Madison, WI) were added to the protein solution and proteins were digested overnight at 37°C. Generated peptides were subjected to phosphopeptide enrichment by immobilized metal ion affinity chromatography (IMAC) using metal chelate $ZipTip_{MC}$™ columns (Millipore, Bedford, MA) and $FeCl_3$ as a source of metal ions, according to manufacturer's instructions. Resultant peptide solutions were dried by vacuum centrifugation and resuspended in 5 μl of 50 mM ammonium bicarbonate. The matrix, α-cyano-4-hydroxycinnamic acid (HCCA), was prepared by dissolving 8 mg of HCCA in 1 ml of acetonitrile/water (50:50, v/v) containing 0.1% trifluoroacetic acid (TFA). The matrix solution was vortexed until all solids were dissolved. Samples were spotted as 1:1 (v/v) of protein digest:HCCA directly onto MALDI sample targets. Samples were desalted by spotting 0.7 μl 0.1% TFA on each dried sample spot, followed immediately by pipetting off the surface liquid.

Samples were air-dried in the dark and were cleared of particulate matter with compressed gas prior to sample plate loading into the mass spectrometer.

Positive ion MALDI-TOF mass spectra were acquired using an Applied Biosystems (Foster City, CA) AB4700 protein analyzer operating in reflectron mode and with ion source pressure ~0.5 μTorr. After a 400 ns time-delayed ion extraction period, the ions were accelerated to 20kV for TOF mass spectrometric analysis. A total of 600 to 1000 laser shots (355nm Nd:YAG solid state laser operating at 200Hz) were acquired and signal averaged. Data was analyzed using Mascot assuming a) monoisotopic peptides masses, b) cysteine carbamidomethylation, c) variable oxidation of methionine, d) a maximum of one missed trypsin cleavage, and e) a mass accuracy of 100 ppm or better. Limitation of the original protein mass was not employed within the Mascot search.

The protein candidates with Mascot significance scores of $p<0.05$ were a) analyzed for theoretical tryptic fragmentation masses using Peptide Cutter (EXPASY) and b) reanalyzed by Mascot using an additional Mascot scoring parameter of serine/threonine phosphorylation. Peaks identified within the acquired MALDI TOF spectrum matching to the predicted phosphopeptide masses were subjected MALDI TOF-TOF analysis by collision- induced fragmentation (CID) using 1 KeV collision energy and atmospheric gases. Mascot search of the MALDI TOF-TOF data proceeded with search parameters listed above with the inclusion of a mass accuracy of 0.6 Da for peptide fragment masses. MALDI TOF-TOF spectra were used for combined MS/(MSMS) analysis using Global Protein Server software (Applied Biosystems, Forster City, CA) and Mascot. The resultant data were used to determine the presence or absence of phosphorylation and the sequence of the peptide.

Expression of Recombinant Wild Type and Mutant MRP-14

Total RNA from human neutrophils was isolated using RNeasy Mini kit (Qiagen, Germantown, MD). RT-PCR primers were designed according to the cDNA sequence of human MRP-14. The forward primer (5'-CTGTGTGGATCCTCGGCTTTGG-3') incorporated a BamHI restriction enzyme site and the reverse primer (5'-CACTGTAAGCTTAGGGGGTGCC-3') incorporated a HindIII restriction enzyme site. RT-PCR was performed using the SuperScript One-Step RT-PCR kit (Invitrogen) under following conditions: 30 min at 50°C for cDNA synthesis, 2 min at 94°C for strand denaturation, followed by 40 cycles of 30 sec steps at 94 °C (denaturation), 55°C (annealing), and 68°C (extension), and the final extension step of 72°C for 10 min. The PCR product was digested with BamHI and HindIII (Promega) and ligated into pRSET-A plasmid (Invitrogen) using T4 DNA ligase (Promega). Plasmids were propagated in DH5α chemically competent *E. coli* cells (Invitrogen). Threonine 113 mutation to alanine was carried out using the Transformer Site-Directed Mutagenesis kit from BD Biosciences according to manufacturer's instructions. The mutation primer for Thr^{113} to Ala^{113} was 5'-GGGAGGGCGCCCCCTAAG-3' and the selection primer for pRSETA-MRP-14 (mutating the XbaI site) was 5'-CAACGGTTTCCCTCCAGAAATA-3'. Cloning and mutation were confirmed by DNA sequencing. Expression of pRSET-MRP-14 and pRSET-MRP-14^{T113A} plasmids was carried out in BL21(DE3)pLysS chemically competent *E. coli* cells, and protein was purified using the ProBond Purification System (Invitrogen).

Assessment of MRP-14 Phosphorylation *Ex Vivo*

Neutrophils were loaded with [^{32}P]orthophosphate, as previously described by Grinstein *et al.* [286]. Briefly, 8×10^7 cells were suspended in 4 ml of loading buffer (6 mM HEPES, pH 7.4, 150 mM NaCl, 5 mM KCl, 1 mM $MgCl_2$, 0.25 mM $CaCl_2$, 10 mM Glucose) for 5 min and divided into four 1 ml tubes. Two mCi of [^{32}P]orthophosphate was added to each tube, and the cells and were rotated at 37°C for 60 min. SB203580 was added to appropriate tubes to a final concentration of 3 μM simultaneously with orthophosphate. After one hour, fMLP (final concentration 300 nM) was added to appropriate tubes. After 5 min, cells were pelleted at 500 × g, washed once in loading buffer, and the pellet was solubilized in 600 μl of rehydration buffer (7 M urea, 2 M thiourea, 2% CHAPS, 0.01 M dithiothreitol, 2% ampholytes 3–10, and 0.01% bromophenol blue). The lysates were cleared by centrifugation at 14,000 × g, and 155 μl of the supernatant was loaded onto pH 3-10 IPG Zoom™ strips (Invitrogen, Carlsbad, CA) by overnight rehydration at 27°C. Strips were focused on Zoom IPG Runner™ using the following IEF protocol at 200 mA maximum current setting: 200 V for 20 min, 450 V for 15 min, 750 V for 15 min, 2000 V for 30 min. After focusing, strips were sequentially incubated for 10 min in equilibration buffers I (6 M urea, 1% SDS, 2% dithiothreitol, 30% glycerol) and II (6 M urea, 1% SDS, 2.5% iodoacetamide, 30% glycerol). IPG strips were then applied to 4-12% Novex™ bis-tris gels (Invitrogen) and proteins were separated at 200 V for 1 h in X-Cell Sure Lock electrophoresis apparatus. Gels were stained with Coomassie blue dye, and phosphorylation was visualized by autoradiography.

Confocal Microscopy

Neutrophils were resuspended in KRPB supplemented with 1.2 mM Mg^{2+} and 0.5 mM Ca^{2+} at a concentration of 5×10^6 cells/ml. Cells (200 µl) were added to each well of the Lab-Tek Chambered Coverglass (Nalge Nunc, Naperville, IL) and chambers incubated for 15 min at room temperature. SB203580 (3 µM) was added to appropriate wells, and the cells were incubated at 37°C for one hour prior to addition of 300 nM fMLP for 5 minutes at 37°C. Cells were washed with ice-cold KRPB, and 200 µl of 0.5% TX-100 in KRPB were added to each well for 5 min at room temperature to extract cytosolic MRP-14 from cells. Neutrophils were fixed with 3.7% paraformaldehyde for 30 minutes at 4°C, blocked with 2% goat serum and 2% BSA in phosphate buffered saline (PBS), and incubated with mouse monoclonal anti-MRP-14 (Kamiya Biomedical, Seattle, WA) overnight at 4°C (1:200 dilution in blocking buffers). Cells were washed with PBS and incubated at 4°C for one hour with rhodamine-conjugated goat anti-mouse IgG (Molecular Probes, Eugene, OR) for one hour at (1:1000). Cells were also stained with BODIPY-conjugated phalloidin (Molecular Probes) for 1 hr at 4°C (to visualize F-actin). Imaging was carried out on a Zeiss Axiovert 100 M microscope using LSM510 software.

Two-dimensional Electrophoretic Analysis of Granule and Plasma Membrane Fractions

Neutrophil subcellular fractionation was carried out by the method of Kjeldsen *et al* [19]. Briefly, isolated neutrophils (8×10^8/ml) were pre-treated with 10 µM diisopropyl fluorophosphate, resuspended in disruption buffer containing 100 mM KCl, 1 mM NaCl, 1 mM $ATPNa_2$, 3.5 mM $MgCl_2$, 10 mM PIPES, 0.5 mM PMSF, and cells

were disrupted by nitrogen cavitation for 10 min at 380 psi and 4°C. Cavitate was collected into 1.5 mM EGTA, and nuclei and intact cells were removed by centrifugation at 500 × g for 5 minutes. The postnuclear supernatant was layered onto a Percoll gradient formed from three 9 ml layers of Percoll, of density 1.090 g/ml, 1.050 g/ml and 1.120 g/ml. Percoll solutions were prepared in buffer containing 100 mM KCl, 3 mM NaCl, 1 mM Na_2ATP, 3.5 mM $MgCl_2$, 1.25 mM EGTA, 10 mM PIPES, and 0.5 mM PMSF. The gradient was centrifuged at 37,000 × g for 30 minutes in SS-34 fixed angle rotor in a Sorvall RC-5B centrifuge. The separated granules were recovered from the gradient interfaces by aspiration, and the Percoll removed by ultracentrifugation at 100,000 × g for 90 minutes using the Ti-50.3 rotor (Beckman, Fullerton, CA). Granule and plasma membrane/secretory vesicle devoid of Percoll were washed in disruption buffer by centrifugation. Washed material was dissolved in 300 µl of rehydration buffer, and lysates were cleared by centrifugation at 14,000 × g. Supernatant was loaded onto pH 3-10 IPG Zoom™ strips by overnight rehydration at 27°C. Proteins were separated by 2DE using Zoom IPG Runner™ IEF apparatus and X-Cell Sure Lock electrophoresis apparatus, as described above. Gels were stained with Coomassie blue dye.

Purity of granule fractions was determined by immunoblot analysis for CD66b (a marker of specific granules) and an ELISA for gelatinase and myeloperoxidase (a marker of azurophil granules). CD66b was found only in specific granule fractions. Distribution of gelatinase was 75% in gelatinase granules, 18% in specific granules, 5% in plasma membrane/secretory vesicles, and 2% in azurophil granules. Myeloperoxidase distribution was 76% in azurophil granules, 20% in specific granules, 3% in gelatinase

granules, and 1% in plasma membrane/secretory vesicles. This degree of granule enrichment is similar to that previously reported [19].

Association of MRP-14 With Neutrophil Granules and Plasma Membranes

Neutrophils (9×10^8 cells) were resuspended in Krebs-Ringer buffer supplemented with Ca^{2+} and Mg^{2+}, and incubated with or without 300 nM fMLP for 5 minutes with or without pretreatment with 3 μM SB203580 for 40 min. Cells were subjected to subcellular fractionation, as described above. Granule and plasma membrane/secretory vesicle proteins were separated by SDS-PAGE on 15% gels, the gels were cut at the level of the 25 kDa marker, and the lower portions of gels were subjected to immunoblotting using standard methods. Blotted membranes were probed with mouse monoclonal anti-MRP-14 (Kamiya Biomedicals, Seattle, WA) at 1:500 dilution and HRP-conjugated goat anti-mouse IgG (Upstate Biotechnology) at 1:2000 dilution. To ensure equal protein loading, upper portions of the cut gels were stained with Coomassie blue dye, and the staining intensities of protein bands were compared.

F-actin Co-sedimentation Assay.

F-actin filaments (500 μg of 5-10 μm length) were generated using the Actin Filament Biochem Kit (Cytoskeleton, Denver CO) according to manufacturer's instructions. MRP-14/MRP-8 complexes (150 μg of protein) prepared from human neutrophils were incubated overnight at 30°C in 100 μl of kinase buffer containing 25 mM HEPES, 100 mM KCl, 40 mM $MgCl_2$, pH 7.2 and 5 mM Na_2ATP (pH adjusted to 7.4), in the presence or absence of 2 μg of active recombinant p38 MAPK. After

overnight incubation, unphosphorylated (no kinase) and phosphorylated (kinase added) MRP-14/MRP-8 complexes (100 µl) were mixed with 350 µl F-actin filaments (250 µg of actin) in the Actin Polymerization Buffer supplied with the kit. To determine the amount of nonspecific MRP-14/MRP-8 sedimentation, 100 µl of unphosphorylated and phosphorylated complexes were added to 350 µl of Actin Polymerization Buffer without actin. All solutions were incubated at 37 °C for 30 minutes and centrifuged at 100,000 x g for 1 hr in a Ti55 rotor (Beckman) at 37°C. Supernatants (450 µl) were removed completely, and pellets were dissolved in 100 µl of SDS-PAGE gel loading buffer. Twenty µl of the dissolved pellets and 20 µl of supernatant were loaded onto 4-12% Bis-Tris SDS-PAGE gels (Invitrogen), proteins were separated, and the gels were stained with colloidal Coomassie blue dye (Genomic Solutions). Gels were scanned and the intensities of MRP14 bands were measured by densitometry.

Results

Identification of p38 MAPK Substrates

To screen for p38 MAPK substrates, human neutrophil lysates were incubated with [γ-^{32}P]ATP in the presence and absence of active recombinant p38 MAPKα. Proteins were separated by two-dimensional gel electrophoresis, gels were stained with Coomassie blue dye, and phosphorylated proteins were visualized by autoradiography. Autoradiographs were compared with Coomassie stained gels to identify proteins that were p38 MAPK substrates. Protein phosphorylation was not observed on autoradiographs of neutrophil lysates incubated with [γ-^{32}P]ATP in the absence of active recombinant kinase, indicating that method of neutrophil lysate preparation eliminated

endogenous kinase activity (data not shown). In the presence of active recombinant p38 MAPK, autoradiography demonstrated at least 15 phosphorylated proteins. Three of these could be matched to Coomassie blue-stained protein spots, while no stained protein spots could be visualized for the remainder. Figure 9 shows the location on two dimensional gels of the three proteins identified by MALDI-TOF MS, MRP-14, coronin, and Ly-GDI. MRP-14 is a known phosphoprotein that binds Ca^{2+} [275-281] and arachidonic acid [287,288]. MRP-14 also acts as a binding partner for the cytosolic factors of the NADPH oxidase [282,283]. As these findings suggest MRP-14 may mediate some p38 MAPK-dependent neutrophil responses, additional experiments were performed to confirm that MRP-14 is a true substrate of p38 MAPK.

***In Vitro* Phosphorylation of MRP-14 by p38 MAPK**

The possibility that MRP-14 phosphorylation represented a false positive was addressed by performing *in vitro* kinase reactions under non-denaturing conditions. In cells, MRP-14 is predominantly found in a heterodimeric complex with MRP-8 [277,278]. In order to assess the ability of p38 MAPK to phosphorylate MRP-14 while complexed with MRP-8, MRP-14/MRP-8 complexes were purified from human neutrophils under non-denaturing conditions. Purified complexes were incubated with active recombinant p38 MAPK and [γ-^{32}P]ATP, after which proteins were separated by SDS-PAGE. Figure 10 shows a Coomassie blue-stained gel and the corresponding autoradiograph demonstrating that MRP-14, but not MRP-8, was phosphorylated by p38 MAPK. These data show that MRP-14 is a p38 MAPK substrate while complexed with MRP-8.

Figure 9. Identification of p38 MAPK substrates in human neutrophil lysate. Candidate p38 MAPKα substrates were identified by incubation of neutrophil lysates with [γ-^{32}P]ATP in the presence of active recombinant p38 MAPKα. Proteins were separated by two-dimensional gel electrophoresis, and phosphoproteins were detected by autoradiography. Corresponding proteins were located by matching the autoradiograph with the image of the SYPRO Ruby-stained gel. Phosphoproteins were identified using in-gel trypsin digestion and MALDI-TOF MS of tryptic peptides followed by protein database analysis of obtained spectra. A SYPRO Ruby-stained gel and its corresponding autoradiograph are shown. The arrows show the three proteins identified from the gel, coronin, Ly-GDI and MRP-14.

Figure 9

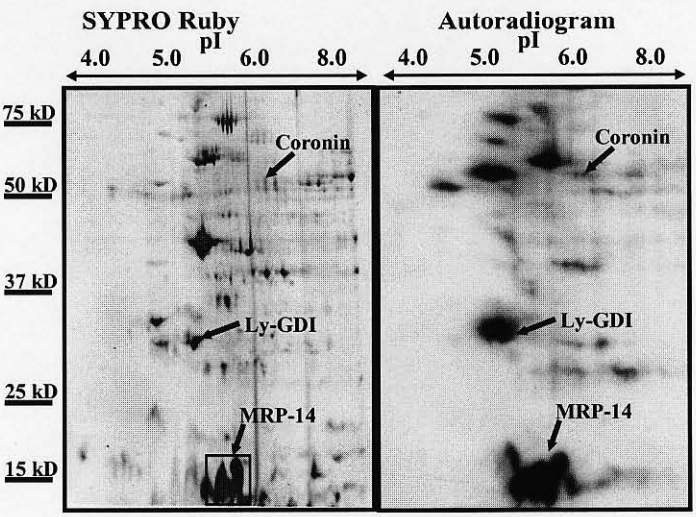
SYPRO Ruby
pI
4.0
5.0
6.0
8.0
Autoradiogram
pI
4.0
5.0
6.0
8.0
75 kD
50 kD
37 kD
25 kD
15 kD
Coronin
Ly-GDI
MRP-14
Coronin
Ly-GDI
MRP-14

Figure 10. ***In vitro*** **phosphorylation of MRP-14 by p38 MAPK.** MRP-14/MRP-8 complexes purified from neutrophil lysates were incubated with [γ-^{32}P]ATP in the presence or absence of active recombinant p38 MAPKα and proteins were separated by SDS-PAGE. Kinase alone (K), MRP-14/MRP-8 alone (p14/8), and kinase plus MRP-14/MRP-8 (K+p14/8) were added to separate lanes and subjected to SDS-PAGE. The Coomassie blue-stained gel and its corresponding autoradiograph are shown. The figure shows that MRP-14, but not MRP-8, was phosphorylated by p38 MAPK.

Figure 10

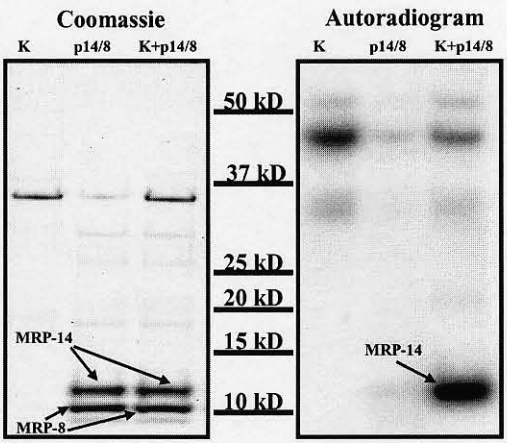
Coomassie
K
p14/8
K+p14/8
MRP-14
MRP-8
50 kD
37 kD
25 kD
20 kD
15 kD
10 kD
Autoradiogram
K
p14/8
K+p14/8
MRP-14

MRP-14 Phosphorylation by p38 MAPK in Intact Neutrophils

To assess whether MRP-14 is phosphorylated by p38 MAPK in intact cells, isolated neutrophils were loaded with [^{32}P]orthophosphate in the absence or presence of the p38 MAPK inhibitor SB203580 prior to stimulation of cells with fMLP. Cells were lysed and proteins separated by two-dimensional electrophoresis. Coomassie blue-stained gels were compared with autoradigraphs to identify phosphorylation events. Figure 11 shows that some phosphorylation of MRP-14 was detected in unstimulated cells, and this basal phosphorylation was reduced by pre-treatment with 3 μM SB203580. Stimulation with 300 nM fMLP for 5 minutes markedly enhanced phosphorylation of MRP-14, while pre-treatment with SB203580 abolished fMLP-induced phosphorylation. These data indicate that MRP-14 is a substrate of p38 MAPK in human neutrophils.

p38 MAPK Phosphorylates Threonine-113 on MRP-14

MRP-14 was reported previously to be phosphorylated on Thr-113, although the kinase was not identified [279]. To determine if Thr-113 is phosphorylated by p38 MAPK, mass spectrometry was used to identify the phosphorylated residue on MRP-14. MRP-14/MRP-8 was incubated with ATP in the presence or absence of active recombinant p38 MAPK. Following phosphorylation, proteolysis by trypsin was performed, and the peptide solution was subjected to phosphopeptide enrichment using metal ion affinity chromatography. MALDI-TOF MS analysis of the tryptic digests confirmed the presence of MRP-14 (Mascot $p<0.05$) in all digests. The unphosphorylated C-terminal 21 amino acid peptide containing Thr-113 was predicted to have a mass to charge ratio (m/z) of 2176.2, while the phosphorylated peptide was predicted to be

Figure 11. Phosphorylation of MRP-14 by p38 MAPK in intact neutrophils. Neutrophils were loaded with [^{32}P]orthophosphate prior to stimulation of cells with fMLP in the absence or presence of 3 μM SB203580. Cells were lysed and proteins separated by two-dimensional electrophoresis. Coomassie stained gels and corresponding autoradiographs used to identify phosphorylation events are shown. MRP-14 was identified from gels using MALDI-TOF MS. The figure shows that basal MRP-14 phosphorylation was increased by treatment with 300 nM fMLP, and pretreatment of cells with SB203580 reduced basal phosphorylation levels and abolished fMLP-induced phosphorylation. The arrows identify the full length and N-terminal truncated MRP-14 isoforms.

Figure 11

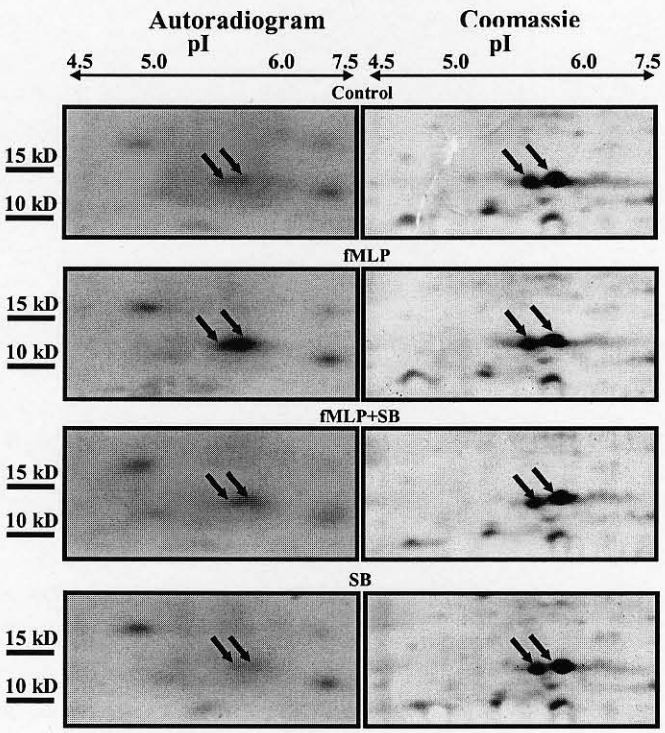
Autoradiogram
pI
4.5
5.0
6.0
7.5
Coomassie
pI
4.5
5.0
6.0
7.5
Control
15 kD
10 kD
fMLP
15 kD
10 kD
fMLP+SB
15 kD
10 kD
SB
15 kD
10 kD

2256.0 *m/z*, due to the 80 Da mass addition of a phosphoryl group (HPO_3) [289]. Analysis of peptide mass spectra showed a peak at 2177.3 m/z in samples from p38 MAPK treated and untreated MRP-14 (Figure 12A and B). An ion of 2257.2 m/z was observed only in the digest from the sample incubated with p38 MAPK (Figure 12B). These results suggest that the C-terminal 21 amino tryptic peptide of MRP-14 was modified by phosphorylation.

To confirm the phosphorylation of this peptide, timed ion selection of 2257 $\pm$ 3 m/z precursor ions, followed by collision induced dissociation fragmentation, yielded a fragmentation pattern with a Mascot ion score of 31 (significant homology ($p<0.05$) at a score >18 and identity at a score of >33) for a sequence of ^{94}MHEGDEGPGHHHKPGLGEGTP^{114}. The TOF-TOF spectrum analysis included an ion of 2158.6 m/z, which corresponds to the neutral loss of 98 m/z (the mass of phosphoric acid, H_3PO_4) from the parent phosphorylated ion (Figure 12C). Appearance of a peptide with this mass to charge ratio in addition to the MH+80 precursor ion confirms that the post-translational modification on the peptide was phosphorylation [227,290-292]. As Thr-113 is the only residue in the peptide that could serve as a phosphate acceptor from p38 MAPK, these data suggest that p38 MAPK phosphorylates MRP-14 on Thr-113.

To confirm that Thr-113 is the residue phosphorylated by p38 MAPK, a mutant recombinant protein was created in which alanine was substituted for Thr-113. Wild-type MRP-14 and mutant MRP-14 were expressed and incorporated in an *in vitro* kinase reaction with recombinant active p38 MAPK. Figure 13 shows that wild type MRP-14 was strongly phosphorylated under the conditions employed, while no phosphorylation

Figure 12. p38 MAPK phosphorylates MRP-14 on Thr-113. To define the site of p38 MAPK phosphorylation, purified MRP-14/MRP-8 complexes were incubated with Na_2ATP in the presence or absence of recombinant p38 MAPK. Following proteolysis by trypsin, the peptide solution was subjected to phosphopeptide enrichment using metal ion affinity chromatography. MALDI-TOF MS analysis of the tryptic digests confirmed the presence of MRP-14 in digests from incubation with and without p38 MAPK. Panel A shows the mass spectra of peptides from digests of the MRP-14/MRP-8 complex alone, which included a peptide with m/z of 2177, corresponding to the C-terminal 21 amino acid tryptic peptide of MRP-14 (MHEGDEGPGHHHKPGLGEGTP) (arrow). Panel B shows the mass spectra for digests of the MRP-14/MRP-8 complex incubated with p38 MAPK. A new major peak at 2257 m/z was found, corresponding to the hypothetical mass (2256.4) of the phosphorylated C-terminal 21 amino acid peptide containing Thr-113.

The peak with the m/z of 2257 was sequenced using the timed ion selection and collision induced dissociation (CID) fragmentation. Panel C shows the spectra of the ions from this fragmentation. Included in this spectra was an ion with a mass of ~2159 m/z (shown with an asterisk on threonine), which corresponds to the neutral loss of phosphoric acid (H_3PO_4) from the parent phosphorylated ion (theoretical mass of 2158). The increase in 80 Da with phosphorylation and the loss of 98 Da with CID confirm that the post-translational modification on the peptide was phosphorylation. Observation of multiple peaks with 1Da differences in m/z (for example, observation of peaks with m/z of 2257, 2258, 2259) arises from the natural presence of isotopes of carbon, nitrogen, oxygen and hydrogen in the peptides.

Figure 12

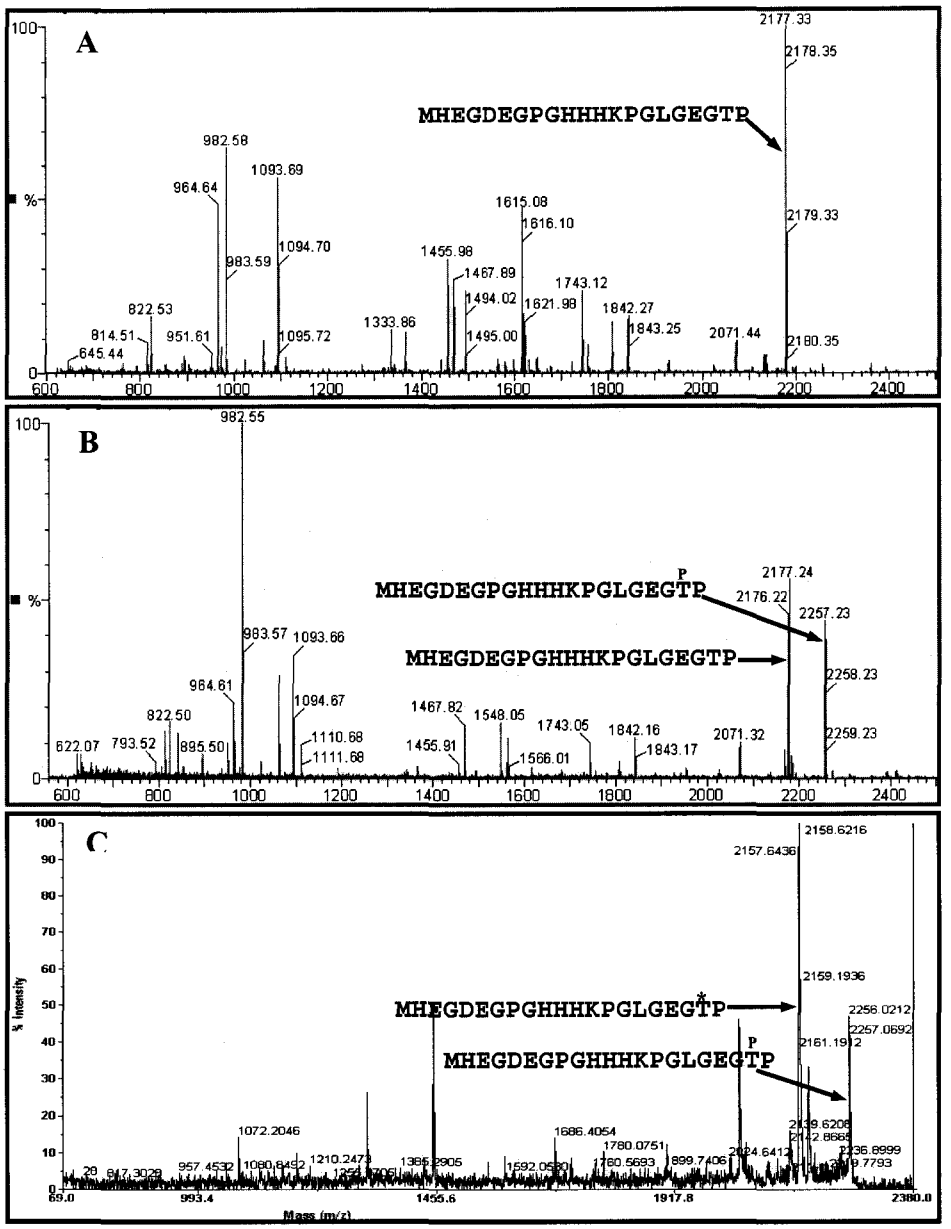
A
MHEGDEGPGHHHKPGLGEGTP
2177.33
2178.35
2179.33
2180.35
982.58
1093.69
964.64
1615.08
1616.10
1094.70
983.59
1455.98
1467.89
1743.12
822.53
1494.02
1621.98
1842.27
814.51
951.61
1095.72
1333.86
1843.25
2071.44
1495.00
645.44
B
MHEGDEGPGHHHKPGLGEGTP
MHEGDEGPGHHHKPGLGEGTP
982.55
2177.24
2176.22
2257.23
2258.23
2259.23
983.57
1093.66
964.61
1094.67
822.50
1467.82
1548.05
1743.05
1842.16
622.07
793.52
895.50
1110.68
1111.68
1455.91
1566.01
1843.17
2071.32
C
MHEGDEGPGHHHKPGLGEGTP
MHEGDEGPGHHHKPGLGEGTP
2158.6216
2157.6436
2159.1936
2256.0212
2257.0892
2161.1912
1072.2046
1686.4054
1780.0751
957.4532
1210.2473
1780.5693
899.7406
2024.6412
1592.0580
% Intensity
Mass (m/z)

Figure 13. P38 MAPK phosphorylates wild type hrMRP-14, but not the T113A mutant. Twenty micrograms of purified recombinant human wild type and T113A mutant MRP-14 were incubated with [γ-^{32}P]ATP in the presence or absence of the 50 ng active recombinant p38 MAPK for 30 min at 30°C. The upper panel shows a Coomassie stained gel, and the lower panel shows the corresponding autoradiograph. Wild type MRP-14 was phosphorylated, while no phosphorylation of the T113A mutant was seen. The mass of the recombinant MRP-14 is about 4.5 kD higher than that of human neutrophil MRP14 due to the additional histidine tag.

Figure 13

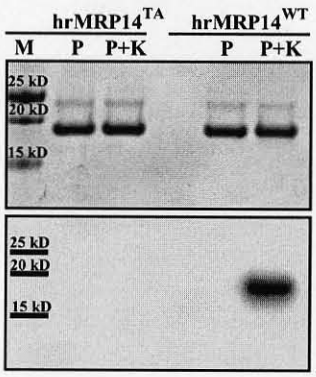

was observed when alanine replaced Thr-113. Taken together, these results firmly establish that p38 MAPK phosphorylates MRP-14 on Thr-113.

p38 MAPK-Dependent Translocation of MRP-14 in Intact Neutrophils

Phosphorylation of MRP-14 in monocytes results in increased calcium binding and translocation from cytosol to membranes and cytoskeleton [281]. To determine if a similar translocation occurred in human neutrophils, confocal microscopy was used to determine co-localization of MRP-14 and F-actin in fMLP-stimulated and unstimulated cells. Initial studies showed that the large amount of cytosolic MRP-14 resulted in intense staining of the whole cell, which obscured visualization of any changes in intracellular distribution (data not shown). Therefore, control and fMLP-stimulated neutrophils that had been plated on confocal microscope slides were permeabilized with TX-100 to remove cytosolic MRP-14. Cells were then fixed and stained for F-actin using BODIPY 650/665-conjugated phalloidin and stained for MRP-14 with monoclonal anti-MRP-14 and rhodamine-conjugated secondary antibody. Figure 14A shows that minimal staining for MRP-14 associated with cortical F-actin was observed in unstimulated cells. FMLP stimulation resulted in a marked increase in MRP-14 staining and in F-actin formation, both of which were associated with lamellipodia. MRP-14 staining was localized at the base of F-actin within lamellipodia, and excluded from the leading edge (Figure 14B). The increased intensity of MRP-14 staining and localization at lamellipodia were completely prevented by pre-treatment with SB203580, while formation of lamellipodia and increased F-actin formation were not affected. These results suggest that MRP-14 translocates to the stable actin cytoskeleton at the base of lamellipodia following fMLP

Figure 14. Phosphorylation-induced redistribution of MRP-14 in intact neutrophils. Control and fMLP-stimulated neutrophils were plated on confocal microscope slides and permeabilized with Triton X-100 prior to fixation and staining. Panel A shows cells stained for F-actin using BODIPY 650/665-conjugated phalloidin (shown in green), and with monoclonal anti MRP-14 and rhodamine-conjugated anti-mouse IgG (shown in red), and the merged pictures of the two. Unstimulated cells show minimal staining for MRP-14, confined to the periphery of the cell and colocalized with cortical F-actin (Control). Neutrophil stimulation with fMLP resulted in increased F actin staining primarily localized to lamellipodia. An increase in MRP-14 staining was seen at the base of lamellipodia. Increased MRP-14 staining and association with lamellipodia were completely reversed by incubation of cells with SB203580 prior to fMLP treatment (fMLP+SB), while F-actin staining and lamellipodia formation was not affected.

Panel B shows analysis of single cell staining profiles using LSM510 software (green lines correspond to the intensity of actin staining and red to MRP-14 staining). This analysis demonstrates colocalization of F-actin and MRP-14 under basal condition (control). Following fMLP stimulation F-actin staining was most prominent in lamellipodia. MRP-14 did not co-localize with the leading edge of F-actin, but was present at the base of lamellipodia. Preincubation with 3 μM SB203580 (fMLP+SB) blocked translocation of MRP-14. Distance in the graphs (the x-axis) corresponds to the distance measured from the base to the tip of the line traversing cells. These results indicate that MRP-14 translocates to Triton X-100 insoluble structures at the base of lamellipodia in human neutrophils upon fMLP treatment, and that the translocation is p38 MAPK-dependent.

Figure 14

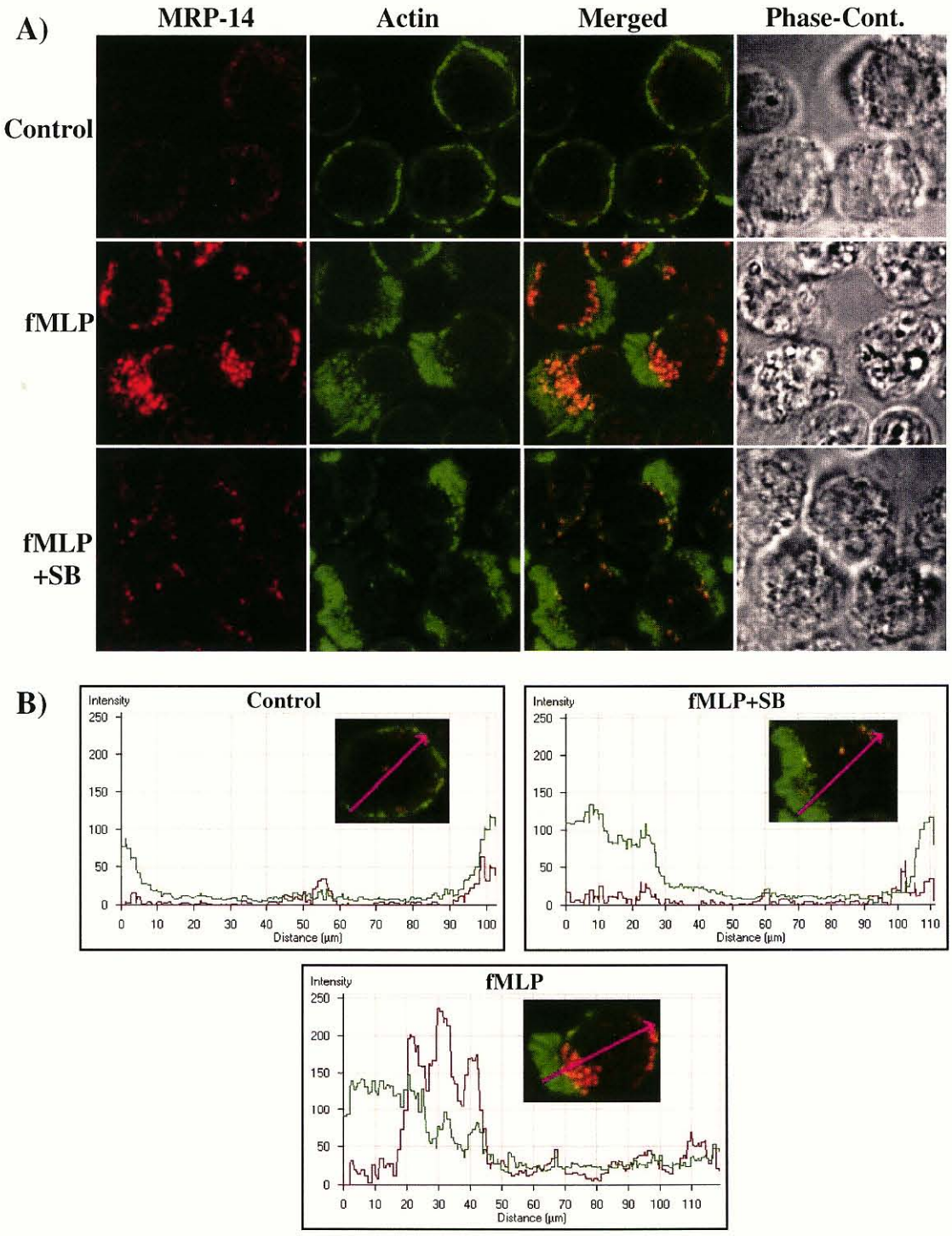
A)
MRP-14
Actin
Merged
Phase-Cont.
Control
fMLP
fMLP +SB
B)
Control
fMLP+SB
fMLP
Intensity
Distance (µm)

stimulation of human neutrophils, and this translocation is dependent p38 MAPK activity.

We and others reported previously that neutrophil exocytosis depends on p38 MAPK activation [15,186,188,195]. Therefore, localization of MRP-14 to neutrophil granule subsets and the effect of fMLP-stimulation on this localization were examined. Two-dimensional electrophoretic separation of neutrophil granule and plasma membrane/secretory vesicle fraction proteins revealed that MRP-14 was present in plasma membrane/secretory vesicle fractions, on gelatinase granules and specific granules, but was absent from azurophilic granules (Figure 15). The amount of MRP-14 associated with plasma membrane/secretory vesicle and granule fractions in control and fMLP-activated neutrophils was examined using western blotting (Figure 16). The amount of MRP-14 associated with specific granules was greater than that associated with plasma membrane/secretory vesicles or gelatinase granules. FMLP stimulation resulted in a significant increase in the amount of MRP-14 associated with plasma membrane/secretory vesicle fractions and gelatinase granules, while no change was observed in MRP-14 association with specific granules. This translocation was abolished by pre-treatment of cells with SB203580. MRP-14 did not associate with azurophilic granules under either basal or stimulated conditions (data not shown). In separate experiments the ability of anti-MRP-14 antibody to recognize both the non-phosphorylated and the phosphorylated form of MRP-14 was examined. Both purified MRP-14/MRP-8 complexes and recombinant MRP-14 were incubated with ATP in the presence and absence of p38 MAPK. Immunoblot analysis showed that phosphorylated and non-phosphorylated MRP-14 were detected equally (data not shown). These results

Figure 15. Association of MRP-14 with neutrophil granule and plasma membrane/secretory vesicle fractions. Neutrophil subcellular fractionation was performed to isolate plasma membrane/secretory vesicle fraction and granules. The figure shows a portion of Coomassie blue-stained two-dimensional gels, after separation of proteins from each fraction, showing the area in which MRP-14 is located. Proteins were identified using MALDI-TOF MS. MRP-14 was identified in plasma membrane/secretory vesicle, gelatinase granule, and specific granule fractions, but was absent from the azurophilic granule fraction.

Figure 15

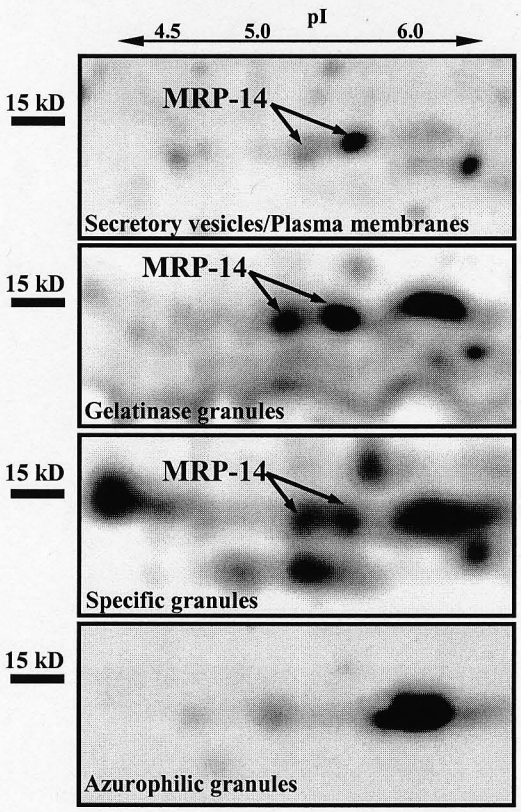
4.5
5.0
pI
6.0
15 kD
MRP-14
Secretory vesicles/Plasma membranes
15 kD
MRP-14
Gelatinase granules
15 kD
MRP-14
Specific granules
15 kD
Azurophilic granules

Figure 16. Translocation of MRP-14 to neutrophil gelatinase granule and plasma membrane/secretory vesicle fractions in fMLP-stimulated neutrophils. Plasma membrane/secretory vesicle and granule fractions were obtained from control (basal) and fMLP-stimulated cells (fMLP) without or with pretreatment with SB203580 (fMLP/SB). Gelatinase granule, specific granule and plasma membrane/secretory vesicle fraction proteins were separated by SDS-PAGE on 15% gels. The gels were cut at 25 kDa marker. The figure shows immunoblots for MRP-14 of lower portions of gels. To ensure equal protein loading, upper portions of each gel were stained with Coomassie blue dye, and the staining intensities of abundant proteins were compared. Actin, gelatinase and lactoferrin bands were confirmed by MALDI-TOF MS and peptide mass fingerprinting as described above. FMLP stimulation resulted in a significant increase in the amount of MRP-14 associated with plasma membrane/secretory vesicle fractions and gelatinase granules, while no change was observed in MRP-14 association with specific granules. This translocation was abolished by treatment of cells with SB203580. A greater amount of MRP-14 was associated with the specific granule fraction than with plasma membrane/secretory vesicle or gelatinase granule fractions (equal amounts of protein were loaded on gels for each fraction). MRP-14 did not associate with azurophilic granules under either basal or stimulated conditions (data not shown).

Figure 16

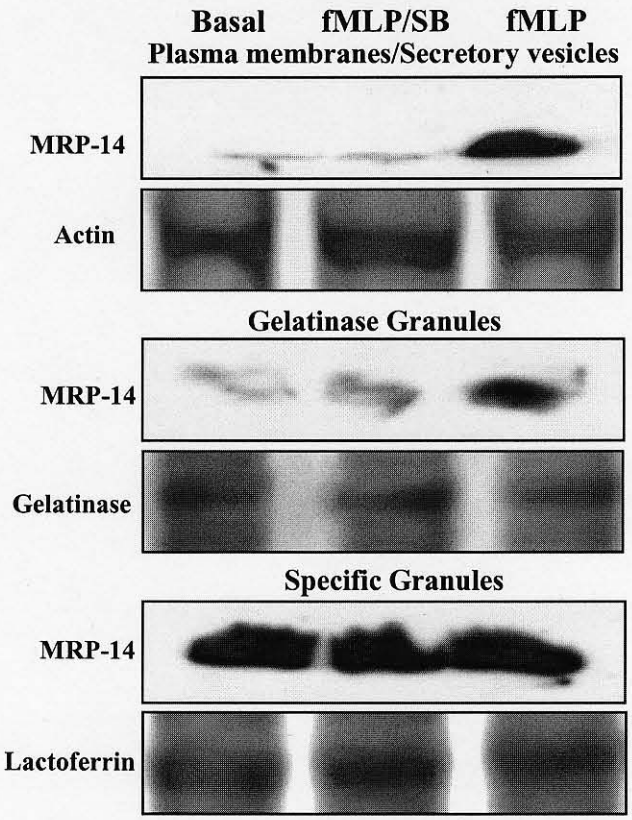
Basal
fMLP/SB
fMLP
Plasma membranes/Secretory vesicles
MRP-14
Actin
Gelatinase Granules
MRP-14
Gelatinase
Specific Granules
MRP-14
Lactoferrin

suggest that p38-MAPK-dependent phosphorylation induces translocation of MRP-14 to plasma membrane and gelatinase granules, possibly due to increased association with the actin cytoskeleton.

To determine if MRP-14 phosphorylation regulates its binding to actin, an *in vitro* F-actin co-sedimentation assay was performed. MRP-14/MRP-8 complexes were incubated with ATP in the presence and absence of recombinant active p38 MAPK. Equal amounts of phosphorylated and non-phosphorylated MRP-14/MRP-8 were added to F-actin filaments, then F-actin was pelleted by ultracentrifugation. Protein in the pelleted F-actin and supernatant were separated by 4-12% gradient electrophoresis. Figure 17A shows a Coomassie blue-stained gel demonstrating increased association of phosphorylated MRP-14/MRP-8 with actin. Figure 17B presents the densitometric analysis of three separate experiments. The data indicate that p38 MAPK phosphorylation doubles the amount of MRP-14/MRP-8 complex associated with F-actin. In the absence of F-actin, MRP-14/MRP-8 complexes failed to pellet following ultracentrifugation (data not shown). These data suggest that phosphorylation by p38 MAPK regulates the translocation of MRP-14/MRP-8 to lamellipodia and granules by mediating binding to F-actin.

Discussion

The p38 MAPK pathway participates in a number of neutrophil functions critical to generation and regulation of the inflammatory response, including chemotaxis, adherence, respiratory burst activity, degranulation, and cytoskeletal reorganization [15,172-174,180,186,188,194,195,267,268,]. Understanding the molecular mechanisms

Figure 17. Phosphorylation by p38 MAPK enhanced actin binding of MRP-14/MRP-8. Purified MRP-14/MRP-8 was incubated overnight with 5 mM ATP in the presence or absence of 2 μg p38 MAPK. Phosphorylated (K+MRP) and non-phosphorylated (MRP) complexes were then incubated with F-actin for 30 min at 37°C. Following centrifugation of F-actin at 100,000 x g, pelleted proteins were separated by 4-12% gradient gel electrophoresis. Panel A shows a Coomassie blue stained gel demonstrating increased binding of phosphorylated MRP-14/MRP-8 to actin. Panel B shows the mean ± S.D. densitometric analysis of MRP-14 bands from three separate experiments, demonstrating that p38 MAPK-mediated phosphorylation of MRP-14 resulted in a 100% increase in actin binding.

Figure 17

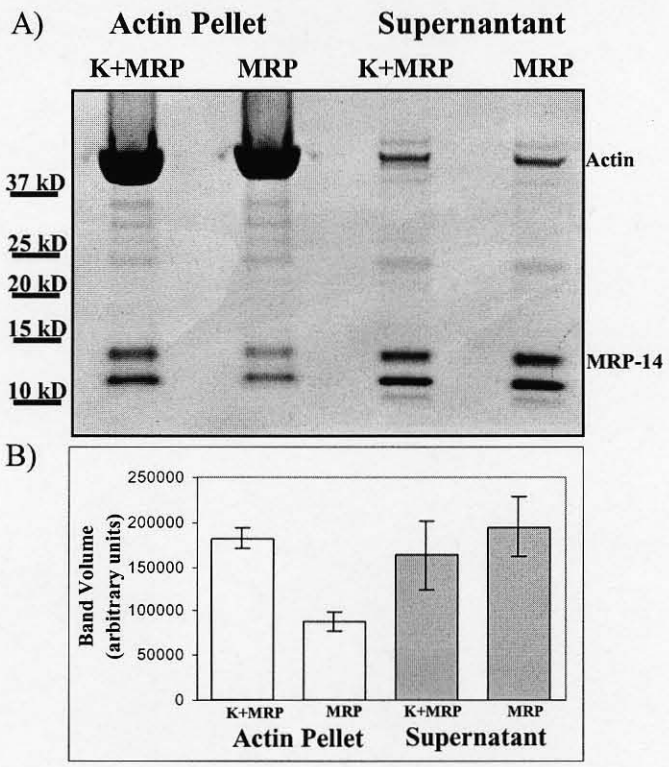
A)
Actin Pellet
Supernantant
K+MRP
MRP
K+MRP
MRP
37 kD
25 kD
20 kD
15 kD
10 kD
Actin
MRP-14
B)
Band Volume (arbitrary units)
250000
200000
150000
100000
50000
0
K+MRP
MRP
K+MRP
MRP
Actin Pellet
Supernatant

by which p38 MAPK participates in these responses is hindered by the limited number of targets of p38 MAPK identified to date in neutrophils. MAPKAPK2 and $p47^{phox}$ are the only clearly identified p38 MAPK targets in human neutrophils [175,194,195,274]. A previous study by Lewis *et al.* [203] determined that 20 of 25 ERK targets identified in a global screen were not previously known. Thus, it is likely that a number of important targets of p38 MAPK that participate in regulation of neutrophil responses remain to be identified. The goal of the present study was to apply a recently developed proteomic approach that allows simultaneous identification of multiple substrates of a single kinase to defining p38 MAPK substrates in human neutrophils. This approach involves *in vitro* phosphorylation of cellular lysate by active recombinant kinase in the presence of [γ-^{32}P]ATP, followed by protein separation by two dimensional gel electrophoresis, alignment of autoradiogram with stained gel, and subsequent identification of phosphoproteins by MALDI-TOF MS. Using this approach, three potential p38 MAPK substrates were identified, MRP-14, Ly-GDI, and coronin.

The identification of only three of more than 15 phosphorylated proteins by the current approach indicates sensitivity remains a limitation to this method. For a number of phosphorylation events identified by autoradiography, no corresponding protein spot was found or an insufficient mass spectrum was obtained for successful protein identification. The limited sensitivity may result from low abundance of these proteins, inadequate transfer of proteins from IPG strips to the second dimension gels, incomplete in-gel digestion of the protein by trypsin, or inefficient processing and ionization of phosphopeptides during mass spectrometric analysis.

All three of the proteins identified as targets of p38 MAPK have the potential of participating in neutrophil functional responses. Coronins are a family of actin binding proteins that directly regulate actin nucleation by Arp2/3 complexes [293], participate in chemotaxis of Dictyostelium [294], associate with the phagocytic cup [295], and bind the cytosolic components of the NADPH oxidase [296]. Ly-GDI inhibits dissociation of GDP from Rho GTPases, including Rac and Cdc42, maintaining them in the inactive state and controlling distribution between cytosol and membrane [297,298]. MRP-14 and its heterodimeric partner, MRP-8, are members of the S100 family of calcium binding proteins. The heterodimer constitutes up to 30% of neutrophil and 1% of monocyte cytosolic proteins [277,278]. The MRP-14/MRP-8 complex was reported to undergo phosphorylation-dependent translocation to the plasma membrane and cytoskeleton in monocytes following cell stimulation [281]. The MRP-14/MRP-8 complexes were also found to bind arachidonic acid [287,288], and to participate in the activation of NADPH oxidase [282,283]. MRP-14/MRP-8 increased the affinity of $p67^{phox}$ for cytochrome b_{558}, and oxidase activity was enhanced [283]. Targeted disruption of the MRP-14 gene in mice does not produce consistent phenotypic changes [299,300], although Manitz *et al.* [300] reported impaired *in vitro* chemotaxis and up-regulation of CD11b. Because of its abundance in human neutrophils, further studies were performed examining MRP-14.

The artificial conditions used for *in vitro* kinase reactions with neutrophil lysates may permit p38 MAPK phosphorylation of proteins that would not be targets in intact neutrophils. The use of cell lysate may permit access of exogenously added kinase to proteins with restricted localization in intact cells. Urea denaturation may expose phosphorylation sites that are inaccessible in properly folded proteins. Disruption of

protein-protein interactions may result in dissociation of signaling modules that restrict kinase-substrate interaction. Finally, protein spots may contain more than one protein, which could lead to identification of false substrates. For these reasons, experiments were performed in which MRP-14 was confirmed to be a p38 MAPK substrate both *in vitro* and *ex vivo*. The MRP-14/MRP-8 complex was isolated under non-denaturing conditions and subjected to an *in vitro* kinase reaction with active recombinant p38 MAPK. Under these conditions, MRP-14, but not MRP-8, was phosphorylated. In intact neutrophils loaded with [^{32}P]orthophosphate, MRP-14 demonstrated basal phosphorylation that was dramatically increased by fMLP stimulation. Basal and fMLP-stimulated phosphorylation of MRP-14 was dependent on p38 MAPK activity. These findings indicate that MRP-14, while in a heterodimeric complex with MRP-8, is a direct target of p38 MAPK in human neutrophils. This conclusion is supported by a recent report by Vogl *et al.* [301] showing that MRP-14 is phosphorylated by p38 MAPK in arsenite-stimulated human monocytes and *in vitro*, using recombinant proteins.

To identify the p38 MAPK phosphorylation site in MRP-14, a combination of phosphopeptide enrichment using immobilized metal affinity chromatography (IMAC) and tandem mass spectrometry was used [227,290-292]. Edgeworth *et al.* [279] showed that the penultimate residue, Thr-113, was the single phosphorylated residue on MRP-14 in ionomycin-activated neutrophils and monocytes, and this phosphorylation was independent of protein kinase C activity. Our data demonstrated that in the presence of p38 MAPK, the 21 amino acid C-terminal MRP-14 tryptic peptide that contains Thr-113 showed an 80 Da increase in mass, as compared to MRP-14 tryptic peptides in the absence of p38 MAPK. This is consistent with phosphorylation of this peptide, as the

mass of a phosphoryl group (HPO_3) is 80 Da [289]. Use of tandem mass spectrometry allowed us to observe the β-elimination, neutral loss of 98 m/z from the precursor peptide ion, which is the mass of phosphoric acid (H_3PO_4) [289,290]. Peptide tag sequencing of the phosphopeptide using collision-induced dissociation showed that the sequence corresponded to that of the 21 amino acid C-terminal peptide of MRP-14. Confirmation that Thr-113 was the amino acid residue phosphorylated by p38 MAPK was obtained by showing that mutation of Thr-113 to alanine prevented phosphorylation. Similarly, Vogl *et al.* [301] identified Thr-113 as the site of p38 MAPK-mediated phosphorylation.

Despite being the most abundant protein in human neutrophils, the functional role of MRP-14 has not been determined. The MRP-14/MRP-8 complex translocates to the plasma membrane and cytoskeleton in monocytes in a phosphorylation-dependent manner following cell stimulation [281]. The present study used confocal microscopy to determine the location of MRP-14 after neutrophil stimulation with fMLP, and to determine if changes in location were dependent on p38 MAPK activity. The abundance of MRP-14 in human neutrophils resulted in marked staining of the entire cell, preventing detection of differences in MRP-14 localization between control and stimulated cells (data not shown). We presumed that the large amount of cytosolic MRP-14 was obscuring any changes in localization that could have occurred as the result of phosphorylation following cell activation. Permeabilization of cells with Triton X-100 prior to fixation and staining resulted in loss of cytosolic MRP-14. Under basal conditions, only a small amount of MRP-14 was present in the sub-plasma membrane area occupied by cortical actin. FMLP stimulation prior to permeabilization resulted in a significant increase in MRP-14 staining that localized to the base of the actin

cytoskeleton forming lamellipodia. The increased staining for MRP-14 and its localization at the base of lamellipodia were dependent on p38 MAPK-mediated phosphorylation, as both were inhibited by SB203580 at concentrations specific for p38 MAPK inhibition [302]. These data suggest that phosphorylation by p38 MAPK results in MRP-14 association with long, unbranched actin filaments that form at the base of lamellipodia. This conclusion is supported by our data demonstrating enhanced F-actin binding of phosphorylated MRP-14. Thus, the MRP-14/MRP-8 complex may play a role in stabilization of the actin network at the base of lamellipodia [303]. Manitz *et al.* [300] reported that neutrophils from mice with targeted deletion of MRP-14 demonstrated impaired chemotaxis to IL-8 and LTB_4. MRP-$14^{-/-}$ neutrophils exhibited increased basal levels of F-actin that did not increase with IL-8 stimulation. Impaired CD11b up-regulation in IL-8-stimulated MRP-$14^{-/-}$ neutrophils suggested that MRP-14 plays a role in exocytosis. Vogl *et al.* [301] reported that deletion of the MRP-14 gene in mice inhibited granulocyte migration, suggesting a functional role for the MRP-14/MRP-8 complex. Thr-113 is absent from the mouse isoform of MRP-14, however, preventing any conclusions regarding the role of p38 MAPK-mediated phosphorylation in MRP-14 functions from studies in mice.

Permeabilization with Triton X-100 prior to confocal microscopic visualization of MRP-14 and F-actin solubilizes many cell structures, thereby preventing detection of translocation of MRP-14 to these structures. However, using two-dimensional gel electrophoresis and MALDI-TOF MS, MRP-14 was shown to be associated with plasma membrane/secretory vesicles, gelatinase granules, and specific granules, but not with azurophilic granules, in resting human neutrophils. Based on previous reports indicating

p38 MAPK regulates neutrophil granule exocytosis [15,186,188,195], the effect of MRP-14 phosphorylation on its association with these structures was determined. The data indicate that MRP-14 translocated to the plasma membrane/secretory vesicle fraction and gelatinase granules following fMLP stimulation, and that this translocation was dependent on p38 MAPK activity. The failure of MRP-14 to translocate to specific and azurophilic granules upon cell activation may be related to the small amount of actin associated with these granules (unpublished observations). The quantitative difference in MRP-14 association with specific granules, compared to gelatinase granules and plasma membrane/secretory vesicle fractions, under basal conditions remains to be explained. Taken together, the results of the present study suggest the hypothesis that phosphorylation of MRP-14 by p38 MAPK contributes to p38 MAPK regulation of cytoskeletal reorganization necessary for exocytosis. Association of MRP-14 with granule subsets may also provide a mechanism by which MRP-14 is released extracellularly at sites of inflammation [304-306].

CHAPTER IV

SUMMARY AND FINAL CONCLUSIONS

Proteomic analysis of neutrophil granules with 2DE revealed that for each granule subset, the quality of protein separation by 2DE paralleled the density of the lumen matrix and the amount of cationic proteins in the granule lumen. Proteins from gelatinase granules, which had the least dense lumen, were the most amenable to analysis by 2DE. Azurophil granule proteins on the other hand, were dominated by large amounts of highly cationic proteins that make up the dense matrix of these granules and did not separate well by 2DE. Specific granules have intermediate density and content of cationic proteins in the lumen, and the quality of specific granule protein separation by 2DE was intermediate to those of gelatinase and azurophil granules. To improve protein separation by 2DE, we fractionated granule proteins prior to analysis by 2DE using either the separation of luminal proteins from membranes by sodium carbonate, or differential precipitation of proteins by ammonium sulfate. We found that the success of each of these two methods depended on the granule subtype. Thus, sodium carbonate treatment removed large amounts of basic luminal proteins from granule membranes, and allowed for improved separation of both membrane-associated cytoskeletal proteins and the luminal proteins. However, it led to losses of low molecular weight proteins and luminal proteins from gelatinase granules. Ammonium sulfate precipitation was most useful at improving the separation of gelatinase granule proteins, which had more cytoskeletal

proteins and fewer basic luminal proteins than specific granules. Neither method succeeded at improving the separation of proteins from azurophil granules, which contained very little cytoskeleton and large amounts of acidic mucopolysaccharide and highly cationic proteins that do not resolve well on 2D gels.

Similarly to other proteomic studies, we found that transmembrane and membrane-associated proteins were strongly underrepresented among the proteins identified by 2DE. To overcome the limitations of 2DE-based protein identification, we used a much higher sensitivity proteomic method, namely, strong cation-exchange reversed-phase two-dimensional chromatography combined with ESI-MS/MS (2D-HPLC ESI-MS/MS). To enhance the sensitivity of this approach for membrane-spanning and membrane-associated proteins, we used sodium carbonate extraction of granules. Based on 2D gels of carbonate treated granule membranes, this treatment allowed for granule membrane-associated proteins to largely remain bound to the membrane, but effectively removed luminal proteins.

The high sensitivity of 2D-HPLC ESI-MS/MS and the resultant identification of proteins from subcellular organelles that contaminated isolated granules, led us to establish a valid list of proteins for each granule type by repeating the 2D-HPLC ESI-MS/MS experiments for each granule subtype three times, and rejecting proteins that were identified in only one of the three experiments. We identified a total of 286 proteins on the three granule subsets, 87 of which were identified by 2DE and MALDI-MS and 247 were identified by 2D HPLC ESI-MS/MS.

Proteomic analysis of neutrophil granules resulted in identification of a number of proteins not previously described in neutrophils, but have been implicated in granule

exocytosis of other hematopoietic cells. Among these proteins were SNARE proteins VAMP-8 and syntaxin 7, SNARE-modulating proteins Munc-18-2 and Munc-13-4, GTPase Rab27A, and synaptotagmin-like protein Slp-1. VAMP-8 associates with, and participates in exocytosis of platelet dense core granules and RBL-2H3 mast cell granules [307,308]. Syntaxin 7 was found on platelet granules [309]. In addition, it was shown that syntaxin 7 interacts with VAMP-8 and may act in granule-to-granule and granule-to-phagosome fusion [310-312]. SNARE modulating protein Munc-18-2 (Hunc-18b) is found on mast cell granules, interacts with microtubules, and participates in compound exocytosis of granules [100]. Munc-18-2 also associates with a complex that contains SNAP-23 and VAMP 3 and participates in platelet exocytosis [313]. Munc-13-4 and synaptotagmin-like protein 1 (Slp-1) are effectors of the GTPase Rab27A. Rab27A regulates granule secretion in a number of cell types, and mutations in Rab27A gene have been found in a human disorder known as Griscelli syndrome characterized by aberrant pigmentation and immunodeficiencies [314]. Munc-13-4 regulates granule secretion in platelets and mast cells by directly binding to GTP-Rab27A and enhancing exocytosis [315,316]. The function of synaptotagmin-like proteins is not known, but they interact with GTP-Rab27A and contain tandem calcium C2 domains found in many proteins involved in exocytosis [317,318].

The identification of a number of proteins on neutrophil granules that are involved in granule exocytosis in other hematopoietic cells suggests a common exocytotic machinery for all hematopoieteic cells. However, signaling pathways that lead to exocytosis are unique for each cell. In neutrophils the p38 MAPK pathway plays a central role. We screened neutrophil granule proteins for substrates of p38 MAPK and its

downstream kinase MAPKAPK-2 (MK2). Novel substrates were not identified for MK2, however, we identified MRP-14 as a novel p38 MAPK substrate and a component of neutrophil granules. Upon phosphorylation by p38 MAPK, MRP-14 translocated to plasma membranes and gelatinase granules. No increase was seen in the amount of MRP-14 associated with specific granules, which had more MRP-14 bound to them under basal conditions than gelatinase granules or plasma membranes. Additionally, confocal microscopy revealed colocalization of MRP-14 and F-actin at the base of lamellipodia in cells stimulated with fMLP and extracted with TX-100. P38 MAPK and its substrate Hsp27 also localized at the base of lamellipodia in migrating aortic smooth muscle cells [319]. Our confocal micrographs revealed punctate distribution of colocalized F-actin and MRP-14 in small round structures at the base of neutrophil lamellipodia. Whether these structures were granules that have been immobilized by binding to TX-100-insoluble cytoskeleton, is not known. MRP-14 also bound to F-actin in vitro in phosphorylation-dependent manner. Thus, MRP-14 may be translocating to F-actin present on granules and plasma membranes. Increased translocation of MRP-14 to gelatinase granules and plasma membranes, but not to specific granules, may reflect an earlier observation of the presence of more actin on plasma membranes and gelatinase granules than on specific granules. Presence of significant amounts of MRP-14 on specific granules under basal conditions, and the lack of change in MRP-14 content upon cell stimulation, suggests that non-phosphorylated MRP-14 binds an unknown membrane component that is abundant in specific granules.

Phosphorylation of threonine 113 of MRP-14 by p38 MAPK is interesting from the standpoint of substrate recognition by this proline-directed kinase. Threonine 113 is a

penultimate residue at the highly disordered C-terminus of the protein [320]. Although it is followed by a proline, it lacks a basic residue at -2 position and its proximity to the protein C-terminus makes it dramatically different from other p38 MAPK phosphorylation sites that are followed by a proline [321].

The MRP-14/MRP-8 complex binds arachidonic acid and can transport it through hydrophilic cytosol and extracellular fluids that would otherwise prevent the diffusion of this hydrophobic signaling molecule [287,322,323]. MK-2, a substrate of p38 MAPK, phosphorylates 5-lipoxygenase (5-LO), an arachidonate-metabolizing enzyme of the leukotriene synthesis pathway [324]. This phosphorylation is augmented in vitro by a direct addition of arachidonate to the reaction mixture containing 5-LO, MK2 and MgATP [324]. Thus, p38 MAPK may modulate arachidonate metabolism by inducing 5-LO activity, as well as transport of arachidonate through cytosol. This process may be involved in granule exocytosis, since arachidonate augments membrane fusion between specific granules and phospholipid vesicles [134,135], and MRP-14 may act in the delivery of this lipid mediator to neutrophil granules during exocytosis.

Using proteomic approaches, we identified a number of proteins that are likely to be involved in neutrophil granule exocytosis, and a novel p38 MAPK substrate that could participate in exocytosis and/or other neutrophil effector functions. Thus, we have provided targets for the studies that may lead to elucidation of the mechanism neutrophil degranulation, as well as improved understanding of the role of p38 MAPK in neutrophil exocytosis or other aspects of neutrophil biology.

REFERENCES

1. Boulay, F., Naik, N., Giannini, E., Tardif, M., Brouchon, L. (1997). Phagocyte chemoattractant receptors. *Annals of New York Academy of Sciences*. **832**, 69-84.

2. Heinzelmann, M., Mercer-Jones, M.A., Passmore, J.C. (1999). Neutrophils and renal failure. *American Journal of Kidney Diseases*. **34**, 384-399.

3. Linas, S.L., Whittenburg, D., Parsons, P.E., Repine, J.E. (1995). Ischemia increases neutrophil retention and worsens acute renal failure: role of oxygen metabolites and ICAM-1. *Kidney International*. **48**, 1584-1591.

4. Hellberg, P.O., Kallskog, T.O. (1989). Neutrophil-mediated post-ischemic tubular leakage in the rat kidney. *Kidney International*. **36**, 555-561.

5. Smith, J.A. (1994). Neutrophils, host defense, and inflammation: a double-edged sword. *Journal of Leukocyte Biology*. **56**, 672-686.

6. Malech, H.L., Gallin, J.I. (1987). Neutrophils in human diseases. *New England Journal of Medicine*. **317**, 687-694.

7. Weiss, S.J. (1989). Tissue destruction by neutrophils. *New England Journal of Medicine*. **320**, 565-576.

8. Borregaard, N., Cowland, J.B. (1997). Granules of the human neutrophilic polymorphonuclear leukocyte. *Blood*. **89**, 3503-3521.

9. Faurschou, M., Borregaard, N. (2003). Neutrophil granules and secretory vesicles in inflammation. *Microbes and Infection*. **5**, 1317-1327.

10. Kjeldsen, L., Sengelov, H., Borregaard, N. (1999). Subcellular fractionation of human neutrophils on Percoll density gradients. *Journal of Immunological Methods*. **232**, 131-143.

11. Sengelov, H., Kjeldsen, L., Borregaard, N. (1993). Control of exocytosis in early neutrophil activation. *Journal of Immunology*. **150**, 1535-1543.

12. Sengelov, H., Follin, P., Kjeldsen, L., Lollike, K., Dahlgren, C., Borregaard, N. (1995). Mobilization of granules and secretory vesicles during *ex vivo* exudation of human neutrophils. *Journal of Immunology*. **154**, 4157-4165.

13. Borregaard, N., Kjeldsen, L., Sengelov, H., Diamond, M.S., Springer, T.A., Anderson, H.C., Kishimoto, T.K., Bainton, D.F. (1994). Changes in subcellular localization and surface expression of L-selectin, alkaline phosphatase, and Mac-1 in human neutrophils during stimulation with inflammatory mediators. *Journal of Leukocyte Biology*. **56**, 80-87.

14. Pugin, J., Widmer, M.C., Kossodo, S., Liang, C.M., Preas, H.L., Suffredini, A.F. (1999). Human neutrophils secrete gelatinase B *in vitro* and *in vivo* in response to endotoxin and proinflammatory mediators. *Am. J. Respir. Cell. Mo. Biol.* **20**, 458-464.

15. Smolen, J.E., Peterson, T.K., Koch, C., O'Keefe, S.J., Hanlon, W.A., Seo, S., Pearson, D., Fossett, M.C., Simon, S.I. (2000). L-selectin signaling of neutrophil adhesion and degranulation involves p38 mitogen-activated protein kinase. *Journal of Biological Chemistry*. **275**, 15876-15884.

16. von Andrian, U.H., Chambers, D.J., McEnvoy, L.M., Bargatze, R.F., Arfors, K-E., Butcher, E.C. (1991). Two-step model of leukocyte endothelial cell interaction in inflammation: distinct roles of LECAM-1 and the leukocyte β2 integrins *in vivo*. *Proc. Natl. Acad. Sci. USA*. **88**, 7538-7542.

17. Sengelov, H., Kjeldsen, L., Diamond, M.S., Springer, T.A., Borregaard, N. (1993). Subcellular localization and dynamics of Mac-1 ($\alpha_m\beta_2$) in human neutrophils. *Journal of Clinical Investigation*. **92**, 1467-1476.

18. Delclaux, C., Delacourt, C., D'Ortho, M.P., Boyer, V., Lafuma, C., Harf, A. (1996). Role of gelatinase B and elastase in human polymorphonuclear neutrophil migration across basement membrane. *Am. J. Respir. Cell. Molec. Biol.* **14**, 288-295.

19. Kjeldsen, L., Sengelov, H., Lollike, K., Nielsen, M.H., Borregaard, N. (1994). Isolation and characterization of gelatinase granules from human neutrophils. *Blood*. **83**, 1640-1649.

20. Karlsson, A., Dahlgren, C. (2002). Assembly and activation of neutrophil NADPH oxidase in granule membranes. *Antioxidants & Redox Signaling*. **4**, 49-60.

21. Hasty, K.A., Hibbs, M.S., Kang, A.H., Mainardi, C.L. (1986). Secreted forms of human neutrophil collagenase. *Journal of Biological Chemistry*. **261**, 5645-5650.

22. Breton-Gorius. J., Mason, D.Y., Buriot, D., Vilde, J-L., Griscelli, C. (1980). Lactoferrin deficiency as a consequence of a lack of specific granules in neutrophils from a patient with recurrent infections. *American Journal of Pathology*. **99**, 413-428.

23. Gallin, J.I. (1985). Neutrophil specific granule deficiency. *Annual Reviews in Medicine*. **36**, 263-274.

24. Gullberg, U., Bengtsson, N., Bulow, E., Garwicz, D., Lindmark, A., Olsson, I. (1999). Processing and targeting of granule proteins in human neutrophils. *Journal of Immunological Methods*. **232**, 201-210.

25. Tapper, H., Grinstein, S. (1997). Fc receptor-triggered insertion of secretory granules into the plasma membrane of human neutrophils. *Journal of Immunology*. **159**, 409-418.

26. N'Diaye, E-N., Darzacq, X., Astarie-Dequeker, C., Daffe, M., Calafat, J., Maridonneau-Parini, I. (1998). Fusion of azurophil granules with phagosomes and activation of the tyrosine kinase Hck are specifically inhibited during phagocytosis of mycobacteria by human neutrophils. *Journal of Immunology*. **161**, 4983-4991.

27. Zeya, H., Spitznagel, J. (1971). Characterization of cationic protein-bearing granules of polymorphonuclear leucocytes. *Laboratory Investigation*. **24**, 229-236.

28. Bartold, P.M., Harkin, D.G., Bignold, L.P. (1989). Proteoglycans synthesized by human polymorphonuclear leucocytes *in vitro*. *Immunology and Cell Biology*. **67**, 9-17.

29. Gardiner, E.E., Mok, S.S., Spiratana, A., Robinson, H.C., Veitch, B.J.A., Lowther, D.A., Handley, C.J. (1994). Polymorphonuclear neutrophils release ^{35}S-labelled proteoglycans into cartilage during frustrated phagocytosis. *European Journal of Biochemistry*. **221**, 871-879.

30. Bainton, D.F., Farquhar, M.C. (1966). Origin of Granules in Polymorphonuclear Leukocytes. *Journal of Cell Biology*. **28**, 287-301.

31. Borregaard, N., Theilgaard-Mönch, K., Sørensen, O.E., Cowland, J.B. (2001). Regulation of human neutrophil granule protein expression. *Current Opinion in Hematology*. **8**, 23-27.

32. Cowland, J.B., Borregaard, N. (1999). The individual regulation of granule protein mRNA levels during neutrophil maturation explains the heterogeneity of neutrophil granules. *Journal of Leukocyte Biology*. **66**, 989–995.

33. Lian, Z., Wang, L., Yamaga, S., Bonds, W., Beazer-Barclay, Y., Kluger, Y., Gerstein, M., Newburger, P.E., Berliner, N., Weissman, S.M. (2001). Genomic and proteomic analysis of the myeloid differentiation program. *Blood*. **98**, 513-524.

34. Lian, Z., Kluger, Y., Greenbaum, D.S., Tuck, D., Gerstein, M., Berliner, N., Weissman, S.M., Neuwburger, P.E. (2002). Genomic and proteomic analysis of the myeloid differentiation program: global analysis of gene expression during induced differentiation of the MRPO cell line. *Blood*. **100**, 3209-3220.

35. Dahms, N.M., Lobel, P., Kornfeld, S. (1989). Mannose 6-phosphate receptors and lysosomal enzyme targeting. *Journal of Biological Chemistry*. **264**, 12115-12118.

36. Stromberg, K., Persson, A-M., Olsson, I. (1985). The processing and intracellular transport of myeloperoxidase. Modulation by lysosomotropic agents and monensin. *European Journal of Cell Biology*. **39**, 424-431.

37. Hasilik, A., Pohlmann, R., Olsen, R.L., von Figura, K. (1984). Myeloperoxidase is synthesized as a larger phosphorylated precursor. *EMBO Journal*. **3**, 2671-2676.

38. Subramaniam, M., Koedam, J.A., Wagner, D.D. (1993). Divergent fates of P- and E-selectins after their expression and the plasma membrane. *Molecular Biology of the Cell*. **4**, 791-801.

39. Disdier, M., Morrissey, J.H., Fugate, R.D., Bainton, D.F., McEver, R.P. (1992). Cytoplasmic domain of P-selectin (CD62) contains the signal for sorting into the regulated secretory pathway. *Molecular Biology of the Cell*. **3**, 309-321.

40. Dahlgren, C., Carlsson S.R., Karlsson, A., Lundqvist, H., Sjolin, C. (1995). The lysosomal membrane glycoproteins Lamp-1 and Lamp-2 are present in mobilizable organelles, but absent from the azurophil granules of human neutrophils. *Biochemical Journal*. **311**, 667-674.

41. Metzelaar, M.J., Wijngaard, P.L., Peters, P.J., Sixma, J.J., Nieuwenhuis, H.K., Clevers, H.C. (1991). CD63 antigen. A novel lysosomal membrane glycoprotein, cloned by a screening procedure for intracellular antigens in eukariotic cells. *Journal of Biological Chemistry*. **266**, 3239-3245.

42. Lemansky, P., Gerecitano-Schmidek, M., Das, R.C., Schmidt, B., Hasilik, A. (2003). Targeting myeloperoxidase to azurophil granules in HL-60 cells. *Journal of Leukocyte Biology*. **74**, 542-550.

43. Reggio, H., Dagorn, J.C. (1978). Ionic interactions between bovine chymotrypsinogen A and chondroitin sulfate A.B.C. A possible model for molecular aggregation in zymogen granules. *Journal of Cell Biology*. **78**, 951-957.

44. Niemann, C.U., Cowland, J.B., Klausen, P., Askaa, J., Calafat, J., Borregaard, N. (2004). Localization of serglycin in human neutrophil granulocytes and their precursors. *Journal of Leukocyte Biology*. **76**, 406-415.

45. Weiss, S.J., Klein, R., Slivka, A., Wei, M. (1982). Chlorination of taurine by human neutorphils. Evidence for hypochlorous acid generation. *Journal of Clinical Investigation*. **70**, 598-607.

46. Lollike, K., Lindau, M., Calafat, J., Borregaard, N. (2002). Compound exocytosis of granules in human neutrophils. *Journal of Leukocyte Biology*. **71**, 973-980.

47. Burgoyne, R.D., Morgan, A. (2002). Secretory granule exocytosis. *Physiological Reviews*. **83**, 581-632.

48. Blott, E.J., Griffiths, G.M. (2002). Secretory lysosomes. *Nature Reviews*. **3**, 122-131.

49. Ammala, C., Eliasson, L., Bokvist, K., Larsson, O., Ashcroft, F.M., Rorsman, P. (1993). Exocytosis elicited by action potentials and voltage-clamp calcium currents in individual mouse pancreatic B-cells. *Journal of Physiology*. **472**, 665-688.
50. Neher, E., Zucker, S. (1993). Multiple calcium-dependent processes related to secretion in bovine chromaffin cell. *Neuron*. **10**, 21-30.

51. Rosenmund, C., Stevens, C.F. (1996). Definition of the ready releasable pool of vesicles at hyppocampal synapses. *Neuron*. **16**, 1197-1207.

52, Gray, E.G. (1959). Axo-somatic and axo-dendritic synapses of the cerebral cortex: an electron microscope study. *Journal of Anatomy*. **93**, 420-433.

53. Hoffstein, S., Goldstein, I.M., Weissmann, G. (1977). Role of microtubule assembly in lysosomal enzyme secretion from human polymorphonuclear leukocytes, a reevaluation. *Journal of Cell Biology*. **73**, 242-256.

54. Kjeldsen, L., Bainton, D.F., Sengelov, H., Borregaard, N. (1993). Structural and functional heterogeneity among peroxidase-negative granules in human neutrophils: Identification of a distinct gelatinase containing granule subset by combined immunocytochemistry and subcellular fractionation. *Blood*. **82**, 3183-3191.

55. Calafat, J., Kuijpers, T.W., Janssen, H., Borregaard, N., Verhoeven, A.J., Roos, D. (1993). Evidence for small intracellular vesicles in human blood phagocytes containing cytochrome b_{558} and the adhesion molecule CD11b/CD18. *Blood*. **81**, 3122-3129.

56. Fernandez-Segura, E., Garcia, J.M., Campos, A. (1996). Topographic distribution of CD18 integrin on human neutrophils as related to shape changes and movement induced by chemotactic peptide and phorbol esters. *Cellular Immunology*. **171**, 120-125.

57. Jahn, R., Sudhof, T.C. (1999). Membrane fusion and exocytosis. *Annual Reviews in Biochemistry*. **68**, 863-911.

58. Sollner, T., Whiteheart, S.W., Brunner, M., Erdjument-Bromage, H., Geromanos, S., Tempst, P., Rothman, J.E. (1993). SNAP receptors implicated in vesicle targeting and fusion. *Nature*. **362**, 318-324.

59. Weimbs, T., Low, S.H., Chapin, S.J., Mostov, K.E., Bucher, P., Hofmann, K. (1997). A conserved domain is present in different families of vesicular fusion proteins: a new superfamily. *Proc. Natl. Acad. Sci. USA*. **94**, 3046-3051.

60. Fasshauer, D., Sutton, R.B., Brunger, A.T., Jahn, R. (1998). Conserved structural features of the synaptic fusion complex: SNARE proteins reclassified as Q- and R-SNAREs. *Proc. Natl. Acad. Sci. USA*. **95**, 15781-15786.

61. Chen, Y.A., Scheller, R.H. (2001). SNARE-Mediated membrane fusion. *Nature Reviews*. **2**, 98-106.

62. Antonin, W., Dulubovam, I., Arac, D., Pabst, S., Plitzner, J. (2002). The N-terminal domains of syntaxin 7 and vti1b form three-helix bundles that differ in their ability to regulate SNARE complex assembly. *Journal of Biological Chemistry*. **277**, 36449-36456.

63. Sutton, R.B., Fasshauer, D., Jahn, R., Brunger, A.T. (1998). Crystal structure of a SNARE complex involved in synaptic exocytosis at 2.4 Å resolution. *Nature*. **395**, 347-353.

64. Hanson, P.I., Roth, R., Morisaki, H., Jahn, R., Heuser, J.E. (1997). Structure and conformational changes in NSF and its membrane receptor complexes visualized by quick-freeze/deep-etch electron microscopy. *Cell*. **90**, 523-535.

65. Fasshauer, D., Eliason, W.K., Brunger, A.T., Jahn, R. (1998). Identification of a minimal core of the synaptic SNARE complex sufficient for reversible assembly and disassembly. *Biochemistry*. **37**, 10354-10362.

66. Hayashi, T., McMahon, H., Yamasaki, S., Binz, T., Hata, Y., Sudhof, T.C., Niemann, H. (1994). Synaptic vesicle membrane fusion complex: action of clostridial neurotoxins on assembly. *EMBO Journal*. **13**, 5051-5061.

67. May, A.P., Whiteheart, S.W., Weis, W.I. (2001). Unraveling the mechanism of the vesicle transport ATPase NSF, the N-ethylmaleimide-sensitive factor. *Journal of Biological Chemistry*. **276**, 21991-21994.

68. Tellam, J.T., Macauley, S.L., McIntosh, S., Hewish, D.R., Ward, C.W., James, D.E. (1997). Characterization of Munc-18c and syntaxin-4 in 3T3-L1 adipocytes. *Journal of Biological Chemistry*. **272**, 6179-6186.

69. De Camilli, P., Emr, S.D., McPherson, P.S., Novick, P. (1996). Phosphoinositides as regulators in membrane traffic. *Science*. **271**, 1533-1539.

70. Fujita, Y., Sasaki, T., Fukui, K., Kotani, H., Kimura, T., Hata, Y., Sudhof, T.C., Scheller, R.H., Takai, Y. (1996). Phosphorylation of Munc-18/nSec1/rbSec1 by protein kinase C. *Journal of Biological Chemistry*. **271**, 7265-7268.

71. Rhee, J-S., Betz,, A., Pyott, S., Reim, K., Varoqueaux, F., Augustin, I., Hesse, D., Sudhoff, T.C., Takahashi, M., Rosenmund, C., Brose, N. (2002). β-Phorbol ester- and diacylglycerol-induced augmentation of transmitter release is mediated by Munc13s and not by PKCs. *Cell*. **108**, 121-133.

72. Brumell, J.H., Volchunk, A., Sengelov, H., Borregaard, N., Cieutat, A.M., Bainton, D.F., Grinstein, S., Klip, A. (1995). Subcellular distribution of docking/fusion proteins in

neutrophils, secretory cells with multiple exocytic compartments. *Journal of Immunology*. **155**, 5750-5759.

73. Martin-Martin, B., Nabokina, S.M., Blasi, J., Lazo, P.A., Mollinedo, F. (2000). Involvement of SNAP-23 and syntaxin-6 in human neutrophil exocytosis. *Blood*. **96**, 2574-2583.

74. Ravichandran, V., Chawla, A., Roche, P.A. (1996). Identification of a novel syntaxin- and synaptobrevin/VAMP-binding protein, SNAP-23, expressed in non-neuronal tissues. *Journal of Biological Chemistry*. **271**, 13300-13303.

75. Mollinedo, F., Lazo, P.A. (1997). Identification of two isoforms of the vesicle-membrane fusion protein SNAP-23 in human neutrophils and HL-60 cells. *Biochem. Biophys. Res. Comm*. **231**, 808-812.

76. Mollinedo, F., Martin-Martin, B., Calafat, J., Nabokina, S.M., Lazo, P. (2003). Role of vesicle-associated membrane protein-2, through Q-soluble N-ethylmaleimide-sensitive factor attachment protein receptor/R-soluble N-ethylmaleimide-sensitive factor attachment protein receptor interaction, in the exocytosis of specific and tertiary granules of human neutrophils. *Journal of Immunology*. **170**, 1034-1042.

77. Martin-Martin, B., Nabokina, S.M., Lazo, P., Mollinedo, F. (1999). Co-expression of several human syntaxin genes in neutrophils and differentiated HL-60 cells: variant isoforms and detection of syntaxin1. *Journal of Leukocyte Biology*. **65**, 397-406.

78. Shukla, A., Berglund, L., Nielsen, P., Hoffmann, H.J., Dahl, R. (2000). Regulated exocytosis in immune function: are SNARE proteins involved? *Respiratory Medicine*. **94**, 10-17.

79. Orci, L., Gabbay, K.H,, Malaisse, W.J. (1972). Pancreatic beta-cell web: its possible role in insulin secretion. *Science*. **175**, 1128-1130.

80. Nemoto, T., Kojima, T., Oshima, A., Bito, H., Kasai, H. (2004). Stabilization of exocytosis by dynamic F-actin coating of zymogen granules in pancreatic acini. *Journal of Biological Chemistry*. **279**, 37544-37550.

81. Dos Remedios, C.G., Chhabra, D., Kekic, M., Dedova, I.V., Tsubakihara, M., Berry, D.A., Nosworthy, N.J. (2003). Actin binding proteins: regulation of cytoskeletal microfilaments. *Physiological Reviews*. **83**, 433:473.

82. Trifaro, J-M., Rose, S.D., Marcu, M.G. (2000). Scinderin, a Ca^{2+}-dependent actin filament severing protein that controls cortical actin network dynamics durin secretion. *Neurochemical Research*. **25**, 133-144.

83. Eitzen, G. (2003). Actin remodeling to facilitate membrane fusion. *Biochimica et Biophysica Acta*. **1641**, 175-181.

84. Doussau, F., Augustine, G.J. (2000). The actin cytoskeleton and neurotransmitter release: an overview. *Biochimie.* **82,** 353-363.

85. Segawa, A., Yamashina, S. (1989). Roles of microfilaments in exocytosis: a new hypothesis. *Cell Structure and Function.* **14,** 531–544.

86. Jahraus, A., Egeberg, M., Hinner, B., Habermann, A., Sackman, E. Pralle, A., Faulstich, H., Rybin, V., Defacque, H., Griffiths, G. (2001). ATP-dependent membrane assembly of F-actin facilitates membrane fusion. *Molecular Biology of the Cell.* **12,** 155–170.

87. Eitzen, G., Wang, L., Thorngren, N., Wickner, W. (2002). Remodeling of organelle-bound actin is required for yeast vacuole fusion. *Journal of Cell Biology.* **158,** 669–679.

88. Ramos, C., Teissie, J. (2000). Electrofusion: a biophysical modification of cell membrane and a mechanism in exocytosis. *Biochimie.* **82,** 511–518.

89. Rose, S.D., Lejen, T., Casaletti, L., Larson, R.E., Pene, T.D., Trifaro, J-M. (2002). Molecular motors involved in chromaffin granule secretion. *Ann. N.Y. Acad. Sci.* **971,** 222-231.

90. Nakano, M., Nogami, S., Sato, S., Terano, A., Shirataki, H. (2001). Interaction of syntaxin with α-fodrin, a major component of the submembranous cytoskeleton. *Biochemical & Biophysical Research Communications.* **288,** 468-475.

91. Ohyama, A., Komiya, Y., Igarashi, M. (2001). Globular tail of myosin-V is bound to vamp/synaptobrevin. *Biochemical & Biophysical Research Communications.* **280,** 988-991.

92. Rothwell, S.W., Nath, J., Wright, D.G. (1989). Interactions of cytoplasmic granules with microtubules in human neutrophils. *Journal of Cell Biology.* **108,** 2313-2326.

93. Rothwell, S.W., Deal, C.C., Pinto, J., Wright, D.G. (1993). Affinity purification and subcellular localization of kinesin in human neutrophils. *Journal of Leukocyte Biology.* **53,** 372-380.

94. Tapper, H., Furuya, W., Grinstein, S. (2002). Localized exocytosis of primary (lysosomal) granules during phagocytosis: role of Ca^{2+}-dependent tyrosine phosphorylation and microtubules. *The Journal of Immunology.* **168,** 5287-5296.

95. Ignarro, L.J. (1974). Stimulation of phagocytic release of neutral protease from human neutrophils by cholinergic amines and cyclic 3',5'-guanosine monophosphate. *Journal of Immunology.* **112,** 210-213.

96. Ignarro, L.J., Cech, S.Y. (1976). Bidirectional regulation of lysosomal enzyme secretion and phagocytosis in human neutrophils by guanosine 3'-5'-monophosphate and

adenosine 3',5'-monophosphate. *Proceedings of the Society of Experimental Biology and Medicine.* **151**, 448-452.

97. Weissmann, G., Goldstein, I., Hoffstein, I., Tsung, P.K. (1975). Reciprocal effects of cAMP and cGMP on microtubule-dependent release of lysosomal enzymes. *Annals of the New York Academy of Sciences.* **253**, 750-762.

98. Pryzwansky, K.B. and Merricks, E. (1998). Chemotactic peptide-induced changes of intermediate filament organization in neutrophils during granule secretion: role of cyclic guanosine monophosphate. *Molecular Biology of the Cell.* **9**, 2933-2947.

99. Faigle, W. Colucci-Guyon, E., Louvard, D., Amigorena, S., Galli, T. (2000). Vimentin filaments fibroblasts are a reservoir for SNAP23, a component of the membrane fusion machinery. *Molecular Biology of the Cell.* **11**, 3485-3494.

100. Martin-Verdaux, S., Pombo, I., Iannascoli, B., Roa, M., Varin-Blank, N., Rivera, J., Blank, U. (2003). Evidence of a role for Munc18-2 and microtubules in mast cell granule exocytosis. *Journal of Cell Science.* **116**, 325-334.

101. Thelen, M., Dewald, B., Baggiolini, M. (1993). Neutrophil signal transduction and activation of the respiratory burst. *Physiological Reviews.* **73**, 797-821.

102. Putney, J. W., McKay, R. R. (1999). Capacitative calcium entry channels *Bioessays.* **21**, 38-46.

103. Demaurex, N., Schlegel, W., Varnai, P., Mayr, G., Lew, D. P., Krause, K. H. (1992). Regulation of Ca^{2+} influx in myeloid cells. Role of plasma membrane potential, inositol phosphates, cytosolic free [Ca^{2+}], and filling state of intracellular Ca^{2+} stores. *Journal of Clinical Investigation.* **90**, 830-839.

104. Andersson, T., Dahlgren, C., Pozzan, T., Stendahl, O., Lew, P.D. (1986). Characterization of fMet-Leu-Phe receptor-mediated Ca^{2+} influx across the plasma membrane of human neutrophils *Molecular Pharmacology.* **30**, 437-443.

105. Pozzan, T., Lew, D.P., Wollheim, C.B., Tsien, R.Y. (1983). Is cytosolic ionized calcium regulating neutrophil activation? *Science.* **221**, 1413-1415.

106. Sham, R.L., Phatak, P.D., Ihne, T.P., Abboud, C.N., Packman, C.H. (1993). Signal pathway regulation of interleukin-8-induced actin polymerization in neutrophils. *Blood.* **82**, 2546-2551.

107. Gerard, C., Gerard, N.P. (1994). C5a anaphylatoxin and its seven transmembrane-segment receptor. *Annual Review of Immunology.* **12**, 775-808.

108. Richter, J., Andersson, T., Olsson, I. (1989). Effect of tumor necrosis factor and granulocyte/macrophage colony-stimulating factor on neutrophil degranulation. *Journal of Immunology*. **142**, 3199-3205.

109. Lew, D.P., Wollheim, C.B., Waldvogel, F.A., Pozzan, T. (1984). Modulation of cytosolic free calcium transients by changes in intracellular calcium-buffering capacity: correlation with exocytosis and O_2^- production in human neutrophils. *Journal of Cell Biology*. **99**, 1212-1220.

110. Lew, D.P., Monod, A., Waldvogel, F.A., Dewald, B., Baggiolini, M., Pozzan, T. (1986). Quantitative analysis of the cytosolic free calcium dependency of exocytosis from three subcellular compartments in intact human neutrophils. *Journal of Cell Biology*. **102**, 2197-2204.

111. Boyhan, A., Casimir, C.M., French, J.K., Teahan, C.G., Segal, A.W. (1992). Molecular cloning and characterization of grancalcin, a novel EF-hand calcium-binding protein abundant in neutrophils and monocytes. *Journal of Biological Chemistry*. **267**, 2928-2933.

112. Teahan, C.G., Totty, N.F., Segal, A.W. (1992). Isolation and characterization of grancalcin, a novel 28-kDa EF-hand calcium-binding protein from human neutrophils. *Biochemical Journal*. **286,** 549-554.

113. Roes, J., Choi, K.B., Power, D., Xu, P., Segal, A.W. (2003). Granulocyte function in grancalcin-deficient mice. *Molecular and Cellular Biology*. **23**, 826–830.

114. Blackwood, R.A., Ernst, J.D. (1990). Characterization of calcium-dependent phospholipid binding, vesicle aggregation, and membrane fusion by annexins. *Biochemical Journal*. **266**, 195-200.

115. Volker, G., Moss, S.E. (2002). Annexins: from structure to function. *Physiological Reviews*. **82**, 331-371.

116. Le Cabec, V., Maridonneau-Parini, I. (1994). Annexin 3 is associated with cytoplasmic granules in neutrophils and monocytes and translocates to the plasma membrane in activated cells. *Biochemical Journal*. **303**, 481-487.

117. Ernst, J.D., Hoye, E., Blackwood, R.A., Jaye, D. (1990). Purification and characterization of an abundant cytosolic protein from human neutrophils that promotes Ca^{2+}-dependent aggregation of isolated specific granules. *Journal of Clinical Investigation*. **85**, 1065–1071.

118. Rosales, J.L. and Ernst, J.D. (1997). Calcium-dependent neutrophil secretion: characterization and regulation by annexins. *Journal of Immunology*. **159**, 6195-6202.

119. Theander, S., Lew, D.P., Nusse, O. (2002). Granule-specific ATP requirements for Ca^{2+}-induced exocytosis in human neutrophils. Evidence for substantial ATP-independent release. *Journal of Cell Science*. **115**, 2975-2983.

120. Baggiolini, M., Dewald, B., Moser, B. (1997). Human chemokines: an update. *Annual Reviews in Immunology*. **15**, 675-705.

121. Barrowman, M.M., Cockroft, S., Gomperts, B.D. (1986). Two roles for guanine nucleotides in the stimulus-secretion sequence of neutrophils. *Nature*. **319**, 504-507.

122. Nusse, O., Lindau, M. (1988). The dynamics of exocytosis in human neutrophils. *Journal of Cell Biology*. **107**, 2117-2123.

123. Smolen, J.E., Stoehr, S.J. (1986). Guanine nucleotides reduce the free calcium requirement for secretion of granule constituents from permeabilized neutrophils. *Biochimica et Biophysica Acta*. **889**, 171-178.

124. Nusse, O., Lindau, M. (1993). The calcium signal in human neutrophils and its relation to exocytosis investigated by patch-clamp capacitance and Fura-2 measurements. *Cell Calcium*. **14**, 255-269.

125. Becker, E.L., Kermode, J.C., Naccache, P.H., Yassin, R., Marsh, M.L., Munoz, J.J., Sha'afi, R.I. (1985). The inhibition of neutrophil granule enzyme secretion and chemotaxis by pertussis toxin. *Journal of Cell Biology*. **100**, 1641-1646.

126. Molski, T.F.P., Naccache P.H., Marsh, M.L., Kermode, J., Becker, E.L., Sha'afi R.I. (1984). Pertussis toxin inhibits the rise in the intracellular concentration of free calcium that is induced by chemotactic factors in rabbit neutrophils: possible role of the "G proteins" in calcium mobilization. *Biochemical and Biophysical Research Communications*. **124**, 644-650.

127. Pinxteren, J.A., O'Sullivan, A.J., Larbi, K.Y., Tatham, P.E.R., Gomperts, B.D. (2000). Thirty years of stimulus-secretion coupling: from Ca^{2+} to GTP in regulation of exocytosis. *Biochimie*. **82**, 385-393.

128. Stephens, L.R., Eguinoa, A., Erdjument, B.H., Lui, M., Cooke, F., Coadwell, J., Smrcka, A.S., Thelen, M., Caldwallader, K., Tempst, P., Hawkins, P.T. (1997). The G beta gamma sensitivity of a PI3K is dependent upon a tightly associated adaptor, p101. *Cell*. **89**, 105-114.

129. Maridonneau-Parini, I. de Gunzburg, J. (1992). Association of rap1 and rap2 proteins with the specific granules of human neutrophils. Translocation to the plasma membrane during cell activation. *Journal of Biological Chemistry*. **267**, 6396-6402.

130. Philips, M.R., Abramson, S.B., Kolasinski, S.L., Haines, K.A., Wessmann, G., Rosenfeld, M.G. (1991). Low molecular weight GTP-binding proteins in human neutrophil granule membranes. *Journal of Biological Chemistry*. **266**, 1289-198.

131. Cicchetti, G., Allen, P.G., Glogauer, M. (2002). Chemotactic signaling pathways in neutrophils: from receptor to actin assembly. *Crit. Rev. Oral Bio. Med.* **13**, 220-228.
132. Zhong, B., Jiang, K., Gilvary, D.L., Epling-Burnette, P.K., Ritchey, C. Liu, J., Jackson, R.J., Hong-Geller, E., Wei, S. (2003). Human neutrophils utilize a Rac/Cdc42-dependent MAPK pathway to direct intracellular granule mobilization toward ingested microbial pathogens. *Blood*. **101**, 3240-3248.

133. Abdel-Latif, D., Steward, M., Macdonald, D.L., Francis, G.A, Dinauer, M.C., Lacy P. (2004). Rac2 is critical for neutrophil primary granule exocytosis. *Blood*. **104**, 832-839.

134. Blackwood, R.A., Transue, A.T., Harsh, D.M., Brower, R.C., Zacharek, S.J., Smolen, J.E., Hessler, R.J. (1996). PLA_2 promotes fusion between PMN-specific granules and complex liposomes. *Journal of Leukocyte Biology*. **59**, 663-670.

135. Forehand, J.R., Johnston, R.B., Bomalaski, J.S. (1993). Phospholipase A2 activity in human neutrophils. Stimulation by lipopolysaccharide and possible involvement in priming for an enhanced respiratory burst. *Journal of Immunology*. **151**, 4918-4925.

136. Harsh, D.M., Blackwood, R.A. (2001). Phospholipase A2-mediated fusion of neutrophil-derived membranes is augmented by phosphatidic acid. *Biochemical and Biophysical Research Communications*. **282**, 480-486.

137. Khan, Y., Kanoh, H., Nozawa, Y. (1991). Activation of phospholipase D in rabbit neutrophjils by fMet-Leu-Phe is mediated by a pertussis toxin-sensitive GTP-binding protein that may be distinct from a phospholipase C-regulating protein. *FEBS Letters*. **279**, 249-252.

138. Mullmann, T.J., Siegel, M.I., Egan, R.W., Billah, M.M. (1990). Complement C5a activation of phospholipase D in human neutrophils. Major route to the production of phosphatidates and diglycerides. *Journal of Immunology*. **144**, 1901-1908.

139. Kanaho, Y., Kanoh, H., Saitoh, K., Nozawa, Y. (1991). Phospholipase D activation by platelet-activating factor, leukotriene B4, and formyl-methionyl-leucyl-phenylalanine in rabbit neutrophils. Phospholipase D activation is involved in enzyme release. *Journal of Immunology*. **146**, 3536-3541.

140. Kaldi, K., Szeberenyi, J., Rada, B.K., Kovacs, P., Geiszt, M., Mocsai, A., Ligeti, E. (2002). Contribution of phospholipase D and brefeldin A-sensitive ARF to chemoattractant-induced superoxide production and secretion of human neutrophils. *Journal of Leukocyte Biology*. **71**, 695-700.

141. Succhard, S.J., Nakamura, T., Abe, A., Shayman, J.A., Boxer, L.A. (1994). Phospholipase D-mediated diradylglycerol formation coincides with H_2O_2 and lactoferrin release in adherent human neutrophils. *Journal of Biological Chemistry.* **269**, 8063-8068.

142. Nadler, M.J.S., Kinet. J-P. (2002). Uncovering new complexities in mast cell signaling. *Nature Immunology.* **3**, 707-708.
143. Korchak, H.M., Rossi, M.W., Kilpatrick, L.E. (1998). Selective role for beta-protein kinase C in signaling for O-2 generation but not degranulation or adherence in differentiated HL60 cells. *Journal of Biological Chemistry.* **273**, 27292-27299.

144. Junger, W.G., Hoyt, D.B., Davis, R.E., Herdon-Remelius, C., Namiki, S., Junger, H., Loomis, W., Altman, A. (1998). Hypertonicity regulates the function of human neutrophils by modulating chemoattractant receptor signaling and activating mitogen-activated protein kinase p38. *Journal of Clinical Investigation.* 101:2768-2779.

145. Silinsky, E.M., Searl, T.J. (2003). Phorbol esters and neurotransmitter release: more than just protein kinase C? *British Journal of Pharmacology.* **138**, 1191–1201.

146. Siddiqui, R.A., English, D. (1997). Phosphatidic acid elicits calcium mobilization and actin polymerization through a tyrosine kinase-dependent process in human neutrophils: A mechanism for induction of chemotaxis. *Bichimica et Biophysica Acta.* **1349**, 81-95.

147. Sergent, S., Waite, K.A., Heravi, J., McPhail, L.C. (2001). Phosphatidic acid regulates tyrosine phosphorylating activity in human neutrophils. Enhancement of Fgr activity. *Journal of Biological Chemistry.* **276**, 4737-4746.

148. Horn, J.M., Lehman, J.A., Alter, G., Horwitz, J., Gomez-Cambronero, J. (2001). Presence of a phospholipase D (PLD) distinct from PLD1 or PLD2 in human neutrophils: Immunochemical characterization and initial purification. *Biochimica et Biophysica Acta.* **1530**, 97-110.

149. Tou, J. (2002). Differential regulation of neutrophil phospholipase D activity and degranulation. *Biochemical and Biophysical Research Communications.* **292**, 951-956.

150. Welch, H., Maridonneau-Parini, I. (1997). Lyn and Fgr are activated in distinct membrane fractions of human granulocytic cells. *Oncogene.* **15**, 2021-2029.

151. Welch, H., Mauran, C., Maridonneau-Parini, I. (1996). Nonreceptor protein-tyrosine kinases in neutrophil activation. *Methods; A Companion to Methods in Enzymology.* **9**, 607-618.

152. Mocsai, A., Banfi, B., Kapus, A., Farkas, G., Geiszt, M., Buday, L., Farago, A., Ligeti, E. (1997). Differential effects of tyrosine kinases inhibitors and an inhibitor of the mitogen-activated protein kinase cascade on degranulation and superoxide production of human neutrophil granulocytes. *Biochemical Pharmacology.* **54**, 781-789.

153. Gutkind, J.S. and Robbins, K. (1989). Translocation of the FGR protein-tyrosine kinase as a consequence of neutrophil activation. *Proc. Natl. Acad. Sci. USA.* **86**, 8783-8787.

154. Mohn, H., Le Cabec, V., Fischer, S., Maridonneau-Parini, I. (1995). The src-family protein-tyrosine kinase p59hck is located on the secretory granules in human neutrophils and translocates towards the phagosome during cell activation. *Biochemical Journal.* **309**, 657-665.

155. Mocsai, A., Ligeti, E., Lowell, C.A., Berton, G. (1999). Adhesion-dependent degranulation of neutrophils requires the Src family kinases Fgr and Hck. *Journal of Immunology.* **162**, 1120-1126.

156. Corey, S., Eguinoa, A., Puyanatheall, K., Bolen, J.B., Cantley, L., Mollinedo, F., Jackson, T.R., Hawkins, P.T., Stephens, L.R. (1993). Granulocyte macrophage-colony stimulating factor stimulates both association and activation of phosphoinositide 3OH-kinase and src- related tyrosine kinase(s) in human myeloid derived cells. *EMBO Journal.* **12**, 2681-2690.

157. Alonso, A., Bayon, Y., Mateos, J.J., Crespo, M.S. (1998). Signaling by leukocyte chemoattractant and Fc receptors in immune-complex tissue injury. *Laboratory Investigation.* **78**, 377-392.

158. Hirsch, E., Katanaev, V.L., Garlanda, C., Azzolino, O., Pirola, L., Silengo, L., Sozzani, S., Mantovani, A., Altruda, F., Wymann, M.P. (2000). Central role for G protein-coupled phosphoinositide 3-kinase γ in inflammation. *Science.* **287**, 1049-1053.

159. Sadhu, C., Dick, K., Tino, W.T., Staunton, D.E. (2003). Selective role of PI3K delta in neutrophil inflammatory responses. (2003). *Biochemical and Biophysical Research Communication.* **308**, 764-769.

160. Sue, A.Q., Fialkow, L., Vlahos, C.J., Schelm, J.A., Grinstein, S., Butler, J., Downey, G.P. (1997). Inhibition of neutrophil oxidative burst and granule secretion by wortmannin: potential role of MAP kinase and renaturable kinases. *Journal of Cell Physiology.* **172**, 94-108.

161. Thelen, M., Wymann, M.P., Langen. H. (1994). Wortmannin binds specifically to 1-phosphatidylinositol 3-kinase while inhibiting guanine nucleotide-binding protein-coupled receptor signaling in neutrophil leukocytes. *Proc. Natl. Acad. Sci. USA.* **91**, 4960-4964.

162. Yamamori, T., O. Inanami, H. Nagahata, Y. Cui, M. Kuwabara. (2000). Roles of p38 MAPK, PKC and PI3-K in the signaling pathways of NADPH oxidase activation and phagocytosis in bovine polymorphonuclear leukocytes. *FEBS Letters.* **467**, 253-258.

163. Bonser, R.W., Thompson, N.T., Randall, R.W., Tateson, J.E., Spacey, G.D., Hodson, H.F., Garland, G.L. (1991). Demethoxyviridin and wortmannin block phospholipase C and D activation in the human neutrophil. *British Journal of Pharmacology*. **103**, 1237-1241.

164. Wyatt, T.A., Lincoln, T.M., Pryzwansky, K.B. (1993). Regulation of human neutrophil degranulation by LY-83583 and L-arginine: role of cGMP-dependent protein kinase. *American Journal of Physiology - Cell Physiology*. **265**, C201-C211.

165. Widmann, C., Gibson, S., Jarpe, M.B., Johnson, G.L. (1999). Mitogen-activated protein kinase: conservation of a three-kinase module from yeast to human. *Physiological Reviews*. **79**, 143-180.

166. Kyriakis, J.M., Avruch, J. (2001). Mammalian mitogen-activated protein kinase signal transduction pathways activated by stress and inflammation. *Physiological Reviews*. **81**, 807-869.

167. Kato, Y., Tapping, R.I., Huang, S., Watson, M.H., Ulevitch, R.J., Lee, J.D. (1998). Bmk1/Erk5 is required for cell proliferation induced by epidermal growth factor. *Nature*. **395**, 713-716.

168. Ono, K., Han, J. (2000). The p38 signal transduction pathway activation and function. *Cellular Signaling*. **12**, 1-13.

169. Nick, J.A., Avdi, N.J., Young, S.K., Lehman, L.A., McDonald, P.P., Frasch, S.C., Billstrom, M.A., Henson, P.M., Johnson, G.L., Worthen, G.S. (1999). Selective activation and functional significance of p38α mitogen-activated protein kinase in lipopolysaccharide-stimulated neutrophils. *Journal of Clinical Investigation*. **103**, 851-858.

170. Goedert, M., Cuenda, A., Craxton, M., Jakes, R., Cohen, P. (1997). Activation of the novel stress-activated protein kinase SAPK4 by cytokines and cellular stresses is mediated by SKK3 (MKK6): comparison of its substrate specificity with that of other SAP kinases. *EMBO Journal*. **16**, 3563-3571.

171. Young, P.R., McLaughlin, M.M., Kumar, S., Kassis, S., Doyle, M.L., McNulty, D., Gallagher, T.F., Fisher, S., McDonnell, P.C., Carr, S.A. (1997). Pyridinyl imidazole inhibitors of p38 mitogen-activated protein kinase bind in the ATP site. *Journal of Biological Chemistry*. **272**, 12116–12121.

172. Nick, J.A., Avdi, N.J., Young, S.K., Knall, C., Gerwins, P., Johnson, G.L., Worthen, G.S. (1997). Common and distinct pathways in human neutrophils utilized by platelet activating factor and fMLP. *Journal of Clinical Investigation*. **99**, 975-986.

173. McLeish, K. R., Knall, C., Ward, R.A., Gerwins, P., Coxon, P.Y., Klein, J.B., Johnson, G.L. (1998). Activation of mitogen-activated protein kinase cascades during

priming of human neutrophils by TNF-α and GM-CSF. *Journal of Leukocyte Biology.* **64**, 537-545.

174. Rane, M. J., Carrithers, S.L., Arthur, J.M., Klein, J.B., McLeish, K.R. (1997). Formyl peptide receptors are coupled to multiple mitogen-activated protein kinases cascades by distinct signal transduction pathways. *Journal of Immunology.* **159**, 5070-5078.

175. Krump, E., Sanghera, J.S., Pelech, S.L., Furuya, W., Grinstein, S. (1997). Chemotactic peptide *N*-formyl-Met-Leu-Phe activation of p38 mitogen-activated protein kinase (MAPK) and MAPK-activated protein kinase-2 in human neutrophils. *Journal of Biological Chemistry.* **272**, 937-944.

176. Knall, C., Young, S., Nick, J.A., Buhl, M.A., Worthen, G.S., Johnson, G.L. (1996). Interleukin-8 regulation of the Ras/Raf/mitogen-activated protein kinase pathway in human neutrophils. *Journal of Biological Chemistry.* **271**, 2832-2838.

177. Bouaounia M., Blouin, E., Halnwachs-Mecarelli, L., Lesavre, P., Rieu, P. (2004). TNF-induced β2 integrin activation involves Src kinases and a redox-regulated activation of p38 MAPK. *Journal of Immunology.* **173**, 1313-1320.

178. Huizinga, T. W., Dolman, K.M., van der Linden, N.J., Kleijer, M., Nuijens, J.H., von dem Borne, A.E., Roos. D. (1990). Phosphatidylinositol-linked FcRIII mediates exocytosis of neutrophil granule proteins, but does not mediate initiation of the respiratory burst. *Journal of Immunology.* **144**, 1432-1437.

179. Coxon, P.Y., Rane, M.J., Powell, D.W., Klein, J.B., McLeish, K.R. (2000). Differential mitogen-activated protein kinase stimulation by Fc gamma receptor IIa and Fc gamma receptor IIIb determines the activation phenotype of human neutrophils. *Journal of Immunology.* **164**, 6530-6537.

180. Nick, J.A., Avdi, N.J., Gerwins, P., Johnson, G.J., Worthen, S.G. (1996). Activation of a p38 mitogen-activated protein kinase in human neutrophils by lipopolysaccharide. *Journal of Immunology.* **156**, 4867-4875.

181. Darren, D., Browning, N., Windes, D., Ye. R.D. (1999). Activation of p38 Mitogen-activated Protein Kinase by Lipopolysaccharide in Human Neutrophils Requires Nitric Oxide-dependent cGMP Accumulation. *Journal of Biological Chemistry.* **274**, 537-542.

182. Browning, D.D., Windes, N.D., Ye, R.D. (1999). Activation of p38 mitogen-activated protein kinase by lipopolysaccharide in human neutrophils requires nitric oxide-dependent cGMP accumulation. *Journal of Biological Chemistry.* **274**, 537-542.

183. Perskvist, N., Zheng, L., Stendahl, O. (2000) Activation of human neutrophils by *Mycobacterium tuberculosis* H37Ra involves phospholipase Cγ2, Shc adaptor protein, and p38 mitogen-activated protein kinase. *Journal of Immunology.* **164**, 959-965

184. Schnyder, B., Meunier, P.C., Car, B.D. (1998). Inhibition of kinases impairs neutrophil activation and killing of Staphylococcus aureus. *Biochemical Journal.* **331**, 489-495.

185. Tandon, R., Sha'afi, R.I., Thrall, R.S. (2000). Neutrophil β2-integrin upregulation is blocked by a p38 MAP kinase inhibitor. *Biochemical and Biophysical Research Communications.* **270**, 858-862.

186. Ward, R.A., Nakamura, M., McLeish, K. (2000). Priming of the neutrophil respiratory burst involves p38 mitogen-activated protein kinase-dependent exocytosis of flavocytochrome b_{558}-containing granules. *Journal of Biological Chemistry.* **275**, 36713-36719.

187. Wyman, T.H., Dinarello, C.A., Banerjee, A., Gamboni-Robertson, F., Hiester, A.A., England, K.M., Kelher, M., Silliman, C.C. (2002). Physiological levels of interleukin-18 stimulate multiple neutrophil functions through p38 MAP kinase activation. *Journal of Leukocyte Biology.* **72**, 401-409.

188. Mocsai, A., Jakus, Z., Vantus, T., Berton, G., Lowell, C.A., Ligeti, E. (2000). Kinase pathways in chemoattractant-induced degranulation of neutrophils: the role of p38 mitogen-activated protein kinase activated by Src family kinases. *Journal of Immunology.* **164**, 4321-4331.

189. Gaudreault, E. Thompson, C., Stankova, J., Rola-Pleszczynski, M. (2005). Involvement of BLT1 endocytosis and Yes kinase activation in leukotriene B_4-induced neutrophil degranulation. *Journal of Immunology.* **174**, 3617-3625.

190. Kasper, B., Brandt, E., Bulfone-Paus, S., Petersen, F. (2003). Platelet factor 4 (PF-4)-induced neutrophil adhesion is controlled by src-kinases, whereas PF-4-mediated exocytosis requires the additional activation of p38 MAP kinase and phosphatidylinositol-3-kinase. *Blood.* **103**, 1602-1610.

191. Capodici, C., Hanft, S., Feoktistov, M., Pillinger, M.H. (1998). Phosphatidylinositol 3-kinase mediates chemoattractant-stimulated, CD11b/CD18-dependent cell-cell adhesion of human neutrophils: evidence for an ERK-independent pathway. *Journal of Immunology.* **160**, 1901-1909.

192. Roberts, A., Kim, C., Zhen, L., Lowe, J., Kapur, R., Petryniak, B., Spaetti, A., Pollock, J., Borneo, J., Bradford, G. (1999). Deficiency of the hematopoietic cell-specific Rho-family GTPase, Rac2, is characterized by abnormalities in neutrophil function and host defense. *Immunity.* **10**, 183-196.

193. Shi, Y., Gaestel, M. (2002). In the cellular garden of forking paths: how p38 MAPKs signal for downstream assistance. *Biological Chemistry.* **383**, 1519-1536.

194. Brown, G.E., Stewart M.Q., Bissonnette, S.A., Elia, A.E.H., Wilker, E., Yaffe, M.B. (2004). Distinct ligand-dependent roles for p38 MAPK in priming and activation of the neutrophil NADPH oxidase. *Journal of Biological Chemistry*. **279**, 27059-27068.

195. Coxon, P.Y., Rane, M.J., Uriarte, S., Powell, D.W., Singh, S., Butt, W., Chen, Q., McLeish, K.R. (2003). MAPK-activated protein kinase-2 participates in p38 MAPK-dependent and ERK-dependent functions in human neutrophils. *Cellular Signaling*. **15**, 993-1001.

196. Nahas, N., Thaddeus, Molski, T.F.P., Fernandez, G.A., Sha'afi, R.I. (1996). Tyrosine phosphorylation and activation of a new mitogen-activated protein (MAP)-kinase cascade in human neutrophils stimulated with various agonists. *Biochemical Journal*. **318**, 246-253.

197. Hannigan, M., Zhan, L., Ai, Y., Kotlyarov, A., Gaestel, M., Huang, C. (2001). Abnormal migration phenotype of mitogen-activated protein kinase-activated protein kinase $2^{-/-}$ neutrophils in Zigmond chambers containing *formyl*-methionyl-leucyl-phenylalanine gradients. *Journal of Immunology*. **167**, 3953-3961.

198. Powell, D.W., Rane, M.J., Joughin, B.A., Kalmukova, R., Hong, J.H., Tidor, B., Dean, W.L., Pierce, W.M., Klein, J.B., Yaffe, M.B., McLeish, K.R. (2003). Proteomic identification of 14-3-3ζ as a mitogen-activated protein kinase-activated protein kinase 2 substrate: role in dimer formation and ligand binding. *Molecular and Cellular Biology*. **23**, 5376-5387.

199. Singh, S., Powell, D., Rane, M., Millard, T.H., Trent, J., Pierce, W., Klein, J., Machesky, L., McLeish K.R. (2003). Identification of the p16-Arc subunit of the Arp 2/3 complex as a substrate of MAPK-activated protein kinase 2 by proteomic analysis. *Journal of Biological Chemistry*. **278**, 36410-36417.

200. Werz, O., Klemm, J., Samuelsson, B., Radmark, O. (2000). 5-lipoxygenase is phosphorylated by p38 kinase dependent MAPKAP kinases. *Proc. Nat. Acad. Sci. USA*. **97**, 5262-5266.

201. Cheng, T.J., Lai, Y.K. (1998). Identification of mitogen-activated protein kinase-activated protein kinase-2 as a vimentin kinase activated by okadaic acid in 9L rat brain tumor cells. *Journal of Cellular Biochemistry*. **71**, 169-181.

202. Komatsu, S. and Hosoya, H. (1996). Phosphorylation by MAPKAP kinase 2 activates Mg^{2+}-ATPase activity of myosin II. *Biochemical and Biophysical Research Communications*. **223**, 741-745.

203. Lewis, T.S., Hunt, J.B., Aveline, L.D., Jonscher, K.R., Louie, D.F., Yeh, J.M., Nahreini T,S., Resing, K.A., Ahn, N.G. (2000). Identification of novel MAP kinase pathway signaling targets by functional proteomics and mass spectrometry. *Molecular Cell*. **6**, 1343-1354.

204. O'Farrell, P. (1975). High resolution two-dimensional electrophoresis of proteins. *Journal of Biological Chemistry*. **250**, 4007-4021.

205. Gorg, A., Obermaier, C. Boguth, G. Harder, A., Scheibe, B., Wildgruber, R., Weiss, W. (2001). The current state of two-dimensional electrophoresis with immobilized pH gradients. *Electrophoresis*. **21**, 1037-1053.

206. Corthals, G.L., Wasinger, V.C., Hochstrasser, D.F., Sanches, J-C. (2000). The dynamic range of protein expression: challenge for proteomic research. *Electrophoresis*. **21**, 1104-1115.

207. Santoni, V., Molloy, M., Rabilloud, T. (2000). Membrane proteins and proteomics: un amour impossible? *Electrophoresis*. **21**, 1054-1070.

208. Santoni, V., Rabilloud, T., Doumas, P., Rouquie, D., Mansion, M., Kieffer, S., Garin, J., Rossignol, M. (1999). Towards the recovery of hydrophobic proteins on two-dimensional electrophoresis gels. *Electrophoresis*. **20**, 705-711.

209. Molloy, M. (2000). Two dimensional electrophoresis of membrane proteins using immobilized pH gradients. *Analytical Biochemistry*. **280**, 1-10.

210. Patton, W.F. (2000). A thousand points of light: the application of fluorescence detection technologies to two-dimensional gel electrophoresis and proteomics. *Electrophoresis*. **21**, 1123-1144.

211. Chevallet, M., Santoni, V., Poinas, A., Rouquie, D., Fuchs, A. Kieffer, S., Rossignol, M., Lunardi, J., Garin, J., Rabilloud, T. (1998). New zwitterionic detergents improve the analysis of membrane proteins by two-dimensional electrophoresis. *Electrophoresis*. **19**, 1901-1909.

212. Tastet, C., Charmont, S., Chevallet, M., Luche, S., Rabilloud, T. (2003). Structure-efficiency relationships of zwitterionic detergents as protein solubilizers in two-dimensional electrophoresis. *Proteomics*. **3**, 111-121.

213. Herbert, B.R., Molloy, M.P., Gooley, A.A., Walsh, B.J., Bryson, W.G., Williams, K. (1998). Improved protein solubility in two-dimensional electrophoresis using tributyl phosphine as reducing agent. *Electrophoresis*. **19**, 845-851.

214. Eng, J.K., McCormack, A.L., Yates, J.R. (1994). An approach to correlate tandem mass spectral data of peptides with amino acid sequences in protein database. *J. Amer. Soc. Mass Spectrom*. **5**, 976-989.

215. Link, A.J. Eng, J., Schieltz, D.M., Carmack, E., Mize, G.J., Morris, D.R., Garvik, B.M., Yates, J.R. (1999). Direct analysis of protein complexes using mass spectrometry. *Nature Biotechnology*. **17**, 676-682.

216. Sanders, S.L., Jennings, J., Canutescu, A., Link, A.J., Weil, A.P. (2002). Proteomics of the eukaryotic transcription machinery: identification of proteins associated with components of yeast TFIID by multidimensional mass spectrometry. *Molecular and Cellular Biology*. **22**, 4723-4738.

217. Aebersold, R., Hoodlett, D. (2001). Mass spectrometry in proteomics. *Chemistry Reviews*. **101**, 269-295.

218. Yates, J.R. (2004). Mass spectral analysis in proteomics. *Annu. Rev. Biophys. Biomol. Struct*. **33**, 297-316.

219. Powell, D.W., Pierce, W.M., McLeish, K.R. (2005). Defining mitogen-activated protein kinase pathways with mass spectrometry-based approaches. *Mass Spectrometry Reviews*. **21**, 1-22.

220. Kaufmann, H., Bailey, J.E., Fussenegger, M. (2001). Use of antibodies for detection of phosphorylated proteins separated by two-dimensional gel electrophoresis. *Proteomics*. **1**, 194-199.

221. Schulenberg, B., Aggeler, R., Beechem, J.M., Capaldi, R.A., Patton, W.F. (2003). Analysis of steady-state protein phosphorylation in mitochondria using a novel fluorescent phosphosensor dye. *Journal of Biological Chemistry*. **278**, 27251-27255.

222. Steinberg, T.H., Agnew, B.J., Gee, K.R. Leung, W-Y., Goodman, T., Schulenberg, B., Hendrickson, J., Beechem, J.M., Haugland, R.P., Patton, W.F. (2003). Global quantitative phosphoprotein analysis using multiplexed proteomics technology. *Proteomics*. **3**, 1128-1144.

223. Gronborg, M., Kristiansen, T.Z., Stensballe, A., Andersen, J.S., Ohara, O., Mann, M., Jensen, O.N., Pandey, A. (2002). A mass spectrometry-based proteomic approach for identification of serine/threoninephosphorylated proteins by enrichment with phospho-specific antibodies: identification of a novel protein, Frigg, as a protein kinase A substrate. *Molecular and Cellular Proteomics*. **1**, 517-527.

224. Andersson, L., Porath, J. (1986). Isolation of phosphoproteins by immobilized metal (Fe-3+) affinity-chromatography. *Analytical Biochemistry*. **154**, 250-254.

225. Li, S., Dass, C. (1999). Iron (III)-immobilized metal ion affinity chromatography and mass spectrometry for the purification and characterization of synthetic phosphopeptides. *Analytical Biochemistry*. **270**, 9-14.

226. Ficarro, S.B., McCleland, M.L., Stukenberg, P.T., Burke, D.J., Ross, M.M., Shabanowitz, J., Hunt, D.F., White, F.M. (2002). Phosphoproteome analysis by mass spectrometry and its application to *Saccharomyces cerevisiae*. *Nature Biotechnology*. **20,** 301-305.

227. Haydon, C.E., Eyers, P.A., Aveline-Wolf, L.D., Resing, K.A., Mallers, J.L., Ahn, N.G. (2003). Identification of novel phosphorylation sites on *Xenopus laevis* aurora A and analysis of phosphopeptide enrichment by immobilized metal-affinity chromatography. *Molecular and Cellular Proteomics.* **2**, 1055-1067.

228. Collins, M.O., Yu, L., Coba, M.P., Husi, H., Campuzano, I., Blackstock, W.P., Choudhary, J.S., Grant, S.G.N. (2005). Proteomic analysis of *in vivo* phosphorylated synaptic proteins. *Journal of Biological Chemistry.* **280**, 5972-5982.

229. Zeller, M., Konig, S. (2004). The impact of chromatography and mass spectrometry on the analysis of protein phosphorylation sites. *Analytical Biochemistry.* **378**, 898-909.

230. Steen, H., Kuester, B., Mann, M. (2001). Quadrupole time-of-flight versus triple-quadrupole mass spectrometry for determination of phosphopeptides by precursor ion scanning. *Journal of Mass Spectrometry.* **36**, 782-790.

231. Borregaard, N., Sehested, M., Nielsen, B.S., Sengelov, H., Kjeldsen, L. (1995). Biosynthesis of granule proteins in normal human bone marrow cells. Gelatinase is a marker for terminal neutrophil differentiation. *Blood.* **85**, 812-822.

232. Le Cabec, V., Cowland, J.B., Calafat, J., Borregaard, N. (1996). Targeting of proteins to granule subsets is determined by timing and not by sorting: The specific granule protein NGAL is localized to azurophil granules when expressed in HL-60 cells. *Proc. Nat. Acad. Sci. USA.* **93**, 6454-6457.

233. Bainton, D.F. (1999). Distinct granule populations in human neutrophils and lysosomal organelles identified by immuno-electron microscopy. *Journal of Immunological Methods.* **232**, 153-168.

234. Robinson, J.M., Kobayashi, T., Seguchi, H., Takizawa, T. (1999). Evaluation of neutrophil structure and function by electron microscopy: cytochemical studies. *Journal of Immunological Methods.* **232**, 169-178.

235. Sørensen, O.E., Follin, P., Johnsen, A.H., Calafat, J., Tjabringa, G.S., Hiemstra, P.S., Borregaard N. (2001). Human cathelicidin, hCAP18, is processed to the antimicrobial peptide LL-37 by extracellular cleavage with proteinase 3. *Blood.* **97**, 3951-3959.

236. Haslett, C., Guthrie, L., Kopaniak, M., Johnston, J., Henson, P. (1985). Modulation of multiple neutrophil functions by preparative methods of trace concentrations of bacterial lipopolysaccharide. *Americn Journal of Pathology.* **119**, 101-110.

237. Amrein, P.C., Stossel, T.P., (1980). Prevention of degradation of human polymorphonuclear leukocyte proteins by diisopropylfluorophosphate. *Blood.* **56**, 442-447.

238. Howell, K.E., Palade, G.E. (1982). Hepatic Golgi fractions resolved into membrane and content subfractions. *Journal of Cell Biology.* **92,** 822-832.
239. Wessel, D., Flugge, U.I. (1984). A method for the quantitative recovery of protein in dilute solution in presence of detergents and lipids. *Analytical Biochemistry.* **138,** 141-143.

240. Fujiki, Y., Hubbard, A.L., Fowler, S., Lazarow, P.B. (1982). Isolation of intracellular membranes by means of sodium carbonate treatment: application to endoplasmic reticulum. *Journal of Cell Biology.* **93,** 97-102.

241. Fujiki, Y., Fowler, S., Shio, H., Hubbard, A.L., Lazarow, P.B. (1982). Polypeptide and phospholipid composition of the membrane of rat liver peroxisomes: comparison with endoplasmic reticulum and mitochondrial membranes. *Journal of Cell Biology.* **93,** 103-110.

242. Nebl, T., Pestonjamasp, K.N., Leszyk, J.D., Crowley, J.L., Oh, S.W., Luna, E.J. (2002). Proteomic analysis of a detergent-resistant membrane skeleton from neutrophil plasma membranes. *Journal of Biological Chemistry.* **277,** 43399-43409.

243. Lin, D., Chang, Y.J., Strauss, J.F., Miller, W.L. (1993). The human peripheral benzodiazepine receptor gene: cloning and characterization of alternative splicing in normal tissues and in a patient with congenital lipoid adrenal hyperplasia. *Genomics.* **18,** 643-650.

244. Ye, Q., Worman, H.J. (1994). Primary structure analysis and lamin B and DNA binding of human LBR, an integral protein of the nuclear envelope inner membrane. *Journal of Biological Chemistry.* **269,** 11306-11311.

245. Malone, C.J., Fixsen, W.D., Horvitz, H.R., and Han, M. (1999). UNC-84 localizes to the nuclear envelope and is required for nuclear migration and anchoring during *C. elegans* development. *Development.* **126,** 3171-3181.

246. Deacona, S.W. and Gelfanda, V.I. (2001). Of yeast, mice, and men: Rab proteins and organelle transport. *Journal of Cell Biology.* **152,** F21-F24.

247. Zerial, M., McBride, H. (2001). Rab proteins as membrane organizers. *Nature Reviews.* **2,** 107-119.

248. Hong-Geller, E., Cerione, R.A. (2000). Cdc42 and Rac stimulate exocytosis of secretory granules by activating the IP(3)/calcium pathway in RBL-2H3 mast cells. *Journal of Cell Biology.* **148,** 481-494.

249. Izumi, T., Gomi, H., Kasai, K., Mizutani, S., Torii, S. (2003). The roles of Rab27 and its effectors in the regulated secretory pathways. *Cell Structure and Function.* **28,** 465-474.

250. Huynh, H., Bottini, N., Williams, S., Cherepanov, V., Musumeci1, L., Saito, K., Bruckner, S., Vachon, E., Wang, X., Kruger, J., Chow, C-W., Pellecchia, M., Monosov, E., Greer, P.A., Trimble, W., Downey, G.P., Mustelin, T. (2004). Control of vesicle fusion by a tyrosine phosphatase. *Nature Cell Biology.* **6**, 831-839.

251. Chen, M., Geng, J.G. (2001). Inhibition of protein tyrosine phosphatases suppresses P-selectin exocytosis in activated human platelets. *Biochemical and Biophysical Research Communications.* **286**, 609-615.

252. Ostenson, C.G., Sandberg-Nordqvist, A.C., Chen, J., Hallbrink, M., Rotin, D., Langel, U., Efendic, S. (2002). Overexpression of protein-tyrosine phosphatase PTP sigma is linked to impaired glucose-induced insulin secretion in hereditary diabetic Goto-Kakizaki rats. *Biochem. Biophys. Res. Commun.* 291, 945–950.

253. Hermel, J.M., Dirkx, R., Solimena, M. (1999). Post-translational modifications of ICA512, a receptor tyrosine phosphatase-like protein of secretory granules. *European Journal of Neuroscience.* **11**, 2609–2620.

254. Michalak, M., Corbett, E.F., Mesaeli, N., Nakamura, K., Opas, M. (1999). Calreticulin: one protein, one gene, many functions. *Biochem. J.* 344, 281–292.

255. Nauseef, W.M., McCormick, S.J., Clark, R.A. (1995). Calreticulin functions as a molecular chaperone in the biosynthesis of myeloperoxidase. *Journal of Biological Chemistry.* **270**, 4741-4747.

256. Ghiran, I., Klickstein, L.B., Nicholson-Weller, A. (2003). Calreticulin is at the surface of circulating neutrophils and uses CD59 as an adaptor molecule. *Journal of Biological Chemistry.* **278**, 21024-21031.

257. Sipione, S., Ewen, K., Shostak, I., Michalak, M., Bleackley, R.C. (2005). Impaired cytolytic activity in calreticulin-deficient CTLs. *Journal of Immunology.* **174**, 3212-3219.

258. Rizo, J., Sudhof, T.C. (1998). C_2-domains, structure and function of a universal Ca^{2+}-binding domain. *Journal of Biological Chemistry.* **273**, 15879-15882.

259. Gygi, S.P., Corthals, G.L., Zhang, Y., Rochon, Y., Aebersold, R. (2000). Evaluation of two-dimensional gel electrophoresis-based proteome analysis technology. *Proc. Natl. Acad. Sci. U.S.A.* **97**, 9390-9395.

260. Olsson, I. (1969). The intracellular transport of glucosaminoglycans (mucopolysaccharides) in human leukocytes. *Experimental Cell Research.* **54**, 318-325.

261. Washburn, M.P., Wolters, D., Yates, J.R. (2001). Large-scale analysis of the yeast proteome by multidimensional protein identification technology. *Nature Biotechnology.* **19**, 242-247.

262. Wu, C.C., MacCoss, M.J., Howell, K.E., Yates, J.R. (2003). A method for the comprehensive proteomic analysis of membrane proteins. *Nature Biotechnology.* **21**, 532-538.

263. Krungkrai, J., Krungkrai, S.R., Bhumiratana, A. (1993). *Plasmodium berghei*: partial purification and characterization of mitochondrial cytochrome c oxidase. *Experimental Parasitology.* **77**, 136-146.

264. Brinkmann, V., Reichard, U., Goosmann, C., Fauler, B., Uhlemann, Y., Weiss, D.S., Weinrauch, Y., Zychlinsky, A. (2004). Neutrophil extracellular traps kill bacteria. *Science.* **303**, 1532-1535.

265. Hiempstra, P.S., Eisenhauer, P.B., Harwig, S.S., van den Barselaar, M.T., van Furth, R., Lehrer, R.I. (1993). Antimicrobial proteins of murine macrophages. *Infection and Immunity.* **61**, 3038-1046.

266. Kim, H.S., Cho, J.J., Park, H.W., Yoon, H., Kim, M.S., Kim, S.C. (2002). Endotoxin-neutralizing antimicrobial proteins of the human placenta. *Journal of Immunology.* **168**, 2356-2364.

267. Zu, Y-L., Qi, J., Gilchrist, A., Fernandez, G.A., Vazque-Abad, D., Kreutzer, D.L., Huang, C.K., Sha'afi, R.I. (1998). p38 mitogen-activated protein kinase activation is required for human neutrophil function triggered by TNF-α or fMLP stimulation. *Journal of Immunology.* **160**, 1982-1989.

268. McLeish, K.R., Klein, J.B., Coxon, P.Y., Head, K.Z., Ward, R.A. (1998). Bacterial phagocytosis activates extracellular signal-regulated kinase and p38 mitogen-activated protein kinase cascades in human neutrophils. *Journal of Leukocyte Biology.* **64**, 835-844.

269. Dong, C., Davis, R.J., Flavell, R.A. (2002). MAP kinases in the immune response. *Annual Reviews in Immunology.* **20**, 55-72.

270. Waas, W.F., Lo, H.H., Dalby, K.N. (2001). The kinetic mechanism of the dual phosphorylation of the ATF2 transcription factor by p38 mitogen-activated protein(MAP) kinase alpha. Implications for signal/response profiles of MAP kinase pathways. *Journal of Biological Chemistry.* **276**, 5676-5684.

271. New, L., Jiang, Y., Zhao, M., Liu, K., Zhu, W., Flood, L.J., Kato, Y., Parry, C.N.G., Han, J. (1998). PRAK, a novel protein kinase regulated by the p38 MAP kinase. *EMBO Journal.* **17**, 3372-3384.

272. Casanovas, O., Miró, F., Estanyol, J.M., Itarte, E., Neus, A., Bachs, O. (2000). Osmotic Stress Regulates the Stability of Cyclin D1 in a p38 SAPK2-dependent Manner *Journal of Biological Chemistry.* **275**, 35091-35097.

273. Sanghera, J.S., Weinstein, S.L., Aluwalia, M., Girn, J., Pelech, S.L. (1996). Activation of multiple proline-directed kinases by bacterial lipopolysaccharide in murine macrophages. *Journal of Immunology.* **156**, 4457-4465.

274. El Benna, J., Han, J., Park, J.W., Schmid, E., Ulevitch, R.J., Babior, B.M. (1996). Activation of p38 in stimulated human neutrophils: phosphorylation of the oxidase component p47phox by p38 and ERK but not by JNK. *Arch. Biochem. Biophys.* **334**, 395-400.

275. Nacken, W., Roth, J., Sorg, C., Kerkhoff, C. (2003). S100A9/S100A8: myeloid representatives of the S100 protein family as prominent players in innate immunity. *Microscopy Res. & Tech.* **60**, 569-580.

276. Schaefer, B.W., Heizmann, C.W. (1996). The S100 family of EF-hand calcium-binding proteins: functions and pathology. *Trends in Biocheical Sciences.* **21**, 134-140.

277. Kerkhoff, C., Klempt, M., Sorg, C. (1998). Novel insights into structure and function of MRP8 (S100A8) and MRP14 (S100A9). *Biochimica et Biophysica Acta.* **1448**, 200-211.

278. Edgeworth, J., Gorman, M., Bennett, R., Freemont, P., Hogg, N. (1991). Identification of p8,14 as a highly abundant heterodimeric calcium-binding protein complex of myeloid cells. *Journal of Biological Chemistry.* **266**, 7706-7713.

279. Edgeworth, J., Freemont, P., Hogg, N. (1989). Ionomycin-regulated phosphorylation of the myeloid calcium-binding protein p14. *Nature.* **342**, 189-192.

280. Bengis-Garber, C., Gruener, N. (1993). Calcium-binding myeloid protein (p8,14) is phosphorylated in fMet-Leu-Phe-stimulated neutrophils. *Journal of Leukocyte Biology.* **54**, 114-118.

281. van den Bos, C., Roth, J., Koch, H.J., Hartmann, M., Sorg, C. (1996). Phosphorylation of MRP14, an S100 protein expressed during monocytic differentiation, modulates Ca^{2+}-dependent translocation from cytoplasm to membranes and cytoskeleton. *Journal of Immunology.* **156**, 1247-1254.

282. Doussiere, J., Bouzidi, F., Vignais, V.P. (2002). The S100A8/A9 protein as a partner for the cytosolic factors of NADPH oxidase activation in neutrophils. *European Journal of Biochemistry.* **269,** 3246-3255.

283. Berthier, S., Paclet, M-H., Lerouge, S., Roux, F., Vergnaud, S., Coleman, A.W., Morel, F. (2003). Changing the conformation state of cytochrome b558 initiates NADPH oxidase activation. *Journal of Biological Chemistry.* **278**, 25499-24508.

284. Jensen, O.N., Wilm, M., Shevchenko, A., Mann, M. (1999). Sample preparation methods for mass spectrometric peptide mapping directly from 2-DE gels. *Methods. Mol. Biol.* **112**, 513-530.

285. van den Bos, C., Rammes, A., Vogl, T., Boynton, R., Zaia, J., Sorg, C., Roth, J. (1998). Copurification of P6, MRP8, and MRP14 from human granulocytes and separation of individual proteins. *Protein Expr. Purif.* **13,** 313-318.

286. Grinstein, S., Butler, J.R., Furuya, W., L'Allemain, G., Downey, G.P. (1994). Chemotactic peptides induce phosphorylation and activation of MEK-1 in human neutrophils. *Journal of Biological Chemistry.* **269**, 19313-19320.

287. Kerkhoff, C., Klempt, M., Kaever, V., Sorg, C. (1999). The two calcium-binding proteins, S100A8 and S100A9, are involved in the metabolism of arachidonic acid in human neutrophils. *Journal of Biological Chemistry.* **274**, 32672-32679.

288. Klempt, M., Melkonyan, H., Nacken, W., Wiesmann, D., Holtkemper, U., Sorg, C. (1997). The heterodimer of the Ca^{2+}-binding protein MRP8 and MRP14 binds arachidonic acid. *FEBS Letters.* **408**, 81-84.

289. Janek, K., Wenschuh, H., Bienert, M., Drause. E. (2001). Phosphopeptide analysis by positive and negative ion matrix-assisted laser desorption/ionization mass spectrometry. *Rapid Commun. Mass Spectrom.* **15**, 1593-1599.

290. Chen, S.L., Huddleston, M.J., Shou, W., Deshales, R.J., Annan, R.S., Carr, S.A. (2002). Mass spectrometry-based methods for phosphorylation site mapping of hyperphosphorylated proteins applied to Net1, a regulator of exit from mitosis in yeast. *Molecular and Cellular Proteomics.* **1**, 186-196.

291. Fuglsang, A.T., Visconti, S., Drumm, K., Jahn, T., Stensballe, A., Mattei, B., Jensen, O., Aducci, P., Palmgren, M.G. (1999). Binding of 14-3-3 protein to the plasma membrane H+-ATPase AHA2 involves the three C-terminal Tyr946-Thr-Val and requires phosphorylation of Thr947. *Journal of Biological Chemistry.* **274**, 36774-36780.

292. Raska, C. S., Parker, C.E., Dominski, Z., Marzluff, W.F. Glish, G.L., Pope, R.M., Borchers, C.H. (2002). Direct MALDI-MS/MS of phosphopeptides affinity-bound to immobilized metal ion affinity chromatography beads. *Analytical Chemistry.* **74**, 3429-3433.

293. Humphries, C.L., Balcer, H.I., D'Agostino, J.L., Winsor, B., Drubin, D.G., Barnes, G., Andrews, B.J., Goode, B.L. (2002). Direct regulation of Arp2/3 complex activity and function by the actin binding protein coronin. *Journal of Cell Biology.* **159**, 993-1004.

294. Gerisch, G., Albrecht, R., Heizer, C., Hodgkinson, S., Maniak, M. (1995). Chemoattractant-controlled accumulation of coronin at the leading edge of Dictyostelium

cells monitored using a green fluorescent protein-coronin fusion protein. *Current Biology*. **5**, 1280-1285.

295. Maniak, M., Rauchenberger, R., Albrecht, R., Murphy, J., Gerisch, G. (1995). Coronin involved in phagocytosis: dynamics of particle induced relocalization visualized by a green fluorescent protein tag. *Cell.* **15**, 915-924.

296. Grogan, A., Reeves, E., Keep, N., Wientjes, F., Totty, N.F., Burlingame, A.L., Hsuan, J.J., Segal, A.W. (1997). Cytosolic phox proteins interact with and regulate the assembly of coronin in neutrophils. *Journal of Cell Science.* **110**, 3071-3081.

297. Scheffzek, K., Stephan, I., Jensen, O.N., Illenberger, D., Gierschik, P. (2000). The Rac-RhoGDI complex and structural basis for the regulation of Rho proteins by RhoGDI. *Nature Structural Biology.* **7**, 122-126.

298. Gorvel, J.P., Chang, T.C., Boretto, J., Azuma, T., Chavrier, P. (1998). Differential properties of D4/LyGDI versus RhoGDI: phosphorylation and rho GTPase selectivity. *FEBS Letters.* **422**, 269-273.

299. Hobbs, J.A.R., May, R., Tanousis, K., McNeill, E., Mathies, M., Gebhardt, C., Henderson, R., Robinson, M.J., Hogg, N. (2003). Myeloid cell function in MRP-14 (S100A9) null mice. *Molecular and Cellular Biology.* **23**, 2564-2576.

300. Manitz, M.-P., Horst, B., Seeliger, S., Strey, A., Skryabin, B.V., Gunzer, M., Frings, W., Schoenlau, F., Roth, J., Sorg, C., Nacken, W. (2003). Loss of S100A9 (MRP14) results in reduced interleukin-8-induced CD11b surface expression, a polarized microfilament system, and diminished responsiveness to chemoattractants *in vitro*. *Molecular and Cellular Biology.* **23**, 1034-1043.

301. Vogl, T., Ludwig, S., Geobeter, M., Strey, A., Thorey, I.S., Reichelt, R., Foell, D., Gerke, V., Manitz, M.P., Nacken, W., Werner, S., Sorg, C., Roth, J. (2004). MRP8 and MRP14 control microtubule reorganization during transendothelial migration of phagocytes. *Blood.* **104**, 4260-4268.

302. Lali, F.V., Hunt, A.E., Turner, S.J., Foxwell. B.M.J. (2000). The pyridinyl imidazole inhibitor SB203580 blocks phosphoinositide-dependent protein kinase activity, protein kinase B phosphorylation, and retinoblastoma hyperphosphorylation in interleukin-2-stimulated T cells independently of p38 mitogen activated protein kinase. *Journal of Biological Chemistry.* **275**, 7395-7402.

303. Svitkina, T.M., Borisy, G.G. (1999). Arp2/3 complex and actin depolymerizing factor/cofilin in dendritic organization and treadmilling of actin filament array in lamellipodia. *Journal of Cell Biology.* **145**, 1009-1026.

304. Shibata, F., Miyama, K., Shinoda, F., Mizumoto, J., Takano, K., Nakagawa, H. (2004). Fibroblast growth-stimulating activity of S100A9 (MRP-14). *European Journal of Biochemistry.* **271**, 2137-2143.

305. Frosch, M., Vogl, T., Seeliger, S., Wulfraat, N., Kuis, W., Viemann, D., Foell, D., Sorg, C., Sunderkotter, C., Roth, J. (2003). Expression of myeloid-related proteins 8 and 14 in systemic-onset juvenile rheumatoid arthritis. *Arthritis Rheumatism.* **48**, 2622-2626.

306. Ahmad, A., Bayley, D.L., He, S., Stockley, R.A. (2003). Myeloid related protein-8/14 stimulates interleukin-8 production in airway epithelial cells. *Am. J. Respir. Cell Mol. Biol.* **29**, 523-530.

307. Polgar, J., Chung, S-H., Reed, G.L. (2002). Vesicle-associated membrane protein 3 (VAMP-3) and VAMP-8 are present in human platelets and are required for granule secretion. *Blood.* **100**, 1081-1083.

308. Paumet, F., Le Mao, J., Martin, S., Galli, T., David, B., Blank, U., Roa, M. (2000). Soluble NSF Attachment Protein Receptors (SNAREs) in RBL-2H3 Mast Cells: Functional Role of Syntaxin 4 in Exocytosis and Identification of a Vesicle-Associated Membrane Protein 8-Containing Secretory Compartment. *Journal of Immunology.* **164**, 5850-5857.

309. Chen, D., Bernstein, A.M., Lemons, P.P., Whiteheart, S.W. (2000). Molecular mechanisms of platelet exocytosis: role of SNAP-23 and syntaxin 2 in dense core granule release. *Blood.* **95**, 921-929.

310. Pryor, P.R., Mullock, B.M., Bright, N.A., Lindsay, M.R., Gray, S.R., Richardson, S.C., Stewart, A., James, D.E., Piper, R.C., Luzio, J.P. (2004). Combinatorial SNARE complexes with VAMP7 or VAMP8 define different late endocytic fusion events. *EMBO Rep.* **6**, 590-595.

311. Ward, D.M., Pevsner, J., Scullion, MA., Vaughn, M., Kaplan, J. (2000). Syntaxin 7 and VAMP-7 are soluble N-ethylmaleimide-sensitive factor attachment protein receptors required for late endosomes-lysosome and homotypic lysosome fusion in alveolar macrophages. *Molecular Biology of the Cell.* **11**, 2327-2333.

312. Mullock, B.M., Smith, C.W., Ihrke, G., Bright, N.A., Lindsay, M., Parkinson, E.J., Brooks, D.A., Parton, R.G., James, D.E., Luzio, J.P., Piper, R.C. (2000). Syntaxin 7 is localized to late endosome compartments, associates with vamp 8, and is required for late endosome-lysosome fusion. *Molecular Biology of the Cell.* **11**, 3137-3153.

313. Schraw, T.D., Lemons, P.P., Dean, W.L., Whiteherat, S.W. (2003). A role for Sec1/Munc18 proteins in platelet exocytosis. *Biochemical Journal.* **374**, 207–217.

314. Menasche, G., Pastural, E., Feldmann, J., Certain, S., Ersoy, F., Dupuis, S., Wulffraat, N., Bianchi, D., Fischer, A., Le Deist, F., de Saint Basile, G. (2000).

Mutations in RAB27A cause Griscelli syndrome associated with haemophagocytic syndrome. *Nature Genetics.* **25**, 173-176.

315. Shirakawa, R., Higashi, T., Tabuchi, A., Yoshioka, A., Nishioka, H., Fukuda, M., Kita, T., Horiuchi, H. (2004). Munc13-4 is a GTP-Rab27-binding protein regulating dense core granule secretion in platelets. *Journal of Biological Chemistry.* **279**, 10730-10737.

316. Neeft, M., Wieffer, M., de Jong, A.S., Negroiu, G., Metz, C.H.G, van Loon, A., Griffith, J., Krijgsveld, J., Wulffraat, N., Koch, H., Heck, A.J.R., Brose, N., Kleijmeer, M., van der Sluijs, P. (2005). Munc13-4 is an effector of rab27a and controls secretion of lysosomes in hematopoietic cells. *Molecular Biology of the Cell.* **16**, 731-741.

317. Kuroda, T.S., Fukuda, M., Ariga, H. and Mikoshiba, K. (2002). The Slp homology domain of synaptotagmin-like proteins 1–4 and Slac2 functions as a novel Rab27A binding domain. *Journal of Biological Chemistry.* **277**, 9212-9218.

318. Kuroda, T.S., Fukuda, M., Ariga, H., Mikoshiba, K. (2002). Synaptotagmin-like protein 5: a novel Rab27A effector with C-terminal tandem C2 domains. *Biochemical and Biophysical Research Communications.* **293**, 899-906.

319. Pichon, S., Bryckaert, M., Berrou, E. (2004). Control of actin dynamics by p38 MAP kinase – Hsp27 distribution in the lamellipodium of smooth muscle cells. *Journal of Cell Science.* **117**, 2569-2577.

320. Itou, H., Yao, M., Fujita, I., Watanabe, N., Suzuki, M., Nishihira, J., Tanaka, I. (2002). The crystal structure of human MRP14 (S100A9), a Ca(2+)-dependent regulator protein in inflammatory process. *Journal of Molecular Biology.* **316**, 265-276.

321. Reynolds, C.H., Betts, J.C., Blackstock, W.P., Nebreda, A.R., Anderton, B.H. (2000). Phosphorylation sites on tau identified by nanoelectrospray mass spectrometry: differences in vitro between the mitogen-activated protein kinases ERK2, c-Jun N-terminal kinase and P38, and glycogen synthase kinase-3beta. *Journal of Neurochemistry.* **74**, 1587-1595.

322. Siegenthaler, G., Roulin, K., Chatellard-Gruaz, D., Hotz, R., Saurat, J.H, Hellman, U., Hagens, G. (1997). A heterocomplex formed by the calcium-binding proteins MRP8 (S100A8) and MRP14 (S100A9) binds unsaturated fatty acids with high affinity. *Journal of Biological Chemistry.* **272,** 9371-9377.

323. Kerkhoff, C., Eue, I., Sorg, C. (1999). The regulatory role of MRP8 (S100A8) and MRP14 (S100A9) in the transendothelial migration of human leukocytes. *Pathobiology.* **67**, 230-232.

324. Werz, O., Szellas, D., Steinhilber, D., Radmark, O. (2002). Arachidonic acid promotes phosphorylation of 5-lipoxygenase at Ser-271 by MAPK-activated protein kinase 2 (MK2). *Journal of Biological Chemistry*. **277**, 14793-14800.

APPENDIX

Supplementary Table 1

Peptides used for identification of proteins from more than one 2D-HPLC ESI-MS/MS experiment

GELATINASE GRANULES					
Receptors and Membrane Anchors					
Entrez Gene	**Entrez Protein**	**Protein Name**	**Peptide Sequences Detected**		
			1st Identification	**2nd Identification**	**3rd Identification**
BZRP	NP_000705	Benzodiazepine receptor	1 R.FVHGEGLR.W	1 R.FVHGEGLR.W	
CEACAM1	NP_001703	CAECAM-1	1 R.TLTLLSVTR.N	1 R.DLTEHKPSVSNHTQDHSNDPPNK.M 2 R.TLTLLSVTR.N	1 R.DLTEHKPSVSNHTQDHSNDPPNK.M 2 R.TLTLLSVTR.N
CANX	NP_001737	Calnexin	1 K.APVPTGEVYFADSFDR.G 2 K.IPDPEAVKPDDWDEDAPAK.I 3 K.IPNPDFFEDLEPFR.M 4 R.KIPNPDFFEDLEPFR.M 5 R.KPEDWDERPK.I 6 K.TPELNLDQFHDK.T 7 K.TPYTIMFGPDK.C	1 K.IPDPEAVKPDDWDEDAPAK.I 2 K.IPNPDFFEDLEPFR.M 3 R.KIPNPDFFEDLEPFR.M 4 R.KPEDWDERPK.I 5 K.TPELNLDQFHDK.T	1 K.IPNPDFFEDLEPFR.M 2 R.IVDDWANDGWGLK.K 3 R.KIPNPDFFEDLEPFR.M 4 K.TPELNLDQFHDK.T
ITGAM	NP_000623	CD11b, complement component receptor 3 (CR3)	1 R.DHVFQVNNFEALK.T 2 R.EGQIQSVVTYDLALDSGRPHSR.A 3 R.FGAALTVLGDVNGDK.L 4 K.FGDPLGYEDVIPEADR.E 5 R.GAVVLFHGTSGSGISPSHSQR.I 6 R.GFGQSVVQLQGSR.V 7 R.LPSHSDFLAELR.K 8 K.LTDVAIGAPGEEDNR.G 9 R.QELNTIASKPPR.D 10 R.QNTGMWESNANVK.G 11 R.SLVKPITQLLGR.T 12 K.TEFQLELPVK.Y 13 K.TLFSLMQYSEEFR.I 14 R.VMQHQYQVSNLGQR.S 15 R.VVVGAPQEIVAANQR.G	1 R.DHVFQVNNFEALK.T 2 K.EFVSTVMEQLKK.S 3 K.ERLPSHSDFLAELR.K 4 K.FGDPLGYEDVIPEADR.E 5 K.FGDPLGYEDVIPEADREGVIR.Y 6 R.GAVVLFHGTSGSGISPSHSQR.I 7 R.GFGQSVVQLQGSR.V 8 K.ILVVITDGEKFGDPLGYEDVIPEADREGVIR.Y 9 R.LPSHSDFLAELR.K 10 R.QNTGMWESNANVK.G 11 R.SLVKPITQLLGR.T 12 R.VMQHQYQVSNLGQR.S 13 R.VQSLVLGAPR.Y 14 R.VVVGAPQEIVAANQR.G 15 R.YVIGVGDAFR.S	1 R.DHVFQVNNFEALK.T 2 K.EFVSTVMEQLKK.S 3 K.FGDPLGYEDVIPEADR.E 4 R.GFGQSVVQLQGSR.V 5 K.ILVVITDGEK.F 6 R.LPSHSDFLAELR.K 7 K.LTDVAIGAPGEEDNR.G 8 R.QELNTIASKPPR.D 9 R.SLVKPITQLLGR.T 10 R.TQVTFFFPLDLSYR.K 11 R.VQSLVLGAPR.Y 12 R.VVVGAPQEIVAANQR.G 13 K.YAVYMVVTSHGVSTK.Y
ADAM8	NP_001100	CD156, ADAM-8	1 R.GPQELVPTTHPGQPAR.H 2 R.SNPLFHQAASR.V 3 R.VLEVVNHVDK.L	1 R.GPQELVPTTHPGQPAR.H	
FCGR3B	NP_000561	CD16, FcγRIIIb	1 K.AVVFLEPQWYSVLEK.D	1 K.YFHHNSDFHIPK.A	
ITGB2	NP_000202	CD18, macrophage antigen 1 (mac-1) beta subunit	1 K.LAENNIQPIFAVTSR.M 2 R.LLVFATDDGFHFAGDGK.L 3 K.SAVGELSEDSSNVVHLIK.N 4 R.SNEFDYPSVGQLAHK.L 5 K.TVLPFVNTHPDK.L 6 R.VFLDHNALPDTLK.V	1 R.LLVFATDDGFHFAGDGK.L 2 K.SAVGELSEDSSNVVHLIK.N 3 R.SNEFDYPSVGQLAHK.L 4 K.SQWNNDNPLFK.S 5 K.TVLPFVNTHPDK.L 6 R.VFLDHNALPDTLK.V	1 R.ALNEITESGR.I 2 R.IGFGSFVDK.T 3 K.LAENNIQPIFAVTSR.M 4 K.LGAILTPNDGR.C 5 K.LGGDLLR.A 6 R.LLVFATDDGFHFAGDGK.L 7 K.LTEIIPK.S 8 K.SAVGELSEDSSNVVHLIK.N 9 R.SNEFDYPSVGQLAHK.L 10 K.SQWNNDNPLFK.S 11 K.TVLPFVNTHPDK.L 12 R.VFLDHNALPDTLK.V
CR1	NP_000564 NP_000642	CD35, complement receptor-1 (CR1)	1 R.HTGTPSGDIPYGK.E 2 R.VLFPVNLQLGAK.V	1 R.HTGTPSGDIPYGK.E	1 R.ENFHYGSVVTYR.C 2 R.HTGTPSGDIPYGK.E 3 R.VLFPVNLQLGAK.V
ITGA2B	NP_000410	CD41, platelet fibrinogen receptor, alpha subunit	1 R.DGYNDIAVAAPYGGPSGR.G 2 R.EGNSLDSWGPK.V 3 R.FGSAIAPLGDLDR.D 4 R.GAVDIDDNGYPDLIVGAYGANQVAVYR.A 5 R.GEAQVWTQLLR.A 6 R.GNSFPASLVVAAEEGER.E 7 R.HDLLVGAPLYMESR.A 8 R.NVGSQTLQTFK.A 9 R.SRPSQVLDSPFPTGSAFGFSLR.G	1 R.VAIVVGAPR.T	1 R.DGYNDIAVAAPYGGPSGR.G 2 R.FGSAIAPLGDLDR.D 3 R.GEAQVWTQLLR.A 4 R.GNSFPASLVVAAEEGER.E 5 R.NVGSQTLQTFK.A
ITGB3	NP_000203	CD61, platelet glycoprotein IIIa	1 K.DDLWSIQNLGTK.L 2 K.GSGDSSQVTQVSPQR.I 3 K.HVLTLTDQVTR.F 4 K.IGDTVSFSIEAK.V 5 R.NDASHLLVFTTDAK.T 6 K.SFTIKPVGFK.D 7 R.VLEDRPLSDK.G 8 K.WDTANNPLYK.E	1 K.GSGDSSQVTQVSPQR.I 2 R.NDASHLLVFTTDAK.T 3 R.SKVELEVR.D	1 K.GSGDSSQVTQVSPQR.I 2 K.IGDTVSFSIEAK.V 3 R.NDASHLLVFTTDAK.T
C5R1	NP_001727	CD88, C5aR1	1 R.NVLTEESVVR.E	1 K.DTLDLNTPVDK.T 2 R.NVLTEESVVR.E	
CD9	NP_001760	CD9, motility related protein	1 K.KDVLETFTVK.S	1 K.KDVLETFTVK.S	
DSG1	NP_001933	Desmoglein preproprotein	1 R.ISGVGIDQPPYGIFVINQK.T 2 K.VGDFVATDLDTGRPSTTVR.Y 3 K.YQGTILSIDDNLQR.T	1 K.VGDFVATDLDTGRPSTTVR.Y 2 K.YQGTILSIDDNLQR.T	
FCER1G	NP_004097	Fc receptor for IgE, high affinity I, gamma polypeptide	1 K.SDGVYTGLSTR.N	1 K.SDGVYTGLSTR.N	1 R.NQETYETLK.H 2 K.SDGVYTGLSTR.N
FLOT1	NP_005794	Flotillin 1	1 K.TEAEIAHIALETLEGHQR.A	1 K.DIHDDQDYLHSLGK.A 2 R.HGVPISVTGIAQVK.I 3 K.LPQVAEEISGPLTSANK.I 4 K.TEAEIAHIALETLEGHQR.A	1 R.SPPVMVAGGR.V
FLOT2	NP_004466	Flotillin 2	1 K.NVVLQTLEGHLR.S 2 K.TAEAQLAYELQGAR.E	1 K.NVVLQTLEGHLR.S 2 R.SILGTLTVEQIYQDR.D 3 K.VDEIVVLSGDNSK.V	
FPR1	NP_002020	Formyl peptide receptor	1 R.LIHALPASLER.A	1 R.LIHALPASLER.A	
GP1BB	NP_000398	Glycoprotein Ib beta precursor	1 R.TAHLGANPWR.C	1 R.TAHLGANPWR.C	
HLA-A	NP_002107	HLA-A1	1 R.APWIEQEGPEYWDQETR.N	1 R.SWTAADTAAQITQR.K	
ICAM3	NP_002153	ICAM-3 precursor	1 R.QPAVEEPAEVTATVLASR.D	1 R.TFVLPVTPPR.L 2 R.WEEELSRQPAVEEPAEVTATVLASR.D	1 R.QPAVEEPAEVTATVLASR.D 2 R.TFVLPVTPPR.L 3 R.TSLTVVLLR.W
LBR	NP_919424 NP_002287	Lamin B receptor	1 K.ENDIKPLTSFR.Q 2 K.VVEGTPLIDGR.R	1 K.VVEGTPLIDGR.R	
LAMP2	NP_002285	LAMP2	1 K.YLDFVFAVK.N	1 K.YLDFVFAVK.N	
LILRB2	NP_005865	Leukocyte Ig-like receptor 2	1 R.KADFQHPAGAVGPEPTDR.G 2 K.NGQFHIPSITWEHTGR.Y	1 K.NGQFHIPSITWEHTGR.Y	
LAIR1	NP_002278 NP_068352 NP_068354	Leukocyte-associated Ig-like receptor 1	1 R.SKDEEQKPQQRPDLAVDVLER.T	1 R.GPVGVQTFR.L	

CLEC12A	NP_612210 NP_963917 NP_963919	Myeloid inhibitory C-type lectin-like receptor	1 R.SYDYWLGLSPEEDSTR.G	1 R.SYDYWLGLSPEEDSTR.G 2 R.VDNIINSSAWVIR.N	
GP9	NP_000165	Platelet glycoprotein IX	1 R.GHGLTALPALPAR.T	1 R.TPEALLQVR.C	
SELPLG	NP_002997	P-selectin glycoprotein ligand-1	1 K.SPGLTPEPR.E	1 K.SPGLTPEPR.E	
UNC84B	NP_056189	Sad1	1 K.EGVIGVTEEQVHHIVK.Q 2 R.LEDQLAGLQQELAALALK.Q 3 R.QGAPGQGGGGGLSHEDTLALLEG LVSR.R 4 R.RLEDQLAGLQQELAALALK.Q 5 R.RPDEGWEAR.D	1 R.DSSPHFQAEQR.V 2 K.EGVIGVTEEQVHHIVK.Q 3 K.ILTHVAEMQGK.S 4 R.LEDQLAGLQQELAALALK.Q 5 R.RPDEGWEAR.D	1 R.QGAPGQGGGGGLSHEDTLALLEG LVSR.R
SCAMP1	NP_004857	SCAMP1	1 K.EHALAQAELLK.R	1 K.EHALAQAELLK.R	
SCAMP2	NP_005688	SCAMP2	1 R.ELQNTVANLHVR.Q	1 R.ELQNTVANLHVR.Q 2 R.TGASFQQAQEEFSQGIFSSR.T	1 R.ELQNTVANLHVR.Q 2 R.TGASFQQAQEEFSQGIFSSR.T
SIGLEC5	NP_003821	Sialic acid binding ig-like lectin	1 R.KKPWPDSPGDQASPPGDAPPLEE QK.E 2 R.MEDTGSYFFR.V	1 K.KPWPDSPGDQASPPGDAPPLEE QK.E	1 K.DQEAPSTTEYSEIK.T
SPN	NP_003114	Sialophorin (CD43)	1 R.TGALVLSR.G	1 R.NGVVDAWAGPAQVPEEGAVTVTVG GSGGDK.G	1 R.NGVVDAWAGPAQVPEEGAVTVTVG GSGGDK.G 2 R.TGALVLSR.G
STOM	NP_004090	Stomatin	1 R.AKVIAAEGEMNASR.A 2 K.EASMVITESPAALQLR.Y 3 R.LLAQTTLR.N 4 K.LPVQLQR.A 5 K.NLSQILSDREEIAHNMQSTLDDATDA WGIK.V 6 K.NLSQILSDREEIAHNMQSTLDDATDA WGIKVER.V 7 R.TISFDIPPQEILTK.D 8 K.VIAAEGEMNASR.A 9 R.VQNATLAVANITNADSATR.L	1 K.DSVTISVDGVVYYR.V 2 R.LLAQTTLR.N 3 K.NLSQILSDR.E 4 K.NLSQILSDREEIAHNMQSTLDDATDA WGIK.V 5 K.NSTIVFPLPIDMLQGIIGAK.H 6 R.TISFDIPPQEILTK.D 7 R.VQNATLAVANITNADSATR.L 8 R.YLQTLTTIAAEK.N	1 K.DSVTISVDGVVYYR.V 2 K.EASMVITESPAALQLR.Y 3 R.EEIAHNMQSTLDDATDAWGIK.V 4 R.LLAQTTLR.N 5 K.LPVQLQR.A 6 K.NLSQILSDR.E 7 R.TISFDIPPQEILTK.D 8 K.VIAAEGEMNASR.A 9 R.VQNATLAVANITNADSATR.L 10 R.YLQTLTTIAAEK.N
VNN1	NP_004657	Vanin 1	1 K.MSENIPNEVYALGAFDGLHTVEGR.Y 2 R.VNFLASNIHYPSK.K	1 K.MSENIPNEVYALGAFDGLHTVEGR.Y 2 K.QNLFMGENQFNVPK.E 3 R.VNFLASNIHYPSK.K 4 R.YQYNTDVVFDSQGK.L	
VNN2	NP_004656 NP_511043	Vanin 2	1 K.DNSIYVLANLGDK.K 2 K.EENEVYVLGAFTGLHGR.R	1 K.DNSIYVLANLGDK.K	1 K.EENEVYVLGAFTGLHGR.R 2 K.TETPVSQEDALNLMNENIDILETAIK.Q

Channels and Transporters

Entrez Gene	Entrez Protein	Protein Name	Peptide Sequences Detected		
			1st Identification	2nd Identification	3rd Identification
SLC25A4	NP_001142	Adenine nucleotide translocator 1	1 K.LLLQVQHASK.Q	1 R.GNLANVIR.Y 2 R.YFPTQALNFAFK.D	
SLC25A5	NP_001143	Adenine nucleotide translocator 2	1 K.DFLAGGVAAAISK.T 2 K.EQGVLSFWR.G	1 K.DFLAGGVAAAISK.T	
SLC25A6	NP_001627	Adenine nucleotide translocator 3	1 K.DFLAGGIAAAISK.T	1 K.DFLAGGIAAAISK.T	1 K.DFLAGGIAAAISK.T
SLC4A1	NP_000333	Anion exchanger, member 1	1 K.GLDLNGGPDDPLQQTGQLFGGLVR.D 2 K.IPPDSEATLVLVGR.A 3 R.LQEAAELEAVELPVPIR.F 4 R.SVTHANALTVMGK.A	1 K.GLDLNGGPDDPLQQTGQLFGGLVR.D	
ATP5F1	NP_001679	ATP synthase, H+ transporting, mitochondrial F0 complex, subunit b	1 K.EQEHMINWVEK.H 2 K.QASIQHIQNAIDTEK.S 3 K.TGVTGPVVLGTGLILYALSK.E	1 K.QASIQHIQNAIDTEK.S	
ATP5H	NP_006347	ATP synthase, H+ transporting, mitochondrial F0 complex, subunit d	1 R.LAALPENPPAIDWAYYK.A 2 K.NLIPFDQMTIEDLNEAFPETK.L 3 K.TIDWVAFAEIIPNQK.A 4 K.YPYWPHQPIENL.-	1 K.YPYWPHQPIENL.-	
ATP5A1	NP_004037	ATP synthase, H+ transporting, mitochondrial F1 complex, alpha subunit	1 R.NVQAEEMVEFSSGLK.G	1 R.EAYPGDVFYLHSR.L 2 K.HALIIYDDLSK.Q	
TCIRG1	NP_006010	ATPase, H+ transporting, 116kD, vacuolar, T cell imune regulator	1 R.LGALQQLQQQSQELQEVLGETER.F 2 R.VNFVAGAVEPHK.A	1 R.TPLLQAPGGPHQDLR.V 2 R.VNFVAGAVEPHK.A	1 R.DLNASVSAFQR.R 2 R.DLPALQEALR.D 3 R.DSSMEEGVSAVAHR.I 4 R.FLSQVLGR.V 5 R.LGALQQLQQQSQELQEVLGETER.F 6 R.VNFVAGAVEPHK.A
ATP6V1C2	NP_653184	ATPase, H+ transporting, lysosomal 42kDa, V1 subunit C isoform 2	1 K.LITEDKEGGLFTVTLFR.K	1 K.LITEDKEGGLFTVTLFR.K	
ATP6V0A1	NP_005168	ATPase, H+ transporting, lysosomal V0 subunit a isoform 1	1 R.DLNPDVNVFQR.K	1 R.DLNPDVNVFQR.K	
ATP6V0A2	NP_036595	ATPase, H+ transporting, lysosomal V0 subunit a isoform 2	1 R.ADIPLPEGEASPPAPPLK.Q	1 R.ADIPLPEGEASPPAPPLK.Q	
ATP6V0D1	NP_004682	ATPase, H+ transporting, lysosomal, V0 subunit D isoform 1	1 R.FFEHEVK.L	1 R.FFEHEVK.L	
SLC25A24	NP_037518	Calcium-binding transporter	1 K.HEGLGAFYK.G	1 R.QLLAGGIAGAVSR.T	
SLC2A3	NP_008862	Glucose transporter type 3	1 R.LWGTQDVSQDIQEMK.D 2 R.LWGTQDVSQDIQEMKDESAR.M	1 K.DGVMEMNSIEPAK.E 2 R.LWGTQDVSQDIQEMK.D	1 R.LWGTQDVSQDIQEMK.D 2 K.QVTVLELFR.V 3 R.TFEDITR.A
MTCH2	NP_055157	Mitochondrial carrier homolog 2	1 R.EEGILGFFAGLVPR.L 2 K.VLQHYQESDKGEELGPGNVQK.E	1 R.GLFTGLTPR.L 2 K.VLIQVGYEPLPPTIGR.N	1 R.GLFTGLTPR.L
SLC25A3	NP_005879 NP_002626	Mitochondrial phosphate carrier precursor isoform 1	1 R.LPRPPPPEMPESLK.K	1 K.GIFNGFSVTLK.E 2 R.IQTQPGYANTLR.D	
PLSCR1	NP_066928	Phospholipid scramblase 1	1 R.EAFTDADNFGIQFPLDLDVK.M	1 R.EAFTDADNFGIQFPLDLDVK.M	1 R.EAFTDADNFGIQFPLDLDVK.M
ATP2A3	NP_005164 NP_777613 NP_777614 NP_777615 NP_777617 NP_777618	Sarco/endoplasmic reticulum Ca2+ - ATPase	1 K.AVGVAVATGLHTELGK.I 2 R.HFSVTAEGGLSPAQVTGAR.E 3 R.IVENLQSFNEITAMTGDGVNDAPA LK.K 4 K.NMLFSGTNITSGK.A 5 R.VDQSILTGESVSVTK.H 6 R.YGPNELPSEEGK.S	1 K.NMLFSGTNITSGK.A 2 R.VDQSILTGESVSVTK.H	
SFXN1	NP_073591	Sideroflexin 1	1 K.IQESHPELR.R 2 R.NILLTNEQLESAR.K 3 R.QGIVPPGLTENELWR.A	1 R.NILLTNEQLESAR.K	1 R.NILLTNEQLESAR.K 2 K.QAITQVVVSR.I 3 R.QGIVPPGLTENELWR.A
SLCO4C1	NP_851322	Solute carrier organic anion transporter family, member 4C1	1 K.SPEPSLPSAPPNVSEEK.L	1 K.ENAVVTNVLAEQDLNK.I 2 K.SPEPSLPSAPPNVSEEK.L	
VDAC1	NP_003365	Voltage-dependent anion channel 1	1 K.SENGLEFTSSGSANTETTK.V 2 K.TDEFQLHTNVNDGTEFGGSIYQK.V	1 K.WNTDNTLGTEITVEDQLAR.G	1 K.SENGLEFTSSGSANTETTK.V 2 K.TDEFQLHTNVNDGTEFGGSIYQK.V
SLCO4C1	NP_003366	Voltage-dependent anion channel 2	1 R.TGDFQLHTNVNDGTEFGGSIYQK.V 2 K.VNNSSLIGVGYTQTLRPGVK.L	1 R.TGDFQLHTNVNDGTEFGGSIYQK	
VDAC3	NP_005653	Voltage-dependent anion channel 3	1 K.AADFQLHTHVNDGTEFGGSIYQK.V 2 K.VNNASLIGLGYTQTLRPGVK.L 3 K.WNTDNTLGTEISWENK.L	1 K.AADFQLHTHVNDGTEFGGSIYQK.V	1 K.WNTDNTLGTEISWENK.L

GTP-ases

Entrez Gene	Entrez Protein	Protein Name	Peptide Sequences Detected		
			1st Identification	2nd Identification	3rd Identification
HSPC121	NP_057479	Butyrate-induced transcript 1 GTPase activating protein	1 R.VELSDVQNPAISITENVLHFK.A	1 K.RPLFLAPDFDR.W 2 R.VELSDVQNPAISITENVLHFK.A	
CDC42	NP_001782	Cdc42	1 K.NVFDEAILAALEPPEPK.K	1 K.NVFDEAILAALEPPEPK.K	1 K.NVFDEAILAALEPPEPK.K
GNAI2	NP_002061	Gi α2	1 K.AMGNLQIDFADPSR.A 2 R.IAQSDYIPTQQDVLR.T	1 R.IAQSDYIPTQQDVLR.T 2 K.YDEAASYIQSK.F	1 K.EFADSLGIPFLETSAK.N 2 R.GAHGIIVVYDVTDQESFNNVK
IQGAP1	NP_003861	IQ motif containing GTPase activating protein 1	1 K.LPYDVTPEQALAHEEVK.T 2 K.TLINAEDPPMVVR.K	1 K.TVLELMNPEAQLPQVYPFAADLYQK	
RAB10	NP_057215	RAB10	1 K.EPNSENVDISSGGGVTGWK.S 2 K.TPVKEPNSENVDISSGGGVTGWK.S	1 K.EPNSENVDISSGGGVTGWK.S	
RAB11A	NP_004654	RAB11A	1 R.ENDMSPSNNVVPIHVPPTTENKPK.V	1 R.ENDMSPSNNVVPIHVPPTTENKPK	
RAB11B	NP_004209	RAB11B	1 R.DDEYDYLFK.V 2 R.DHADSNIVIMLVGNK.S 3 R.GAVGALLVYDIAK.H 4 K.HLTYENVER.W 5 K.STIGVEFATR.S	1 R.DHADSNIVIMLVGNK.S	1 R.DDEYDYLFK.V 2 K.HLTYENVER.W
RAB14	NP_057406	Rab14	1 R.NLTNPNTVIILIGNK.A 2 K.TGENVEDAFLEAAK.K	1 R.NLTNPNTVIILIGNK.A 2 K.QFAEENGLLFLEASAK.T 3 K.TGENVEDAFLEAAK.K	
RAB1A	NP_004152	RAB1A	1 K.EFADSLGIPFLETSAK.N 2 R.GAHGIIVVYDVTDQESFNNVK.Q	1 K.EFADSLGIPFLETSAK.N 2 R.GAHGIIVVYDVTDQESFNNVK	
RAB1B	NP_112243	RAB1B	1 R.MGPGAASGGERPNLK.I	1 R.GAHGIIVVYDVTDQESYANVK.Q 2 K.NATNVEQAFMTMAAEIK.K	1 R.GAHGIIVVYDVTDQESYANVK.Q 2 K.NATNVEQAFMTMAAEIK.K
RAB2	NP_002856	RAB2	1 R.DTFNHLTTWLEDAR.Q 2 K.IQEGVFDINNEANGIK.I	1 K.IQEGVFDINNEANGIK.I 2 K.TASNVEEAFINTAK.E	
RAB21	NP_055814	RAB21	1 R.HVSIQEAESYAESVGAK.H	1 R.HVSIQEAESYAESVGAK.H	
RAB27A	NP_899057 NP_899058 NP_899059 NP_004571	RAB27A	1 K.FLALGDSGVGK.T 2 R.IHLQLWDTAGQER.F 3 K.TSVLYQYTDGK.F 4 R.VVKEEEAIALAEK.Y	1 K.FLALGDSGVGK.T 2 R.IHLQLWDTAGQER.F 3 R.VVKEEEAIALAEK.Y	1 K.FLALGDSGVGK.T 2 R.IHLQLWDTAGQER.F
RAB32	NP_006825	RAB32	1 K.ILVNHQSFPNEENDVDK.I	1 K.DNINIEEAAR.F 2 K.EHGFAGWFETSAK.D 3 K.ILVNHQSFPNEENDVDK.I	
RAB3A RAB3B RAB3C	NP_002857 NP_002858 NP_612462	RAB3	1 K.LQIWDTAGQER.Y	1 K.ILIIGNSSVGK.T	
RAB3B	NP_002858	RAB3B	1 K.TYSWDNAQVILVGNK.C	1 K.TYSWDNAQVILVGNK.C	
RAB3D	NP_004274	RAB3D	1 R.DAADQNFDYMFK.L	1 R.DAADQNFDYMFK.L 2 R.LADDLGFEFFEASAK.E	1 R.DAADQNFDYMFK.L 2 R.LADDLGFEFFEASAK.E
RAB5C	NP_958842 NP_004574	RAB5C	1 R.AVEFQEAQAYADDNSLLFMETSAK.T 2 R.GVDLQENNPASR.S	1 R.GVDLQENNPASR.S	1 R.GVDLQENNPASR.S
RAB7	NP_004628	RAB7	1 R.DPENFPFVVLGNK.I 2 K.EAINVEQAFQTIAR.N 3 K.QETEVELYNEFPEPIK.L	1 R.DPENFPFVVLGNK.I	
RAP2A RAP2B RAP2C	NP_066361 NP_002877 NP_067006	RAP2	1 K.EIEVDSSPSVLEILDTAGTEQFASMR	1 K.VVVLGSGGVGK.S	

Structural Proteins and Adaptors

Entrez Gene	Entrez Protein	Protein Name	Peptide Sequences Detected		
			1st Identification	2nd Identification	3rd Identification
ACTA1 ACTA2	NP_001091 NP_001604	Actin, alpha	1 R.DLTDYLMK.I 2 R.HQGVMVGMGQK.D 3 K.SYELPDGQVITIGNER.F 4 K.YPIEHGIITNWDDMEK.I	1 R.AVFPSIVGRPR.H 2 R.HQGVMVGMGQK.D 3 K.IKIIAPPER.K 4 K.IWHHTFYNELR.V 5 K.YPIEHGIITNWDDMEK.I	1 K.AGFAGDDAPR.A 2 R.AVFPSIVGRPR.H 3 K.EITALAPSTMK.I 4 K.YPIEHGIITNWDDMEK.I
ACTB ACTG1	NP_001092 NP_001605	Actin, beta or gamma	1 K.QEYDESGPSIVHR.K 2 R.TTGIVMDSGDGVTHTVPIYEGYALPHAILR.L 3 R.VAPEEHPVLLTEAPLNPK.A	1 R.GYSFTTTAER.E 2 K.QEYDESGPSIVHR.K 3 K.QEYDESGPSIVHRK.C 4 R.TTGIVMDSGDGVTHTVPIYEGYALPHAILR.L 5 R.VAPEEHPVLLTEAPLNPK.A	1 R.GYSFTTTAER.E 2 R.KDLYANTVLSGGTTMYPGIADR.M 3 K.QEYDESGPSIVHR.K 4 R.VAPEEHPVLLTEAPLNPK.A
ACTN1	NP_001093	Actinin, alpha 1	1 R.DHSGTLGPEEFK.A 2 K.HEAFESDLAAHQDR.V 3 K.KHEAFESDLAAHQDR.V 4 R.VEQIAAIAQELNELDYYDSPSVNAR.C 5 R.VGWEQLLTTIAR.T	1 K.LVSIGAEEIVDGNVK.M 2 R.VEQIAAIAQELNELDYYDSPSVNAR.C	
AP2A1	NP_055018 NP_570603	Adaptin	1 K.LLGFGSALLDNVDPNPENFVGAGIIQTK.A	1 K.LLGFGSALLDNVDPNPENFVGAGIIQTK.A	
ANXA1	NP_000691	Annexin I, (lipocortin I)	1 K.GVDEATIIDILTK.R	1 K.GTDVNVFNTILTTR.S	
CORO1A	NP_009005	Coronin 1A	1 R.KLQATVQELQK.R 2 R.KSDLFQEDLYPPTAGPDPALTAEEWLGGR.D	1 R.AAPEASGTPSSDAVSR.L 2 R.HVFGQPAK.A 3 R.KLQATVQELQK.R	1 R.KLQATVQELQK.R

FLNA	NP_001447	Filamin 1	1 R.AYGPGIEPTGNMVK.K 2 K.DAGEGGLSLAIEGPSK.A 3 K.DAGEGLLAVQITDPEGKPK.K 4 R.DAGYGGLSLSIEGPSK.V 5 R.DAPQDFHPDR.V 6 K.DKGEYTLVVK.W 7 R.DVDIIDHHDNTYTVK.Y 8 R.EAGAGGLAIAVEGPSK.A 9 R.EGPYSISVLYGDEEVPR.S 10 K.FADQHVPGSPFSVK.V 11 R.FGGEHVPNSPFQVTALAGDQPSVQPPLR.S 12 K.FNEEHIPDSPFVVPVASPSGDAR.R 13 K.FNGTHIPGSPFK.I 14 R.GAGTGGLGLAVEGPSEAK.M 15 K.GLVEPVDVVDNADGTQTVNYVPSR.E 16 K.KNGQHVASSPIPVVISQSEIGDASR.V 17 K.KTHIQDNHDGTYTVAYVPDVTGR.Y 18 K.LPQLPITNFSR.D 19 R.LVSNHSLHETSSVFVDSLTK.A 20 R.NGHVGISFVPK.E 21 K.NGQHVASSPIPVVISQSEIGDASR.V 22 R.RLTVSSLQESGLK.V 23 R.SAGQGEVLVYVEDPAGHQEEAK.V 24 K.SPFEVYVDK.S 25 K.SPFSVAVSPSLDLSK.I 26 R.TFSVWYVPEVTGTHK.V 27 K.TGVAVNKPAEFTVDAK.H 28 K.THIQDNHDGTYTVAYVPDVTGR.Y 29 R.VANPSGNLTETYVQDR.G 30 R.VGEPGHGGDPGLVSAYGAGLEGGVTGNPAEFVVNTSNAGAGALSVTIDGPSK.V 31 K.VGSAADIPINISETDLSLLTATVVPPSGR.E 32 K.VNQPASFAVSLNGAK.G 33 R.VSGQGLHEGHTFEPAEFIIDTR.D 34 K.VTAQGPGLEPSGNIANK.T 35 K.VTVLFAGQHIAK.S 36 R.YAPSEAGLHEMDIR.Y 37 K.YNEQHVPGSPFTAR.V	1 K.AFGPGLQGGSAGSPAR.F 2 R.ALTQTGGPHVK.A 3 R.AWGPGLEGGVVGK.S 4 R.DAEMPATEKDLAEDAPWKK.I 5 K.FNEEHIPDSPFVVPVASPSGDAR.R 6 R.GAGTGGLGLAVEGPSEAK.M 7 R.IANLQTDLSDGLR.L 8 R.TFSVWYVPEVTGTHK.V 9 K.YGGPYHIGGSPFK.A	1 K.FNEEHIPDSPFVVPVASPSGDAR.R 2 K.GLVEPVDVVDNADGTQTVNYVPSR.E 3 K.SPFSVAVSPSLDLSK.I 4 K.TGVAVNKPAEFTVDAK.H
GSN	NP_000168 NP_937895	Gelsolin	1 R.EVQGFESATFLGYFK.S 2 K.HVVPNEVVVQR.L 3 K.QTQVSVLPEGGETPLFK.Q 4 K.TPSAAYLWVGTGASEAEK.T 5 K.VSNGAGTMSVSLVADENPFAQGALK.S	1 K.HVVPNEVVVQR.L 2 K.TGAQELLR.V	1 K.TGAQELLR.V
CORO7	NP_078811	Coronin 7	1 R.LPDTALPTLQNGAAVTDLAWDPFDPHR.L	1 R.LPDTALPTLQNGAAVTDLAWDPFDPHR.L	
LCP1	NP_002289	L-plastin	1 K.AYYHLLEQVAPK.G 2 K.IGNFSTDIK.D 3 K.VNDDIVNWVVNETLR.E 4 R.VYALPEDLVEVNPK.M 5 R.YPALHKPENQDIDWGALEGETR.E	1 R.EITENLMATGDLDQDGR.I 2 K.GDEEGVPAVVIDMSGLR.E 3 K.ISTSLPVLDLIDAIQPGSINYDLLK.T 4 R.NEALIALLR.E 5 R.NWMNSLGVNPR.V 6 K.VNDDIVNWVVNETLR.E 7 R.VNIHLYSDLSDALVIFQLYEK.I 8 R.VYALPEDLVEVNPK.M 9 R.YPALHKPENQDIDWGALEGETR.E	1 K.FSLVGIGGQDLNEGNR.T 2 K.GDEEGVPAVVIDMSGLR.E
MYH9	NP_002464	Myosin, heavy chain	1 R.AGVLAHLEEER.D 2 K.AKQTLENERGELANEVK.V 3 K.ALELDSNLYR.I 4 K.DFSALESQLQDTQELLQEENRQK.L 5 K.HSQAVEELAEQLEQTKR.V 6 R.IMGIPEEEQMGLLR.V 7 K.KVEAQLQELQVK.F 8 K.LQVELDNVTGLLSQSDSK.S 9 R.LTEMETLQSQLMAEK.L 10 K.LTKDFSALESQLQDTQELLQEENR.Q 11 R.NWQWWR.L 12 R.QAQQERDELADEIANSSGK.G 13 K.TELEDTLDSTAAQQELR.S 14 R.TEMEDLMSSKDDVGK.S 15 K.THEAQIQEMR.Q 16 K.TLEEEAKTHEAQIQEMR.Q 17 K.VSHLLGINVTDFTR.G	1 K.ANLQIDQINTDLNLER.S 2 K.DFSALESQLQDTQELLQEENR.Q 3 R.ELEDATETADAMNR.E 4 K.FDQLLAEEK.T 5 R.FLSNGHVTIPSQQDK.D 6 R.HEMPPHIYAITDTAYR.S 7 K.HSQAVEELAEQLEQTK.R 8 R.IAEFTTNLTEEEEK.S 9 R.IAQLEEELEEEQGNTELINDR.L 10 K.IAQLEEQLDNETK.E 11 R.IMGIPEEEQMGLLR.V 12 K.KEEELQAALAR.V 13 R.KLEGDSTDLSDQIAELQAQIAELK.M 14 K.LEGDSTDLSDQIAELQAQIAELK.M 15 R.LQQELDDLLVDLDHQR.Q 16 R.LTEMETLQSQLMAEK.L 17 K.NFINNPLAQADWAAK.K 18 K.NKHEAMITDLEER.L 19 K.NLPIYSEEIVEMYK.G 20 K.NMDPLNDNIATLLHQSSDK.F 21 R.QLLQANPILEAFGNAK.T 22 K.SGFEPASLKEEVGEEAIVELVENGK.K 23 K.SGFEPASLKEEVGEEAIVELVENGKK.V 24 K.SMEAEMIQLQEELAAAER.A 25 K.TELEDTLDSTAAQQELR.S 26 K.TQLEELEDELQATEDAK.L 27 K.VEAQLQELQVK.F	1 K.DFSALESQLQDTQELLQEENR.Q 2 K.VKPLLQVSR.Q
PFN1	NP_005013	Profilin 1	1 K.TFVNITPAEVGVLVGK.D	1 R.DSLLQDGEFSMDLR.T 2 R.SSFYVNGLTLGGQK.C 3 K.STGGAPTFNVTVTK.T 4 K.TFVNITPAEVGVLVGK.D	1 K.TFVNITPAEVGVLVGK.D
MYL6	NP_066299 NP_524147 NP_524149 NP_524148	Myosin alkali light chain	1 R.HVLVTLGEK.M	1 R.HVLVTLGEK.M	
TLN1	NP_006280	Talin 1	1 K.AAAFEEQENETVVVK.E 2 K.AVSSAIAQLLGEVAQGNENYAGIAAR.D 3 R.DDILNGSHPVSFDK.A 4 R.DLDQASLAAVSQQLAPR.E 5 K.EAAYHPEVAPDVR.L 6 K.EADESLNFEEQILEAAK.S 7 R.EQGVEEHETLLLR.R 8 K.EVIQEWNLTNIK.R 9 R.GSQAQPDSPSAQLALIAASQSFLQPGGK.M 10 K.GTEWVDPEDPTVIAENELLGAAAAIEAAAK.K 11 R.GVAALTSDPAVQAIVLDTASDVLDK.A 12 R.GVGAAATAVTQALNELLQHVK.A 13 R.IPEAPAGPPSDFGLFLSDDDPK.K 14 K.NGNLPEFGDAISTASK.A 15 K.QAAASATQTIAAAQHAASTPK.A 16 R.SGASGPENFQVGSMPPAQQQITSGQMHR.G 17 K.SKQHFGLEGDEESTMLEDSVSPK.K 18 K.SNTSPEELGPLANQLTSDYGR.L 19 K.TLSHPQQMALLDQTK.T 20 R.VAGSVTELIQAAEAMK.G 21 K.VGAIPANALDDGQWSQGLISAAR.M 22 K.VGDDPAVWQLK.N 23 K.VLGEAMTGISQNAK.N	1 R.GSQAQPDSPSAQLALIAASQSFLQPGGK.M 2 R.IGITNHDEVSLVR.E 3 R.VAGSVTELIQAAEAMK.G 4 K.VGDDPAVWQLK.N	
TUBA1 TUBA2	NP_005991 NP_005992 NP_524575	Tubulin alpha 1,2	1 K.VGINYQPPTVVPGGDLAK.V	1 R.AVFVDLEPTVIDEIR.N 2 R.NLDIERPTYTNLNR.L 3 K.VGINYQPPTVVPGGDLAK.V	1 K.VGINYQPPTVVPGGDLAK.V
TUBA3	NP_006000	Tubulin alpha 3	1 R.AVFVDLEPTVIDEVR.T	1 R.AVFVDLEPTVIDEVR.T	
TUBB1	NP_110400	Tubulin beta 1	1 K.EVDQQLLSVQTR.N 2 K.FWEMIGEEHGIDLAGSDR.G 3 K.LGALFQPDSFVHGNSGAGNNWAK.G	1 K.EVDQQLLSVQTR.N 2 K.FWEMIGEEHGIDLAGSDR.G 3 K.LGALFQPDSFVHGNSGAGNNWAK.G	

TUBB2	NP_001060	Tubulin beta 3	1 R.AILVDLEPGTMDSVR.S 2 K.EVDEQMLNVQNK.N 3 R.SGPFGQIFRPDNFVFGQSGAGNN WAK.G	1 K.EVDEQMLNVQNK.N 2 R.FPGQLNADLR.K 3 K.GHYTEGAELVDSVLDVVR.K 4 K.NSSYFVEWIPNNVK.T 5 R.SGPFGQIFRPDNFVFGQSGAGNN WAK.G	1 R.FPGQLNADLR.K
URP2	NP_848537 NP_113659	UNC-112 related protein 2	1 K.EKEPEEELYDLSK.V 2 R.HPEELSLLR.A 3 R.ILEAHQNVAQLSLAEAQLR.F 4 K.LSQSGEVGEPAGTDPGLDDLDVALS NLEVK.I 5 K.SQDEAPGDPIQQLNLK.G 6 R.VFVGEEDPEAESVTLR.V 7 R.VTGESHIGGVLLK.I	1 R.VFVGEEDPEAESVTLR.V 2 R.VTGESHIGGVLLK.I	
VIM	NP_003371	Vimentin	1 K.FADLSEAANR.N 2 K.ILLAELEQLKGQGK.S 3 R.LLQDSVDFSLADAINTEFKNTR.T	1 K.FADLSEAANR.N 2 K.ILLAELEQLKGQGK.S 3 R.LLQDSVDFSLADAINTEFKNTR.T	
RP2	NP_008846	XRP2	1 K.APDFLPLLNK.G	1 K.APDFLPLLNK.G	

Kinases and Phosphatases

Entrez Gene	Entrez Protein	Protein Name	Peptide Sequences Detected		
			1st Identification	2nd Identification	3rd Identification
HCK	NP_002101	Hck tyrosine kinase	1 R.IPYPGMSNPEVIR.A	1 R.IPYPGMSNPEVIR.A	
FGR	NP_005239	Fgr tyrosine kinase	1 K.FHILNNTEGDWWEAR.S	1 R.IPYPGMNK.R 2 R.QLLSPGNPQGAFLIR.E 3 R.SYGAADHYGPDPTK.A	1 R.QLLSPGNPQGAFLIR.E
PTPNS1	NP_542970	Protein tyrosine phosphatase, non-receptor type substrate 1	1 R.VPPTLEVTQQPVR.A	1 R.VPPTLEVTQQPVR.A	
PTPN7	NP_002823 NP_542155	Protein tyrosine phosphatase, non-receptor type 7	1 R.RGSNVALMLDVRSLGAVEPICSVNT PR.E	1 R.RGSNVALMLDVRSLGAVEPICSVNT PR.E	
PTPRJ	NP_002834	Protein tyrosine phosphatase, receptor type J	1 R.AGSPTAPVHDESLVGPVDPSSG QQSR.D 2 K.NIQTSESHPLR.Q	1 R.AGSPTAPVHDESLVGPVDPSSG QQSR.D 2 K.KDFIATQGPLPNTLK.D 3 K.NNEVSFSQIKPK.K 4 K.TPSSTGPSPVFDIK.A	1 K.KDFIATQGPLPNTLK.D 2 K.TPSSTGPSPVFDIK.A
PTPRC	NP_002829 NP_563578 NP_563579 NP_563580	Protein tyrosine phosphatase, receptor type C	1 K.DLQYSTDYTFK.A 2 R.DPPSEPSPLEAEFQR.L 3 K.ELISMIQVVK.Q 4 R.EVTHIQFTSWPDHGVPEDPHLLLK.L 5 K.KRDPPSEPSPLEAEFQR.L 6 K.LENLEPEHEYK.C 7 R.SEAAHQGVITWNPPQR.S 8 R.TVYQYQYTNWSVEQLPAEPK.E 9 R.VELSEINGDAGSNYINASYIDGFK.E 10 R.VPLKHELEMSK.E 11 K.YDLQNLKPYTK.Y 12 R.YHLEVEAGNTLVR.N	1 K.DLQYSTDYTFK.A 2 R.EVTHIQFTSWPDHGVPEDPHLLLK.L 3 K.KRDPPSEPSPLEAEFQR.L 4 K.RDPPSEPSPLEAEFQR.L 5 R.SEAAHQGVITWNPPQR.S 6 R.VPLKHELEMSK.E 7 K.YDLQNLKPYTK.Y	

Luminal and Host Defense Proteins

Entrez Gene	Entrez Protein	Protein Name	Peptide Sequences Detected		
			1st Identification	2nd Identification	3rd Identification
BPI	NP_001716	Bactericidal/permeability-increasing protein precursor, BPI	1 K.FFGTFLPEVAK.K 2 K.GLDYASQQGTAALQK.E	1 K.GLDYASQQGTAALQK.E	1 K.FSISNANIK.I 2 K.GLDYASQQGTAALQK.E
CTSG	NP_001902	Cathepsin G preproprotein	1 R.NVNPVALPR.A 2 R.TIQNDIMLLQLSR.R 3 R.VSSFLPWIR.T	1 R.IFGSYDPRR.Q 2 R.NRNVNPVALPR.A 3 R.NVNPVALPR.A 4 R.TIQNDIMLLQLSR.R 5 R.VSSFLPWIR.T	1 R.IFGSYDPR.R 2 R.NVNPVALPR.A 3 R.TIQNDIMLLQLSR.R 4 R.VSSFLPWIR.T
C10orf42	NP_612366	Chromosome 10 ORF 42	1 R.DLLSHENAATLNDVK.T 2 R.DPLQVHLPLR.Q 3 R.LEDLKEQLAPLEK.V	1 R.DLLSHENAATLNDVK.T 2 R.DPLQVHLPLR.Q 3 R.VAASTGIDLLLLDDFK.L	
DCD	NP_444513	Dermcidin precursor	1 R.SSLLEKGLDGAKK.A	1 K.DAVEDLESVGK.G 2 K.LGKDAVEDLESVGK.G	1 K.DAVEDLESVGK.G
EPX	NP_000493	Eosinophil peroxidase	1 R.IGLDLAALNMQR.S 2 R.IVYEGGIDPILR.G 3 R.NGFLLPLVR.A 4 R.RPLLGASNQALAR.W 5 R.TNYLGLLAINQR.F 6 R.VANVFTLAFR.F	1 R.IGLDLAALNMQR.S 2 R.IVYEGGIDPILR.G 3 R.NGFLLPLVR.A 4 R.TNYLGLLAINQR.F 5 R.VANVFTLAFR.F	1 R.NGFLLPLVR.A 2 R.NQINALTSFVDASMVYGSEVSLSLR.L 3 R.TNYLGLLAINQR.F
MMP9	NP_004985	Gelatinase	1 R.AFALWSAVTPLTFTR.V 2 R.FTEGPPLHK.D 3 R.FTEGPPLHKDDVNGIR.H 4 R.GSRPQGPFLIADK.W 5 R.KLDSVFEEPLSK.K 6 K.QLSLPETGELDSATLK.A 7 R.QVWVYTGASVLGPR.R 8 K.SLGPALLLLQK.Q	1 R.FTEGPPLHK.D 2 R.KLDSVFEEPLSK.K 3 K.LGLGADVAQVTGALR.S 4 K.QLSLPETGELDSATLK.A 5 R.QSTLVLFPGDLR.T 6 K.SLGPALLLLQK.Q	1 R.FTEGPPLHK.D 2 R.KLDSVFEEPLSK.K 3 K.SLGPALLLLQK.Q
SPCS2	NP_055567	KIAA0102 gene product (signal peptidase)	1 R.LHDSLAIER.K	1 K.FFDHSGTLVMDAYEPEISR.L 2 K.SIFLVAHR.K	
LTF	NP_002334	Lactoferrin	1 K.GGSFQLNELQGLK.S 2 R.THYYAVAVVK.K	1 K.EDAIWNLLR.Q 2 K.FQLFGSPSGQK.D 3 K.GGSFQLNELQGLK.S 4 R.IDSGLYLGSGYFTAIQNLR.K 5 K.KGGSFQLNELQGLK.S 6 K.LRPVAAEVYGTER.Q 7 R.THYYAVAVVK.K	1 R.DGAGDVAFIR.E 2 K.EDAIWNLLR.Q 3 K.FQLFGSPSGQK.D 4 K.GGSFQLNELQGLK.S 5 R.IDSGLYLGSGYFTAIQNLR.K 6 K.KGGSFQLNELQGLK.S 7 K.LRPVAAEVYGTER.Q 8 R.THYYAVAVVK.K 9 K.YLGPQYVAGITNLK.K
LCN2	NP_005555	Lipocalin 2; NGAL	1 K.VPLQQNFQDNQFQGK.W	1 K.VPLQQNFQDNQFQGK.W	
MGAM	NP_004659	Maltase-glucoamylase	1 R.DASLNHPPYMPHLESR.D 2 R.EIEELYNNPQNPER.S 3 R.KNPLGLIIALDENK.E 4 K.NLPSSPVFGSNVDNVLLTAEYQTS NR.F 5 K.NPFGIEIR.R 6 K.SSVYANAFPSTPVNPLR.L	1 R.DASLNHPPYMPHLESR.D 2 R.LPSTNVYGLGEHVHQQYR.H 3 K.NPFGIEIR.R	1 K.DPNNLAFNEIK.I 2 R.EIEELYNNPQNPER.S 3 R.GVEDDVFIK.Y 4 K.HNGVPSQTSPTVTYDSNLK.V 5 R.KNPLGLIIALDENK.E 6 K.NLPSSPVFGSNVDNVLLTAEYQTS NR.F 7 K.NPFGIEIR.R 8 K.SSVYANAFPSTPVNPLR.L 9 K.YPNDGDIWWGK.V
MMP25	NP_071913 NP_073209	Matrix metalloproteinase 25 (leukolysin)	1 R.DLSLWEGAPPSPDDVTVSNAGDTY FFK.G	1 R.DLSLWEGAPPSPDDVTVSNAGDTY FFK.G	1 R.DGLQQLYGK.A
ANPEP	NP_001141	Membrane alanine aminopeptidase	1 R.DHSAIPVINR.A 2 R.ENSLLFDPLSSSSSNK.E 3 R.FSTEYELQQLEQFK.K 4 R.GVGGSQPPDIDKTELVEPTEYL VVHLK.G 5 R.KVVATTQMQAADAR.K	1 R.DHSAIPVINR.A 2 R.ENSLLFDPLSSSSSNK.E 3 K.EVVLQWFTENSK.- 4 R.FSTEYELQQLEQFK.K 5 R.GVGGSQPPDIDK.T	1 R.DHSAIPVINR.A 2 R.ENSLLFDPLSSSSSNK.E

MPO	NP_000241	Myeloperoxidase	1 R.FPTDQLTPDQER.S 2 R.IANVFTNAFR.Y 3 R.NQINALTSFVDASMVYGSEEPLAR.N 4 R.QALAQISLPR.I 5 R.VVLEGGIDPILR.G	1 R.DHGLPGYNAWR.R 2 R.FPTDQLTPDQER.S 3 R.IGLDLPALNMQR.S 4 R.NQINALTSFVDASMVYGSEEPLAR.N	1 R.DHGLPGYNAWR.R 2 R.FPTDQLTPDQER.S 3 R.IANVFTNAFR.Y 4 R.NGFPVALAR.A 5 R.QALAQISLPR.I 6 R.QNQIAVDEIR.E 7 R.VVLEGGIDPILR.G
MME	NP_000893 NP_009218 NP_009219 NP_009220	Neprilysin	1 R.LPIDENQLALEMNK.V 2 K.NSVNHVIHIDQPR.L	1 K.DGDLVDWWTQQSASNFK.E 2 R.LPIDENQLALEMNK.V	
PADI4	NP_036519	Peptidyl arginine deiminase IV	1 R.ELGLAESDIIDIPQLFK.L 2 R.GPQTGGISGLDSFGNLEVSPPVT VR.G 3 K.LFQEQQNEGHGEALLFEGIK.K	1 R.ELGLAESDIIDIPQLFK.L 2 R.GPQTGGISGLDSFGNLEVSPPVT VR.G 3 K.LFQEQQNEGHGEALLFEGIK.K	
PRTN3	NP_002768	Proteinase 3	1 R.TQEPTQQHFSVAQVFLNNYDAENK.L	1 R.LVNVVLGAHNVR.T 2 R.TQEPTQQHFSVAQVFLNNYDAENK.L	
PRG2	NP_002719	Proteoglycan 2	1 R.GNLVSIHNFNINYR.I	1 R.GNLVSIHNFNINYR.I	1 R.GNLVSIHNFNINYR.I
THBS1	NP_003237	Thrombospondin 1 precursor	1 R.FTGSQPFGQGVEHATANK.Q 2 K.GPDPSSPAFR.I 3 R.IEDANLIPPVPDDKFQDLVDAVR.A	1 R.DDDYAGFVFGYQSSSR.F 2 K.DHSGQVFSVVSNGK.A 3 K.FQDLVDAVR.A 4 R.FTGSQPFGQGVEHATANK.Q 5 K.GGVNDNFQGVLQNVR.F 6 K.GPDPSSPAFR.I 7 R.IEDANLIPPVPDDK.F 8 R.IEDANLIPPVPDDKFQDLVDAVR.A 9 R.IPESGGDNSVFDIFELTGAAR.K 10 R.KDHSGQVFSVVSNGK.A 11 K.MENAELDVPIQSVFTR.D 12 R.NALWHTGNTPGQVR.T 13 K.QHVVSVEEALLATGQWK.S 14 R.TIVTTLQDSIR.K 15 K.VTEENKELANELR.R	1 R.FTGSQPFGQGVEHATANK.Q 2 R.IEDANLIPPVPDDKFQDLVDAVR.A

Membrane Traffic and Fusion Proteins

Entrez Gene	Entrez Protein	Protein Name	Peptide Sequences Detected		
			1st Identification	2nd Identification	3rd Identification
DNAJC5	NP_079495	DnaJ (Hsp40) homolog, subfamily C, member 5	1 K.APEGEETEFYVSPEDLEAQLQS DER.E 2 K.EINNAHAILTDATK.R	1 K.YHPDKNPDNPEAADKFK.E	1 K.APEGEETEFYVSPEDLEAQLQS DER.E
DYSF	NP_003485	Dysferlin	1 R.AEDLPQMDDAVMDNVK.Q 2 K.DSFSDPYAIVSFLHQSQK.T 3 R.EFTGFPDPYTELNTGK.G 4 R.IETQNQLLGIADR.L 5 R.IPNPHLGPVEER.L 6 K.IYPLPEDPAIPMPPR.Q 7 R.KDPSEDKEDIESNLLRPTGVALR.G 8 K.LGHSELPAALEQAEDWLLR.L 9 K.NLVDPFVEVSFAGK.M 10 R.RPDTSFLWFTSPYK.T 11 K.TGPAAVFALEGALGGVMDDK.S 12 R.THHLSQITEAALALK.L 13 K.TQEETEDPSVIGEFK.G 14 R.VPAHQVLFSR.R	1 K.EYSIEEIEAGRIPNPHLGPVEER.L 2 K.HWVPAEK.M 3 K.IGETVVDLENR.L 4 R.IPNPHLGPVEER.L 5 K.IYPLPEDPAIPMPPR.Q 6 K.LGHSELPAALEQAEDWLLR.L 7 K.LVEHSEQKVEDLPADDILR.V	1 K.DSFSDPYAIVSFLHQSQK.T 2 R.DVILDDLSLTGEK.M 3 R.EFTGFPDPYTELNTGK.G 4 R.GSQPSGELLASFELIQR.E 5 R.IETQNQLLGIADR.L 6 K.IGETVVDLENR.L 7 K.IYPLPEDPAIPMPPR.Q 8 R.LEAGLEQVHLALK.A 9 K.NLVDPFVEVSFAGK.M 10 R.SLGGEGNFNWR.F 11 R.TDALLGEFR.M 12 K.TGPAAVFALEGALGGVMDDK.S 13 K.TQEETEDPSVIGEFK.G
TMED9	NP_059980	gp25L2 protein	1 R.VHLDIQVGEHANDYAEIAAK.D	1 R.VHLDIQVGEHANDYAEIAAK.D	
MBC2	NP_056107	KIAA0747 protein	1 R.IHVLEAQDLIAK.D 2 R.LLVPLVPDLQDVAQLR.S	1 R.KPHTESLELQVR.G 2 R.LLVPLVPDLQDVAQLR.S 3 R.LTHVDSPLEAPAGPLGQVK.L 4 K.VLQASVLDDWFPLQGGQGGQVHLR.L	
SNAP23	NP_003816	SNAP-23A	1 K.QPGPVTNGQLQQPTTGAASGGYIK.R	1 K.QPGPVTNGQLQQPTTGAASGGYIK.R	
SACM1L	NP_054735	Synaptojanin	1 R.GIDSEGHAANFVETEQIVHYNGSK.A	1 R.ELSAQPEVHR.F	
STX7	NP_003560	Syntaxin 7	1 R.TLNQLGTPQDSPELR.Q	1 R.TLNQLGTPQDSPELR.Q	1 R.LVAEFTTSLTNFQK.V 2 R.TLNQLGTPQDSPELR.Q
UNC13D	XP_113950 NP_954712	Unc-13 homolog D	1 R.LGHPEPNHVTEASELLR.Y	1 R.EVPGLSGSEEPGEVPQTR.L 2 R.LGHPEPNHVTEASELLR.Y 3 R.LPLTYPAPNGDPILQLLEGR.K 4 R.YLQEAFHVEPEEHQQTLQR.V	
VAMP2	NP_055047 NP_004772	VAMP 2	1 R.ADALQAGASQFETSAAK.L	1 R.ADALQAGASQFETSAAK.L	1 R.ADALQAGASQFETSAAK.L
VAMP8	NP_003752	VAMP 8	1 R.NKTEDLEATSEHFK.T 2 R.NLQSEVEGVK.N 3 K.TEDLEATSEHFK.T	1 K.NIMTQNVER.I	1 K.NIMTQNVER.I 2 R.NKTEDLEATSEHFK.T 3 R.NLQSEVEGVK.N 4 K.TEDLEATSEHFK.T

Redox Proteins

Entrez Gene	Entrez Protein	Protein Name	Peptide Sequences Detected		
			1st Identification	2nd Identification	3rd Identification
DIA1	NP_000389 NP_015565	Cytochrome b5 reductase	1 K.DILLRPELEELR.N 2 R.GPSGLLVYQGK.G	1 R.APEAWDYGQGFVNEEMIR.D 2 K.DILLRPELEELR.N 3 R.GPSGLLVYQGK.G 4 R.IDGNLVVRPYTPISSDDDK.G 5 R.STPAITLESPDIK.Y 6 K.SVGMIAGGTGITPMLQVIR.A	1 R.GPSGLLVYQGK.G
NQO3A2	NP_057327	Cytochrome b5 reductase 1 (B5R.1)	1 R.GPSGLLTYTGK.G 2 R.RPQVTLLDPNEK.Y	1 R.GPSGLLTYTGK.G	
DHRS8	NP_057329	Dehydrogenase/reductase member 8	1 K.NPSTSLGPTLEPEEVVNR.L	1 K.NPSTSLGPTLEPEEVVNR.L 2 K.SVTGEIVLITGAGHGIGR.L	1 K.NPSTSLGPTLEPEEVVNR.L 2 K.SVTGEIVLITGAGHGIGR.L
PDIA3	NP_005304	Grp58	1 R.TADGIVSHLK.K 2 K.TFSHELSDFGLESTAGEIPVVAIR.T	1 R.TADGIVSHLK.K	
GSTK1	NP_057001	Glutathione transferase kappa 1	1 R.NEDITEPQSILAAAEK.A	1 K.DSGNKPPGLLPR.K	
CYBB	NP_000388	gp91-phox	1 K.DVITGLK.Q 2 R.GVHFIFNK.E 3 R.KLLGSALALAR.A 4 K.LLGSALALAR.A 5 K.TIELQMK.K	1 R.GVHFIFNK.E 2 R.GVHFIFNKENF.- 3 K.LLGSALALAR.A 4 K.TLYGRPNWDNEFK.T	1 K.LLGSALALAR.A 2 K.MEVGQYIFVK.C
NDUFB8	NP_004995	NADH dehydrogenase 1 β subcomplex 8	1 R.DPWYSWDQPGLR.L	1 R.DPWYSWDQPGLR.L	
ND5	NP_536853 NP_776061	NADH dehydrogenase subunit 5	1 R.FPTLTNINENNPTLLNPIK.R	1 R.FPTLTNINENNPTLLNPIK.R 2 K.TISQHQISTSIITSTGK.G	1 R.FPTLTNINENNPTLLNPIK.R 2 K.TISQHQISTSIITSTGK.G
NDUFB11	NP_061929	Neuronal protein 17.3	1 K.RPPEPTTPWQEDPEPEDENLYEK.N	1 K.RPPEPTTPWQEDPEPEDENLYEK.N	
CYBA	NP_000092	p22-phox	1 R.ERPQIGGTIK.Q 2 R.KKPSEEEAAAAAGGPPGGPQVN PIPVTDEVV.-	1 R.ERPQIGGTIK.Q 2 R.KKPSEEEAAAAAGGPPGGPQVN PIPVTDEVV.-	
HSD17B12	NP_057226	Steroid dehydrogenase homolog	1 K.GVFVQSVLPYFVATK.L 2 R.KPTLDKPSPETFVK.S 3 R.TIAVDFASEDIYDK.I	1 R.SKDKLDQVSSEIK.E	

SQRDL	NP_067022	Sulfide dehydrogenase	1 K.YADALQEIIQER.N	1 R.HFYQPIWTLVGAGAK.Q 2 K.VGAENVAIVEPSER.H	1 K.EGNAIFTFPNTPVK.C
TXNDC	NP_110382	Thioredoxin-related transmembrane protein	1 R.RPQPYPYPSK.K	1 R.RPQPYPYPSK.K	1 K.DFINFISDK.E

Other Proteins

Entrez Gene	Entrez Protein	Protein Name	Peptide Sequences Detected		
			1st Identification	2nd Identification	3rd Identification
C20orf3	NP_065392	C20 ORF 3; adipocyte plasma membrane-associated	1 R.DYLLLVMEGTDDGR.L 2 K.EPPLLLGVLHPNTK.L 3 R.FPNGVQLSPAEDFVLVAETTMAR.I 4 R.LFENQLVGPESIAHIGDVMFTGTAD GR.V 5 R.RPLRPQVVTDDDGQAPEAK.D	1 R.LFENQLVGPESIAHIGDVMFTGTAD GR.V 2 R.RPLRPQVVTDDDGQAPEAK.D 3 R.VVKLENGEIETIAR.F	1 R.DYLLLVMEGTDDGR.L 2 K.EPPLLLGVLHPNTK.L
CGI-51	NP_056195	CGI-51 protein	1 K.DVVVQHVHFDGLGR.T	1 K.DVVVQHVHFDGLGR.T	
DSP	NP_004406	Desmoplakin	1 R.LLEAQIATGGIIDPK.E 2 R.QLQNIIQATSR.E	1 R.AVTGYNDPETGNIISLFQAMNK.E 2 R.LKNTLTQTTENLR.R 3 R.LLEAQIATGGIIDPK.E	
FGB	NP_005132	Fibrinogen β chain preproprotein	1 K.DNENVVNEYSSELEK.H 2 R.EEAPSLRPAPPPISGGGYR.A 3 K.QGFGNVATNTDGK.N	1 K.DNENVVNEYSSELEK.H	
FGG	NP_000500N P_068656	Fibrinogen γ chain precursor	1 R.LTIGEGQQHHLGGAK.Q	1 K.EGFGHLSPTGTTEFWLGNEK.I 2 K.YEASILTHDSSIR.Y	
GPI	NP_000166	Glucose phosphate isomerase	1 K.TLAQLNPESSLFIIASK.T	1 K.HFVALSTNTTK.V 2 R.VWYVSNIDGTHIAK.T	
GSTK1	NP_057001	Glutathione transferase kappa 1	1 K.DSGNKPPGLLPR.K	1 R.NEDITEPQSILAAAEK.A	
GCA	NP_036330	Grancalcin	1 R.DHLQQGSANFIYDDFLQGTMAI.- 2 K.ELWAALNAWK.E 3 K.ENFMTVDQDGSGTVEHHELR.Q	1 K.ENFMTVDQDGSGTVEHHELR.Q 2 R.LSPQTLTTIVK.R	1 R.LSPQTLTTIVK.R
E2IG5	NP_055182	Growth and transformation-dependent protein	1 K.EDEIPETVSLEMLDAAK.N	1 K.EDEIPETVSLEMLDAAK.N	
HIST1H1C	NP_005310	Histone H1 family	1 K.ALAAAGYDVEK.N 2 K.ALAAAGYDVEKNNSR.I 3 K.GTGASGSFKLNK.K	1 K.KALAAAGYDVEK.N 2 R.KASGPPVSELITK.A	
HIST1H2BG	NP_003509	Histone H2B	1 K.AMGIMNSFVNDIFER.I 2 K.HAVSEGTKAVTKYTSSK.- 3 K.QVHPDTGISSK.A 4 K.VLKQVHPDTGISSK.A	1 R.KESYSVYVYK.V 2 R.LLLPGELAK.H	
HIST1H4I	NP_003486	Histone H4	1 R.DNIQGITKPAIR.R 2 R.TLYGFGG.- 3 K.TVTAMDVVYALK.R	1 R.DNIQGITKPAIR.R 2 R.ISGLIYEETR.G 3 K.RISGLIYEETR.G 4 K.VFLENVIR.D	1 R.DNIQGITKPAIR.R 2 R.ISGLIYEETR.G 3 R.TLYGFGG.- 4 K.TVTAMDVVYALK.R 5 K.VFLENVIR.D
HNRPU	NP_004492 NP_114032	hnRNP U protein	1 K.EKPYFPIPEEYTFIQNVPLEDR.V	1 K.EKPYFPIPEEYTFIQNVPLEDR.V	
ATAD3A	NP_060658	Hypothetical protein FLJ10709	1 K.GEGAGPPPPLPPAQPGAEGGGDR.G 2 R.INEMVHFDLPGQEER.E	1 R.NILMYGPPGTGK.T	
TNFAIP9	NP_078912	Hypothetical protein FLJ23153	1 R.NLGLTPMDQGSLMAAK.E	1 K.TTLLPSGAEVLSYSEAAK.K	
TMEM43	NP_077310	Hypothetical protein MGC3222	1 R.GDFFYHSENPK.Y 2 K.TATSLAEGLSLVVSPDSIHSVAPE NEGR.L 3 R.VSFSYAGLSGDDPDLGPAHVVTV IAR.Q	1 K.TATSLAEGLSLVVSPDSIHSVAPE NEGR.L	
EFHA1	NP_689939	Hypothetical protein FLJ34588	1 K.VATGQELSNNILDTVFK.I	1 K.TNETGYQEAIVKEPEINTTLQMR.F	
LOC199675	NP_777578	Hypothetical protein LOC199675	1 R.LETTLAGIK.N 2 K.NQGAHDPDYENITLAFK.N	1 R.GWDSVQQSITMVR.S 2 R.LETTLAGIK.N 3 K.NQGAHDPDYENITLAFK.N	
LOC255809	XP_172995	Hypothetical protein XP_172995	1 R.GGQVVQLLQAPTDQR.G	1 R.GGQVVQLLQAPTDQR.G 2 K.RPTSTSSSPETPEFSTFR.A	
KIAA0792	XP_375848	KIAA0792 gene product	1 R.TLFITGLPR.D	1 R.TLFITGLPR.D	
LAP1B	NP_056417	Lamina-associated polypeptide 1B	1 R.ISHLVLPVQPENALK.R	1 R.FESFPAGSTLIFYK.Y 2 R.ISHLVLPVQPENALK.R 3 R.QVTGQPQNASFVK.R	1 R.ISHLVLPVQPENALK.R
LST1	NP_995309 NP_995310 NP_995311 NP_995312	Leukocyte specific transcript 1	1 R.LPVPSSEGPDLR.G	2 R.LPVPSSEGPDLR.G	
S100A9	NP_002956	MRP-14	1 K.DLQNFLK.K 2 R.KDLQNFLK.K 3 K.LGHPDTLNQGEFK.E 4 R.NIETIINTFHQYSVK.L 5 K.VIEHIMEDLDTNADK.Q	1 K.LGHPDTLNQGEFK.E 2 R.LTWASHEK.M 3 R.NIETIINTFHQYSVK.L	1 R.NIETIINTFHQYSVK.L 2 K.VIEHIMEDLDTNADK.Q
S100A8	NP_002955	MRP-8	1 K.ALNSIIDVYHK.Y 2 K.ELDINTDGAVNFQEFLILVIK.M 3 K.GADVWFK.E 4 K.GNFHAVYR.D 5 K.KGADVWFK.E	1 K.ALNSIIDVYHK.Y 2 K.GNFHAVYR.D	1 K.ALNSIIDVYHK.Y
P4HB	NP_000909	PDI	1 R.TGPAATTLPDGAAAESLVESSEVA VIGFFK.D	1 K.VDATEESDLAQQYGVR.G	
PHB	NP_002625	Prohibitin	1 R.IFTSIGEDYDER.V 2 R.NITYLPAGGSVLLQLPQ.-	1 R.FDAGELITQR.E	1 R.NITYLPAGGSVLLQLPQ.-
PHB2	NP_009204	Prohibitin-like	1 R.IGGVQQDTILAEGLHFR.I 2 R.IPWFQYPIIYDIR.A	1 R.IGGVQQDTILAEGLHFR.I 2 R.IPWFQYPIIYDIR.A	1 K.FNASQLITQR.A 2 R.IGGVQQDTILAEGLHFR.I 3 R.IPWFQYPIIYDIR.A
PKM2	NP_002645 NP_872270 NP_872271	Pyruvate kinase 3 isoform	1 K.GADFLVTEVENGGSLGSK.K 2 R.TATESFASDPILYRPVAVALDTK.G	1 K.GVNLPGAAVDLPAVSEK.D 2 K.KGVNLPGAAVDLPAVSEK.D	1 R.LAPITSDPTEATAVGAVEASFK.C 2 R.TATESFASDPILYRPVAVALDTK.G
RTN4	NP_065393 NP_722550 NP_008939 NP_997403 NP_997404	Reticulon 4	1 R.GPLPAAPPVAPER.Q	1 R.GPLPAAPPVAPER.Q	
RPN1	NP_002941	Ribophorin I	1 R.FPLFGGWK.T	1 R.APDELHYTYLDTFGRPVIVAYK.K 2 K.ISVIVETVYTHVLHPYPTQITQSEK.Q 3 K.NLVEQHIQDIVVHYTFNK.V 4 K.VTAEVVLAHLGGGSTSR.A	
RPN2	NP_002942	Ribophorin II precursor	1 R.YHVPVVVVPEGSASDTHEQAILR.L	1 K.EDQVIQLMNAIFSK.K 2 K.EETVLATVQALQTASHLSQQADLR.S 3 K.FPEEEAPSTVLSQNLFTPK.Q 4 R.LQVTNVLSQPLTQATVK.L 5 K.NFESLSEAFSVASAAAVLSHNR.Y 6 K.NPILWNVADVVIK.F 7 R.SIVEEIEDLVAR.L 8 K.TGQEVVFVAEPDNK.N 9 R.YHVPVVVVPEGSASDTHEQAILR.L	

HRNR	XP_373868	Similar to hornerin	1 R.GPYESGSGHSSGLGHR.E	1 R.GPYESGSGHSSGLGHR.E 2 R.HGSGSGQSSSYSPYGSGSGWSSSR	
196527	XP_113743	Similar to RIKEN cDNA F730003B03	1 K.LPLKPNDLK.N 2 K.VLSVDESIIKPEQEFFTAPFEK.N	1 K.VLSVDESIIKPEQEFFTAPFEK.N	
LOC388015	XP_370776	Similar to RTI1	1 R.NFIEFVFPYR.H	1 R.NFIEFVFPYR.H	
RPS27A UBB UBA52 UBC	NP_002945 NP_061828 NP_003324 NP_066289	Ubiquitin precursor	1 K.ESTLHLVLR.L 2 K.IQDKEGIPPDQQR.L 3 K.TITLEVEPSDTIENVK.A 4 R.TLSDYNIQK.E	1 K.ESTLHLVLR.L 2 K.TITLEVEPSDTIENVK.A	1 K.ESTLHLVLR.L 2 K.TITLEVEPSDTIENVK.A

SPECIFIC GRANULES

Receptors and Membrane Anchors

Entrez Gene	Entrez Protein	Protein Name	Peptide Sequences Detected		
			1st Identification	2nd Identification	3rd Identification
ADAM8	NP_001100	ADAM-8 (CD156)	1 R.GPQELVPTTHPGQPAR.H	1 R.GPQELVPTTHPGQPAR.H 2 R.HLHDNVQLITGVDFTGTTVGFAR.V 3 R.VLEVVNHVDK.L	
CANX	NP_001737	Calnexin	1 K.APVPTGEVYFADSFDR.G 2 K.IPDPEAVKPDDWDEDAPAK.I 3 K.IPNPDFFEDLEPFR.M 4 K.TPELNLDQFHDK.T	1 R.IVDDWANDGWGLK.K 2 R.KIPNPDFFEDLEPFR.M	1 K.IPDPEAVKPDDWDEDAPAK.I
CEACAM1	NP_001703	CAECAM-1	1 R.TLTLLSVTR.N	1 R.DLTEHKPSVSNHTQDHSNDPPNK.M 2 R.TLTLLSVTR.N	1 R.DLTEHKPSVSNHTQDHSNDPPNK.M 2 R.TLTLLSVTR.N
ITGAM	NP_000623	CD11b	1 R.DHVFQVNNFEALK.T 2 K.ERLPSHSDFLAELR.K 3 K.FGDPLGYEDVIPEADR.E 4 K.FGDPLGYEDVIPEADREGVIR.Y 5 R.GAVYLFHGTSGSGISPSHSQR.I 6 R.GFGQSVVQLQGSR.V 7 R.LPSHSDFLAELR.K 8 R.QELNTIASKPPR.D 9 R.QNTGMWESNANVK.G 10 R.VMQHQYQVSNLGQR.S 11 R.VQSLVLGAPR.Y 12 R.VVVGAPQEIVAANQR.G	1 R.DHVFQVNNFEALK.T 2 K.FGDPLGYEDVIPEADR.E 3 R.GAVYLFHGTSGSGISPSHSQR.I 4 R.GFGQSVVQLQGSR.V 5 R.LFTALFPFEK.N 6 R.LPSHSDFLAELR.K 7 R.QELNTIASKPPR.D 8 K.TEFQLELPVK.Y 9 R.VQSLVLGAPR.Y 10 R.VVVGAPQEIVAANQR.G 11 R.YVIGVGDAFR.S	1 K.AIMEFNPR.E 2 R.DHVFQVNNFEALK.T 3 K.EFVSTVMEQLK.K 4 K.FGDPLGYEDVIPEADR.E 5 R.GAVYLFHGTSGSGISPSHSQR.I 6 R.GFGQSVVQLQGSR.V 7 K.ILVVITDGEK.F 8 R.LFTALFPFEK.N 9 K.LTDVAIGAPGEEDNR.G 10 R.QNTGMWESNANVK.G 11 R.SLVKPITQLLGR.T 12 K.TEFQLELPVK.Y 13 R.TQVTFFFPLDLSYR.K 14 R.VQSLVLGAPR.Y 15 R.VVVGAPQEIVAANQR.G 16 R.YVIGVGDAFR.S
ITGB2	NP_000202	CD18	1 R.IGFGSFVDK.T 2 K.LAENNIQPIFAVTSR.M 3 K.LGAILTPNDGR.C 4 R.LLVFATDDGFHFAGDGK.L 5 K.SAVGELSEDSSNVVHLIK.N 6 R.SNEFDYPSVGQLAHK.L 7 K.SQWNNDNPLFK.S 8 R.VFLDHNALPDTLK.V	1 R.ALNEITESGR.I 2 R.IGFGSFVDK.T 3 R.LLVFATDDGFHFAGDGK.L 4 K.LTEIIPK.S 5 K.RSNEFDYPSVGQLAHK.L 6 K.SAVGELSEDSSNVVHLIK.N 7 R.SNEFDYPSVGQLAHK.L 8 K.SQWNNDNPLFK.S 9 K.TVLPFVNTHPDK.L 10 R.VFLDHNALPDTLK.V	1 R.IGFGSFVDK.T 2 K.LAENNIQPIFAVTSR.M 3 K.LGAILTPNDGR.C 4 K.LGGDLLR.A 5 R.LLVFATDDGFHFAGDGK.L 6 K.LTEIIPK.S 7 K.SAVGELSEDSSNVVHLIK.N 8 R.SNEFDYPSVGQLAHK.L 9 K.SQWNNDNPLFK.S 10 R.VFLDHNALPDTLK.V
C5R1	NP_001727	CD88 C5aR1	1 R.NVLTEESVVR.E	1 R.NVLTEESVVR.E	1 R.NVLTEESVVR.E
ITGA2B	NP_000410	CD41	1 R.ALSNVEGFER.L 2 R.DGYNDIAVAAPYGGPSGR.G 3 R.GEAQVWTQLLR.A 4 K.IVLLDVPVR.A 5 R.NVGSQTLQTFK.A 6 R.VAIVVGAPR.T 7 R.VYLFLQPR.G	1 R.VYLFLQPR.G	
ITGB3	NP_000203	CD61	1 K.GSGDSSQVTQVSPQR.I 2 K.HVLTLTDQVTR.F 3 R.NDASHLLVFTTDAK.T 4 K.SFTIKPVGFK.D	1 K.GSGDSSQVTQVSPQR.I	
FCER1G	NP_004097	FCER1G gene product	1 K.SDGVYTGLSTR.N	1 K.SDGVYTGLSTR.N	1 K.SDGVYTGLSTR.N
FPR1	NP_002020	Formyl peptide receptor	1 R.LIHALPASLER.A	1 R.LIHALPASLER.A	
GP1BB	NP_000398	Glycoprotein Ib beta precursor	1 R.TAHLGANPWR.C	1 R.TAHLGANPWR.C	
LILRB2	NP_005865	Leukocyte Ig-like receptor 2	1 R.KADFQHPAGAVGPEPTDR.G	1 K.NGQFHIPSITWEHTGR.Y	
CLEC12A	NP_612210 NP_963917	Myeloid inhibitory C-type lectin-like receptor isoform	1 R.SYDYWLGLSPEEDSTR.G	1 R.SYDYWLGLSPEEDSTR.G	
SIGLEC5	NP_003821	Sialic acid binding Ig-like lectin 5	1 R.KKPWPDSPGDQASPPGDAPPLEEQK.E 2 R.MEDTGSYFFR.V	1 R.KKPWPDSPGDQASPPGDAPPLEEQK.E	
STOM	NP_004090	Stomatin	1 K.EASMVITESPAALQLR.Y 2 R.LLAQTTLR.N 3 K.LPVQLQR.A 4 K.NLSQILSDR.E 5 R.TISFDIPPQEILTK.D 6 R.VQNATLAVANITNADSATR.L 7 R.YLQTLTTIAAEK.N	1 K.EASMVITESPAALQLR.Y 2 R.LLAQTTLR.N 3 R.LPDSFKDSPSK.G 4 K.VIAAEGEMNASR.A 5 R.VQNATLAVANITNADSATR.L 6 R.YLQTLTTIAAEK.N	1 K.EASMVITESPAALQLR.Y 2 R.EEIAHNMQSTLDDATDAWGIK.V 3 R.LLAQTTLR.N 4 K.LPVQLQR.A 5 K.NLSQILSDR.E 6 K.NSTIVFPLPIDMLQGIIGAK.H 7 R.TISFDIPPQEILTK.D 8 K.VIAAEGEMNASR.A 9 R.VQNATLAVANITNADSATR.L 10 R.YLQTLTTIAAEK.N

Channels and Transporters

Entrez Gene	Entrez Protein	Protein Name	Peptide Sequences Detected		
			1st Identification	2nd Identification	3rd Identification
SLC25A4	NP_001142	Adenine nucleotide translocator 1	1 R.LWGTQDVSQDIQEMK.D 2 K.QVTVLELFR.V	1 R.LWGTQDVSQDIQEMK.D 2 K.QVTVLELFR.V 3 R.TFEDITR.A	1 R.LWGTQDVSQDIQEMK.D 2 K.QVTVLELFR.V
ATP2A3	NP_005164 NP_777613 NP_777614 NP_777615 NP_777617 NP_777618	Sarco/endoplasmic reticulum Ca^{2+} - ATPase	1 R.VDQSILTGESVSVTK.HD	1 R.LGIFGDTEDVAGK.A	
MVP	NP_059447 NP_005106	Major vault protein	1 R.LAQDPFPLYPGEVLEK.D	1 K.AQQLAEVEVK.K 2 R.LAQDPFPLYPGEVLEK.D 3 K.LKAQALAIETEAELQR.V	

GTP-ases

Entrez Gene	Entrez Protein	Protein Name	Peptide Sequences Detected		
			1st Identification	2nd Identification	3rd Identification
RAB3A RAB3B RAB3C	NP_002857 NP_002858 NP_612462	RAB3	1 R.YADDSFTPAFVSTVGIDFK.V	1 K.LQIWDTAGQER.Y	
RAB3D	NP_004274	RAB3D	1 R.LADDLGFEFFEASAK.E	1 R.LADDLGFEFFEASAK.E	1 R.DAADQNFDYMFK.L 2 R.LADDLGFEFFEASAK.E 3 K.LLLIGNSSVGK.T 4 K.MNESLEPSSSSGSNGK.G
RAB5C	NP_958842 NP_004574	RAB5C	1 R.GVDLQENNPASR.S	1 R.GVDLQENNPASR.S	
RAB27A	NP_004571 NP_899057 NP_899058 NP_899059	RAB27A	1 R.IHLQLWDTAGQER.F	1 R.IHLQLWDTAGQER.F	1 K.FLALGDSGVGK.T 2 K.TSVLYQYTDGK.F
GNAI2	NP_002061	Gi α2	1 K.AMGNLQIDFADPSR.A 2 R.IAQSDYIPTQQDVLR.T	1 K.AMGNLQIDFADPSR.A 2 R.IAQSDYIPTQQDVLR.T	1 K.AMGNLQIDFADPSR.A 2 R.IAQSDYIPTQQDVLR.T 3 K.YDEAASYIQSK.F
RAP1A RAP1B	NP_002875 NP_056461	RAP1	1 K.LVVLGSGGVGK.S	1 K.LVVLGSGGVGK.S	1 K.SALTVQFVQGIFVEK.Y
RAB31	NP_006859	RAB31	1 K.NAINIEELFQGISR.Q	1 K.NAINIEELFQGISR.Q	

Structural Proteins and Adaptors

Entrez Gene	Entrez Protein	Protein Name	Peptide Sequences Detected		
			1st Identification	2nd Identification	3rd Identification
ACTN1	NP_001093	Actinin, alpha 1	1 R.FAIQDISVEETSAK.E 2 R.LAILGIHNEVSK.I 3 R.VGWEQLLTTIAR.T	1 R.FAIQDISVEETSAK.E	1 R.TINEVENQILTR.D
ACTA1 ACTA2	NP_001091 NP_001604	Actin, alpha	1 K.EITALAPSTMK.I 2 K.YPIEHGIITNWDDMEK.I	1 K.SYELPDGQVITIGNER.F 2 R.VAPEEHPTLLTEAPLNPK.A 3 K.YPIEHGIITNWDDMEK.I	1 K.AGFAGDDAPR.A 2 K.SYELPDGQVITIGNER.F
ACTB ACTG1	NP_001092 NP_001605	Actin, beta or gamma	1 R.GYSFTTTAER.E 2 K.QEYDESGPSIVHR.K 3 R.TTGIVMDSGDGVTHTVPIYEGYALP HAILR.L 4 R.VAPEEHPVLLTEAPLNPK.A	1 R.GYSFTTTAER.E 2 K.QEYDESGPSIVHR.K 3 R.VAPEEHPVLLTEAPLNPK.A	1 R.GYSFTTTAER.E
CALD1	NP_149129 NP_004333 NP_149347 NP_149130 NP_149131	Caldesmon 1	1 K.KGFTEVKSQNGEFMTHKLK.H	1 K.KGFTEVKSQNGEFMTHKLK.H	1 K.KGFTEVKSQNGEFMTHKLK.H
CYLC2	NP_001331	Cylicin 2	1 K.ADEKKDEDGKKDANK.G	1 K.ADEKKDEDGKKDANK.G	
CORO1A	NP_009005	Coronin 1A	1 R.AAPEASGTPSSDAVSR.L 2 R.HVFGQPAK.A	1 R.AAPEASGTPSSDAVSR.L 2 R.DAGPLLISLK.D	
FLNA	NP_001447	Filamin 1	1 R.AEAGVPAEFSIWTR.E 2 K.AFGPGLQGGSAGSPAR.F 3 K.AGVAPLQVK.V 4 R.AWGPGLEGGVVGK.S 5 R.EAGAGGLAIAVEGPSK.A 6 R.EGPYSISVLYGDEEVPR.S 7 K.FADQHVPGSPFSVK.V 8 K.FNEEHIPDSPFVVPVASPSGDAR.R 9 R.IANLQTDLSDGLR.L 10 K.KTHQDNHDGTYTVAYVPDVTGR.Y 11 R.NGHVGISFVPK.E 12 K.SPFSVAVSPSLDLSK.I 13 K.TGVAVNKPAEFTVDAK.H 14 R.VANPSGNLTETYVQDR.G 15 K.VNQPASFAVSLNGAK.G 16 K.VTAQGPGLEPSGNIANK.T 17 K.VTVLFAGQHIAK.S 18 K.YGGQPVPNFPSK.L 19 K.YNEQHVPGSPFTAR.V	1 K.AFGPGLQGGSAGSPAR.F	
GSN	NP_000168 NP_937895	Gelsolin	1 K.HVVPNEVVVQR.L	1 K.TGAQELLR.V 2 K.TPSAAYLWVGTGASEAEK.T	1 K.AGALNSNDAFVLK.T 2 R.EVQGFESATFLGYFK.S
LCP1	NP_002289	L-plastin	1 K.AYYHLLEQVAPK.G 2 K.FSLVGIGGQDLNEGNR.T 3 K.GDEEGVPAVVIDMSGLR.E 4 K.LSPEELLLR.W 5 R.VYALPEDLVEVNPK.M	1 K.VNDDIIVNWVNETLR.E 2 R.YPALHKPENQDIDWGALEGETR.E	
MSN	NP_002435	Moesin	1 K.APDFVFYAPR.L 2 K.KAPDFVFYAPR.L	1 K.ESEAVEWQQK.A	1 K.FYPEDVSEELIQDITQR.L
MYH9	NP_002464	Myosin heavy chain	1 R.AGVLAHLEEER.D 2 K.ANLQIDQINTDLNLER.S 3 K.DFSALESQLQDTQELLQEENR.Q 4 R.FLSNGHVTIPGQQDK.D 5 R.IAEFTTNLTEEEEK.S 6 K.KFDQLLAEEK.T 7 R.KLEGDSTDLSDQIAELQAQIAELK.M 8 K.LDPHLVLDQLR.C 9 R.LQQELDDLLVDLDHQR.Q 10 R.QLLQANPILEAFGNAK.T 11 R.RGDLPFVVPR.R 12 K.TDLLLEPYNK.Y 13 K.TELEDTLDSTAAQQELR.S 14 K.TQLEELRDELQATEDAK.L 15 K.VSHLLGINVTDFTR.G	1 K.DFSALESQLQDTQELLQEENRQK.L 2 K.FDQLLAEEK.T 3 R.IAEFTTNLTEEEEK.S 4 R.KKVEAQLQELQVK.F 5 R.LTEMETLQSQLMAEK.L 6 K.NLPIYSEEIVEMYK.G 7 R.QLLQANPILEAFGNAK.T 8 R.RGDLPFVVPR.R 9 K.VSHLLGINVTDFTR.G	1 K.ANLQIDQINTDLNLER.S 2 K.DFSALESQLQDTQELLQEENR.Q 3 K.EQADFAIEALAK.A 4 K.IAQLEEQLDNETK.E 5 K.VKPLLQVSR.Q
TLN1	NP_006280	Talin 1	1 R.IGITNHDEVSLVR.E 2 K.NLGTALAELR.T	1 R.IGITNHDEVSLVR.E 2 K.NLGTALAELR.T	
TUBA1 TUBA2 TUBA3	NP_005991 NP_005992 NP_524575 NP_006000 NP_116093 NP_061816	Tubulin alpha 1,2,3	1 K.VGINYQPPTVVPGGDLAK.V	1 K.VGINYQPPTVVPGGDLAK.V	1 K.VGINYQPPTVVPGGDLAK.V
TUBA4	NP_079295	Tubulin alpha 4	1 R.QIFHPEQLITGK.E	1 R.QIFHPEQLITGK.E	
TUBB2	NP_001060	Tubulin, beta 3	1 R.FPGQLNADLR.K	1 R.FPGQLNADLR.K 2 K.NSSYFVEWIPNNVK.T	1 R.SGPFGQIFRPDNFVFGQSGAGNN WAK.G

Kinases and Phosphatases

Entrez Gene	Entrez Protein	Protein Name	Peptide Sequences Detected		
			1st Identification	2nd Identification	3rd Identification
FGR	NP_005239	Fgr tyrosine kinase	1 R.QLLSPGNPQGAFLIR.E	1 R.QLLSPGNPQGAFLIR.E	1 K.FHILNNTEGDWWEAR.S
PTPNS1	NP_542970	Protein tyrosine phosphatase, non-receptor type substrate 1	1 R.VPPTLEVTQQPVR.A	1 R.AKPSAPVVSGPAAR.A	
PTPRC	NP_002829 NP_563578 NP_563579	Protein tyrosine phosphatase, receptor type, C	1 K.KRDPPSEPSPLEAEFQR.L 2 R.LFLAEFQSIPR.V 3 R.SEAAHQGVITWNPPQR.S 4 K.YDLQNLKPYTK.Y 5 R.YVDILPYDYNR.V	1 R.DPPSEPSPLEAEFQR.L 2 R.LFLAEFQSIPR.V 3 R.SEAAHQGVITWNPPQR.S 4 R.YHLEVEAGNTLVR.N 5 R.YVDILPYDYNR.V	1 K.ATVIVMVTR.C 2 K.DLQYSTDYTFK.A 3 R.DPPSEPSPLEAEFQR.L 4 R.EVTHIQFTSWPDHGVPEDPHLLLK.L 5 K.KRDPPSEPSPLEAEFQR.L 6 K.LENLEPEHEYK.C 7 R.LFLAEFQSIPR.V 8 K.VDVYGYVVK.L 9 K.YDLQNLKPYTK.Y 10 R.YHLEVEAGNTLVR.N
PTPRJ	NP_002834	Protein tyrosine phosphatase, receptor type J	1 R.AGSPTAPVHDESLVGPVDPSSG QQSR.D 2 K.NIQTSESHPLR.Q 3 K.TPSSTGPSPVFDIK.A	1 K.TPSSTGPSPVFDIK.A	
TTBK2	NP_775771	Tau tubulin kinase	1 K.LALDIKIATYR.K	1 K.LALDIKIATYR.K	

Luminal and Host Defense Proteins

Entrez Gene	Entrez Protein	Protein Name	Peptide Sequences Detected		
			1st Identification	2nd Identification	3rd Identification
AZU1	NP_001691	Azurocidin 1 preproprotein	1 R.QFPFLASIQNQGR.H	1 R.QFPFLASIQNQGR.H	1 R.QFPFLASIQNQGR.H
BPI	NP_001716	Bactericidal/permeability-increasing protein	1 K.FFGTFLPEVAK.K 2 K.GLDYASQQGTAALQK.E	1 K.GLDYASQQGTAALQK.E 2 K.IDSVAGINYGLVAPPATTAETLDV QMK.G 3 R.IKIPDYSDSFK.I	1 K.FFGTFLPEVAK.K
CAT	NP_001743	Catalase	1 K.LNVITVGPR.G	1 R.FNTANDDNVTQVR.A	
CAMP	NP_004336	hCAP-18	1 R.FALLGDFFR.K	1 R.FALLGDFFR.K	1 R.FALLGDFFR.K
CTSG	NP_001902	Cathepsin G preproprotein	1 R.IFGSYDPR.R 2 R.NVNPVALPR.A 3 R.TIQNDIMLLQLSR.R 4 R.VSSFLPWIR.T	1 R.IFGSYDPR.R 2 R.NVNPVALPR.A 3 R.TIQNDIMLLQLSR.R 4 R.VSSFLPWIR.T	
CHGA	NP_001266	Chromogranin A	1 R.RPEDQELESLSAIEAELEK.V	1 R.RPEDQELESLSAIEAELEK.V	
DCD	NP_444513	Dermcidin precursor	1 K.LGKDAVEDLESVGK.G 2 R.SSLLEKGLDGAKK.A	1 K.DAVEDLESVGK.G	1 K.DAVEDLESVGK.G
EPX	NP_000493	Eosinophil peroxidase	1 R.IGLDLAALNMQR.S 2 R.IICDNTGITTVSR.D 3 R.IVYEGGIDPILR.G 4 R.NGFLLPLVR.A 5 R.RPLLGASNQALAR.W 6 R.TNYLGLLAINQR.F 7 R.VANVFTLAFR.F	1 R.DFLPLVLGK.A 2 R.IGLDLAALNMQR.S 3 R.IVYEGGIDPILR.G 4 K.LNRQDAMLVDELR.D 5 R.NGFLLPLVR.A 6 R.RPLLGASNQALAR.W 7 R.TNYLGLLAINQR.F	1 R.IVYEGGIDPILR.G 2 R.RPLLGASNQALAR.W 3 R.TNYLGLLAINQR.F
FCN1	NP_001994	Ficolin 1 precursor	1 R.VDLVDFEGNHQFAK.Y	1 K.LVLGAFVGGSAGNSLTGHNNNFFS TK.D	
MMP9	NP_004985	Gelatinase	1 R.AVIDDAFAR.A 2 R.FQTFEGDLK.W 3 R.FTEGPPLHK.D 4 R.FTEGPPLHKDDVNGIR.H 5 R.GSRPQGPFLIADK.W 6 R.KLDSVFEEPLSK.K 7 K.QLSLPETGELDSATLK.A 8 R.QSTLVLFPGDLR.T 9 K.SLGPALLLLQK.Q	1 R.FTEGPPLHK.D 2 R.KLDSVFEEPLSK.K 3 K.LGLGADVAQVTGALR.S 4 K.QLSLPETGELDSATLK.A 5 R.QSTLVLFPGDLR.T 6 K.SLGPALLLLQK.Q	1 R.KLDSVFEEPLSK.K 2 K.LGLGADVAQVTGALR.S 3 K.QLSLPETGELDSATLK.A
OLFM4	NP_006409	GW112	1 K.LDIVMHK.M 2 R.LEFTAHVLSQK.F 3 K.LYVVNDGYLLNYDLSVLQKPQ.- 4 R.TEEIFYYYDTNTGK.E 5 K.VQSINYNPFDQK.L	1 K.LYVVNDGYLLNYDLSVLQKPQ.-	
LTF	NP_002334	Lactoferrin	1 R.DGAGDVAFIR.E 2 K.DSAIGFSR.V 3 K.EDAIWNLLR.Q 4 K.GGSFQLNELQGLK.S 5 R.IDSGLYLGSGYFTAIQNLR.K 6 K.KGGSFQLNELQGLK.S 7 K.LRPVAAEVYGTER.Q 8 R.RSDTSLTWNSVK.G 9 R.SVNGKEDAIWNLLR.Q 10 R.THYYAVAVVK.K	1 R.DGAGDVAFIR.E 2 K.DSAIGFSR.V 3 R.ESTVFEDLSDEAER.D 4 K.FQLFGSPSGQK.D 5 K.KGGSFQLNELQGLK.S 6 K.LRPVAAEVYGTER.Q 7 R.THYYAVAVVK.K	1 R.DGAGDVAFIR.E 2 K.DSAIGFSR.V 3 R.ESTVFEDLSDEAER.D 4 K.FQLFGSPSGQK.D 5 K.GGSFQLNELQGLK.S 6 R.IDSGLYLGSGYFTAIQNLR.K 7 K.YLGPQYVAGITNLK.K
LCN2	NP_005555	Lipocalin 2; NGAL	1 K.VPLQQNFQDNQFQGK.W	1 K.VPLQQNFQDNQFQGK.W	1 K.VPLQQNFQDNQFQGK.W
LYZ	NP_000230	Lysozyme precursor	1 K.RLGMDGYR.G 2 R.STDYGIFQINSR.Y	1 R.STDYGIFQINSR.Y	1 R.STDYGIFQINSR.Y
MGAM	NP_004659	Maltase-glucoamylase	1 R.EIEELYNNPQNPER.S 2 K.FAGFPALINR.M	1 R.DASLNHPPYMPHLESR.D 2 K.DPNNLAFNEIK.I 3 R.EIEELYNNPQNPER.S 4 K.NLPSSPVFGSNVDNVLLTAEYQTS NR.F 5 K.VEMELPGDK.I	
MPO	NP_000241	Myeloperoxidase	1 R.FPTDQLTPDQER.S 2 R.QNQIAVDEIR.E	1 R.DHGLPGYNAWR.R 2 R.FPTDQLTPDQER.S 3 R.IANVFTNAFR.Y 4 R.QALAQISLPR.I	1 R.DHGLPGYNAWR.R 2 R.FPTDQLTPDQER.S 3 R.IANVFTNAFR.Y 4 R.QALAQISLPR.I
MMP8	NP_002415	Neutrophil collagenase	1 K.DISNYGFPSSVQAIDAAVFYR.S 2 K.FYQLPSNQYQSTR.K 3 R.NYTPQLSEAEVER.A	1 R.NYTPQLSEAEVER.A	
PTX3	NP_002843	Pentraxin-3	1 R.ADLHAVQGWAAR.S 2 R.LTSALDELLQATR.D	1 R.ADLHAVQGWAAR.S	
PRTN3	NP_002768	Proteinase 3	1 R.TQEPTQQHFSVAQVFLNNYDAENK.L	1 R.LVNVVLGAHNVR.T	
PRG2	NP_002719	Proteoglycan 2	1 R.FQWVDGSR.W 2 R.GNLVSIHNFNINYR.I 3 R.RFQWVDGSR.W	1 R.RFQWVDGSR.W	1 R.FQWVDGSR.W 2 R.GNLVSIHNFNINYR.I
SIGLEC5	NP_003821	Sialic acid binding Ig-like lectin	1 R.KKPWPDSPGDQASPPGDAPPLEE QK.E 2 R.MEDTGSYFFR.V	1 R.KKPWPDSPGDQASPPGDAPPLEE QK.E	

Membrane Traffic and Fusion Proteins

Entrez Gene	Entrez Protein	Protein Name	Peptide Sequences Detected		
			1st Identification	2nd Identification	3rd Identification
CLTC	NP_004850	Clathrin heavy chain 1	1 R.NNLAGAEELFAR.K	1 K.NNRPSEGPLQTR.L 2 K.SVNESLNNLFITEEDYQALR.T	1 K.LLYNNVSNFGR.L

DYSF	NP_003485	Dysferlin	1 R.EFTGFPDPYTELNTGK.G 2 K.HWVPAEK.M 3 K.LGHSELPAALEQAEDWLLR.L 4 K.LVEHSEQKVEDLPADDILR.V	1 R.EFTGFPDPYTELNTGK.G 2 K.IGETVVDLENR.L 3 R.TDALLGEFR.M	1 R.DVILDDLSLTGEK.M 2 R.GSQPSGELLASFELIQR.E 3 R.IETQNQLLGIADR.L 4 K.IGETVVDLENR.L 5 R.IPNPHLGPVEER.L 6 K.NLVDPFVEVSFAGK.M 7 R.THHLSQITEAALALK.L 8 K.TDEETEDPSVIGEFK.G
VAMP8	NP_003752	VAMP 8	1 K.NIMTQNVER.I 2 R.NKTEDLEATSEHFK.T	1 K.NIMTQNVER.I 2 R.NKTEDLEATSEHFK.T 3 R.NLQSEVEGVK.N 4 K.TEDLEATSEHFK.T	

Redox Proteins

Entrez Gene	Entrez Protein	Protein Name	Peptide Sequences Detected		
			1st Identification	2nd Identification	3rd Identification
DHRS8	NP_057329	Dehydrogenase/reductase member 8	1 K.NPSTSLGPTLEPEEVVNR.L	1 K.NPSTSLGPTLEPEEVVNR.L	
CYBB	NP_000388	gp91-phox	1 R.GVHFIFNK.E 2 K.LLGSALALAR.A 3 K.MEVGQYIFVK.C 4 R.VNNSDPYSVALSELGDR.Q	1 R.GVHFIFNK.E 2 R.GVHFIFNKENF.- 3 K.TLYGRPNWDNEFK.T	1 K.DVITGLK.Q 2 R.GVHFIFNK.E 3 R.VNNSDPYSVALSELGDR.Q
GAPD	NP_002037	Glyceraldehyde-3-phosphate dehydrogenase	1 K.LISWYDNEFGYSNR.V	1 R.GALQNIIPASTGAAK.A 2 K.LVINGNPITIFQER.D 3 K.VGVNGFGR.I	1 R.GALQNIIPASTGAAK.A 2 K.LVINGNPITIFQER.D
CYBA	NP_000092	p22-phox	1 R.ERPQIGGTIK.Q 2 R.KKPSEEEAAAAAGGPPGGPQVN PIPVTDEVV.- 1 K.VGDAIPAVEVFEGEPGNKVNLAEL FK.G	1 R.ERPQIGGTIK.Q	1 R.KKPSEEEAAAAAGGPPGGPQVN PIPVTDEVV.-
PRDX5	NP_036226	Peroxiredoxin 5 precursor		1 K.THLPGFVEQAEALK.A	

Other Proteins

Entrez Gene	Entrez Protein	Protein Name	Peptide Sequences Detected		
			1st Identification	2nd Identification	3rd Identification
B3GTL	NP_919299	β 3-glycosyltransferase-like	1 R.IQIPKLLETLR.R	1 R.IQIPKLLETLR.R	
C9orf19	NP_071738	C9orf19, glioma pathogenesis-related protein	1 K.ASASDGSSFVVAR.Y 2 R.EAQQYSEALASTR.I	1 K.ASASDGSSFVVAR.Y	
C20orf3	NP_065392	C20 ORF 3; adipocyte plasma membrane-associated	1 K.GLFEVNPWK.R 2 K.LLLSSETPIEGK.N	1 R.RPLRPQVVTDDDGQAPEAK.D	
EP300	NP_001420	E1A binding protein p300	1 R.LQEWYKK.M	1 R.LQEWYKK.M	
GALIG	NP_919308	Galectin-3 internal gene	1 K.LEPCFSSSRFGKKAR.Q	1 K.LEPCFSSSRFGKKAR.Q	
GCA	NP_036330	Grancalcin	1 K.ENFMTVDQDGSGTVEHHELR.Q	2 K.ENFMTVDQDGSGTVEHHELR.Q	
HIST1H4I	NP_003486	Histone H4	1 R.DNIQGITKPAIR.R 2 R.ISGLIYEETR.G 3 K.RISGLIYEETR.G 4 K.VFLENVIR.D	1 R.ISGLIYEETR.G 2 K.VFLENVIR.D	1 K.VFLENVIR.D
HSPA5	NP_005338	Hsp70 5A	1 K.ELEEIVQPIISK.L	1 K.ELEEIVQPIISK.L	1 R.IINEPTAAAIAYGLDK.R
TMEM30A	NP_060717	Hypothetical protein FLJ10856, transmembrane protein 30A	1 K.FRNPPGGDNLEER.F	1 R.KSDLHPTLPAGR.Y	
LOC199675	NP_777578	Hypothetical protein LOC199675	1 R.GWDSVQQSITMVR.S	1 R.GWDSVQQSITMVR.S 2 K.NQGAHDPDYENITLAFK.N	1 R.GWDSVQQSITMVR.S 2 R.LETTLAGIK.N
PHB	NP_002625	Prohibitin	1 R.FDAGELITQR.E	1 R.FDAGELITQR.E	
PKM2	NP_002645 NP_872270 NP_872271	Pyruvate kinase 3 isoform	1 K.GADFLVTEVENGGSLGSK.K	1 K.GVNLPGAAVDLPAVSEK.D	
S100A8	NP_002955	MRP-8	1 K.ALNSIIDVYHK.Y 2 K.GADVWFK.E 3 K.GNFHAVYR.D	1 K.ALNSIIDVYHK.Y	1 K.ALNSIIDVYHK.Y
S100A9	NP_002956	MRP-14	1 K.LGHPDTLNQGEFK.E 2 R.NIETIINTFHQYSVK.L	1 K.LGHPDTLNQGEFK.E 2 R.NIETIINTFHQYSVK.L 3 K.VIEHIMEDLDTNADK.Q	1 K.VIEHIMEDLDTNADK.Q
LOC388015	XP_370776	Similar to RTI1	1 R.NFIEFVFPYR.H	1 R.NFIEFVFPYR.H	
RPS27A UBB UBA52 UBC	NP_002945 NP_061828 NP_003324 NP_066289	Ubiquitin precursor	1 K.TITLEVEPSDTIENVK.A 2 R.TLSDYNIQK.E	1 K.ESTLHLVLR.L 2 K.TITLEVEPSDTIENVK.A 3 R.TLSDYNIQK.E	1 K.TITLEVEPSDTIENVK.A 2 R.TLSDYNIQK.E

AZUROPHIL GRANULES

Receptors and Membrane Anchors

Entrez Gene	Entrez Protein	Protein Name	Peptide Sequences Detected		
			1st Identification	2nd Identification	3rd Identification
CD63	NP_001771	CD63, LAMP-3	1 K.VMSEFNNNFR.Q	1 K.VMSEFNNNFR.Q	
ITGB5	NP_002204	Integrin β 5	1 R.LGFGSFVDK.D	1 R.LGFGSFVDK.D	
TM7SF3	NP_057635	Seven transmembrane receptor	1 R.VTNILDPSYHIPPLR.E	1 R.VTNILDPSYHIPPLR.E	

STOM	NP_004090	Stomatin	1 R.AKVIAAEGEMNASR.A 2 R.DSEAQRLPDSFKDSPSK.G 3 K.EASMVITESPAALQLR.Y 4 R.LLAQTTLR.N 5 K.VIAAEGEMNASR.A 6 R.VQNATLAVANITNADSATR.L	1 R.AKVIAAEGEMNASR.A 2 R.ALKEASMVITESPAALQLR.Y 3 K.EASMVITESPAALQLR.Y 4 K.VIAAEGEMNASR.A	1 R.AKVIAAEGEMNASR.A 2 R.ALKEASMVITESPAALQLR.Y 3 K.EASMVITESPAALQLR.Y 4 R.LPDSFKDSPSK.G 5 K.NLSQILSDR.E 6 K.NLSQILSDREEIAHNMQSTLDDATDAWGIK.V 7 K.NLSQILSDREEIAHNMQSTLDDATDAWGIKVER.V 8 R.TISFDIPPQEILTK.D 9 K.VIAAEGEMNASR.A 10 R.VQNATLAVANITNADSATR.L 11 R.YLQTLTTIAAEK.N
STOML3	NP_660329	Stomatin-like	1 R.IPVQLQR.S	1 R.IPVQLQR.S	

Channels and Transporters

Entrez Gene	Entrez Protein	Protein Name	Peptide Sequences Detected		
			1st Identification	2nd Identification	3rd Identification
ATP6V0D1	NP_004682	ATPase, H+ transporting, lysosomal, V0 subunit D, isoform 1	1 K.LLFEGAGSNPGDK.T	1 K.LLFEGAGSNPGDK.T	
TCIRG1	NP_006010	ATPase, H+ transporting, 116kD, vacuolar, T cell imune regulator	1 R.AGLVLPPPK.G 2 R.LGALQQLQQQSQELQEVLGETER.F 3 R.TPLLQAPGGPHQDLR.V 4 R.VLQLLPPGQVQVHK.M 5 R.VNFVAGAVEPHK.A	1 R.AGLVLPPPK.G 2 R.LGALQQLQQQSQELQEVLGETER.F 3 R.TPLLQAPGGPHQDLR.V 4 R.VLQLLPPGQVQVHK.M 5 R.VNFVAGAVEPHK.A	
ATP8A1	NP_006086	Aminophospholipid trasporter ATPase	1 K.HLEQFATEGLR.T 2 K.IIYQAASPDEGALVR.A 3 K.LQDQVPETIETLMK.A 4 K.NLQLLGATAIEDK.L 5 R.NTQWVHGIVVYTGHDTK.L 6 R.QGLPATSDIKDVDSLMR.I 7 K.SQDPGAVVLGK.S 8 R.TSNLNEELGQVK.Y	1 K.HLEQFATEGLR.T 2 K.IIYQAASPDEGALVR.A 3 K.LQDQVPETIETLMK.A 4 K.NLQLLGATAIEDK.L 5 R.NTQWVHGIVVYTGHDTK.L 6 R.QGLPATSDIKDVDSLMR.I 7 K.SQDPGAVVLGK.S 8 R.TSNLNEELGQVK.Y	
VAT1	NP_006364	Vesicle amine transport protein 1	1 K.GVDIVMDPLGGSDTAK.G 2 K.VVTYGMANLLTGPK.R	1 K.GVDIVMDPLGGSDTAK.G 2 K.GYNLLKPMGK.V 3 R.LPPLPVTPGMEGAGVVIAVGEGVSDR.K 4 K.TEAASDPQHPAASEGAAAAAASPPLLR.C 5 R.TVENVTVFGTASASK.H 6 K.VLLVPGPEK.E 7 K.VLLVPGPEKEN.- 8 K.VVTYGMANLLTGPK.R	

GTP-ases

Entrez Gene	Entrez Protein	Protein Name	Peptide Sequences Detected		
			1st Identification	2nd Identification	3rd Identification
CDC42	NP_001782	CDC42	1 K.NVFDEAILAALEPPEPK.K	1 K.NVFDEAILAALEPPEPK.K	
GNAI2	NP_002061	Gi α2	1 R.IAQSDYIPTQQDVLR.T	1 R.IAQSDYIPTQQDVLR.T	1 K.AMGNLQIDFADPSR.A 2 R.IAQSDYIPTQQDVLR.T
GNB1 GNB2	NP_002065 NP_005264	G β 1,2	1 K.IYAMHWGTDSR.L	1 K.IYAMHWGTDSR.L	
RAB27A	NP_004571 NP_899057 NP_899058 NP_899059	RAB27A	1 R.IHLQLWDTAGQER.F	1 R.IHLQLWDTAGQER.F	1 K.FLALGDSGVGK.T 2 R.IHLQLWDTAGQER.F 3 R.VVKEEEAIALAEK.Y
RAP1A RAP1B	NP_002875 NP_056461	RAP1	1 K.INVNEIFYDLVR.Q	1 K.INVNEIFYDLVR.Q 2 K.LVVLGSGGVGK.S	1 K.INVNEIFYDLVR.Q 2 K.LVVLGSGGVGK.S
RAB1A	NP_004152	RAB1A	1 K.NATNVEQSFMTMAAEIK.K	1 K.NATNVEQSFMTMAAEIK.K	1 K.NATNVEQSFMTMAAEIK.K
RAB1B	NP_112243	RAB1B	1 K.NATNVEQAFMTMAAEIK.K	1 K.NATNVEQAFMTMAAEIK.K	
RAB3A RAB3B RAB3C	NP_002857 NP_002858 NP_612462	RAB3	1 K.ILIIGNSSVGK.T	1 K.LQIWDTAGQER.Y	

Structural Proteins and Adaptors

Entrez Gene	Entrez Protein	Protein Name	Peptide Sequences Detected		
			1st Identification	2nd Identification	3rd Identification
ACTA1 ACTA2	NP_001091 NP_001604	Actin, alpha	1 K.EITALAPSTMK.I 2 R.HQGVMVGMGQK.D	1 R.DLTDYLMK.I 2 R.HQGVMVGMGQK.D	
ACTB ACTG1	NP_001092 NP_001605	Actin, beta or gamma	1 R.GYSFTTTAER.E 2 K.QEYDESGPSIVHR.K 3 R.TTGIVMDSGDGVTHTVPIYEGYALPHAILR.L 4 R.VAPEEHPVLLTEAPLNPK.A	1 R.TTGIVMDSGDGVTHTVPIYEGYALPHAILR.L 2 R.VAPEEHPVLLTEAPLNPK.A	
HCLS1	NP_005326	Hematopoietic lineage cell-specific protein 1	1 K.KISSEAWPPVGTPPSSESEPVR.T	1 K.KISSEAWPPVGTPPSSESEPVR.T	
MYH9	NP_002464	Myosin heavy chain	1 K.DFSALESQLQDTQELLQEENRQK.L 2 K.LQVELDNVTGLLSQSDSK.S 3 R.QLLQANPILEAFGNAK.T 4 R.RGDLPFVVPR.R	1 K.ANLQIDQINTDLNLER.S 2 K.DFSALESQLQDTQELLQEENRQK.L 3 R.ELEDATETADAMNR.E 4 R.GDLPFVVPR.R 5 K.HSQAVEELAEQLEQTKR.V 6 K.LTKDFSALESQLQDTQELLQEENR.Q 7 R.RGDLPFVVPR.R 8 K.TELEDTLDSTAAQQELR.S 9 K.TLEEEAKTHEAQIQEMR.Q	1 K.DFSALESQLQDTQELLQEENRQK.L 2 R.VISGVLQLGNIVFK.K
TUBB2	NP_001060	Tubulin, beta 3	1 R.SGPFGQIFRPDNFVFGQSGAGNNWAK.G	1 R.SGPFGQIFRPDNFVFGQSGAGNNWAK.G	1 R.AILVDLEPGTMDSVR.S 2 R.SGPFGQIFRPDNFVFGQSGAGNNWAK.G
VIM	NP_003371	Vimentin	1 K.FADLSEAANR.N 2 K.ILLAELEQLK.G 3 K.ILLAELEQLKGQGK.S 4 K.NLQEAEEWYK.S 5 R.TNEKVELQELNDRFANYIDK.V	1 K.FADLSEAANR.N	
ZYX	NP_003452	Zyxin	1 K.VNPFRPGDSEPPPAPGAQR.A	1 K.VNPFRPGDSEPPPAPGAQR.A	

Kinases and Phosphatases

Entrez Gene	Entrez Protein	Protein Name	Peptide Sequences Detected		
			1st Identification	2nd Identification	3rd Identification
PTPRC	NP_002829 NP_563578 NP_563579	Protein tyrosine phosphatase, receptor type C	1 K.KRDPPSEPSPLEAEFQR.L 2 K.RDPPSEPSPLEAEFQR.L	1 K.KRDPPSEPSPLEAEFQR.L	

Luminal and Host Defense Proteins

Entrez Gene	Entrez Protein	Protein Name	Peptide Sequences Detected		
			1st Identification	2nd Identification	3rd Identification
AZU1	NP_001691	Azurocidin 1 preproprotein	1 R.QFPPLASIQNQGR.H	1 R.QFPPLASIQNQGR.H	
BPI	NP_001716	Bactericidal/permeability-increasing protein prec.	1 K.FFGTFLPEVAK.K 2 K.GHYSFYSMDIR.E 3 K.GLDYASQGGTAALQK.E 4 R.IKIPDYSDSFK.I 5 K.LQPYFQTLPVMTK.I 6 R.LTTKFFGTFLPEVAK.K 7 R.LVGELKLDR.L	1 K.FFGTFLPEVAK.K 2 K.GHYSFYSMDIR.E 3 K.GLDYASQGGTAALQK.E 4 R.IKIPDYSDSFK.I	1 R.EFQLPSSQISMVPNVGLK.F 2 K.FFGTFLPEVAK.K 3 K.FSISNANIK.I 4 K.GHYSFYSMDIR.E 5 K.GLDYASQGGTAALQK.E 6 K.IDSVAGINYGLVAPPATTAETLDV QMK.G 7 R.IKIPDYSDSFK.I 8 R.LLLELK.H 9 R.LVGELKLDR.L 10 K.VGWLIQLFHK.K 11 R.VQLYNVVLQPHQNFLLFGADVVYK.-
PPGB	NP_000299	Cathepsin A	1 K.YGDSGEQIAGFVK.E	1 K.HLHYWFVESQK.D 2 K.YGDSGEQIAGFVK.E	
CTSC	NP_001805	Cathepsin C (dipeptidyl-peptidase I)	1 K.NSWGTGWGENGYFR.I 2 R.NVHGINFVSPVR.N	1 K.NSWGTGWGENGYFR.I 2 R.NVHGINFVSPVR.N	
CTSG	NP_001902	Cathepsin G preproprotein	1 R.IFGSYDPR.R 2 R.NRNVNPVALPR.A 3 K.SSGVPPEVFTR.V 4 R.TIQNDIMLLQLSR.R 5 R.VSSFLPWIR.T	1 R.IFGSYDPR.R 2 R.IFGSYDPRR.Q 3 R.NVNPVALPR.A 4 K.SSGVPPEVFTR.V 5 K.SSGVPPEVFTRVSSFLPWIR.T 6 R.TIQNDIMLLQLSR.R 7 R.VSSFLPWIR.T	1 R.IFGSYDPR.R 2 R.IFGSYDPRR.Q 3 R.NRNVNPVALPR.A 4 R.NVNPVALPR.A 5 K.SSGVPPEVFTR.V 6 R.TIQNDIMLLQLSR.R 7 R.VSSFLPWIR.T
DPP7	NP_037511	Dipeptidyl peptidase 7 preproprotein	1 R.APDPGFQER.F 2 R.LDHFNFER.F	1 R.ASHPEDPASVVEAR.K 2 R.LDHFNFER.F	1 R.ASHPEDPASVVEAR.K 2 K.DLFLQGAYDTVR.W 3 R.LDHFNFER.F
ELA2	NP_001963	Elastase 2	1 R.VVLGAHNLSR.R	1 R.REPTRQVFAVQR.I	
EPX	NP_000493	Eosinophil peroxidase	1 R.IGLDLAALNMQR.S 2 R.IVYEGGIDPILR.G 3 K.LNRQDAMLVDELR.D 4 K.LNRQDAMLVDELRDR.L 5 R.NGFLLPLVR.A 6 R.QDAMLVDELR.D 7 R.RIGLDLAALNMQR.S 8 R.RNGFLLPLVR.A 9 R.RPLLGASNQALAR.W 10 R.TNYLGLLAINQR.F 11 R.WNGDKLYNEAR.K	1 R.IGLDLAALNMQR.S 2 R.IVYEGGIDPILR.G 3 R.NGFLLPLVR.A 4 R.QDAMLVDELR.D	1 R.ASAPNSHVPLSSAFFASWR.I 2 R.DFLPLVLGK.A 3 R.FGHTMLQPFMFR.L 4 R.IGLDLAALNMQR.S 5 R.IVYEGGIDPILR.G 6 K.LNRQDAMLVDELR.D 7 R.NGFLLPLVR.A 8 R.QDAMLVDELR.D 9 R.RIGLDLAALNMQR.S 10 R.RNGFLLPLVR.A 11 R.RPLLGASNQALAR.W 12 R.TNYLGLLAINQR.F 13 R.VANVFTLAFR.F 14 R.WNGDKLYNEAR.K
FTL	NP_000137	Ferritin, light polypeptide	1 R.LGGPEAGLGEYLFER.L	1 R.LGGPEAGLGEYLFER.L 2 K.LNQALLDLHALGSAR.T	
GGH	NP_003869	Gamma-glutamyl hydrolase precursor	1 K.NLDGISHAPNAVK.T 2 K.TAFYLAEFFVNEAR.K	1 K.TAFYLAEFFVNEAR.K	1 K.NLDGISHAPNAVK.T 2 K.TAFYLAEFFVNEAR.K
MMP9	NP_004985	Gelatinase	1 R.KLDSVFEEPLSK.K 2 K.KLFFFSGR.Q 3 R.QLAEEYLYR.Y 4 K.QLSLPETGELDSATLK.A 5 R.QVWVVTGASVLGPR.R 6 K.SLGPALLLLQK.Q	1 R.KLDSVFEEPLSK.K 2 K.QLSLPETGELDSATLK.A	1 R.GSRPQGPFLIADK.W 2 R.KLDSVFEEPLSK.K 3 K.QLSLPETGELDSATLK.A 4 R.QSTLVLFPGDLR.T 5 K.SLGPALLLLQK.Q
GUSB	NP_000172	Glucuronidase, beta	1 R.GFEEQWYR.R	1 K.SLLEQYHLGLDQK.R	
CAMP	NP_004336	hCAP-18	1 R.FALLGDFFR.K 2 R.FALLGDFFRK.S	1 R.FALLGDFFRK.S	1 R.FALLGDFFR.K
HEXA	NP_000511	Hexosaminidase A preproprotein	1 R.ALLSAPWYLNR.I 2 R.ISYGPDWKDFYVVEPLAFEGTP EQK.A	1 R.ALLSAPWYLNR.I 2 R.ISYGPDWKDFYVVEPLAFEGTP EQK.A,A	
HEXB	NP_000512	Hexosaminidase B preproprotein	1 R.VLPEFDTPGHTLSWGK.G	1 K.KLESFYIQK.V 2 K.LAPGTIVEVWKDSAYPEELSR.V 3 R.VLPEFDTPGHTLSWGK.G	
HYAL3	NP_003540	Hyaluronidase 3	1 K.NQLGLYPYFGPR.G	1 K.NQLGLYPYFGPR.G	
LTF	NP_002334	Lactoferrin	1 K.DLLFKDSAIGFSR.V 2 K.DSAIGFSR.V 3 K.EDAIWNLLR.Q 4 K.FQLFGSPSGQK.D 5 K.FQLFGSPSGQKDLLFK.D 6 K.KGGSFQLNELQGLK.S 7 R.SVNGKEDAIWNLLR.Q	1 K.FQLFGSPSGQK.D 2 K.FQLFGSPSGQKDLLFK.D 3 K.KGGSFQLNELQGLK.S 4 R.SVNGKEDAIWNLLR.Q	1 R.DGAGDVAFIR.E 2 K.EDAIWNLLR.Q 3 K.FQLFGSPSGQK.D 4 K.GGSFQLNELQGLK.S 5 K.KGGSFQLNELQGLK.S 6 K.LRPVAAEVYGTER.Q 7 R.RSDTSLTWNSVK.G 8 R.SVNGKEDAIWNLLR.Q
CST7	NP_003641	Leukocystatin; Cystatin	1 K.TNDPGVLQAAR.Y	1 K.TNDPGVLQAAR.Y	
LCN2	NP_005555	Lipocalin 2; NGAL	1 K.ELTSELKENFIR.F 2 K.VPLQQNFQDNQFQGK.W	1 K.VPLQQNFQDNQFQGK.W	1 K.ELTSELKENFIR.F 2 K.VPLQQNFQDNQFQGK.W
ACP6	NP_057445	Lysophosphatidic acid phosphatase	1 K.VGMQQMFALGER.L	1 K.VGMQQMFALGER.L	
ACP2	NP_001601	Lysosomal acid phosphatase 2	1 K.TYPKDPYQEEEWPQGFGQLTK.E	1 K.TYPKDPYQEEEWPQGFGQLTK.E	
GAA	NP_000143	Lysosomal alpha-glucosidase	1 R.VTSEGAGLQLQK.V	1 R.AGYIIPLQGPGLTTTESR.Q 2 R.APSPLYSVEFSEEPFGVIVHR.Q 3 R.VTSEGAGLQLQK.V	
LYZ	NP_000230	Lysozyme precursor	1 R.ATNYNAGDRSTDYGIFQINSR.Y 2 R.LGMDGYR.G 3 K.RLGMDGYR.G 4 R.STDYGIFQINSR.Y 5 K.WESGYNTR.A	1 R.ATNYNAGDRSTDYGIFQINSR.Y 2 R.LGMDGYR.G 3 K.RLGMDGYR.G 4 R.STDYGIFQINSR.Y	1 R.STDYGIFQINSR.Y
MAN2B1	NP_000519	Mannosidase, alpha B, lysosomal	1 R.DGSLELMVHR.R 2 R.DLFSTFTITR.L 3 K.ELVDYFLNVATAQGR.Y 4 R.LQETTLVANQLR.E	1 R.GVSEPLMENGSGAWVR.G	1 R.ASTSLKPPTADLFTGVLPNGYNP PR.N 2 R.DGSLELMVHR.R 3 K.ELVDYFLNVATAQGR.Y

MPO	NP_000241	Myeloperoxidase	1 R.DHGLPGYNAWR.R 2 R.FPTDQLTPDQER.S 3 R.IANVFTNAFR.Y 4 R.IGLDLPALNMQR.S 5 R.NQINALTSFVDASMVYGSEEPLAR.N 6 R.QNQIAVDEIR.E 7 R.VVLEGGIDPILR.G 8 R.WLPAEYEDGFSLPYGWTPGVKR.N	1 R.AVSNEIVRFPTDQLTPDQER.S 2 R.FPTDQLTPDQER.S 3 R.IANVFTNAFR.Y 4 R.IGLDLPALNMQR.S 5 R.NQINALTSFVDASMVYGSEEPLAR.N 6 R.VVLEGGIDPILR.G 7 R.WLPAEYEDGFSLPYGWTPGVKR.N 8 R.YGHTLIQPFMFR.L	1 R.AVSNEIVRFPTDQLTPDQER.S 2 R.DHGLPGYNAWR.R 3 R.DYLPLVLGPTAMR.K 4 R.FPTDQLTPDQER.S 5 R.IANVFTNAFR.Y 6 R.IGLDLPALNMQR.S 7 R.KLMEQYGTPNNIDIWMGGVSEPLK.R 8 K.LMEQYGTPNNIDIWMGGVSEPLK.R 9 K.LMEQYGTPNNIDIWMGGVSEPLKR.K 10 R.NQINALTSFVDASMVYGSEEPL AR.N 11 R.QNQIAVDEIR.E 12 R.SRDHGLPGYNAWR.R 13 R.VVLEGGIDPILR.G 14 R.WLPAEYEDGFSLPYGWTPGVK.R 15 R.WLPAEYEDGFSLPYGWTPGVKR.N
PRTN3	NP_002768	Proteinase 3	1 R.LVNVVLGAHNVR.T 2 R.TQEPTQQHFSVAQVFLNNYDAENK.L	1 R.LVNVVLGAHNVR.T 2 R.TQEPTQQHFSVAQVFLNNYDAENK.L	
PRG2	NP_002719	Proteoglycan 2	1 R.FQWVDGSR.W 2 R.RFQWVDGSR.W	1 R.GNLVSIHNFNINYR.I 2 R.RFQWVDGSR.W 3 R.WNFAYWAAHQPWSR.G	
TPP1	NP_000382	Tripeptidyl-peptidase I	1 R.LFGGNFAHQASVAR.V	1 R.LYQQHGAGLFDVTR.G	1 R.LFGGNFAHQASVAR.V 2 R.LYQQHGAGLFDVTR.G

Membrane Traffic and Fusion Proteins

Entrez Gene	Entrez Protein	Protein Name	Peptide Sequences Detected		
			1st Identification	2nd Identification	3rd Identification
SYTL1	NP_116261	Synaptotagmin-like 1	1 K.ILTGDWFQEAR.S	1 K.ILTGDWFQEAR.S	
C20orf178	NP_789782	Snf7 homologue associated with Alix 1	1 R.EALENANTNTEVLK.N 2 K.GGPTPQEAIQR.L	1 R.LRDTEEMLSK.K	
STX7	NP_003560	Syntaxin 7	1 R.TLNQLGTPQDSPELR.Q	1 R.TLNQLGTPQDSPELR.Q	1 R.TLNQLGTPQDSPELR.Q
VAMP8	NP_003752	VAMP 8	1 K.NIMTQNVER.I 2 R.NKTEDLEATSEHFK.T 3 R.NLQSEVEGVK.N	1 K.NIMTQNVER.I	1 K.NIMTQNVER.I 2 R.NKTEDLEATSEHFK.T

Redox Proteins

Entrez Gene	Entrez Protein	Protein Name	Peptide Sequences Detected		
			1st Identification	2nd Identification	3rd Identification
PDIA3	NP_005304	Grp58	1 R.TADGIVSHLK.K	1 R.FLQDVFDGNLKR.Y 2 R.KTFSHELSDFGLESTAGEIP VVAIR.T 3 K.MDATANDVPSPYEVR.G	
CYBB	NP_000388	gp91-phox	1 R.GVHFIFNKENF.- 2 K.TLYGRPNWDNEFK.T	1 K.TLYGRPNWDNEFK.T	1 R.GVHFIFNKENF.- 2 K.TLYGRPNWDNEFK.T

Other Proteins

Entrez Gene	Entrez Protein	Protein Name	Peptide Sequences Detected		
			1st Identification	2nd Identification	3rd Identification
C9orf19	NP_071738	C9orf19, glioma pathogenesis-related protein	1 R.YFPAGNVVNEGFFEENVLPPKK.-	1 K.ASASDGSSFVVAR.Y 2 R.YFPAGNVVNEGFFEENVLPPKK.-	
DDX4	NP_061912	DEAD (Asp-Glu-Ala-Asp) box polypeptide 4	1 R.ELVNQIYLEAR.K	1 R.ELVNQIYLEAR.K	1 R.ELVNQIYLEAR.K
HCLS1	NP_005326	Hematopoietic cell-specific Lyn substrate 1	1 K.KISSEAWPPVGTPPSSESEPVR.T	1 K.KISSEAWPPVGTPPSSESEPVR.T	
HIST1H1C	NP_005310	Histone H1 family	1 K.ALAAAGYDVEK.N	1 K.ALAAAGYDVEK.N 2 K.ALAAAGYDVEKNNSR.I	
HIST1H2BG	NP_003509	Histone H2B	1 K.AMGIMNSFVNDIFER.I 2 K.VLKQVHPDTGISSK.A	1 K.AMGIMNSFVNDIFER.I	
HIST1H4I	NP_003486	Histone H4	1 K.VFLENVIR.D	1 R.ISGLIYEETR.G	
ARL10B	NP_620150	Hypothetical protein BC015408	1 R.DLPGALDEKELIEK.M 2 K.LWDIGGQPR.F	1 R.DLPGALDEKELIEK.M 2 K.LWDIGGQPR.F	
TMEM30A	NP_060717	Hypothetical protein FLJ10856	1 R.KSDLHPTLPAGR.Y	1 K.FRNPPGGDNLEER.F	1 K.FRNPPGGDNLEER.F 2 R.KSDLHPTLPAGR.Y
FLJ22662	NP_079105	Hypothetical protein FLJ22662	1 K.LGLDYSYDLAPR.A 2 K.TTGWGILEIR.A	1 K.LGLDYSYDLAPR.A	
SQSTM1	NP_003891	Sequestosome 1	1 R.AGEARPGPTAESASGPSEDPSVN FLK.N	1 R.AGEARPGPTAESASGPSEDPSVN FLK.N	
TOLLIP	NP_061882	Toll-interacting protein	1 R.GNKDAAINSLLQMGEEP.- 2 R.GPVYIGELPQDFLR.I	1 R.GPVYIGELPQDFLR.I	1 R.GPVYIGELPQDFLR.I
RPS27A UBB UBA52 UBC	NP_002945 NP_061828 NP_003324 NP_066289	Ubiquitin precursor	1 K.IQDKEGIPPDQQR.L 2 K.TITLEVEPSDTIENVK.A 3 K.TLTGKTITLEVEPSDTIENVK.A	1 K.TITLEVEPSDTIENVK.A 2 K.TITLEVEPSDTIENVKAK.I	1 K.ESTLHLVLR.L 2 -.MQIFVK.T 3 K.TITLEVEPSDTIENVK.A

The table lists the peptides used to identify proteins in at least two of three 2D-HPLC ESI-MS/MS experiments. Proteins with corresponding gene and protein designation are listed according to the literature-based functional classification for each granule subset, as described in Table 3.

Supplementary Table 2

Peptides used for identification of proteins from a single 2D-HPLC ESI-MS/MS Experiment

GELATINASE GRANULES				
Receptors and Membrane Anchors				
Entrez Gene	**Entrez Protein**	**Protein Name**	**Peptides Detected**	**% Coverage**
ITGB5	NP_002204	Integrin, β 5	1 R.LGFGSFVDK.D	1.13

Channels and Transporters				
Entrez Gene	**Entrez Protein**	**Protein Name**	**Peptides Detected**	**% Coverage**
MVP	NP_059447 NP_005106	Major vault protein	1 R.LAQDPFPLYPGEVLEK.D	1.79

GTPases				
Entrez Gene	**Entrez Protein**	**Protein Name**	**Peptides Detected**	**% Coverage**
GNB1 GNB2	NP_002065 NP_005264	G β1,2	1 K.VHAIPLR.S	2.82

Structural Proteins				
Entrez Gene	**Entrez Protein**	**Protein Name**	**Peptides Detected**	**% Coverage**
CFL1	NP_005498 NP_068733 NP_619579	Cofilin 1	1 K.KEDLVFIFWAPESAPLK.S	10.24

Luminal and Host Defense Proteins				
Entrez Gene	**Entrez Protein**	**Protein Name**	**Peptides Detected**	**% Coverage**
FCN1	NP_001994	Ficolin 1 precursor	1 R.VDLVDFEGNHQFAK.Y	4.29
AZU1	NP_001691	Azurocidin 1 preproprotein	1 R.QFPFLASIQNQGR.H	5.18
OLFM4	NP_006409	GW112	1 R.LEFTAHVLSQK.F	2.16

Other Proteins				
Entrez Gene	**Entrez Protein**	**Protein Name**	**Peptides Detected**	**% Coverage**
ALB	NP_000468	Albumin	1 K.KVPQVSTPTLVEVSR.N	2.46
SEMG1	NP_002998 NP_937782	Semenogelin I	1 K.DIFSTQDELLVYNK.N 2 K.GHYQNVVEVR.E 3 R.KQGGSQSSYVLQTEELVANK.Q 4 R.KSQQYDLNALHK.T 5 R.LPSEFSQFPHGQK.G	10.14
SEMG2	NP_002999	Semenogelin II	1 K.DIFTTQDELLVYNK.N 2 K.DVSQSSISFQIEK.L 3 R.TQGGSQSSYVLQTEELVVNK.Q	7.27
TOLLIP	NP_061882	Toll-interacting protein	1 R.GPVYIGELPQDFLR.I	5.11
HCLS1	NP_005326	Hematopoietic cell-specific Lyn substrate 1	1 K.KISSEAWPPVGTPPSSESEPVR.T	4.53
HSPA1A	NP_005336	Hsp70 1A	1 K.HWPFQVINDGDKPK.V 2 K.NQVALNPQNTVFDAK.R	4.21

SPECIFIC GRANULES				
Receptors and Membrane Anchors				
Entrez Gene	**Entrez Protein**	**Protein Name**	**Peptides Detected**	**% Coverage**
DSG1	NP_001933	Desmoglein preproprotein	1 R.ISGVGIDQPPYGIFVINQK.T 2 K.YQGTILSIDDNLQR.T	3.15

FLOT1	NP_005794	Flotillin-1	1 K.LPQVAEEISGPLTSANK.I	3.98
HLA-A	NP_002107 NP_002108	HLA-A1	1 R.FIAVGYVDDTQFVR.F	3.84
ICAM3	NP_002153	ICAM-3 precursor	1 R.TFVLPVTPPR.L	1.83
ITGB5	NP_002204	Integrin, β 5	1 R.LGFGSFVDK.D	1.13
LAMP2	NP_002285 NP_054701	LAMP2	1 K.YLDFVFAVK.N	2.20
LAIR1	NP_002278 NP_068352 NP_068354	Leukocyte-associated Ig-like receptor 1	1 R.GPVGVQTFR.L 2 R.IDSVSEGNAGPYR.C	11.15
VNN1	NP_004657	Vanin 1	1 R.FGQTPVQER.L 2 K.MSENIPNEVYALGAFDGLHTVEGR	6.43
VNN2	NP_004656 NP_511043	Vanin 2	1 K.DNSIYVLANLGDK.K	2.78

Channels and Transporters				
Entrez Gene	**Entrez Protein**	**Protein Name**	**Peptides Detected**	**% Coverage**
ATP5F1	NP_001679	ATP synthase, H+ transporting, mitochondrial F0 complex, subunit b	1 R.HYLFDVQR.N	3.13
ATP5H	NP_006347	ATP synthase, H+ transporting, mitochondrial F0 complex, subunit d	1 R.LAALPENPPAIDWAYYK.A	10.56
TCIRG1	NP_006010	ATPase, H+ transporting, 116kD, vacuolar, T cell imune regulator	1 R.TPLLQAPGGPHQDLR.V	4.58
ATP6V0D1	NP_004682	ATPase, H+ transporting, lysosomal, V0 subunit D isoform 1	1 R.FFEHEVK.L	1.99
SLC25A24	NP_037518	Calcium-binding transporter	1 R.QLLAGGIAGAVSR.T	2.73
SLC25A3	NP_005879 NP_002626	Mitochondrial phosphate carrier precursor isoform 1a or 1b	1 R.LPRPPPPEMPESLK.K	3.87
PLSCR1	NP_066928	Phospholipid scramblase 1	1 R.EAFTDADNFGIQFPLDLDVK.M	6.29
HRNR	XP_373868	Similar to hornerin	1 R.GPYESGSGHSSGLGHR.E	2.26
VDAC1	NP_003365	Voltage-dependent anion channel 1	1 K.TDEFQLHTNVNDGTEFGGSIYQK.V	8.13
VDAC3	NP_005653	Voltage-dependent anion channel 3	1 K.AADFQLHTHVNDGTEFGGSIYQK.V 2 K.LTLDTIFVPNTGK.K	12.72

GTPases				
Entrez Gene	**Entrez Protein**	**Protein Name**	**Peptides Detected**	**% Coverage**
CDC42	NP_001782	Cdc42	1 K.NVFDEAILAALEPPEPK.K	1.4
RAB1A RAB1B	NP_004152 NP_112243	RAB1	1 K.EFADSLGIPFLETSAK.N	7.8
RAB2	NP_002856	RAB2	1 K.IQEGVFDINNEANGIK.I 2 K.TASNVEEAFINTAK.E	14.1
GNB1 GNB2	NP_002065 NP_005264	G β1,2	1 K.LIIWDSYTTNK.V	3.2

Structural Proteins				
Entrez Gene	**Entrez Protein**	**Protein Name**	**Peptides Detected**	**% Coverage**
PFN1	NP_005013	Profilin 1	1 K.STGGAPTFNVTVTK.T 2 K.TFVNITPAEVGVLVGK.D	21.4
VIM	NP_003371	Vimentin	1 R.EEAENTLQSFR.Q 2 R.FANYIDK.V 3 R.ISLPLPNFSSLNLR.E	8.8

Kinases and Phosphatases				
Entrez Gene	Entrez Protein	Protein Name	Peptides Detected	% Coverage
PTPN7	NP_002823NP_542155	Protein tyrosine phosphatase, non-receptor type 7	1 R.RGSNVALMLDVRSLGAVEPICSVNTPR.E	7.5

Luminal and Host Defense Proteins				
Entrez Gene	Entrez Protein	Protein Name	Peptides Detected	% Coverage
CHIT1	NP_003456	Chitotriosidase	1 R.FTTLVQDLANAFQQEAQTSGK.E	4.51
CALR	NP_004334	Calreticulin precursor	1 K.EQFLDGDGWTSR.W	2.88
ELA2	NP_001963	Elastase 2	1 R.VVLGAHNLSR.R	3.75
MMP25	NP_071913 NP_073209	Matrix metalloproteinase 25 (leukolysin)	1 R.DGLQQLYGK.A	1.6
ANPEP	NP_001141	Membrane alanine aminopeptidase	1 R.FSTEYELQQLEQFK.K	1.45
PADI4	NP_036519	Peptidyl arginine deiminase, type IV	1 R.ELGLAESDIIDIPQLFK.L 2 R.GPQTGGISGLDSFGNLEVSPPVTVR.G 3 K.LFQEQQNEGHGEALLFEGIK.K	9.35
THBS1	NP_003237	Thrombospondin 1 precursor	1 K.FQDLVDAVR.A 2 R.FQMIPLDPK.G 3 R.FTGSQPFGQGVEHATANK.Q 4 K.GGVNDNFQGVLQNVR.F 5 K.GPDPSSPAFR.I 6 R.IPESGGDNSVFDIFELTGAAR.K 7 R.KDHSGQVFSVVSNGK.A 8 K.MENAELDVPIQSVFTR.D 9 R.NALWHTGNTPGQVR.T	10.85

Membrane Traffic and Fusion Proteins				
Entrez Gene	Entrez Protein	Protein Name	Peptides Detected	% Coverage
DNAJC5	NP_079495	DnaJ (Hsp40) homolog, subfamily C, member 5	1 K.YHPDKNPDNPEAADK.F	7.58
STX7	NP_003560	Syntaxin 7	1 K.EFGSLPTTPSEQR.Q 2 R.LVAEFTTSLTNFQK.V 3 R.TLNQLGTPQDSPELR.Q	16.09
VAMP2	NP_004772 NP_055047	VAMP 2	1 R.ADALQAGASQFETSAAK.L	17.00

Redox Proteins				
Entrez Gene	Entrez Protein	Protein Name	Peptides Detected	% Coverage
PDIA3	NP_005304	Glucose regulated protein, 58kDa	1 K.VVVAENFDEIVNNENK.D	1.98

Other Proteins				
Entrez Gene	Entrez Protein	Protein Name	Peptides Detected	% Coverage
ALB	NP_000468	Albumin	1 K.VPQVSTPTLVEVSR.N	2.3
DSP	NP_004406	Desmoplakin	1 R.AELIVQPELK.Y 2 K.QQIQNDLNQWK.T 3 K.SAIYQLEEEYENLLK.A 4 K.SVQNDSQAIAEVLNQLK.D 5 R.TLELQGLINDLQR.E	2.3
FGB	NP_005132	Fibrinogen β chain preproprotein	1 K.DNENVVNEYSSELEK.H	3.05
RTN4	NP_065393 NP_722550 NP_008939 NP_997403 NP_997404	Reticulon 4	1 R.GPLPAAPPVAPER.Q	2.27-7.24
EHD1	NP_006786	Testilin	1 R.EHQISPGDFPSLR.K	2.43
PPIA	NP_066953 NP_982254 NP_982255	Cyclophilin A	1 K.VKEGMNIVEAMER.F	12.38

HCLS1	NP_005326	Hematopoietic cell-specific Lyn substrate 1	1 K.KISSEAWPPVGTPPSSESEPVR.T	4.53
HIST1H1C	NP_005310	Histone H1 family	1 K.ALAAAGYDVEK.N	5.16
HIST1H2BG	NP_003509	Histone H2B	1 K.AMGIMNSFVNDIFER.I 2 R.KESYSVYVYK.V 3 K.VLKQVHPDTGISSK.A	30.95

AZUROPHIL GRANULES

Receptors and Membrane Anchors

Entrez Gene	Entrez Protein	Protein Name	Peptides Detected	% Coverage
CANX	NP_001737	Calnexin	1 R.KIPNPDFFEDLEPFR.M	2.53
FLOT1	NP_005794	Flotilin	1 K.VSAQYLSEIEMAK.A	3.04
FCER1G	NP_004097	FCER1G gene product	1 K.SDGVYTGLSTR.N	12.79
LAMP2	NP_002285 NP_054701	LAMP2	1 K.YLDFVFAVK.N	2.20

GTPases

Entrez Gene	Entrez Protein	Protein Name	Peptides Detected	% Coverage
RAB3D	NP_004274	RAB3D	1 R.DAADQNFDYMFK.L	5.48

Structural Proteins and Adaptors

Entrez Gene	Entrez Protein	Protein Name	Peptides Detected	% Coverage
ANXA1	NP_000691	Annexin I, (lipocortin I)	1 K.GGPGSAVSPYPTFNPSSDVAALHK.A	6.94
FLNA	NP_001447	Filamin 1	1 K.AFGPGLQGGSAGSPAR.F	0.6
LCP1	NP_002289	L-plastin	1 K.VNDDIIVNWVNETLR.E	2.39
PFN1	NP_005013	Profilin 1	1 R.DSLLQDGEFSMDLR.T 2 K.TFVNITPAEVGVLVGK.D	21.43
TUBA1	NP_005991	Tubulin alpha 1	1 R.QLFHPEQLITGKEDAANNYAR.G 2 K.VGINYQPPTVVPGGDLAK.V	8.71

Luminal and Host Defense Proteins

Entrez Gene	Entrez Protein	Protein Name	Peptides Detected	% Coverage
CALR	NP_004334	Calreticulin precursor	1 R.FYALSASFEPFSNK.G 2 K.FYGDEEKDKGLQTSQDAR.F	7.67
CHIT1	NP_003456	Chitotriosidase	1 R.FTTLVQDLANAFQQEAQTSGK.E 2 R.FTTLVQDLANAFQQEAQTSGKER.L 3 K.RQEESGAAASLNVDAAVQQWLQK.G 4 R.VGAPATGSGTPGPFTK.E	13.3
OLFM4	NP_006409	GW112	1 R.LEFTAHVLSQK.F 2 K.LYVYNDGYLLNYDLSVLQKPQ.-	2.16
CTSZ	NP_001327	Cathepsin Z (X)	1 R.NVDGVNYASITR.N 2 R.VGDYGSLSGR.E	7.26
CRISP3	NP_006052	sgp-28, CRISP-3	1 K.MEWNKEAAANAQK.W	5.31

Membrane Traffic and Fusion Proteins

Entrez Gene	Entrez Protein	Protein Name	Peptides Detected	% Coverage
DNAJC5	NP_079495	DnaJ (Hsp40) homolog, subfamily C, member 5	1 K.EINNAHAILTDATK.R 2 K.YHPDKNPDNPEAADKFK.E	8.59
VAMP2	NP_004772 NP_055047	VAMP 2	1 R.LQQTQNQVDEVVDIMR.V	16.0

Redox Proteins

Entrez Gene	Entrez Protein	Protein Name	Peptides Detected	% Coverage
CYBA	NP_000092	p22-phox	1 R.KKPSEEEAAAAAGGPPGGPQVNPIPVTDEVV	5.13

Other Proteins				
Entrez Gene	Entrez Protein	Protein Name	Peptides Detected	% Coverage
PPIA	NP_066953 NP_982254 NP_982255	Cyclophilin A	1 K.VKEGMNIVEAMER.F	12.38
HSPA5	NP_005338	Hsp70 5A	1 K.DNHLLGTFDLTGIPPAPR.G 2 K.NQLTSNPENTVFDAK.R 3 K.SQIFSTASDNQPTVTIK.V 4 R.TWNDPSVQQDIK.F	9.48
S100A8	NP_002955	MRP-8	1 K.GADVWFK.E	7.53
S100A9	NP_002956	MRP-14	1 R.KDLQNFLK.K 2 K.LGHPDTLNQGEFK.E 3 K.LGHPDTLNQGEFKELVR.K 4 R.NIETIINTFHQYSVK.L	31.58

The table lists peptides used for protein identification from a given granule subset by only one 2D-HPLC ESI-MS/MS experiment, but identified by either 2DE or at least twice by 2D-HPLC ESI-MS/MS in another granule subset. Sequences of corresponding peptides and the percent coverage of proteins are shown.

Supplementary Table 3
Proteins Rejected as Granule Components

GELATINASE GRANULE REJECTED PROTEINS (349)		
Number of peptides	% coverage	Protein Name
1	7.42 %	1-acylglycerol-3-phosphate O-acyltransferase 1
1	2.88 %	6-phosphofructo-2-kinase/fructose-2,6-biphosphatase 3
1	1.07 %	a disintegrin and metalloprotease domain 10
1	3.55 %	AAA-ATPase TOB3
1	5.22 %	AAIR8193
2	5.18 %	acidic (leucine-rich) nuclear phosphoprotein 32 family, member B
1	3.46 %	aconitase 2
1	3.76 %	actin related protein 2/3 complex subunit 1B
1	1.58 %	acyl-CoA synthetase long-chain family member 1
1	1.83 %	acyl-Coenzyme A dehydrogenase, very long chain precursor
1	3.64 %	acyl-Coenzyme A oxidase
1	4.84 %	adenylyl cyclase-associated protein
1	2.65 %	aldehyde dehydrogenase 3A
1	3.85 %	aldolase A; fructose-bisphosphate aldolase
1	3.06 %	alkaline sphingomyelinase
1	1.55 %	alpha 1 type XI collagen preproprotein
2	6.15 %	amine oxidase (flavin-containing)
1	.88 %	amyotrophic lateral sclerosis 2 (juvenile) chromosome region, candidate 3
2	10.69 %	androgen-regulated short-chain dehydrogenase/reductase 1
1	5.53 %	angiopoietin-like 6; angiopoietin-related protein 5
1	4.56 %	apoptosis inhibitor 5; fibroblast growth factor 2-interacting factor 2
1	.61 %	ash1 (absent, small, or homeotic)-like
1	19.12 %	ATP synthase F0 subunit 8
1	10.14 %	ATP synthase, H+ transporting, mitochondrial F0 complex, subunit e
1	13 %	ATP synthase, H+ transporting, mitochondrial F0 complex, subunit g
1	3.59 %	ATP synthase, H+ transporting, mitochondrial F1 complex, beta polypeptide
1	1 %	ATPase, Class V, type 10A; ATPase type IV, phospholipid transporting (P-type)
1	1.92 %	ATPase, Class VI, type 11
1	1.42 %	ATP-binding cassette, sub-family A
1	1.08 %	ATP-binding cassette, sub-family B
1	.58 %	ATP-binding cassette, sub-family C
1	3.79 %	ATP-binding cassette, sub-family D
1	1.94 %	B-cell CLL/lymphoma 9
1	3.66 %	B-cell receptor-associated protein 31
1	2.21 %	beta 3-glycosyltransferase-like
1	2.18 %	beta adrenergic receptor kinase 1
1	2.27 %	beta-galactoside alpha-2,6-sialyltransferase II
1	4.09 %	bone marrow stromal cell antigen 1 precursor
1	2.52 %	calpain 1, large subunit
1	5.81 %	cAMP responsive element binding protein 1
1	17.59 %	cAMP responsive element modulator
3	12.32 %	carcinoembryonic antigen-related cell adhesion molecule 8
2	13.69 %	CD226 antigen; adhesion glycoprotein
1	4.41 %	cell death-regulatory protein GRIM19; CGI-39 protein
1	3.02 %	cell division cycle 2-like
1	4.31 %	cell division cycle associated 1
1	4.21 %	CG9886-like; glycerate kinase
1	10.14 %	CGI-141 protein
2	12.18 %	chemokine-like factor superfamily 5
1	13.89 %	chromosome 10 open reading frame 70
1	20.69 %	chromosome 14 open reading frame 2
1	2.7 %	chromosome 20 open reading frame 75
1	1.76 %	chromosome 5 open reading frame 7; putative zinc finger protein
1	2.09 %	chromosome 6 open reading frame 60
1	5.8 %	chromosome 9 open reading frame 77; CGI-67 protein
1	2.6 %	cisplatin resistance related protein CRR9p
1	.55 %	coagulation factor VIII isoform a precursor
2	2.32 %	coagulation factor XIII A1 subunit precursor
2	12.44 %	coated vesicle membrane protein
1	1.44 %	complement component 3 precursor
1	3.4 %	corneodesmosin precursor
1	2.68 %	COX15 homolog

1	3.85 %	CTD
1	.67 %	CUB and Sushi multiple domains 1
1	3.5 %	cytochrome b reductase 1
1	23.29 %	cytochrome b5 outer mitochondrial membrane precursor
3	21.3 %	cytochrome c oxidase subunit IV isoform 1 precursor
2	4.04 %	cytochrome P450, family 4
1	2.2 %	cytoskeleton associated protein 2
2	10.64 %	cytoskeleton related vitamin A responsive protein
1	3.2 %	DEK oncogene (DNA binding)
1	10.5 %	delta sleep inducing peptide, immunoreactor isoform 1
2	1.19 %	desmocollin 1
1	1.82 %	diaphanous 2
1	3.09 %	dihydrolipoamide S-succinyltransferase
1	1.04 %	dipeptidylpeptidase VI isoform 1
1	1.95 %	DKFZP434D146 protein
3	11.46 %	DKFZP564J0863 protein
1	6.15 %	DKFZP586A0522 protein
1	3.02 %	Dok-like protein
2	4.82 %	dolichyl-diphosphooligosaccharide-protein glycosyltransferase
1	.5 %	dynein, cytoplasmic, heavy polypeptide 1
1	.85 %	early endosome antigen 1, EEA1
2	6.25 %	ecotropic viral integration site 2B
1	2.26 %	elastin microfibril interfacer 1
1	3 %	electron transfer flavoprotein, alpha polypeptide
2	4.55 %	endothelin converting enzyme 1
3	8.01 %	eukaryotic translation elongation factor 1
1	1 %	fatty acid synthase
1	2.12 %	fibroblast growth factor receptor 4
1	4.49 %	FK506-binding protein 8; FK506-binding protein 8 (38kD)
1	4.03 %	flavin containing monooxygenase 2
1	2.65 %	FLJ20160 protein
1	8.1 %	FLJ44290 protein
1	7.14 %	frataxin
1	2.95 %	G protein-coupled receptor kinase 6 (GRK6)
4	38.97 %	galectin 7; lectin galactoside-binding soluble 7
2	11.11 %	GL004 protein
1	4.37 %	glucose transporter protein 10; glucose transporter protein 11
1	3.41 %	glutamate dehydrogenase 1
1	2.3 %	glutamate receptor, metabotropic 4
1	3.73 %	glutathione-S-transferase omega 1
1	3.25 %	glycoprotein, synaptic 2; synaptic glycoprotein SC2
1	16.18 %	guanine nucleotide binding protein (G protein), gamma 5
2	5.29 %	guanine nucleotide binding protein (G protein), q polypeptide
1	1.17 %	guanylate cyclase 2F; RetGC-2
1	7.28 %	heme oxygenase (decyclizing) 2
1	4.1 %	heterogeneous nuclear ribonucleoprotein F
1	1.79 %	heterogeneous nuclear ribonucleoprotein L
1	6.22 %	high-mobility group box 2
1	4.84 %	HLA-B associated transcript 5
1	3.57 %	HMG-box transcription factor TCF-3
1	3.67 %	hydroxysteroid (17-beta) dehydrogenase 4
1	1.89 %	hypothetical protein BC001584
1	2.7 %	hypothetical protein BC009732
1	4.84 %	hypothetical protein BC015408
1	4.3 %	hypothetical protein DJ971N18.2
1	1.94 %	hypothetical protein DKFZp434I1610
1	3.08 %	hypothetical protein DKFZp761D0211
1	10.12 %	hypothetical protein DKFZp762O076
2	11.14 %	hypothetical protein FLJ10842
1	1.53 %	hypothetical protein FLJ12649
1	4.77 %	hypothetical protein FLJ14743; homolog of yeast FAR11 protein 1
1	1.46 %	hypothetical protein FLJ20200
2	6.62 %	hypothetical protein FLJ20245
2	5.62 %	hypothetical protein FLJ20481
2	14.91 %	hypothetical protein FLJ20625
1	2.67 %	hypothetical protein FLJ20626
1	5.04 %	hypothetical protein FLJ22390
1	4.12 %	hypothetical protein FLJ22555
1	6.67 %	hypothetical protein FLJ22649 similar to signal peptidase SPC22/23
1	.67 %	hypothetical protein FLJ25045
1	10.5 %	hypothetical protein FLJ25084

1	2.53 %	hypothetical protein FLJ25477
2	4.69 %	hypothetical protein FLJ32001
1	2.72 %	hypothetical protein FLJ32009
1	10.8 %	hypothetical protein FLJ32809
1	4.92 %	hypothetical protein FLJ33718
1	3.85 %	hypothetical protein FLJ35728
1	4.93 %	hypothetical protein LOC144501
1	1.68 %	hypothetical protein LOC259173
1	1.87 %	hypothetical protein LOC283431
1	1.46 %	hypothetical protein LOC51061
1	5.46 %	hypothetical protein MGC10084
1	5.98 %	hypothetical protein MGC13251
1	6.79 %	hypothetical protein MGC15396
1	6.06 %	hypothetical protein MGC26610
1	4.55 %	hypothetical protein MGC35140
1	3.45 %	hypothetical protein MGC39827
1	2.47 %	hypothetical protein MGC4562
1	9.45 %	hypothetical protein MGC48998
1	15.45 %	hypothetical protein XP_376840
1	8.05 %	hypothetical protein XP_378325
1	20.91 %	hypothetical protein XP_379678
1	9.49 %	hypothetical protein XP_379754
1	6.51 %	hypothetical protein ZD52F10
1	6.86 %	immunity associated protein 1
1	.82 %	inositol 1,4,5-triphosphate receptor, type 3
1	1.28 %	integrin alpha L precursor; antigen CD11A (p180)
3	2.84 %	integrin alpha X precursor
2	4.76 %	integrin VLA-4 beta subunit
1	3.32 %	integrin-linked kinase
1	5.82 %	intercellular adhesion molecule 2 precursor
1	14.4 %	interferon induced transmembrane protein 1 (9-27)
3	5.91 %	junction plakoglobin; gamma-catenin
1	4.51 %	KH domain containing, RNA binding, signal transduction associated 1
1	3.17 %	KIAA0095 gene product
2	12.33 %	KIAA0152 gene product
2	4.97 %	KIAA0830 protein
1	2.75 %	KIAA0937 protein
1	3.09 %	KIAA1185 protein
3	10.4 %	KIAA1271 protein
1	2.97 %	KIAA1340 protein
1	1.4 %	KIAA1614 protein
1	1.57 %	KIAA1836 protein
1	4.52 %	lactate dehydrogenase A
1	4.21 %	LAG1 longevity assurance homolog 2
1	.72 %	laminin, alpha 4 precursor
3	11.52 %	lectin, mannose-binding 2; endoplasmic reticulum glycoprotein
1	3.92 %	lectin, mannose-binding, 1 precursor; intracellular mannose specific lectin
2	6.77 %	leucine zipper-EF-hand containing transmembrane protein 1
1	10.96 %	lipoma HMGIC fusion partner-like 2
1	.13 %	lipoprotein, Lp(a); Apolipoprotein Lp(a)
1	3.57 %	major histocompatibility complex, class I
1	2.15 %	mannosyl-oligosaccharide glucosidase
1	5.31 %	mel transforming oncogene
1	3.51 %	membrane cofactor protein
4	6.53 %	meta-vinculin
1	3.86 %	metaxin 1
1	1.14 %	MICAL-like 2 isoform 2
1	9.21 %	microsomal glutathione S-transferase 3
1	.82 %	microtubule-associated protein 2
1	3.33 %	mitogen-activated protein kinase 1; ERK 2
1	2.34 %	molybdenum cofactor synthesis-step 1
1	1.71 %	multimerin 1; glycoprotein Ia*
2	3.05 %	myosin IG
1	.74 %	myosin IXB
1	4.51 %	NADH dehydrogenase (ubiquinone) 1
1	5.4 %	NADH dehydrogenase (ubiquinone) Fe-S protein 2, 49kDa
1	1.41 %	NADPH oxidase 3; NADPH oxidase catalytic subunit-like 3
1	2.44 %	NEDD9 interacting protein with calponin homology and LIM domains
1	17.95 %	neurogranin; protein kinase C substrate; calmodulin-binding protein
1	4.56 %	neutrophil cytosolic factor
1	7.22 %	NK6 transcription factor related, locus 2

1	32.81 %	nucleolar protein family A, member 3; homolog of yeast Nop10p
1	1.67 %	optic atrophy 1
1	1.4 %	oxoglutarate (alpha-ketoglutarate) dehydrogenase (lipoamide)
1	3.76 %	p21-activated kinase 7; protein kinase PAK5
2	2.7 %	phosphatidate cytidylyltransferase 2; CDP-diglyceride synthetase 2
2	4.97 %	phosphogluconate dehydrogenase
1	1.58 %	phospholipase D1, phophatidylcholine-specific
1	2.98 %	PITPNM family member 3; PYK2 N-terminal domain-interacting receptor 1
1	6.11 %	platelet-activating factor acetylhydrolase, isoform Ib, beta subunit 30kDa
1	1.76 %	pleckstrin homology domain containing, family C (with FERM domain) member 1
1	6.86 %	pleckstrin; p47
1	.33 %	plectin 1
2	2.17 %	plexin C1; receptor for virally-encoded semaphorin
1	1.01 %	polymerase (RNA) III (DNA directed) (155kD)
1	4.5 %	PP1201 protein
1	8.52 %	progesterone membrane binding protein
1	2.28 %	ProSAPiP2 protein
3	9.68 %	prostaglandin-endoperoxide synthase 1
3	.75 %	protein kinase, DNA-activated, catalytic polypeptide
1	4.73 %	protein phosphatase 1, regulatory (inhibitor) subunit 16A
1	3.36 %	protein tyrosine phosphatase, non-receptor type 6
1	3.49 %	protocadherin 21 precursor; MT-protocadherin
1	5.19 %	purine nucleoside phosphorylase
1	4.05 %	putative breast adenocarcinoma marker
1	8.81 %	putative NFkB activating protein HNLF
1	7.28 %	RAB18
1	5.42 %	RAB30
1	4.8 %	RAB33B
1	5.47 %	RAB35
1	5.09 %	RAB37
1	5.16 %	RAB39B
1	5.19 %	RAB41 protein
1	5.05 %	RAB4A
1	4.44 %	RAB4B
1	5.12 %	RAB5A
1	5.12 %	RAB5B
1	5.31 %	RAB8B
1	1.93 %	Ras and Rab interactor 3; RAB5 interacting protein 3
1	1.79 %	RAS guanyl releasing protein 2
1	8.9 %	ras homolog gene family, member G (rho G); RhoG
1	8.85 %	ras-related C3 botulinum toxin substrate 1; Rac1
1	3.3 %	reticulon 2 isoform A
1	1.34 %	retinoblastoma binding protein 2; retinoblastoma-binding protein 2
1	10.17 %	retinoblastoma-binding protein 6
1	3.19 %	Rho GTPase activating protein 1; RhoGAP
1	.46 %	Rho guanine nucleotide exchange factor (GEF) 11
1	8.59 %	ribonuclease 6 precursor
1	5.45 %	ribosomal protein L12; 60S ribosomal protein L12
2	12.23 %	ribosomal protein L18; 60S ribosomal protein L18
1	5.11 %	ribosomal protein L28; 60S ribosomal protein L28
1	2.23 %	ribosomal protein L3; 60S ribosomal protein L3
1	2.11 %	ribosomal protein L4; 60S ribosomal protein L4
2	5.9 %	ribosomal protein L6; 60S ribosomal protein L6
1	7.66 %	ribosomal protein L7; 60S ribosomal protein L7
1	3.47 %	ribosomal protein P0; 60S acidic ribosomal protein P0
1	9.93 %	ribosomal protein S13; 40S ribosomal protein S13
1	7.28 %	ribosomal protein S14; 40S ribosomal protein S14
1	10.77 %	ribosomal protein S15a; 40S ribosomal protein S15a
1	5.26 %	ribosomal protein S18; 40S ribosomal protein S18
1	5.35 %	ribosomal protein S3; 40S ribosomal protein S3
1	6.46 %	ribosomal protein S4, X-linked X isoform
2	7.22 %	ribosomal protein S4, Y-linked 2
1	4.64 %	ribosomal protein S9; 40S ribosomal protein S9
1	7.59 %	ring finger protein 8 isoform 2; C3HC4-type zinc finger protein
1	1.33 %	RNA binding motif protein 15; one twenty two protein
1	6.7 %	RNA binding motif, single stranded interacting protein 1
1	.34 %	ryanodine receptor 2
1	15.24 %	S100 calcium binding protein A11 (calgizzarin)
1	3.77 %	secernin 3
1	5.01 %	serine (or cysteine) proteinase inhibitor
1	4.23 %	serine palmitoyltransferase subunit 1

1	2.8 %	serine/threonine protein kinase TAO1 homolog
1	1.86 %	serologically defined colon cancer antigen 1
1	5.9 %	signal recognition particle receptor, beta subunit
1	5.24 %	signal sequence receptor, alpha
1	10.98 %	signal sequence receptor, delta
1	3.38 %	signal transducer and activator of transcription 3
1	6.1 %	similar to 1810012H11Rik
1	16.13 %	similar to 60S ribosomal protein L29 (Cell surface heparin binding protein HIP)
1	3.76 %	similar to anaphase promoting complex subunit 1
1	1.81 %	similar to CAGL79
1	3.68 %	similar to carbonic anhydrase XV
1	.11 %	similar to Centromeric protein E (CENP-E protein)
1	6.73 %	similar to CGI-62 protein
1	6.78 %	similar to dJ14N1.2 (novel S-100/ICaBP type calcium binding domain protein)
1	10.17 %	similar to Elongation factor 1-alpha 1
1	.59 %	similar to embryonic blastocoelar extracellular matrix protein precursor
1	3.81 %	similar to KIAA0408 protein
1	14.15 %	similar to KIAA0563 gene product
1	3.85 %	similar to mouse fat 1 cadherin
1	1.3 %	similar to RIKEN cDNA 4632411J06
1	8.88 %	similar to tropomyosin 3
1	1.75 %	SKI-like; ski-related oncogene snoN
1	2.61 %	SNF-1 related kinase
1	4.08 %	solute carrier family 16, member 10; T-type amino acid transporter 1
1	2.77 %	solute carrier family 2 member 10; sugar transporter GLUT10
1	2.79 %	solute carrier family 9 (sodium/hydrogen exchanger)
1	1.69 %	source of immunodominant MHC-associated peptides
1	52.38 %	S-phase response (cyclin-related)
1	2.6 %	sphingomyelin phosphodiesterase 3
1	8.54 %	splicing factor, arginine/serine-rich 3
1	2.19 %	sterol carrier protein 2
1	4.21 %	stomatin (EPB72)-like 2; stomatin-like protein 2
1	5.24 %	stratifin
2	5.4 %	stromal interaction molecule 1 precursor
1	5.82 %	surfeit 6; surfeit locus protein 6
1	3.64 %	synaptobrevin-like 1
1	6.27 %	syntaxin 11
1	4.5 %	syntaxin 3A
2	3.96 %	t-complex 1; T-complex locus TCP-1
1	3.35 %	tektin 1
1	.97 %	testis expressed gene 10
1	2.86 %	tetracycline transporter-like protein
1	3.26 %	thromboxane A synthase 1
1	.32 %	thyroid hormone receptor interactor 8
1	3.24 %	tigger transposable element derived 2
1	2.33 %	timeless-interacting protein; tipin
1	.58 %	transcription factor-like nuclear regulator
1	.84 %	transcriptional regulator ATRX
1	.86 %	transient receptor potential cation channel, subfamily M, member 2
3	10.59 %	transketolase
1	2.11 %	transmembrane 9 superfamily member 2
1	2.99 %	transmembrane protein (63kD), endoplasmic reticulum/Golgi
2	12.33 %	transmembrane trafficking protein
1	5.59 %	trans-prenyltransferase
1	5.14 %	triggering receptor expressed on myeloid cells-like 1
2	8.13 %	Tu translation elongation factor, mitochondrial
1	6.87 %	tumor necrosis factor alpha
1	3.1 %	tumor-associated calcium signal transducer 2 precursor
1	26.98 %	ubiquinol-cytochrome c reductase complex 7.2kDa protein
1	3.97 %	ubiquinol-cytochrome c reductase core protein II
1	2.17 %	ubiquitin-activating enzyme E1-like; ubiquitin-activating enzyme-2
1	1.55 %	uveal autoantigen with coiled-coil domains and ankyrin repeats
1	3.68 %	vasodilator-stimulated phosphoprotein
1	6.51 %	vesicle trafficking protein sec22b
1	.64 %	von Willebrand factor precursor
1	.49 %	Werner syndrome protein; Werner Syndrome helicase
1	8.05 %	zinc finger protein 435
1	3.16 %	zinc finger, CW-type with coiled-coil domain 2
1	4.21 %	zinc metalloproteinase STE24 homolog; CAAX prenyl protease

SPECIFIC GRANULE REJECTED PROTEINS (212)		
Number of peptides	% coverage	Protein Name
1	3.53 %	1-acylglycerol-3-phosphate O-acyltransferase 1
1	3.11 %	3-hydroxyisobutyryl-Coenzyme A hydrolase isoform 1
1	2.88 %	6-phosphofructo-2-kinase/fructose-2,6-biphosphatase 3
1	2.01 %	a disintegrin and metalloprotease domain 10
1	1.82 %	a disintegrin and metalloproteinase domain 17
2	5.56 %	aldehyde dehydrogenase 3B1; aldehyde dehydrogenase 7
1	2.58 %	alkylglycerone phosphate synthase precursor
1	1.28 %	alpha 1 type II collagen
1	.88 %	amyotrophic lateral sclerosis 2 (juvenile) chromosome region, candidate 3
1	2.97 %	annexin A11; annexin XI
2	5.05 %	annexin VI (p68)
1	.49 %	antigen identified by monoclonal antibody Ki-67
1	3.74 %	APG12 autophagy 12-like
1	2.51 %	arsenate resistance protein ARS2
1	.4 %	asp (abnormal spindle)-like, microcephaly associated
1	13.83 %	ATP synthase, H+ transporting, mitochondrial F0 complex, subunit f
1	12.62 %	ATP synthase, H+ transporting, mitochondrial F0 complex, subunit g
1	2.01 %	ATPase, Class VI, type 11B
1	1.76 %	ATPase, Na+/K+ transporting
1	.85 %	ATP-binding cassette, sub-family A
1	.78 %	ATP-binding cassette, sub-family C
1	13.6 %	basic leucine zipper transcription factor, ATF-like
1	4.09 %	bone marrow stromal cell antigen 1 precursor
1	.29 %	bullous pemphigoid antigen 1 isoform 1
1	4.2 %	C21orf80 protein isoform C
1	.54 %	cadherin EGF LAG seven-pass G-type receptor 3
1	1.4 %	calpain 1, large subunit
1	.98 %	caspase recruitment domain protein 12; ICE-protease activating factor
1	1.75 %	CD44 antigen; homing function
1	1.4 %	CDC42-binding protein kinase alpha
1	.79 %	chromosome 20 open reading frame 104
1	8.97 %	chromosome 6 open reading frame 82; divalent cation tolerant protein CUTA
1	8.88 %	chromosome 8 open reading frame 13
1	.77 %	coagulation factor VIII isoform a precursor
1	1.67 %	colony stimulating factor 2 receptor, beta, low-affinity
1	4.78 %	concentrative Na+-nucleoside cotransporter
1	3.4 %	corneodesmosin precursor
2	9.79 %	cytochrome b reductase 1
1	4.41 %	cytochrome c oxidase II
1	6.51 %	cytochrome c oxidase subunit IV isoform 1 precursor
2	27.71 %	cytochrome c oxidase subunit VIIa polypeptide 2 (liver) precursor
1	3.69 %	cytochrome c-1
1	.96 %	cytoplasmic linker 2 isoform 1; Williams-Beuren syndrome chromosome region 4
1	.34 %	dedicator of cytokinesis 6
4	2.8 %	desmocollin 1
1	3.85 %	DNA methyltransferase 1-associated protein 1
1	1.83 %	DNA2 DNA replication helicase 2-like
1	9.72 %	downregulated in renal cell carcinoma
1	.32 %	dynein, cytoplasmic, heavy polypeptide
1	4.58 %	EF hand domain containing 2
1	6.28 %	endometrial bleeding associated factor preproprotein
1	1.4 %	evolutionarily conserved G-patch domain containing
1	.26 %	Fc fragment of IgG binding protein
1	.67 %	FERM, RhoGEF, and pleckstrin domain protein
1	4.81 %	FLJ44290 protein
1	2.3 %	FLJ44299 protein
1	1.03 %	formin 2
1	1.02 %	FYVE-finger-containing Rab5 effector protein rabenosyn-5
1	3.8 %	G6B protein; immunoglobulin receptor
1	6.07 %	gasdermin
1	4 %	glycogenin
1	8.95 %	growth and transformation-dependent protein
1	2.89 %	guanine nucleotide binding protein (G protein) alpha 12
1	2.92 %	guanine nucleotide binding protein (G protein), alpha 13

1	5.43 %	H2A histone family
1	5.15 %	H3 histone family
1	1.91 %	heat shock 90kDa protein
1	3.79 %	heterogeneous nuclear ribonucleoprotein H
2	7.18 %	high-mobility group box 2
1	6.15 %	hypothetical protein 669
1	1.89 %	hypothetical protein BC001584
1	1.72 %	hypothetical protein DKFZp566M1046
1	3.08 %	hypothetical protein DKFZp761D0211
1	2 %	hypothetical protein ET
1	3.03 %	hypothetical protein FLJ10211
1	4.78 %	hypothetical protein FLJ10213
1	3.79 %	hypothetical protein FLJ10350
1	9.75 %	hypothetical protein FLJ12598
1	4.6 %	hypothetical protein FLJ13612
1	6.52 %	hypothetical protein FLJ13902
1	2.14 %	hypothetical protein FLJ20272
1	2.67 %	hypothetical protein FLJ20626
1	.99 %	hypothetical protein FLJ23577
1	3.2 %	hypothetical protein LOC92912
1	4.55 %	hypothetical protein LOC92922
1	6.06 %	hypothetical protein MGC26610
1	3.45 %	hypothetical protein MGC39827
1	6.71 %	hypothetical protein MGC50809
1	6.52 %	hypothetical protein XP_172995
1	11.01 %	hypothetical protein XP_378656
1	4.13 %	hypothetical protein XP_379226
1	.64 %	insulin receptor substrate 1
1	2.05 %	involucrin
1	3.54 %	isocitrate dehydrogenase 2 (NADP+), mitochondrial precursor
6	11.68 %	junction plakoglobin; gamma-catenin
1	.4 %	KIAA0100 gene product
1	1.59 %	KIAA0645 gene product
1	1.45 %	KIAA0747 protein
1	3.11 %	KIAA0767 protein
1	1.5 %	KIAA0999 protein
2	.93 %	KIAA1093 protein
1	1.75 %	KIAA1627 protein
1	3.95 %	KIAA1948 protein
1	6.59 %	killer cell immunoglobulin-like receptor
1	1.56 %	leukocyte antigen CD97
1	1.25 %	leukocyte receptor cluster (LRC) member 8
1	1.8 %	likely ortholog of mouse 5-azacytidine induced gene 1
1	.13 %	apolipoprotein Lp(a)
1	1.11 %	LYST-interacting protein LIP8
1	5.31 %	mel transforming oncogene; mel transforming oncogene
1	.53 %	microtubule-associated protein 1B
1	5.62 %	mitochondrial malate dehydrogenase precursor
1	1.07 %	MMS19-like (MET18 homolog, S. cerevisiae)
1	.55 %	nebulin
1	1.47 %	neurofilament, heavy polypeptide 200kDa
1	2.28 %	neuropilin 1
1	3.59 %	neutrophil cytosolic factor 1
1	1.2 %	nicotinamide nucleotide transhydrogenase
1	2.82 %	nuclear receptor subfamily 1, group H, member 2
1	2.67 %	opioid growth factor receptor-like 1
1	3.23 %	origin recognition complex, subunit 3
1	6.71 %	osteoglycin preproprotein; osteoinductive factor; mimecan
1	8.42 %	oxidised low density lipoprotein (lectin-like) receptor 1
1	2.38 %	paraneoplastic cancer-testis-brain antigen
1	2.7 %	perforin 1 (pore forming protein)
1	1.17 %	peroxisome biogenesis factor 1
1	5.1 %	PFTAIRE protein kinase 1
1	1.59 %	phosphoinositide-3-kinase, catalytic susbunit
2	4.4 %	phosphoinositide-3-kinase, regulatory subunit
1	4.34 %	platelet-activating factor acetylhydrolase 2
1	6.86 %	pleckstrin; p47
1	1.97 %	podocan
1	3.01 %	poly(rC)-binding protein 2
1	3.73 %	potassium inwardly-rectifying channel J15
1	4.5 %	PP1201 protein

1	.24 %	protein kinase, DNA-activated, catalytic polypeptide
1	2.69 %	protein phosphatase 1, regulatory subunit 9B; neurabin II
1	10.31 %	putative nuclear protein ORF1-FL49
1	5.42 %	RAB30
1	4.8 %	RAB33B
1	5.09 %	RAB37
1	5.16 %	RAB39B
1	5.19 %	RAB41 protein
1	5.05 %	RAB4A
1	5.31 %	RAB8B
2	1.89 %	radixin
1	1.53 %	regulator of G-protein signalling 3
1	5.69 %	repressor of estrogen receptor activity; B-cell associated protein
1	1.04 %	Rho guanine nucleotide exchange factor (GEF) 12
1	9.38 %	ribonuclease, RNase A family, 3 (eosinophil cationic protein)
1	5.32 %	ribosomal protein L18; 60S ribosomal protein L18
1	3.28 %	ribosomal protein L4; 60S ribosomal protein L4
1	7.66 %	ribosomal protein L7; 60S ribosomal protein L7
1	3.47 %	ribosomal protein P0; 60S acidic ribosomal protein P0
1	11.3 %	ribosomal protein P2; 60S acidic ribosomal protein P2
1	7.28 %	ribosomal protein S14; 40S ribosomal protein S14
1	4.18 %	ribosomal protein S4, X-linked X isoform
1	4.18 %	ribosomal protein S4, Y-linked Y isoform
1	11.86 %	ribosomal protein S7; 40S ribosomal protein S7
1	6.25 %	ribosomal protein S8; 40S ribosomal protein S8
1	1.43 %	ribosome binding protein 1
1	4.95 %	ring finger protein 8; C3HC4-type zinc finger protein
1	1.33 %	RNA binding motif protein 15; one twenty two protein
1	1.16 %	RNA binding motif protein 6
1	1.85 %	sarcosine dehydrogenase
1	4.31 %	serine (or cysteine) proteinase inhibitor
1	6.96 %	serine/threonine protein kinase SSTK
1	2.8 %	serine/threonine protein kinase TAO1 homolog
1	5.69 %	SH3 domain containing ring finger 2
1	1.78 %	similar to 4930579E17Rik protein
1	3.27 %	similar to F-box only protein 2
1	5.91 %	similar to mCBP
1	11.47 %	similar to Phosphorylase B kinase alpha regulatory chain
1	5.31 %	similar to retina and anterior neural fold homeobox
1	4.39 %	similar to Ribonuclease-like protein 9 precursor
1	3 %	similar to RIKEN cDNA 0610009J22
1	2.05 %	similar to RIKEN cDNA E230015L20 gene
1	8.33 %	similar to Spermatogenesis associated protein 2
1	1.68 %	skeletal myosin light chain kinase
1	2.8 %	solute carrier family 16, member 3; monocarboxylate transporter 3
1	4.46 %	solute carrier family 25 (mitochondrial carrier; oxoglutarate carrier)
1	1.87 %	solute carrier family 4, anion exchanger, member 1 band 4.1
1	2.35 %	solute carrier organic anion transporter family, member 4C1
1	.76 %	splicing coactivator subunit SRm300; RNA binding protein
1	2.8 %	splicing factor 3a, subunit 2, 66kDa; Spliceosome protein SAP-62
1	1.88 %	step II splicing factor SLU7
1	2.04 %	stromal interaction molecule 1 precursor
1	7.79 %	superoxide dismutase 1, soluble; Cu/Zn superoxide dismutase
1	1.5 %	surface glycoprotein, Ig superfamily member
1	6.27 %	syntaxin 2
1	4.22 %	syntaxin binding protein 3; syntaxin 4 binding protein
1	5.99 %	TG-interacting factor; homeobox protein TGIF
1	12.38 %	thioredoxin
1	5.75 %	thyroid autoantigen 70kDa (Ku antigen)
1	.06 %	titin isoform; connectin
1	7.23 %	transcription factor MLR1
1	2.32 %	transcription factor NRF; ITBA4 gene
1	1.97 %	translation initiation factor IF2
1	6.87 %	tumor necrosis factor alpha
1	1.25 %	tumor rejection antigen (gp96)
1	4.24 %	uncharacterized hematopoietic stem/progenitor cells protein MDS031
1	.5 %	utrophin; dystrophin-related protein
1	1.25 %	vesicle docking protein p115; transcytosis-associated protein
1	1.52 %	vesicular inhibitory amino acid transporter
1	2.16 %	vitrin
1	1.68 %	wingless-type MMTV integration site family, member 9B precursor

1	1.05 %	zinc finger CCCH type domain containing 3
1	3.32 %	zinc finger protein 185 (LIM domain)
1	2.37 %	zinc finger protein 226
1	1.85 %	zinc finger protein 536
1	2.61 %	zinc finger protein 596

AZUROPHILIC GRANULE REJECTED PROTEINS (231)		
Number of peptides	% coverage	Protein Name
1	5.62 %	acidic (leucine-rich) nuclear phosphoprotein 32 family, member A
1	5.5 %	adaptor-related protein complex 3, mu 1 subunit; mu-adaptin 3A
1	2.62 %	adenylate cyclase 5; adenylate cyclase, type V
1	2.99 %	aldehyde dehydrogenase 3B
1	3.85 %	aldolase A; fructose-bisphosphate aldolase
1	1.3 %	alpha 1 type III collagen; Collagen III, alpha-1 polypeptide
1	1.98 %	alpha 2 type I collagen; Collagen I, alpha-2 polypeptide
1	1.87 %	alpha 2 type V collagen preproprotein; Collagen V, alpha-2 polypeptide
1	10.4 %	alternative reading frame p14; multiple tumor suppressor 1
1	.86 %	androgen-induced prostate proliferative shutoff associated protein
2	4.15 %	arachidonate 5-lipoxygenase
1	3.35 %	arylsulfatase precursor
1	2.13 %	ataxin 7
1	.67 %	ATP-binding cassette, sub-family A
1	.98 %	ATP-binding cassette, sub-family B (MDR/TAP)
1	4.59 %	BCL2-like 14; apoptosis regulator BCL-G
1	2.01 %	block of proliferation 1
1	4.09 %	bone marrow stromal cell antigen 1 precursor
1	5.11 %	BTB (POZ) domain containing 14A
1	6.4 %	C21orf19-like protein; CGI-27 protein
1	2.46 %	calmegin
1	1.53 %	CAP-binding protein complex interacting protein 1
1	.61 %	CASP8 associated protein 2; FLICE associated huge; human FLASH
1	3.72 %	cat eye syndrome critical region protein 1
1	3.6 %	CD36 antigen (collagen type I receptor, thrombospondin receptor)
1	.94 %	CDC42-binding protein kinase beta
1	5.84 %	chromosome 9 open reading frame 87
1	1.89 %	c-Maf-inducing protein
1	1.67 %	colony stimulating factor 2 receptor, beta, low-affinity
1	1.71 %	complement component 8, alpha polypeptide precursor
1	1.35 %	cyclic AMP-regulated phosphoprotein, 21 kD isoform
1	8.74 %	cytochrome b reductase 1
1	1 %	discs large homolog 5; placenta and prostate DLG
1	1.06 %	discs large homolog 7; Drosophila discs large-1 tumor suppressor-like
1	.66 %	Dmx-like 1
1	7.58 %	DOK5 protein isoform b; downstream of tyrosine kinase 5
1	.29 %	dynein, axonemal, heavy polypeptide
1	2.43 %	elongation protein 4 homolog; PAX6 neighbor gene
1	2.94 %	F-box only protein 10
1	1.66 %	F-box only protein 11
1	3.9 %	fibrinogen C domain containing 1
1	2.07 %	FKSG42
1	2.39 %	fucosidase, alpha-L- 1, tissue
1	1.85 %	fuse-binding protein-interacting repressor
1	6.83 %	G protein-coupled receptor MRGX1
2	5.36 %	galactosidase, alpha
1	2.22 %	galactosidase, beta
1	1.71 %	gene near HD on 4p16.3 with homology to hypothetical S. pombe gene
1	3.04 %	general transcription factor IIIC, polypeptide 4, 90kDa
1	2.36 %	glucosamine (N-acetyl)-6-sulfatase precursor
1	6.42 %	glutathione S-transferase M1; HB subunit 4
1	1.41 %	Golgi autoantigen, golgin subfamily a, 2; golgin-95
1	4.19 %	growth differentiation factor 5 preproprotein
1	2.89 %	guanine nucleotide binding protein (G protein) alpha 12
1	2.92 %	guanine nucleotide binding protein (G protein), alpha 13
1	1.54 %	guanylate cyclase 2D, membrane
2	13.24 %	H3 histone family
1	1.79 %	heat shock protein 12A

1	.39 %	hemicentin-2
1	6.86 %	hepatocyte nuclear factor 4, gamma
1	1.37 %	heterogeneous nuclear ribonucleoprotein M
1	4.4 %	homeo box D3; homeobox protein Hox-D3
3	17.2 %	hypothetical protein BC015408
1	2.71 %	hypothetical protein DKFZp434B227
1	1.58 %	hypothetical protein DKFZp686A17109
1	3.41 %	hypothetical protein FLJ10252
1	4.09 %	hypothetical protein FLJ10891
1	1.8 %	hypothetical protein FLJ12994
1	10.5 %	hypothetical protein FLJ13448
1	6.47 %	hypothetical protein FLJ13646
1	6.8 %	hypothetical protein FLJ14281
1	6.13 %	hypothetical protein FLJ20249
1	8.07 %	hypothetical protein FLJ20625
1	3.35 %	hypothetical protein FLJ21128
1	1.41 %	hypothetical protein FLJ21308
1	3.32 %	hypothetical protein FLJ22301
1	5.63 %	hypothetical protein FLJ36031
1	1.85 %	hypothetical protein FLJ40342
1	1.78 %	hypothetical protein FLJ40722
2	5.11 %	hypothetical protein LOC51244
1	2.1 %	hypothetical protein MGC13125
1	13.56 %	hypothetical protein MGC15619
1	3.47 %	hypothetical protein MGC16044
1	5.49 %	hypothetical protein MGC24132
1	2.7 %	hypothetical protein MGC34763
1	4.88 %	hypothetical protein XP_096852
1	9.88 %	hypothetical protein XP_294867
1	12.07 %	hypothetical protein XP_375081
1	4.23 %	hypothetical protein XP_377074
1	15.22 %	hypothetical protein XP_378234
1	6.08 %	hypothetical protein XP_378322
1	6.8 %	hypothetical protein XP_378509
1	17.35 %	hypothetical protein XP_378680
1	4.89 %	hypothetical protein XP_378730
1	11.54 %	hypothetical protein XP_379024
1	9.32 %	hypothetical protein XP_379139
1	11.32 %	hypothetical protein XP_379482
1	18.18 %	hypothetical protein XP_379573
1	11.32 %	hypothetical protein XP_380098
1	1.09 %	inositol polyphosphate-5-phosphatase, 145kDa
1	5.73 %	isopentenyl-diphosphate delta isomerase 2
1	3.66 %	KIAA0220 protein
1	1.18 %	KIAA0553 protein
1	1.44 %	KIAA0676 protein
1	1.89 %	KIAA0720 protein
1	3.67 %	KIAA0889 protein
1	.69 %	KIAA1117 protein
1	1.22 %	KIAA1210 protein
1	2.82 %	KIAA1465 protein
1	1.03 %	KIAA1509
1	2.72 %	l(3)mbt-like isoform l; lethal (3) malignant brain tumor l(3)
1	2.66 %	leucine rich repeat containing 16
1	1.08 %	leucine-rich PPR motif-containing protein
1	.81 %	low density lipoprotein receptor-related protein 4
1	1.57 %	LU1 protein
1	2.66 %	macrophage scavenger receptor 1
1	8.13 %	MAD4; Mad4 homolog
1	3.49 %	MAP/microtubule affinity-regulating kinase 4
1	.96 %	melanoma antigen, family C, 1
1	2.1 %	metalloprotease related protein 1
1	2.78 %	minichromosome maintenance protein 4
1	1.29 %	myosin XVIIIB; myosin 18B
1	1.91 %	NACHT, leucine rich repeat and PYD containing 4
1	4.89 %	natrium-phosphate cotransporter IIa C-terminal-associated protein 2
1	1.54 %	nephroretinin
1	4.55 %	niban protein
1	1.27 %	nicastrin
1	7.22 %	NK6 transcription factor related, locus 2
1	1.95 %	NOD9 protein

1	1.46 %	NPF/calponin-like protein
1	1.59 %	nuclear factor related to kappa B binding protein
1	3.82 %	nucleolin
1	13.9 %	nucleoside-diphosphate kinase 4
1	4 %	nucleosome assembly protein 1-like 4
1	1.94 %	NY-REN-24 antigen
1	.45 %	odd Oz/ten-m homolog 4
1	8.42 %	oxidised low density lipoprotein (lectin-like) receptor 1
1	.84 %	pericentriolar material 1
1	5.46 %	peroxisome biogenesis factor 13
1	.39 %	phosphatidylinositol 4-kinase, catalytic, alpha polypeptide isoform 2
1	5.53 %	phosphoglycerate mutase 2
1	1.3 %	phospholipase D1, phophatidylcholine-specific
1	3.88 %	phosphorylase kinase
1	.3 %	PI-3-kinase-related kinase SMG-1
1	.78 %	plexin D1
1	1.74 %	positive cofactor 2, glutamine/Q-rich-associated protein
1	5.5 %	potassium inwardly-rectifying channel J14
1	1.76 %	PRIP-interacting protein PIPMT
1	1.22 %	PRO2000 protein
1	.36 %	progestin-induced protein; ubiquitin-protein ligase
1	.73 %	programmed cell death 11
1	9.09 %	pro-melanin-concentrating hormone
1	6.69 %	proteasome activator subunit 2; proteasome activator hPA28 subunit beta
1	3.09 %	protein kinase, AMP-activated, alpha 1 catalytic subunit; AMPK alpha 1
1	4.46 %	pyruvate dehydrogenase (lipoamide) beta
1	1.6 %	RAB GTPase activating protein 1
2	6.02 %	RAB37
2	12.08 %	RAB8B
1	5.99 %	rab-related GTP-binding protein
1	3.12 %	Ras-interacting protein
1	5.29 %	Rab-15
1	3.47 %	REC8-like 1
1	.7 %	retinitis pigmentosa RP1 protein
1	3.78 %	RGM domain family, member A
1	2.26 %	Rho GTPase activating protein 18
1	.56 %	Rho GTPase activating protein 21
1	5.32 %	ribosomal protein L18; 60S ribosomal protein L18
1	5.65 %	ribosomal protein L7; 60S ribosomal protein L7
1	14.04 %	ribosomal protein P1; 60S acidic ribosomal protein P1
1	9.93 %	ribosomal protein S13; 40S ribosomal protein S13
1	5.26 %	ribosomal protein S18; 40S ribosomal protein S18
1	3.96 %	S-adenosylhomocysteine hydrolase-like 1
1	3.32 %	serine carboxypeptidase 1 precursor protein
1	2.45 %	serine/threonine protein phosphatase with EF-hand motifs 1
1	1.2 %	SH3 and multiple ankyrin repeat domains 2 isoform 1
2	1.04 %	SH3-domain binding protein 4
1	15.24 %	similar to Alpha-endosulfine
1	.17 %	similar to Centromeric protein E (CENP-E protein)
1	14.88 %	similar to crystallin, zeta; NADPH:quinone reductase
1	2.9 %	similar to dJ25J6.2 (novel zinc finger protein)
1	36.52 %	similar to DKFZP434O047 protein
1	9.41 %	similar to High mobility group protein 1 (HMG-1) (Amphoterin)
1	2.19 %	similar to hypothetical protein DKFZp434A171
1	24.3 %	similar to hypothetical protein FLJ30921
1	3.25 %	similar to hypothetical protein MGC57211
1	1.07 %	similar to KIAA2026 protein
1	2.95 %	similar to MGC76216 protein
1	5.16 %	similar to MGC9515 protein
1	2.27 %	similar to orphan sodium- and chloride-dependent neurotransmitter transporter
1	3.05 %	similar to osteotesticular protein tyrosine phosphatase
1	5.3 %	similar to putative transmembrane protein
2	10.88 %	similar to Rab12 protein
1	6.53 %	similar to retina and anterior neural fold homeobox
1	6.4 %	similar to RIKEN cDNA 0610012A05
1	2.79 %	similar to RIKEN cDNA 9430067K14 gene
1	1.56 %	similar to RIKEN cDNA E430004N04 gene
1	5.12 %	similar to Serine/threonine protein kinase PRKX
1	4.63 %	similar to zinc finger protein 495
1	3.9 %	single Ig IL-1R-related molecule
1	4.23 %	sirtuin 6; sir2-related protein type 6; sirtuin type 6

2	1.85 %	skeletal myosin light chain kinase
1	6.87 %	small GTPase protein E-Ras;
1	13.54 %	small inducible cytokine A1 precursor; inflammatory cytokine I-309
1	1.48 %	smooth muscle cell associated protein-1
1	.97 %	spectrin, alpha, non-erythrocytic 1 (alpha-fodrin)
1	1.94 %	sperm associated antigen 1; infertility-related sperm protein
1	2.9 %	sphingomyelin phosphodiesterase 3, neutral membrane
1	5.32 %	SPRY domain-containing SOCS box protein SSB-2
1	1.29 %	suppressor of Ty 5 homolog
1	4.16 %	surfeit 6; surfeit locus protein 6
1	5.45 %	synaptobrevin-like 1
1	3.61 %	syntaxin 10
1	7.63 %	syntaxin 8
1	5.59 %	tachykinin receptor 3; NK-3 receptor; neurokinin B receptor
1	2.64 %	target of myb1
1	2.88 %	three prime repair exonuclease 1
1	2.33 %	timeless-interacting protein; tipin
1	.06 %	titin isoform; connectin
1	4.21 %	transcription elongation factor B polypeptide 3C (elongin A3)
1	1.18 %	transcriptional co-repressor Sin3A
1	2.24 %	transmembrane protein 16C; chromosome 11 open reading frame 25
1	3.66 %	tripartite motif protein 15 isoform alpha
6	9.09 %	tumor rejection antigen (gp96)
1	3.43 %	ubiquitin-conjugating enzyme E2-like; signaling molecule ATTP
1	.43 %	vacuolar protein sorting 13C protein
1	5.15 %	Williams Beuren syndrome critical region 20A
1	3.26 %	Wilms tumor 1
1	3.77 %	zinc finger protein 205; zinc finger protein 210
1	.38 %	zinc finger protein 469
1	3.06 %	zinc finger protein AP4

The table shows the number of peptides and the percent coverage for proteins identified only once by 2D-HPLC ESI-MS/MS.

CURRICULUM VITAE

Name: George Lominadze

DOB: Tbilisi, Rep. of Georgia (USSR), November 1, 1978.

Education:

B.S., Biological Sciences, 2000
University of Louisville, Louisville, KY

Ph.D., Biochemistry and Molecular Biology, 2005
University of Louisville, Louisville, KY

Academic Honors:

Summa Cum Laude (University of Lousville, 2000).
University Fellowship (University of Louisville, August 2000-July 2002).
American Heart Association Predoctoral Fellowship (July 2002-June 2004).
American Heart Association Predoctoral Fellowship (July 2004-June 2005).

Publications:

Lominadze, G., Rane, M.J., Merchant, M., Cai, J., Ward, R.A., McLeish, K.R. Myeloid-Related Protein-14 Is a p38 MAPK Substrate in Human Neutrophils. *The Journal of Immunology,* 2005, 174: 7257-7267.

Lominadze, G., Ward, R.A., Klein, J.B., McLeish, K.R. Proteomic Analysis of Human Neutrophils. In *Transmembrane Signaling Protocols*, Second Edition (Methods in Molecular Biology, Vol. 84). Editors: Hydar Ali and Bodduluri Haribabu. Accepted for publication.

Lominadze, G., Powell, D.W., Luerman, G.C., Link, A.J., Ward, R.A., McLeish, K.R. Proteomic Analysis of Human Neutrophil Granules. Molecular and Cellular Proteomics. Accepted, pre-published online, June 28, 2005.

National Meeting Presentations:

Lominadze, G., Ward, R., McLeish, K.R. Identification of Human Neutrophil Specific Granule Proteins by Proteomic Analysis. Poster Presentation, 36th Annual Meeting of the Society for Leukocyte Biology (Philadelphia, October, 2003).

Rane, M.J., Lominadze G., Sachleben, L.R., Wu, R., Gozal, E. Hypoxia Induces AKT-Mediated HSP 70 Phosphorylation in PC-12 Cells. Poster Presentation, Society for Neuroscience 34th Annual Meeting (San Diego, October 2004).

Lominadze, G., Chaddha, K., Brinkley, K., Ward, R.A., McLeish, K.R. Comparison of Human Neutrophil Gelatinase and Specific Granule Proteomes. Poster Presentation, IUBMB/ASBMB Annual Meeting (Boston, June, 2004).

Lominadze, G., Powell, D., Brinkley, K., Link, J.A., Ward, R.A., McLeish, K.R. Comprehensive Analysis of Human Neutrophil Myeloperoxidase-negative Granule Proteomes. Poster Presentation, 37th Annual Meeting of the American Society of Nephrology. (St. Louis, October, 2004)

Lominadze, G., Rane, M.J., McLeish, K.R. Identification of MRP-14 as a Substrate of p38 MAPK in Human Neutrophils. Poster Presentation, 37th Annual Meeting of the Society for Leukocyte Biology (Toronto, October, 2004).

Lominadze, G., Powell, D.W., Luerman, G.C., Link, A.J., Ward, R.A., McLeish, K.R. A Comprehensive Proteomic Analysis of Human Neutrophil Granules. Poster Presentation, 13th Gordon Research Conference on Phagocytes (New London, CT., June, 2005).

Jog, N., Lominadze, G., Ward, R.A., McLeish, K.R. The Actin Cytoskeleton Regulates Stimulated Exocytosis and Endocytosis in Human Neutrophils. Poster Presentation, 38th Annual Meeting of the American Society of Nephrology. (Philadelphia, November, 2005).